EVALUATION OF AN INTERDIGITATED GATE ELECTRODE FIELD-EFFECT TRANSISTOR FOR DETECTING ORGANOPHOSPHORUS COMPOUNDS

THESIS

Charles P. Brothers Jr.
Captain, USAF
AFIT/GE/ENG/90D-07

AFIT/GE/ENG/90D-07

EVALUATION OF AN INTERDIGITATED GATE ELECTRODE FIELD-EFFECT TRANSISTOR FOR DETECTING ORGANOPHOSPHORUS COMPOUNDS

THESIS

Charles P. Brothers Jr.
Captain, USAF
AFIT/GE/ENG/90D-07

AFIT/GE/ENG/90D-07

EVALUATION OF AN INTERDIGITATED GATE ELECTRODE FIELD-EFFECT TRANSISTOR FOR DETECTING ORGANOPHOSPHORUS COMPOUNDS

THESIS

Presented to the Faculty of the School of Engineering

of the Air Force Institute of Technology

Air University

In Partial Fulfillment of the

Requirements for the Degree of

Master of Science in Electrical Engineering

Charles P. Brothers Jr.

Captain, USAF

December 1990

Acknowledgements

The assistance I received from many individuals during this research effort was indispensable. The counsel provided by my thesis advisor, Lt Col E. Kolesar, has been invaluable. His assistance kept the investigation focused and on track. Captain Thomas Jenkins was very helpful in repeatedly providing background and reference data. Captain Jenkins provided a level of continuity that is rarely available at AFIT.

The advise and assistance provided by Mr. Don Smith and Mr. William Trop of the AFIT Electronics and Materials Cooperative Laboratory was extremely beneficial in accomplishing the IGEFET evaluation. Without the assistance of Mr. Orville Wright in ordering materials and equipment for the fabrication of the test cell, the IGEFET evaluations would not have been nearly as efficient.

This Thesis would not have been possible without the assistance and continuous support from my wife Heidi; her endless sacrifices were greatly appreciated. My children, Stacy and Scott were very supportive, and their tolerance during this period was exemplary.

Table of Contents

List of Figures

List of Tables

Abstract

This study used an integrated circuit microsensor (designed by Captain Thomas Graham, a GE-90D graduate student) to detect organophosphorus compounds. Chemically-sensitive thin films were applied to interdigitated gate electrode (IGE) structures on the integrated circuit. Electrical performance characteristics of the thin films were measured for several parameters, including: DC resistance, AC impedance, time-domain, gain-phase, and spectral responses from 10 Hz to 1 MHz. Each microsensor contained nine IGEs; each IGE possessed an *in situ* field-effect transistor (FET) amplifier. The chemically-sensitive films evaluated were: copper phthalocyanine, DFPase, succinyl chloride, succinylcholine chloride, 2-naphthol(β), and L-histidine dihydrochloride. Each film was applied to at least one IGE structure on each microsensor with an average thickness of 2000 angstroms. After purging each sensor with filtered laboratory air, the sensor was exposed to one or a combination of two of the following gases: diisopropyl fluorophosphate (DFP), diisopropyl methylphosphonate, and dimethyl methylphosphonate at concentrations spanning 100 ppb to 10 ppm (at 90% relative humidity and 23° C). Testing was conducted with microsensors heated to 30, 50, and 70° C. All six candidate films investigated demonstrated various degrees of sensitivity to the challenge gases at 30° C. DFPase was especially sensitive to the challenge gases at the lowest concentration measured (100 ppb). Only copper phthalocyanine and L-histidine dihydrochloride demonstrated

sensitivity at 50 and 70° C. In particular, 2-naphthol(β) showed complete reversibility and succinylcholine chloride and succinyl chloride demonstrated partial reversibility at 30° C. Copper phthalocyanine was sensitive and reversible only at 70° C. Succinylcholine chloride demonstrated a unique band-reject filter response to the presence of DFP in any challenge gas sample presented to the sensor.

EVALUATION OF AN INTERDIGITATED GATE ELECTRODE FIELD-EFFECT TRANSISTOR FOR DETECTING ORGANOPHOSPHORUS COMPOUNDS

I. Introduction

Background

The detection and measurement of environmentally-sensitive compounds has many widespread applications. The Air Force is particularly interested in sensing and measuring low concentrations of organophosphorus compounds (especially chemical warfare nerve agents), which have the ability to cross the blood-brain barrier. From a more encompassing perspective, the same sensing techniques could be used to detect and measure other organophosphorus compounds, including common pesticides, such as Parathion and Malathion (1:1). A method of sensing and identifying these chemical compounds using an Interdigitated Gate Electrode Field-Effect Transistor (IGEFET) has been under investigation at the Air Force Institute of Technology (AFIT) (2; 3; 4).

The Air Force is primarily interested in detecting organophosphorus compounds in order to prevent or minimize performance degradation of flight crews who may be exposed to low concentrations of the nerve agents during flight, battle field engagements, or at air bases where the aircraft are deployed. Studies on agricultural pilots (that is, crop dusters) have shown significant degradation in flying performance

after exposure to organophosphorus based pesticides (5), which are notably less toxic compared to the known chemical warfare organophosphate nerve agents.

The development of solid-state chemical sensors for measuring hazardous chemicals has several potential advantages compared to current detection methods. The sensor would likely be more rugged, less massive, smaller, and less expensive when produced in volume compared to the laboratory-grade instrumentation currently used. Numerous laboratories in several countries are currently experimenting with various solid-state sensor technological developments (6; 7; 8; 9).

The IGEFET's interdigitated gate electrode (IGE) structure consists of a metallized driven-electrode which is electrically isolated from the floating-electrode component that connects to the Metal-Oxide-Semiconductor Field-Effect Transistor's (MOSFET)'s gate contact, as shown in Figure 1. The driven- and floating-electrodes electrically interact via an applied chemical membrane. A pulsed-voltage excitation of the driven-electrode produces a characteristic low-pass filter response that is reflected in the MOSFET's corresponding amplified drain-to-source signal. The Fourier transform of the time-domain signal can be used to produce an equivalent frequency-domain representation of the signal (Figure 2). The Fourier transform of a time-domain signal contains an ensemble of frequency components that can be correlated with the state of the chemical reaction of the membrane which coats the interdigitated gate electrode structure.

The modified IGEFET investigated in this thesis research consisted of an interdigitated gate electrode structure which is composed of a driven-electrode and a floating-electrode component which are dielectrically-supported above a metal ground plane (metal level-1) to reduce the effects of electromagnetic noise on the structure and

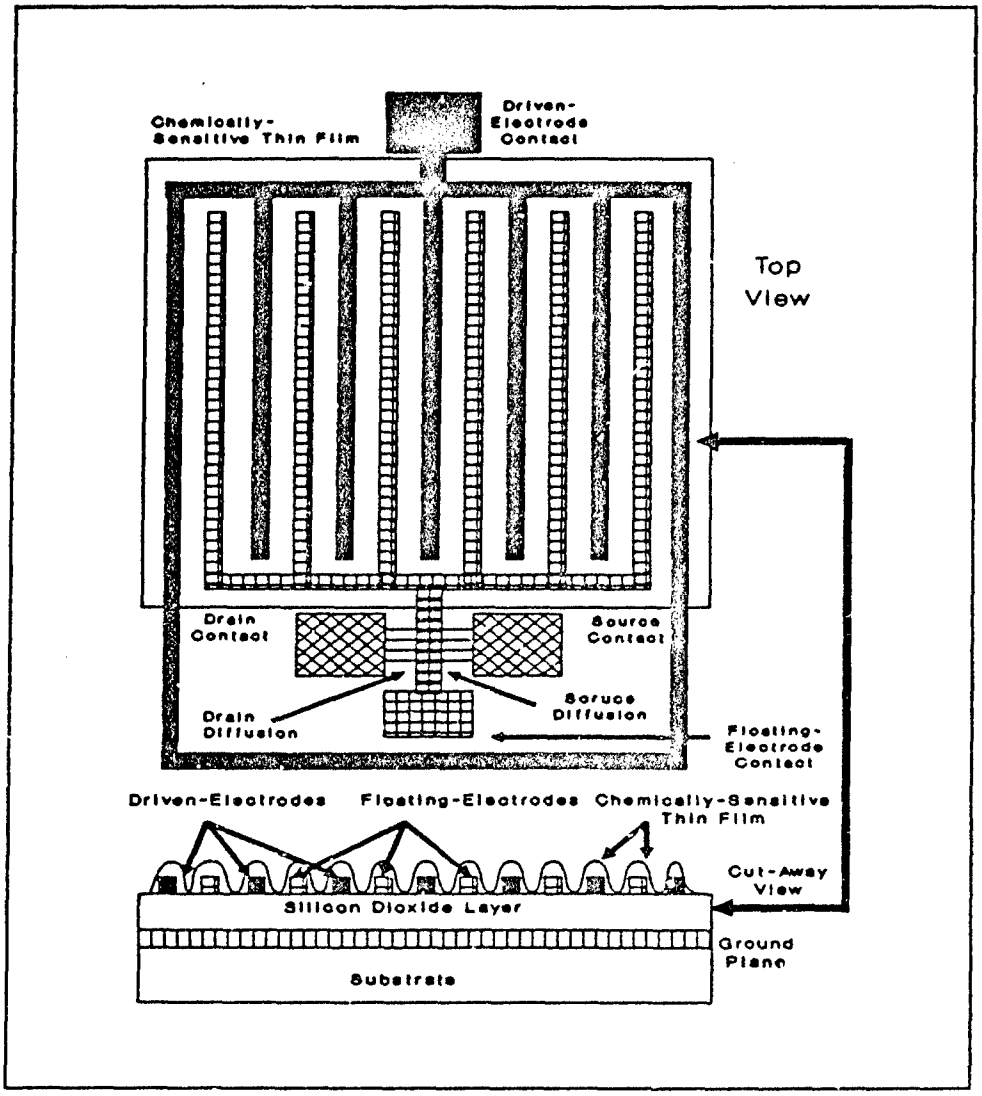

Figure 1. Interdigitated Gate Electrode Field-Effect Transistor (IGEFET) Physical Structure (2:I-3).

to provide a uniform ground plane, as shown in Figure 1. The uniform ground plane is desired to insure a constant ground plane coupling impedance from the driven-electrode and floating-electrode components to the microsensor substrate, eliminating the voltage dependance of the placing the electrode dielectric directly on the semiconductor

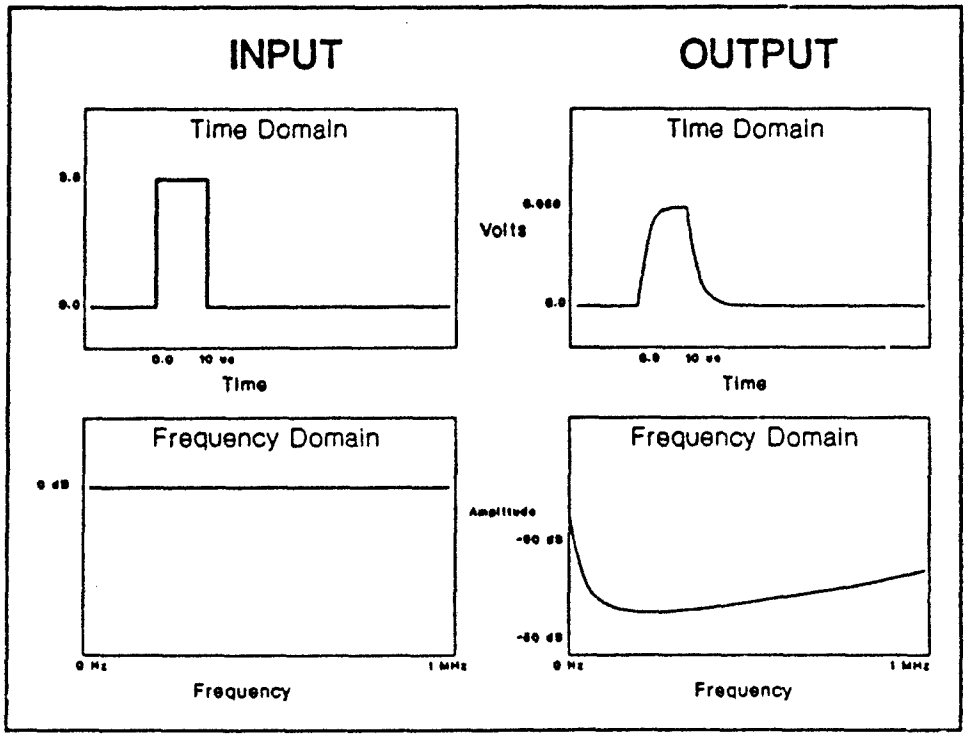

Figure 2. Illustrative Time-Domain Versus Frequency-Domain Response of the IGE Input and Output Signals.

substrate surface. The IGE structure is operated by applying a logic select signal to a demultiplexer on the microsensor's IC, see Figure 3. The output signal of the demultiplexer is passed to the appropriate selected driven-electrode. The floating-electrode component is connected to the gate contact of a conventional MOSFET. The MOSFET is then connected to a sense-element amplifier. The sense-element amplifier is connected to a multiplexer, and its output is branched to a final operational amplifier, and a voltage-follower stage.

The entire integrated circuit (IC) is fabricated using modular design concepts. The connections to each modular block of the integrated circuit are routed to an external pin

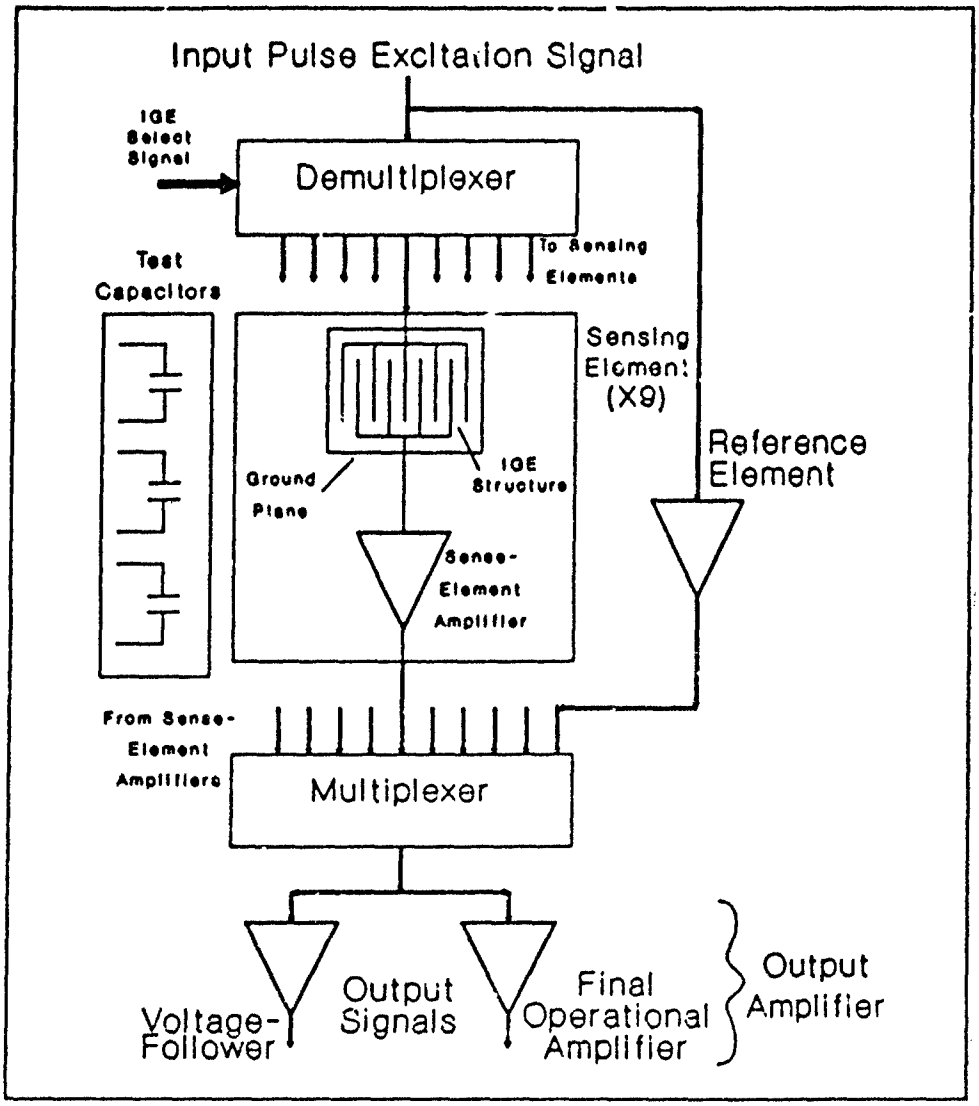

Figure 3. Interdigitated Gate Electrode Field-Effect Transistor Block Diagram.

or the 64-pin dual-inline-package (DIP) used to interface with the integrated circuit. Should any modular block of the integrated circuit fail to operate, the modular block can be bypassed by cutting the node link and then connecting the node via a circuit bond pad to an external equivalent circuit function.

Problem Statement

The interdigitated gate electrode field-effect transistor (IGEFET) has been shown to be capable of detecting trace quantities of organophosphorus compounds (3). Current research is focused on investigating if the IGEFET sensor is capable of discriminating the components in a multiple gas mixture. This thesis evaluated the capabilities of the IGEFET to measure discrete concentrations of diisopropyl fluorophosphate (DFP), diisopropyl methylphosphonate (DIMP), dimethyl methylphosphonate (DMMP), and binary mixtures of these gases.

History of Development

An IGEFET is a MOSFET with an interdigitated gate electrode structure which has a chemically-sensitive film applied on and between the driven- and floating-electrode components, see the cutaway view for the chemically-sensitive thin film, as shown in Figure 1. Thesis research at AFIT has investigated this device for use as a solid-state sensor for detecting several environmentally-sensitive compounds. Captain John Wiseman demonstrated the feasibility of using an IGEFET to detect trace quantities of DIMP, a chemical warfare nerve agent analog compound (simulant) (2). Captain Jenny Shin expanded the evaluation of the IGEFET by characterizing the microsensor's response to DIMP and DMMP (another chemical warfare nerve agent analog compound) (3).

Scope

This thesis research consisted of three major sections. First, the IGEFET has been redesigned. A three-by-three, two-dimensional matrix of the IGEFET sensory elements incorporating the interdigitated gate electrode (IGE) structure, as shown in Figure 4, was designed with individual preamplifiers (sense-element amplifiers) attached to each sensing element to provide an impedance match to the chemically-sensitive film. In addition to the nine IGEFET sensing elements, there is a reference element included on the IC die. A solid metal ground plane of aluminum (metal level-1) is sandwiched between the semiconductor substrate and the silicon dioxide dielectric which supports the interdigitated gate electrode structure, see Figure 1. Three test capacitors are located on the IC die to determine the oxide's thickness. Included in the design are a demultiplexer, IGE sense elements, sense-element amplifiers, a multiplexer, and an output amplifier composed of a final operational amplifier and a voltage-follower stage (Figure 3). The sense-element amplifiers, multiplexer, and output amplifiers are designed to provide an impedance match between the various functional elements and to yield sufficient gain over a bandwidth of 800 kHz.

Second, a completely new test cell was designed for evaluating the IGEFET response to the different gases and their mixtures, as shown in Figure 5. The new test cell consists of a chemically-nonreactive, stainless-steel, challenge gas test chamber which also shields the microsensor from external electromagnetic interference. The test chamber is mounted on an aluminum panel box which contains 64 BNC connectors which provide noise-free connections to each pin on the 64-pin DIP which contains the microsensor under evaluation. Each BNC center conductor is connected to one pin on

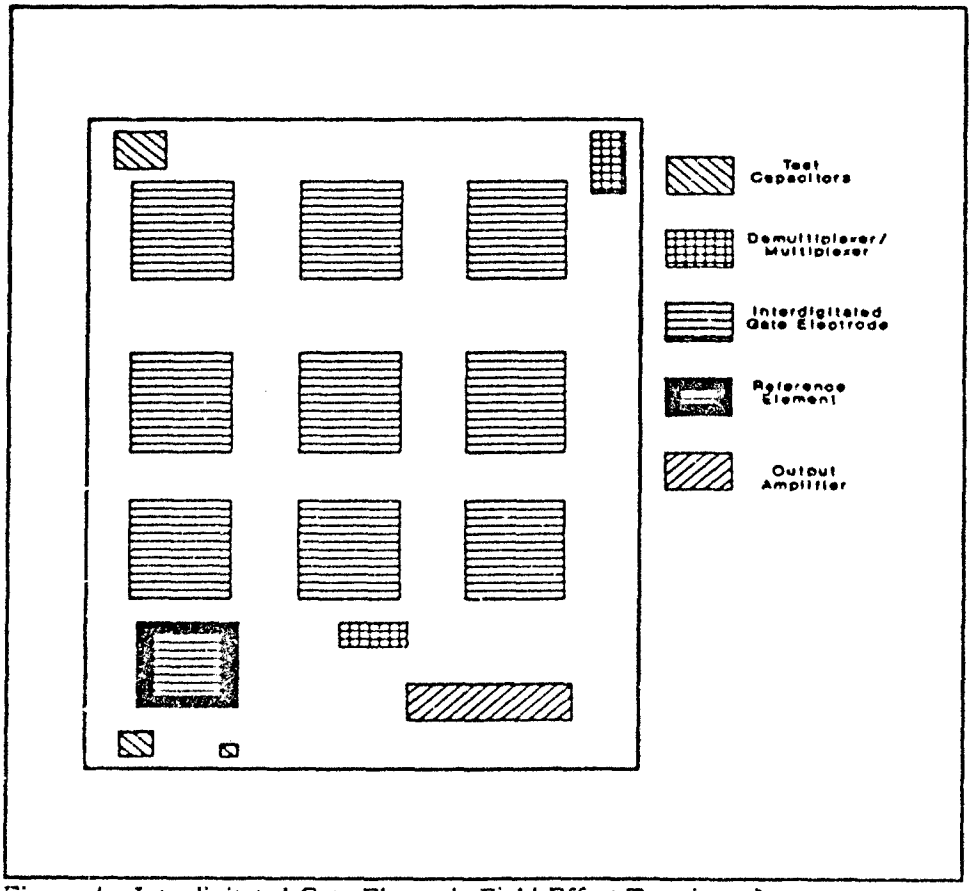

Figure 4. Interdigitated Gate Electrode Field-Effect Transistor Layout.

the 64-pin DIP socket using 50Ω RG-174 coaxial cable. Each coaxial cable is grounded to the aluminum panel box at both ends to minimize ground loops and to reduce the cross-talk between a set of connections.

Third, several different chemically-sensitive thin film candidates were deposited on the interdigitated gate electrode structures in the form of thin film membranes. The candidate materials included: copper phthalocyanine, 2-naphthol(β), L-histidine dihydrochloride, succinylcholine chloride, succinyl chloride, and DFPase. Copper phthalocyanine has been used as a candidate material by many researchers, including

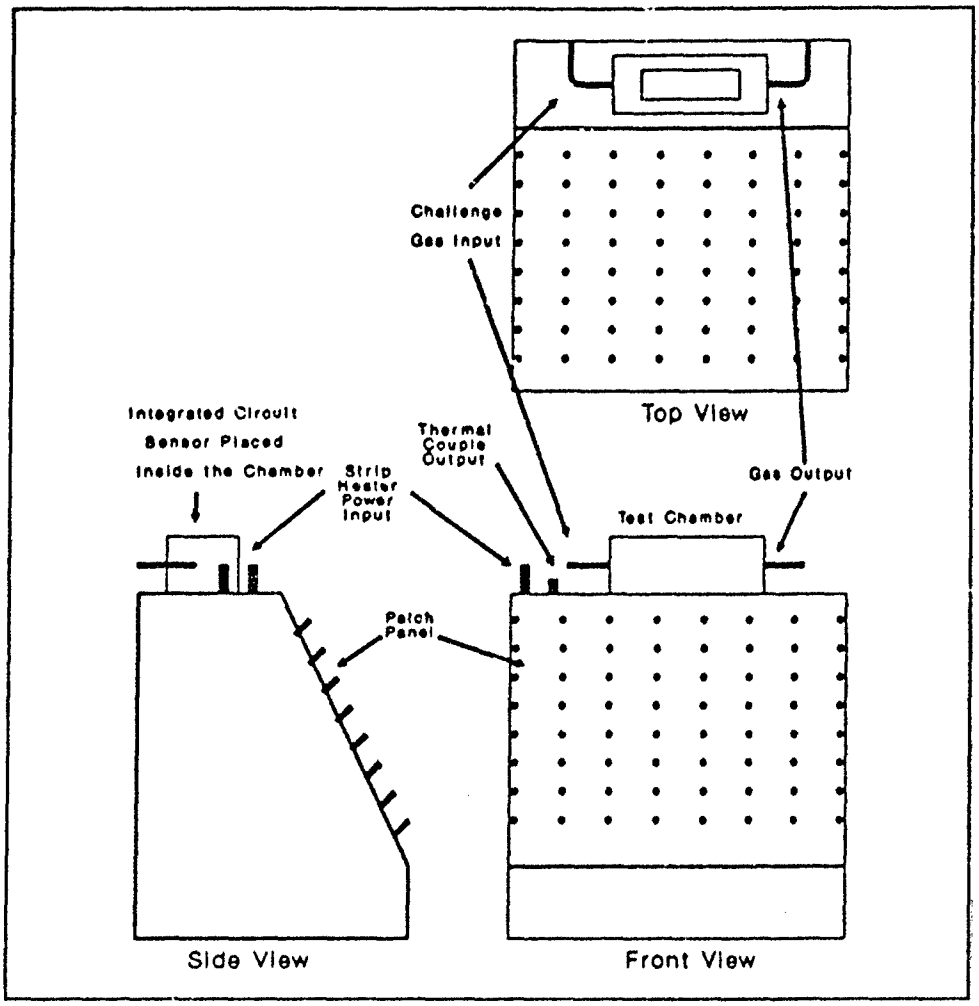

Figure 5. Interdigitated Gate Electrode Field-Effect Transistor Test Cell.

Captain John Wiseman, Captain Jenny Shin, and Captain Thomas Jenkins (2; 3; 4). The 2-naphthol(β), L-histidine dihydrochloride, succinylcholine chloride, and succinyl chloride materials were all used as candidate membranes in experiments conducted by Captain Jenny Shin (3). In those initial experiments, the film deposition process was crude, and thickness was not controlled. In Captain Shin's research, as many as four different organic thin film membranes were applied to each IGEFET device and

evaluated to discern a characteristic frequency-domain signature for each specific gas while various environmental parameters were varied. Tests were conducted with the IGEFET being operated at a temperature of 25° C. The challenge gases were delivered to the test chamber at room temperature: DIMP was delivered at 7.5 ppm, and DMMP was delivered at 3 ppm (3). The relative humidity of the challenge gas atmosphere in the test chamber was not reported.

For this research effort, one of the six chemically-sensitive thin film candidates was applied to each IGEFET microsensor element; this arrangement facilitated evaluating each thin film candidate in every challenge gas test at 30° C. A subset of the thin film candidates (copper phthalocyanine, L-histidine dihydrochloride, and DFPase) were evaluated at 50° C, and copper phthalocyanine and L-histidine dihydrochloride at 70° C. Redundancy testing was accomplished by applying some of the thin film candidates to more than one IGEFET microsensor element. For all evaluations, the challenge and purge gas was delivered at room temperature (23° C) with the relative humidity set at 90 percent.

This investigation also included the evaluation of six different membranes with each deposited on an individual IGE structure in the IGEFET microsensor. A comparison of the differences in the time-domain signals using an oscilloscope (Hewlett-Packard, Model HP 54100A, Palo Alto, CA 94304), spectral signals using a spectrum analyzer (Hewlett-Packard, Model HP 8556B, Palo Alto, CA 94304) and gain-phase analyzer (Hewlett-Packard, Model HP 4194A, Palo Alto, CA 94304) over a frequency range extending from 10 Hz to 1 MHz. A block diagram of the test equipment configuration is provided in Figure 6. The different chemically-sensitive thin films were

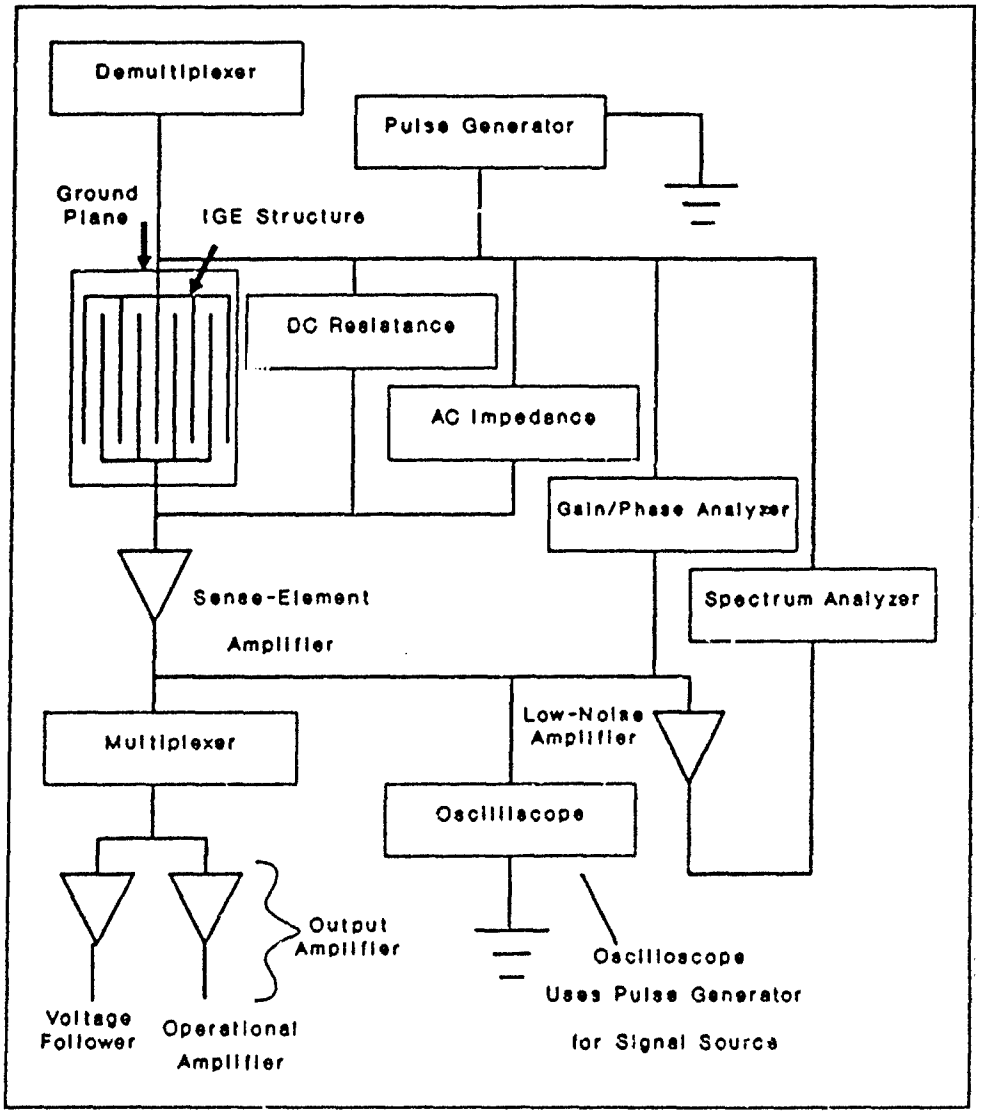

Figure 6. Test Configuration for Evaluating the Interdigitated Gate Electrode Field-Effect Transistor.

evaluated based upon their sensitivity and selectivity to determine the best combination of films for detecting a particular organophosphorus compound or mixture of compounds. Fourier transform analysis was performed on the data to determine if useful selectivity results could be discerned. Fourier transform analysis allows the

signal changes caused by the low-pass filtering effects of the thin films applied to the IGE structure to be quantified. Subtle differences in the time-domain representation of the IGE output can manifest themselves as dramatic changes in the corresponding frequency-domain representation of the IGE output (Figure 2).

Areas of interest in the Fourier transform analysis included: determining the sensitivity to the challenge gas concentration, selectivity to the various challenge gases, and finally, the reversibility characteristics of the IGEFET membrane. The environmental parameters against which the IGEFET sensors were evaluated included: temperature, humidity, and challenge gas concentration (DIMP, DMMP, and DFP). Reversibility for each challenge gas exposure was evaluated by using a purge of filtered laboratory air. The laboratory air purge simulated the effect of the IGEFET being removed from the challenge gas environment. The IGEFET's response, when repeatedly exposed to a challenge gas, was also evaluated.

The IGEFET was tested initially with individual challenge gases. Signatures produced by the IGEFET in response to the individual gases were evaluated, and unique differences were noted. The IGEFET was then evaluated using binary multi-component gas mixtures to generate signature specificity data. For the IGEFET to be immediately useful for analyzing multi-component gas mixtures, its response signature should approximate the superposition of the sum of the signatures generated by using individual challenge gases.

Assumptions

This study initially assumed that the IGEFET, the deposited chemically-sensitive thin films, and the microsensor's reaction with the challenge gases operate as a linear, time-invariant system. This assumption of linearity permits the principle of superposition to be applied in the initial analysis. This assumption is necessary if two signals are to be added to form a composite response, which implies that the transfer function of the system is independent of the magnitude of the input signals (3:I-5).

Real systems, however, are seldom totally linear or time-invariant. Nevertheless, any system that is continuous and differentiable may be considered linear over a sufficiently small range of input values. While real-world systems are not usually linear or time-invariant, it is common practice to model these systems as being linear knowing that, if the range of operation is very large, errors will occur causing the real and modeled values to diverge. Therefore, any non-linear system may be considered to be linear if variations of the input signal are kept sufficiently small, allowing superposition to apply (2:I-7). Careful control of the input signals was necessary to insure the nonlinear effects remained small in the IGEFET. This assumption was critical if the IGEFET was to be useful for discriminating different gases when a mixture of the gases occur in the challenge atmosphere.

The issue of time invariance required that the IGEFET's response be allowed to stabilize after exposure to the challenge gas and before the measurements were accomplished. Previous experience has indicated that stabilization scans last a few seconds to several minutes (3; 4).

Methodology

The IGEFET design used in this research was modified from that used by Captain Thomas Jenkins (4). The revised IGEFET design was accomplished by Captain Thomas Graham, and it includes the following features: a 3 × 3 matrix of interdigitated gate electrodes, a conventional MOSFET reference element, a sense-element amplifier, a multiplexer, a final operational amplifier, a voltage-follower stage, and an IGE aluminum ground plane (metal level-1) to reduce noise and control the interdigitated gate electrode to substrate capacitance (Figure 4). The MOSFET reference element was used for temperature compensation by using its signal as a baseline to which the outputs of the IGE microsensor structures were normalized. After completing the redesign phase, the Metal Oxide Semiconductor Implementation Service (MOSIS) was used to fabricate the integrated circuit (IC).

Discussions with Captain Jenny Shin and Captain John Wiseman indicated a need for redesigning the IGEFET test cell (10; 11). Particular attention was taken to eliminate the stray electromagnetic interference problem by shielding the test cell and the lead wires emerging from the cell. Data from the previous research indicates that extraneous noise corrupts the data at frequencies below 1 kHz (4:V). The bulk of the low-frequency noise is likely due to the 60 Hz harmonics from the IGEFET power supplies, test instrumentation, and laboratory lighting.

New chemically-sensitive thin film deposition masks were fabricated to match the IGE configuration used in the revised IGEFET sensor design. Mask fabrication involved machining a steel bar to the dimensions of the array element. The steel bar was then used as a punch to produce the proper sized hole in an aluminum foil mask.

Deposition of the films on the IGEFET involved two techniques. In the first technique, the copper phthalocyanine thin films were deposited using an electron-beam vacuum evaporation process (Electron-Beam Vacuum Deposition System, Denton Vacuum, Model DV-602, Cherry Hill, NJ 08003). In the second technique, the organic materials (2-naphthol(β), L-histidine dihydrochloride, succinylcholine chloride, succinyl chloride, and DFPase) were applied with an external mix airbrush using nitrogen as the propellant. To apply L-histidine dihydrochioride and succinylcholine chloride, a mixture of 80% deionized water and 20% isopropyl alcohol was used as a carrier (3:I-9). To apply 2-naphthol(β), acetone was used a carrier (3:I-10). No carrier was required to apply DFPase and succinyl chloride since both are liquids at room temperature. The thickness of the organic films was determined using the interferometer configured microscope; errors in the measurements are estimated to be on the order of 100 angstroms.

Evaluating the IGEFET's performance consisted of two phases. The IGEFET, as received from MOSIS, was evaluated for compliance with the design specifications. After insuring that the IGEFET satisfied the specifications, the sensors were fabricated and used for data collection. For those IGEFETs that did not satisfy the design specifications, modifications were implemented to facilitate using the functional sections of the IC. This option was readily executed due to the modular design of the IGEFET IC.

Past research indicated that elevated temperatures are necessary to obtain reversibility of the IGEFET when the metal-doped phthalocyanines are used as the chemically-sensitive thin film. Captain Jenny Shin's research indicated that minimal

reversibility below 70° C was achieved. Since these high temperatures are incompatible with DFPase, when temperatures higher than 50° C were used, DFPase was not considered in the reversibility test.

The chemically-sensitive films were deposited with nominal thicknesses of 1000 angstroms and 2000 angstroms. No previous research has been reported concerning the influence of thickness for the organic films (2-naphthol(β), L-histidine dihydrochloride, succinylcholine chloride, succinyl chloride, and DFPase). Research concerning the copper phthalocyanine material suggests the best results are obtained with films just slightly thicker than 500 angstroms (3:V-41). One possible explanation for this minimum thickness requirement is the extremely high impedance associated with very thin films (<500 angstroms). Information provided by Captain Thomas Jenkins and Captain Jenny Shin indicates that very thin films have DC resistances in excess of 100 GΩ, which is on the order of the gate contact impedances of the MOSFETs in the IGEFET. This feature causes the very thin films to appear as open circuits, and small changes in the film's conductivity becomes unmeasurable (3; 4).

Tests were conducted with the IGEFET being operated at temperatures of 30, 50, and 70° C with the challenge gas relative humidity set to 90% at room temperature (23° C). During elevated temperature tests of the IGEFET, the effective relative humidity at the IGEFET interface was lower, since the challenge gases were supplied to the test chamber at room temperature. The challenge gas concentrations were: one hundred parts-per-billion (ppb), one part-per-million (ppm), and ten ppm (three ppm for DFP).

Spectral analysis of the IGEFET's response was accomplished over frequencies spanning 10 Hz to 1 MHz, with the lower end of the frequency range being limited by the spectrum analyzer capabilities. The interdigitated gate electrode's response was evaluated to discern changes in its time-domain response using an oscilloscope, and its DC resistance was evaluated using an electrometer and AC impedance was evaluated using a gain-phase/impedance analyzer (to include the resistive component and reactive component). The frequency-domain response of the IGEFET was measured using the spectrum analyzer (Hewlett-Packard, Model HP 4195A, Palo Alto, CA 94304) and an amplifier (Low-Noise Amplifier, Stanford Research Systems, Model SR560, 1290-D Reamwood Avenue, Sunnyvale, CA 94089) to provide impedance matching. The IGEFET's response was characterized for its time-domain response which included: time delays, waveform shape changes, and magnitude changes. The corresponding frequency-domain responses were evaluated to discern changes in the spectral signature, along with the behavior of the gain and phase responses. The reference element was used to normalize the output from the IGEFET containing the chemically-sensitive thin film being evaluated. After the initial testing, differential signals between those IGEFETs containing the different chemically-sensitive thin film membranes were analyzed and compared to determine if the IGEFET sensor can be used to discriminate the components of a gas mixture.

Plan of Development

Chapter II reviews the current literature concerning organophosphorus compound effects on human physiology and solid state sensors which have been applied to detect

organophosphorus compounds. A discussion regarding the chemically-sensitive thin films that were evaluated in this thesis is also included. Chapter III discusses the revised design of the IGEFET and the test cell used in the performance evaluation of the microsensor. Chapter IV describes the methods of depositing the chemically-active thin films, experimental methodology, and the microsensor's electrical response data collection process. Chapter V reports the data reduction and analysis techniques, as well as the findings and results. The conclusions and recommendations are presented in Chapter VI.

II. Literature Review

Introduction

The detection of certain organophosphorus compounds, especially chemical warfare nerve agents, is of extreme importance to the military due to their potential use in theater warfare. There are very accurate analytical methods for measuring the presence and concentration of organophosphorus compounds, the most accurate being the gas chromatograph with demonstrated sensitivities to organophosphorus compounds of one nanogram, which corresponds to approximately 15 parts-per-billion (ppb) for gas sample sizes of 10 milliliters (12). However, this equipment is expensive, bulky, and weighs on the order of 12 pounds (12; 13). The military needs to develop a chemical warfare nerve agent detector that is simple to operate, light weight, and inexpensive. The development of solid state sensors capable of detecting and measuring organophosphorus compounds appears to be the technological answer to this critical need. The solid state sensors could possibly be manufactured in very small packages, requiring little electrical power, and one can envision the whole sensor and associated electronics being worn on a soldiers' uniform or possibly on the wrist, much like a wrist watch (8).

This chapter reviews the toxicological background information concerning organophosphorus compounds, different types of solid state sensors, and the thin films which have been applied to microsensors to detect the nerve agent analog compounds. An extensive background on various solid state chemical sensors is presented in Captain Jenny Shin's thesis for the interested reader (3).

Organophosphorus Compounds

There are several toxic organophosphorus compounds of interest to the military. These toxic organophosphorus compounds inhibit the cholinesterase (ChE) enzyme which regulates nerve action. The compounds of interest in this research, diisopropyl fluorophosphate (DFP), diisopropyl methylphosphonate (DIMP), and dimethyl methylphosphonate (DMMP), are analog compounds of the more toxic organophosphorus compounds, such as tabun (GA), sarin (GB), soman (GD), and the V-agents. The chemical structure of several of these organophosphorus compounds are shown in Figure 7. Each compound has a central phosphorus atom with a cationic charge which is double bonded to an oxygen atom. This bond is broken when the phosphorous atom in the compound combines with the ChE enzyme.

Certain organophosphorus compounds are extremely potent ChE enzyme inhibitors in the human body, making them very toxic. The ChE enzyme hydrolyses acetylcholine (ACh) in the human body and produces choline and acetic acid as shown in Figure 8. The normal function of the biochemical process is for the ChE enzyme to terminate the ACh's nerve firing actions at the synaptic junctions. The ChE enzyme, in simple terms, acts as a governor and terminates the firing action of a nerve by converting the ACh and water into choline and acetic acid after the nerve junction has fired (13).

Toxic organophosphorus compounds are those that form a subset of certain alkoxy groups that contain a doubly-bonded oxygen or sulfur atom which readily reacts with the phosphorus atom bonding with the ChE enzyme (Figure 8). When the ChE enzyme is bonded with the nerve agent, the enzyme becomes inhibited and is unable to hydrolyze the acetylcholine. When this happens, the ACh begins to accumulate at the nerve

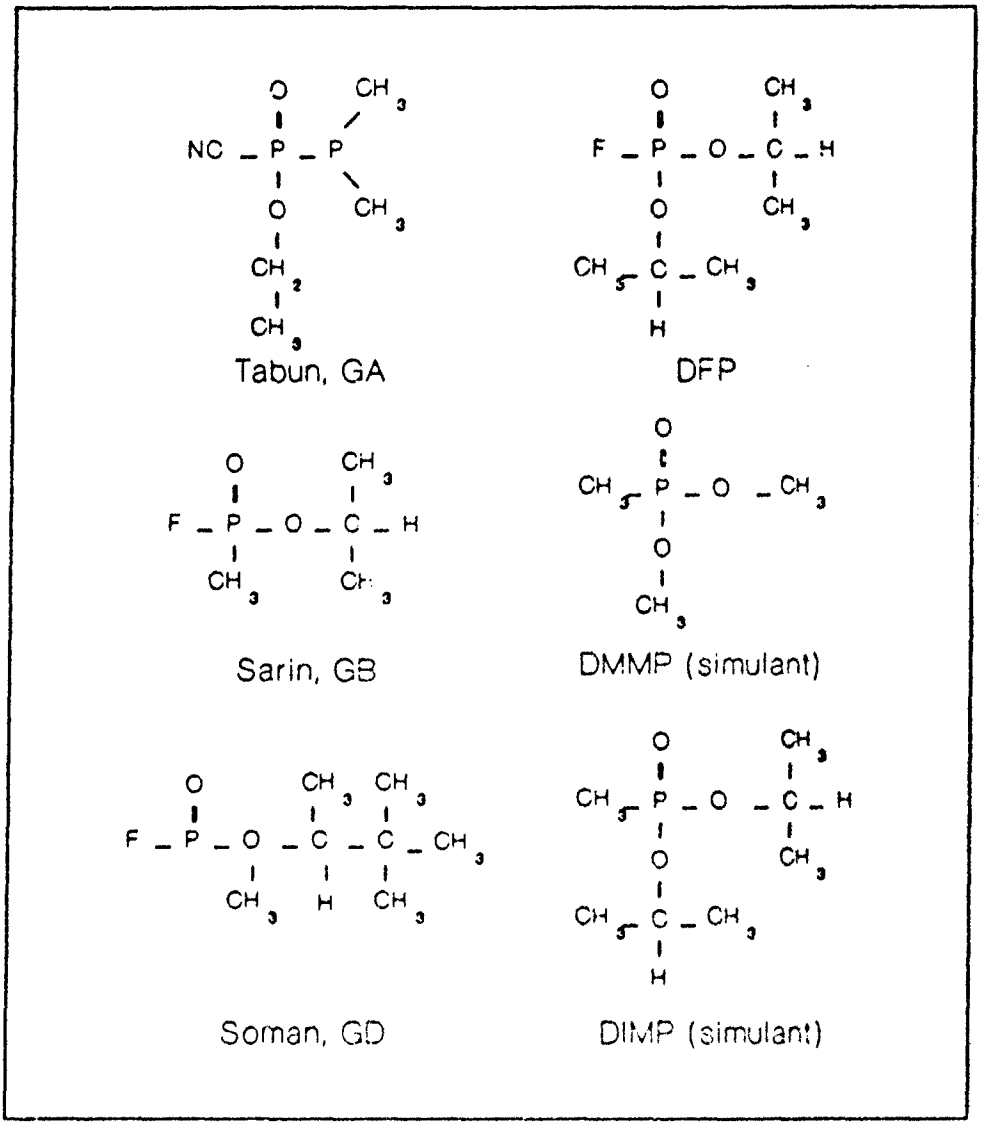

Figure 7. Representative Toxic Organophosphorus Compound Chemical Structures (3:II-3).

receptor sites to a sufficient degree so as to induce desensitization of the receptor sites, and this condition causes a state of continuous nerve firing. This poisoning action by the organophosphorus compound causes the following symptoms: increased fluid

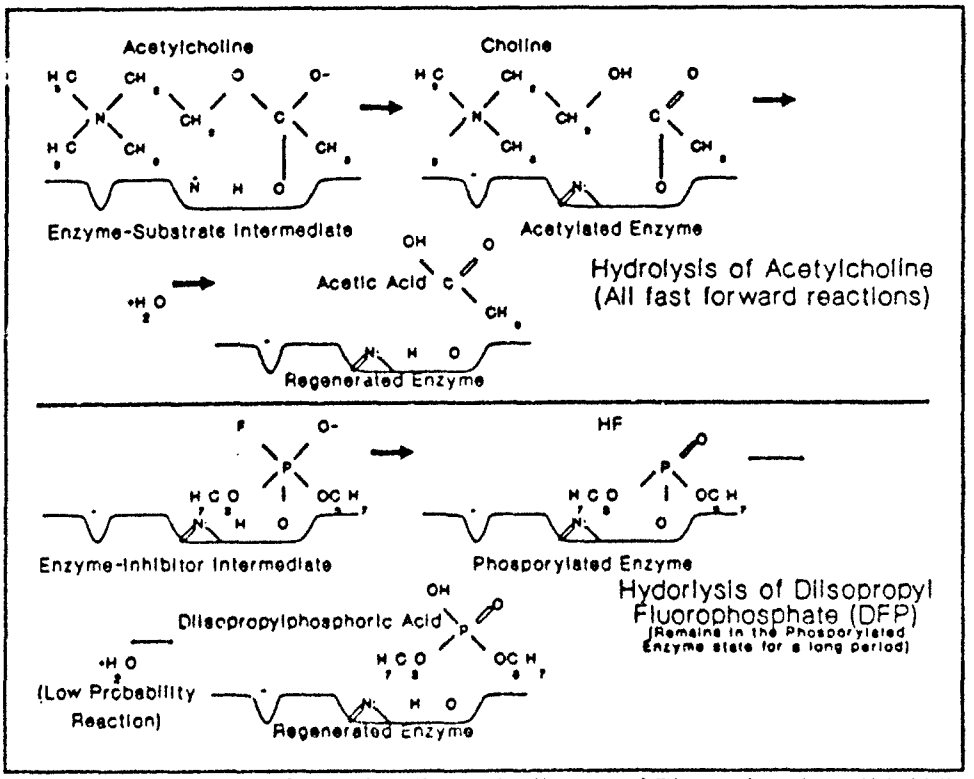

Figure 8. Hydrolysis of Acetylcholine and Diisopropyl Fluorophosphate (14:444).

secretion, gastrointestinal disturbance, miosis (severe constriction of the pupils), tremors, convulsions, and finally death through anoxia. Death by anoxia (loss of oxygen to vital tissues) is attributed to a combination of factors such as central respiratory paralysis, severe bronchoconstriction, and paralysis of the accessory muscles of respiration (6:97-108).

The detection of the toxic organophosphorus compounds is currently accomplished with a series of chemicals that react with and change their chemical structure upon exposure to the compound of interest. The change in chemical structure manifests itself in one of three forms. The chemical may: gain mass, change electrical behavior, or

change color. Sensors that indicate the presence of chemical species using color change include: sugar sensors (used by diabetics), ph sensors, alcohol sensors, etc. The discussions in this thesis will be limited to several of the solid state sensors that detect chemical species through changes in mass or electrical behavior.

Solid State Chemical Sensors

There are two classes of solid state detectors currently being investigated for the detection of toxic organophosphorus compounds. The first class of detectors measure a change in mass of the detectant chemical. These detectors include electrochemical sensors, piezoelectric quartz crystal microbalance sensors, and surface acoustic wave (SAW) devices. Many experiments were conducted in the seventies and early eighties on various electrochemical and piezoelectric crystal sensors. However, recent investigators have focused on the SAW device with an applied chemical sensing film for detecting the toxic organophosphorus compounds (7; 8:36; 15:34R).

Piezoelectric Devices. Piezoelectric sensors depend upon the change in crystal frequency associated with the change in mass of the piezoelectric crystal structure. Like any physical structure, the piezoelectric crystal structure has a natural resonant frequency of oscillation. This crystal can be made to oscillate by exciting it with an electrical excitation signal which modulates its amplitude at the crystal's fundamental oscillation frequency. The piezoelectric device is used as a chemical sensor because the applied film adsorbs the detectant species, which increases the mass of the piezoelectric

crystal structure and correspondingly decreases the oscillation frequency by a measurable amount, as indicated in the following empirical equation (7:2-3):

$$\Delta F = -2.3 * 10^6 * F^2 * \frac{\Delta m}{A} \quad (1)$$

where, ΔF is the change in the natural resonant frequency in Hertz, F is the natural resonant frequency in Hertz, Δm is the change in mass in grams, and A is the detector's surface area in cm^2.

The piezoelectric sensor relies upon the applied chemically-sensitive thin film to adsorb a particular chemical in the environment to cause a decrease in the piezoelectric crystal's oscillation frequency. As noted by Jenkins (4), piezoelectric sensors may be very sensitive, on the order of ppb. However, there is a major problem with regard to selectivity. To be selective the chemically-sensitive thin film must be very selective in its adsorption of the challenge gas. Additionally, any contaminant, such as the condensation of moisture or volatile chemicals, can change the mass of the piezoelectric sensor's chemically-sensitive thin film to the extent that the sensor becomes saturated and is unable to measure the desired chemical species.

Surface Acoustic Wave Devices. In 1986, Susan Rose-Pehrsson and David Ballantine conducted a series of tests using an array of SAW devices which had different chemical coatings (7) (Figure 9). The SAW device operates similar to the piezoelectric device described above. The SAW's resonant frequency decreases whenever the chemically-sensitive thin film absorbs a detectant species. When a particular chemically-sensitive thin film absorbs an organophosphorus compound, the film increases in mass,

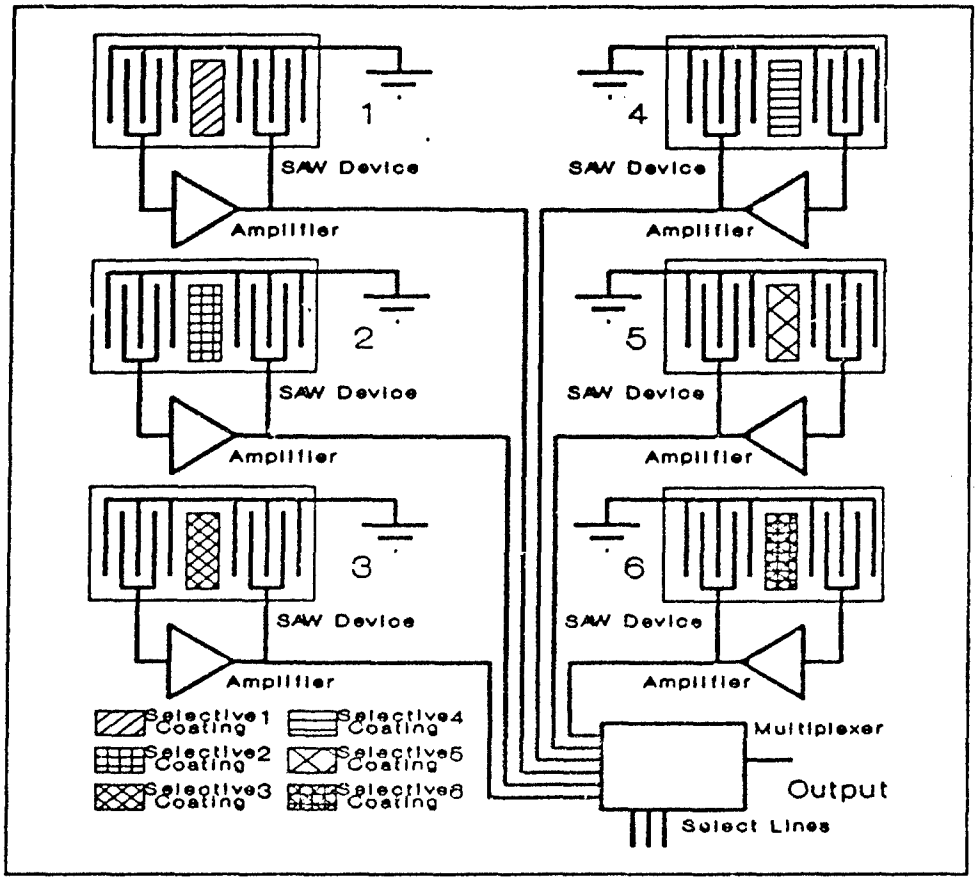

Figure 9. Six-Element Surface Acoustic Wave (SAW) Device (4:420).

which decreases the oscillation frequency of the SAW device. By combining eleven SAW devices, each coated with a different chemically-sensitive thin film, these researchers were able to detect different organophosphorus compounds in a gas mixture (7:421).

Several different coatings are required for the SAW device to be sufficiently selective to detect particular compounds (16). In the Rose-Pehrsson experiments, a total of twelve different sensor coatings were evaluated using eleven different test gases. By using cluster analysis on the sensor data, the investigators were able to determine a

particular gas or mixture of gases being evaluated. One difficulty in the experiment was the variability in coating quality. Sensitivity and selectivity varied dramatically between the different batches of sensors evaluated (7:421-427). While the results are not conclusive, the concept of using multiple sensor elements to measure a gas or mixture of gases warrants attention.

As noted by Jenkins (4:II-5), SAW devices suffer from the same problems as the piezoelectric devices because contaminates can swamp the device and negate its usefulness for measuring the desired chemical species. This limitation can render the device useless in field conditions.

The second class of solid state sensors use the changes in DC resistance as well as AC impedances that occur in a sensing thin film to detect particular organophosphorus compounds. The critical advantage this class of sensors has, compared to the sensors that rely on mass change, is greater selectivity using fewer sensor elements (17:110). There are several types of sensors that use this method of detecting organophosphorus compounds. These sensors include the chemically-sensitive field-effect transistor (CHEMFET), chemically-sensitive resistor, multi-layered interdigitated devices, and the IGEFET (2; 3; 4; 5; 18; 19; 20).

Chemically-Sensitive Field-Effect Transistor. The first device investigated, the CHEMFET, uses a chemically-sensitive film placed on the gate oxide of a field-effect transistor (FET). This device relies upon the chemical reaction between the chemically-sensitive thin film and the challenge material to create ions at the thin film's interface

with the gate oxide which causes a change in the drain to source conductance in the FET. The CHEMFET's gate voltage equation is given by the following equation:

$$v_M=\phi_g+\phi_i+\phi_s \qquad (2)$$

where v_M is the bulk gate potential, ϕ_g is the potential resulting from a sheet charge at the film interface with the gate oxide, ϕ_i is the potential dropped across the insulator, and ϕ_s is the potential across the gate oxide and semiconductor interface. Early CHEMFETs were operated in a direct current mode and measurements were made associated with changes in I_{DS}. Later versions of the device were operated using a sinusoidal input signal and a feedback electrode to excite resonant frequencies in the sensing device (Figure 10). The primary problem with this device is that the sensor is very sensitive to external noise due to the imperfect gate oxide dielectric and the weak reaction of most sensor chemicals. Any noise impressed across the circuit's high impedance gate contact makes the sensor very sensitive to external noise.

Chemically-Sensitive Resistor. A chemically-sensitive resistor (chemiresistor) is a device in which an interdigitated metal electrode structure is deposited on an insulating substrate and a chemically-sensitive thin film then is applied to the interdigitated electrodes (Figure 11). Use of the device involves monitoring changes in the film's electrical conductivity when the chemiresistor is exposed to a challenge gas. Chemiresistors have been fabricated using chemically-sensitive thin films of metal doped phthalocyanine and copper + cuprous oxide (4; 17; 20). The first generation

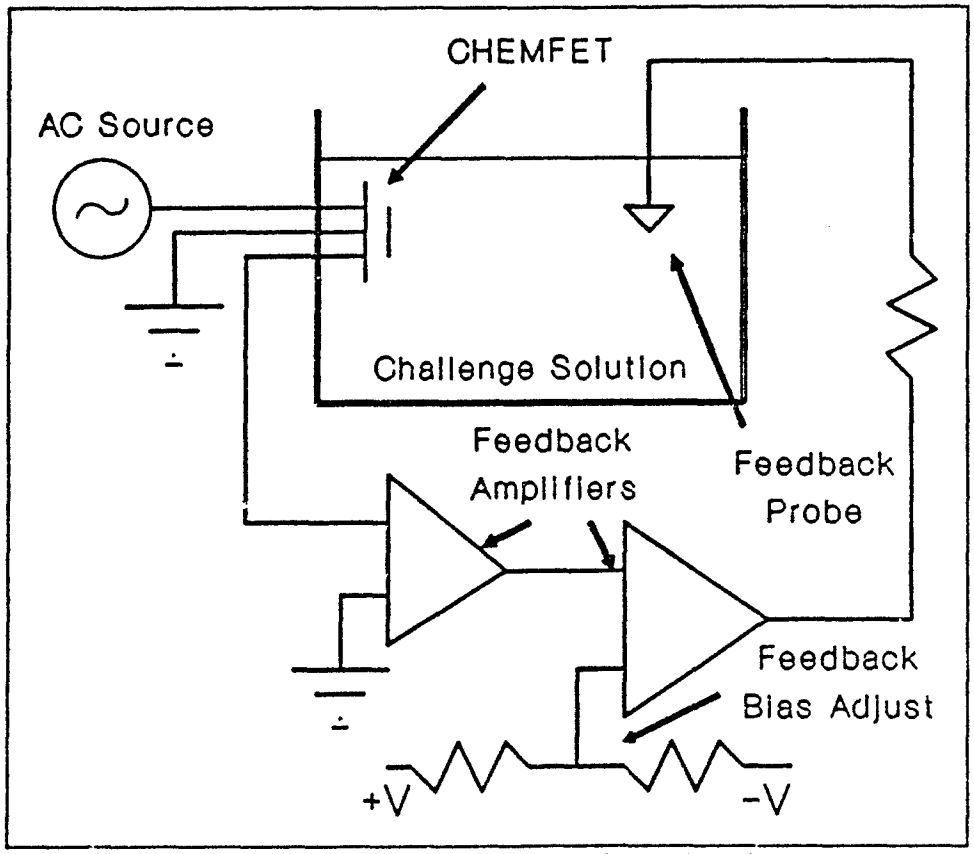

Figure 10. Chemically-Sensitive Field Effect Transistor (Sinusoidally Driven) (22).

chemiresistors were evaluated for their direct current behavior, while later generations expanded the use of the chemiresistor to monitor the changes in AC impedance when the device is exposed to a challenge gas (20).

Multilayered Interdigitated Devices. To minimize some of the disadvantages of the early CHEMFETs, two devices have been developed, the multi-layer interdigitated device and the IGEFET. The multi-layer interdigitated device incorporates a gas-sensitive thin film which is applied to a planar electrode; next, a thin interdigitated

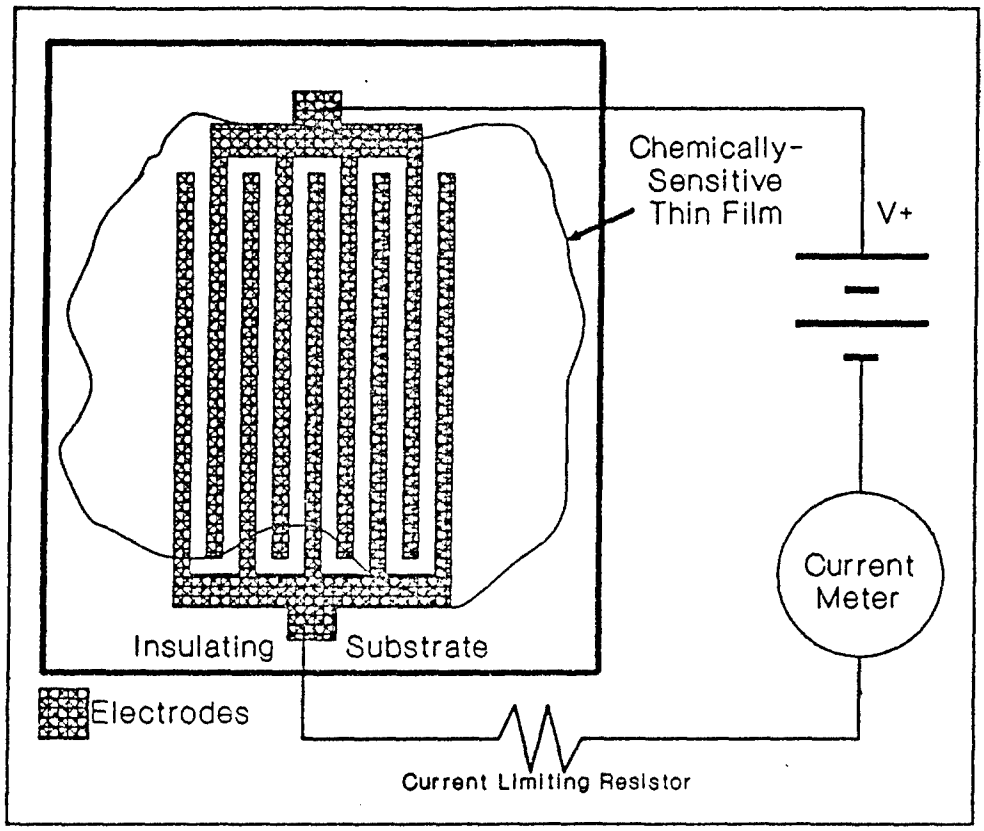

Figure 11. Chemically-Sensitive Resistor Structure (2-D:1175).

electrode is applied to the surface of the chemically-sensitive thin film (Figure 12). This configuration significantly increases the effective gas-sensing surface area which, in-turn, yields increases in sensitivity several orders of magnitude greater than that attained with the standard CHEMFET configuration (9:33). The primary difficulty with this microsensor configuration is its fabrication complexity, which limits the type of gas-sensitive thin films that may be used. Since the top interdigitated electrode is deposited using a vacuum evaporation process, many organic gas-sensitive thin films, including 2-naphthol(β), L-histidine dihydrochloride, succinylcholine chloride, succinyl chloride,

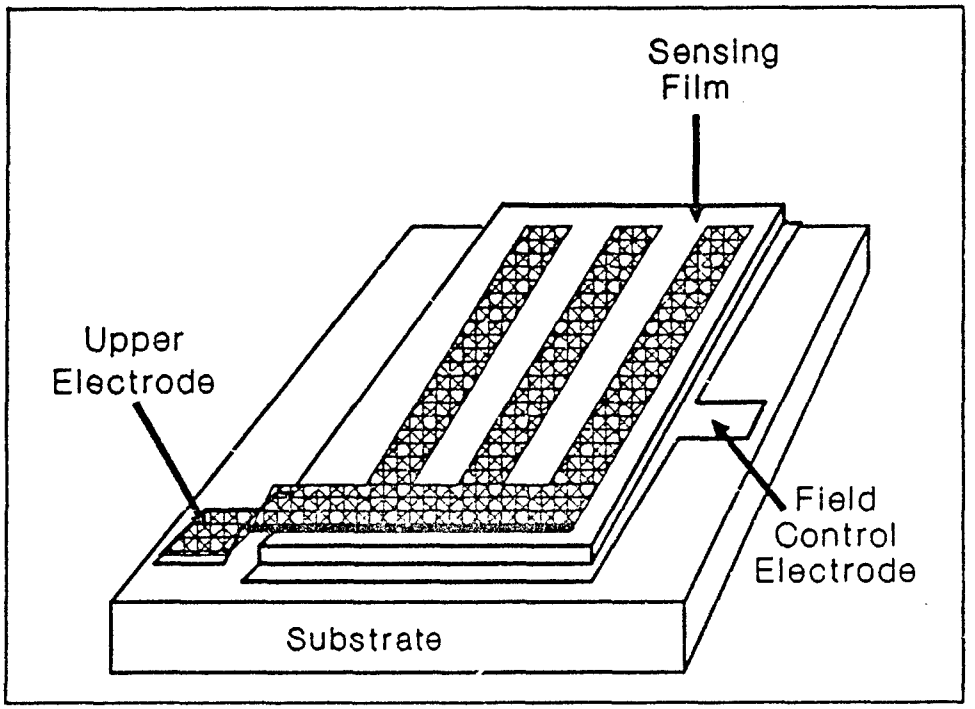

Figure 12. Multi-layered Interdigitated Electrode Chemical Sensor (10:32).

and DFPase, cannot be used because their chemical sensitivity would be compromised by the deposition process of the upper electrode on the chemically-sensitive thin film (9:37). This configuration poses no problem when working with the metal-doped phthalocyanines, since they will survive the electrode's vacuum evaporation deposition process. The fabrication methods used for multilayered interdigitated devices, therefore, limit the potential chemically-sensitive thin film candidates.

Interdigitated Gate Electrode Field Effect-Transistor. The IGEFET is solid-state device that was evaluated in this investigation. One major advantage of using the IGEFET is that all the vacuum and high temperature processing steps required to

fabricate the microsensor are completed prior to the deposition of the chemically-sensitive thin film. This fabrication method allows for a greater number of sensor chemicals to be evaluated than would otherwise be possible with the multi-layer interdigitated device while retaining high sensitivity (2; 3).

Chemically-Sensitive Thin films

Many different thin film sensor candidates have been evaluated to detect and measure organophosphorus compounds. A considerable amount of research has been accomplished in the last two years using several metal-doped phthalocyanine compounds, which include: cobalt, copper, manganese, nickel, titanium, and tin (2; 3; 4; 17). More recently, Captain Shin accomplished an initial evaluation of several gas-sensitive organic compounds that are known to react with nerve agents. These compounds included: 2-naphthol(β), L-histidine dihydrochloride, succinylcholine chloride, and succinyl chloride (3). Table I shows the chemical properties for five of the chemically-sensitive thin films evaluated in this research effort.

Several researchers including Captain John Wiseman, Captain Thomas Jenkins, and Captain Jenny Shin all used copper phthalocyanine as a chemically-sensitive thin film (2; 3; 4). The copper phthalocyanine chemical structure is shown in Figure 13. In this thesis copper phthalocyanine is used as the baseline thin film to compare the performance of the gas-sensitive organic compounds that were evaluated in this thesis effort.

A new area of interest in the detection of chemical warfare nerve agents include a category of compounds that are "scavengers" of organophosphorus compounds. These

Table I. Chemically-Sensitive Thin Film Properties (21).

Chemical Name	Chemical Formula	Molecular Weight	Melting Point	Solvent
Copper Phthalocyanine	$C_{32}H_{18}N_8Cu$	577.79	Sublimes	Acetone
L-Histidine Dihydrochloride	$C_6H_9N_3O_2 \cdot 2HCl$	228.08	245°C	Water
2-Naphthol(β)	$C_{10}H_8O$	144.18	122°C	Acetone
Succinylcholine Chloride	$C_{14}H_{30}Cl_2N_2O_4 \cdot 2H_2O$	387.36	164°C	Water
Succinyl Chloride	$C_4H_4Cl_2O_2$	154.98	20°C	Ether

scavengers bind with the organophosphorus compounds preventing the phosphorus atom from binding with the ChE enzyme. In a recent paper, Dr. Rajan reported isolating a "scavenger" compound that is derived from squid tissue (23). This compound, DFPase, reacts with and hydrolyses the nerve agents. The results reported in the paper indicate that DFPase could be an excellent candidate for use in a thin film chemical sensor. DFPase appears to be extremely sensitive, and as such, it could be used in a personal detection sensor. Unfortunately, current information indicates that DFPase will not survive temperatures elevated to any appreciable amount above 37° C (13; 23). This could pose a problem if it is deemed desirable to have DFPase on the same microsensor as a metal-doped phthalocyanine, which is reported to manifest gas-sensitivity at temperatures above 100° C (3; 9).

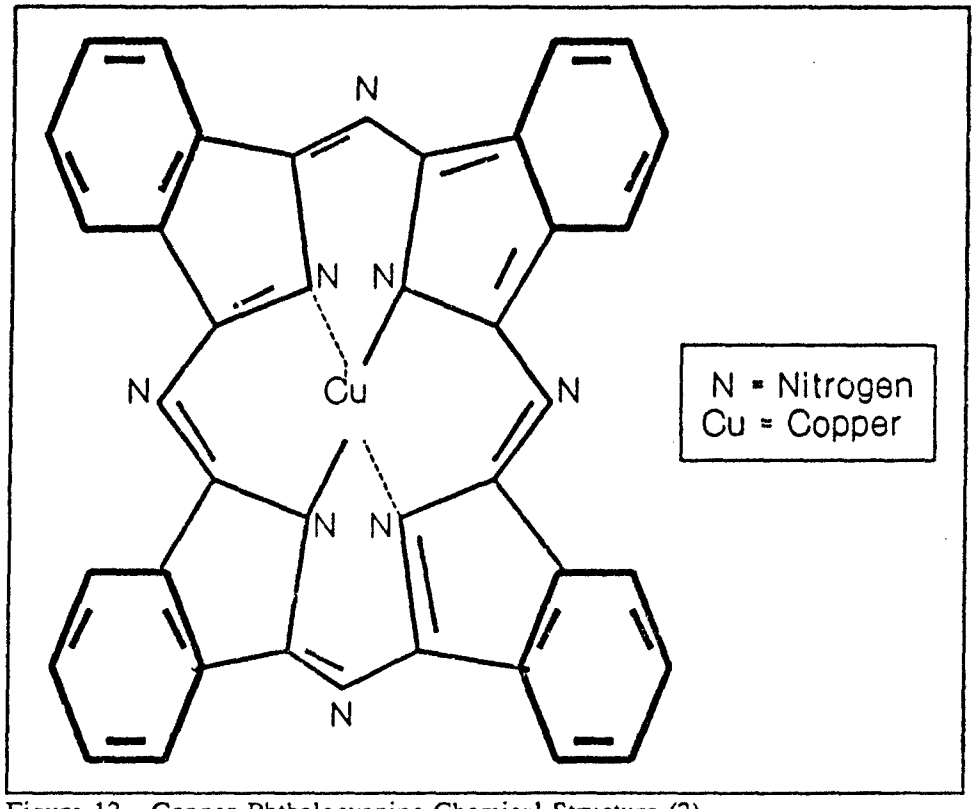

Figure 13. Copper Phthalocyanine Chemical Structure (2).

Summary

Background information concerning toxic organophosphorus compounds, their associated physiological effects and chemical reactions was reviewed. The current state of research concerning solid state sensors including: piezoelectric, SAW, chemiresistor, CHEMFET, multilayered interdigitated electrode, and IGEFET devices was presented. Finally, the candidate chemically-sensitive thin films used in this thesis for detecting and measuring the analog compounds for the chemical warfare nerve agents were reviewed.

III. IGEFET Redesign and Test Cell Design

The redesign of the interdigitated gate electrode field-effect transistor (IGEFET) microsensor is briefly discussed in this chapter. The detailed redesign will be presented in Captain Thomas Graham's thesis (24). However, the microsensor test cell redesign is thoroughly discussed in this chapter. The test cell design section discusses the basis for the revised test cell design. Recognition of the deficiencies discovered in previous test cells used for evaluating the IGEFET microsensor were the basis for the revised test cell design. The layout and basic construction of the new test cell, and the design performance characteristics of the test cell are all discussed in this chapter.

IGEFET Redesign

The redesign of the IGEFET microsensor was primarily influenced by deficiencies discovered during Captain Jenny Shin's and Captain Thomas Jenkins' thesis research (3; 4). The previous microsensors designed by Captain Shin and Captain Jenkins had rectangular IGE structures with a length-to-width ratio of approximately four-to-one. The large length-to-width ratio made it difficult to apply uniform chemically-sensitive thin films to an entire IGE without getting some of the material on an adjacent IGE. Close spacing of adjacent IGEs contributed to the problem of cross contamination.

Captain Jenny Shin's IGEFET microsensor manifested a performance problem caused by the IGE floating gate being connected directly to the input of a multiplexer. The extremely high resistance of the floating gate, on the order of 10^{12} Ω, was higher

than the off-state resistance of the multiplexer, causing the multiplexer to shunt a significant portion of the IGE's output signal. The IGEFET implemented by Captain Thomas Jenkins had a MOSFET amplifier connected directly to each IGE, to reduce the effective output impedance and boost the output signal by approximately 15 decibels. This implementation was incorporated in the redesigned IGEFET microsensor.

A combination of the best individual components in the IGEFETs designed by Captain Jenny Shin and Captain Thomas Jenkins were combined and modified by Captain Thomas Graham in his research effort (Figure 14).

As with the previous designs, the new IGEFET microsensor was fabricated with line-cut links at all major circuit nodes to allow any defective section of the microsensor circuit to be bypassed. These links insure that any single point and most multi-point failures in the microsensor will not seriously compromise its use. Bond pads are also connected to every major node of the microsensor to allow detailed testing and debugging of the microsensor. The redesign of the IGEFET microsensor incorporated a completely modular arrangement allowing individual circuit sections to be arranged with a geometry that facilitates evaluation of the device. The three principal changes made in the IGEFET microsensor included a:

1. three by three array of sensing elements arranged so each sensing element had a square shape.
2. sense-element amplifier connected to the output of each interdigitated gate electrode (IGE) element.
3. demultiplexer connected to each driven gate on the IGEFET to facilitate the automation of microsensor testing.

Test Cell Design

The test cell was redesigned to reconcile the limitations encountered with the previous test cell. The earlier test cell design manifested problems as the result of connecting and disconnecting the signal, power supply and logic select lines. Some of the signal lines became unreliable as the direct result of repeated mating, demating, and handling. Susceptibility to 60 Hertz noise required that the AC signal data was collected only above 1 kHz. Collection of chemically-sensitive thin film's response-time data of the IGEFET microsensor was limited as a result of having to "fill" the one liter test cell a minimum of three times with the challenge gas before measurements could begin. Response-time data could only be accurately collected only for challenge gas concentrations that allowed gas flow rates of several liters per minute. Using a DIMP permeation tube (model G-4942) and delivering the challenge gas at a concentration of 100 parts-per-billion (ppb) required a flow rate of six liters per minute, in order for the response-time data to be accurately collected. Higher concentrations of the challenge gas would not, however, allow an accurate measurement of IGEFET's response-time data.

Test Cell Reliability Factors. Building a reliable test cell which could be used for long-term testing required durable construction and interface connections which will operate reliably after many connect and disconnect cycles. The long-term reliability of the electrical connections was obtained by using chassis mounted BNC connectors for all 64 connections to the microsensor IC (Figure 15). The thermal control heater strip power connections were provided to the test cell chassis using female banana connectors.

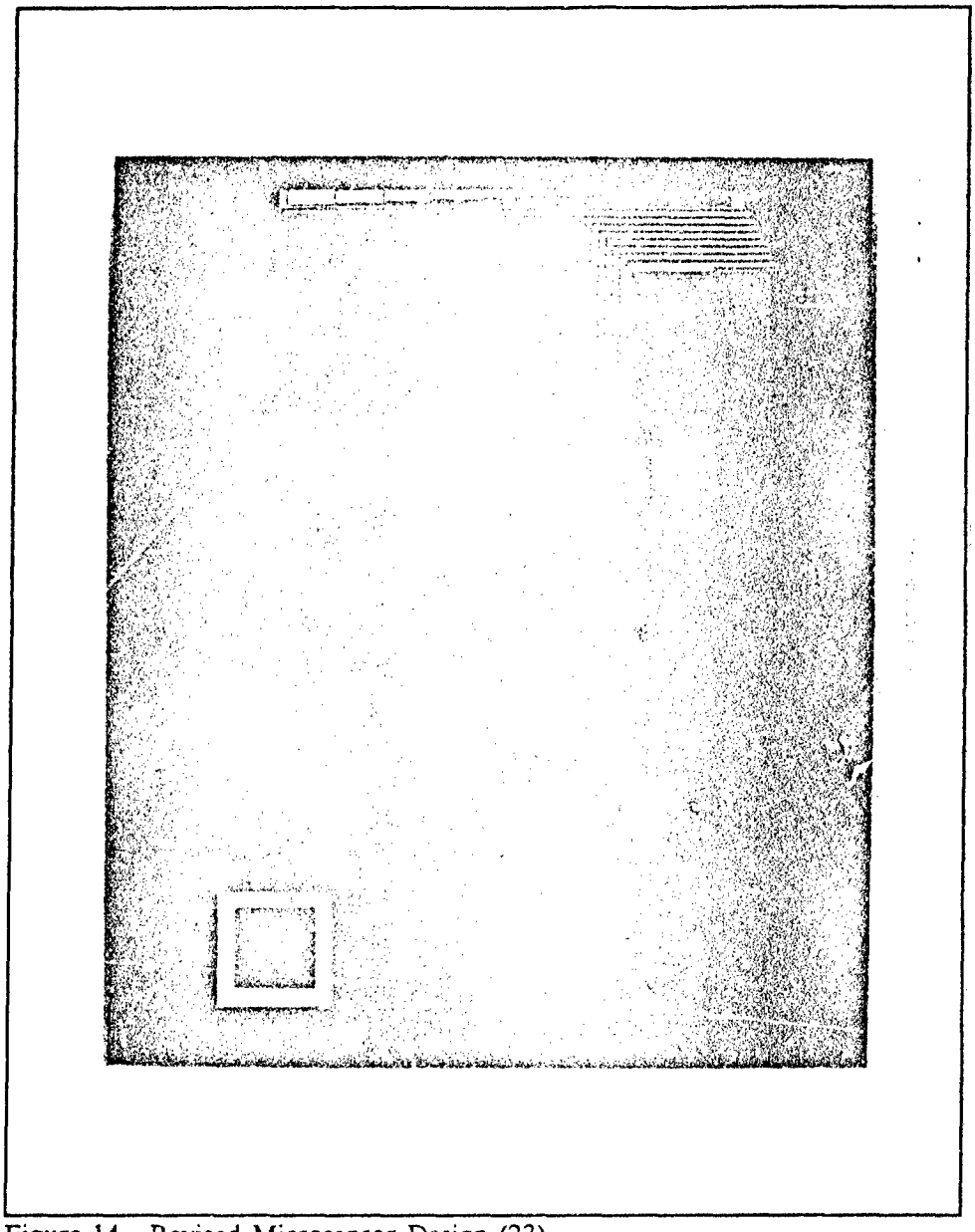

Figure 14. Revised Microsensor Design (23).

The heater strips were easily replaced since small bayonet pin connectors were used inside the test chamber. The thermocouple temperature sensor was routed through the

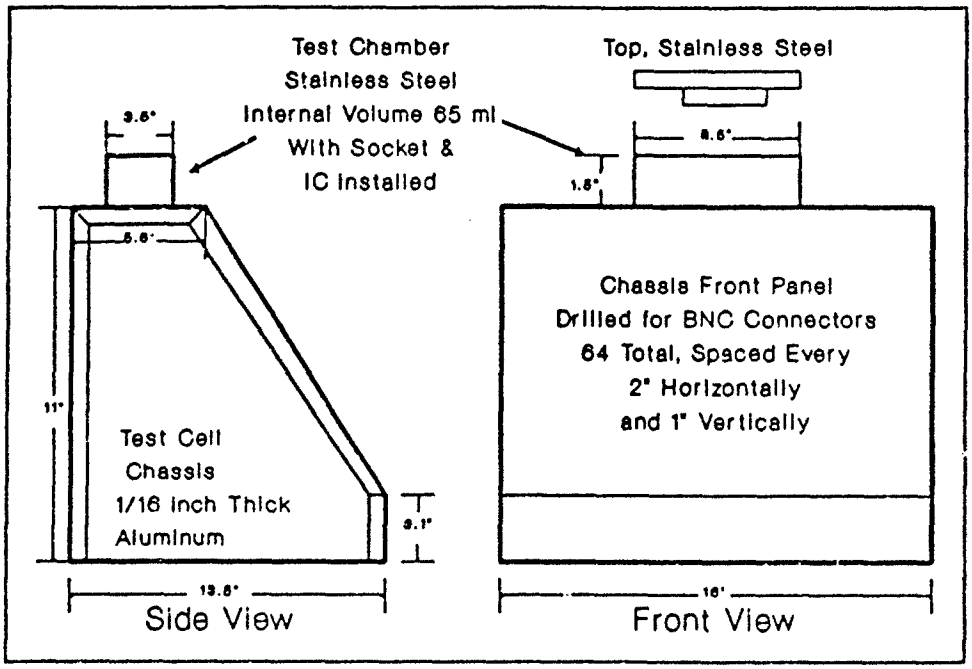

Figure 15. Test Cell Dimensions and Materials.

test cell chassis, and the test chamber circuit card was sealed at the test chamber circuit card interface using conductive a RTV adhesive (Teknit, Model #72-00002, 129 Dermody St, Cranford, NJ 07016).

The microsensor was inserted into and removed from the test chamber by removing the test chamber top, which is held in place with six 8 × 32 hex-head screws, and releasing the clamp lever on the zero insertion force socket (Figure 16). The heater strip and thermocouple were mounted between the socket and the microsensor and did not require adjustment when the microsensor was inserted or removed from the test chamber. The heater strip spans approximately seventy percent of the microsensor's length. The thermocouple was installed under the microsensor at the challenge gas

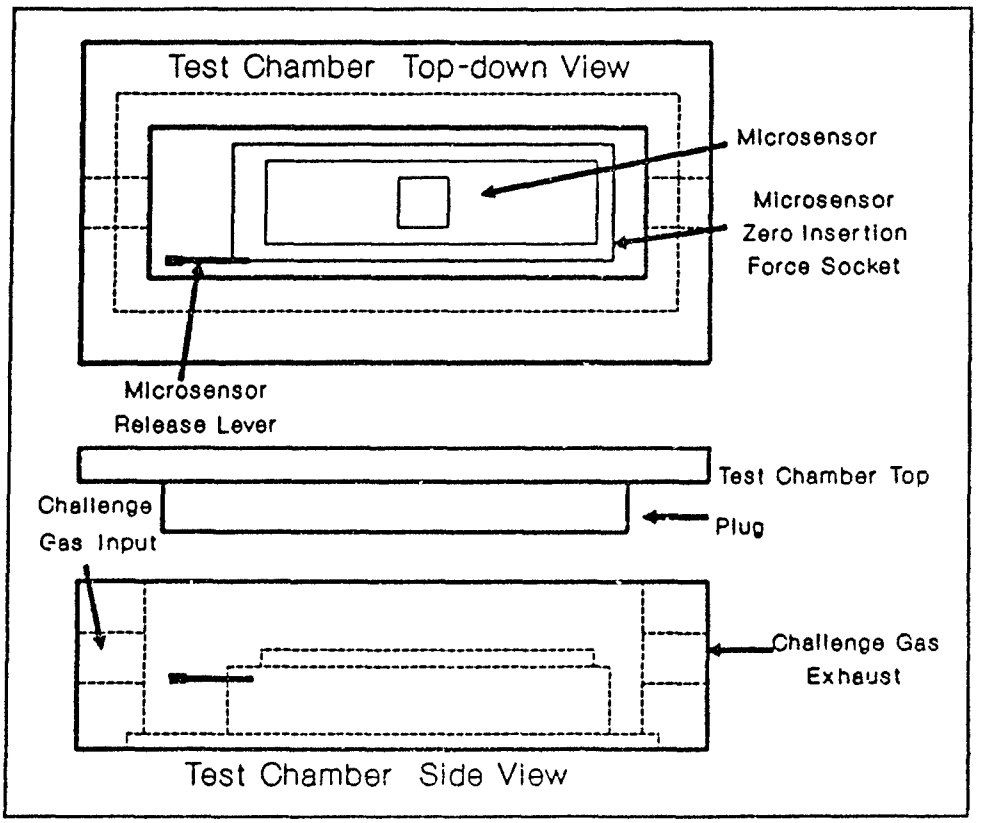

Figure 16. Test Chamber Diagram Showing the Microsensor and the Socket Placement.

exhaust end of the microsensor, to ensure that it measured the microsensor temperature and not the heater strip temperature.

The test chamber challenge gas connections were made using Swagelock quick disconnect couplings to reduce the possibility of damage to the threads on the test chamber when making challenge gas connections.

Electromagnetic Interference. Electromagnetic interference (EMI) was a significant problem with the previous test cell. EMI shielding was incorporated into the design of

the new test cell. The material selection, fabrication techniques, and test cell sealing were all designed to minimize EMI. Aluminum (1/16 inch thick) was selected for the test cell chassis because of its strength and attenuation absorption factor which is approximately three decibels greater than the values in Table II. The reflection factor remains the same as the listed values, yielding an overall shielding effectiveness three decibels better than the values listed in Table II. To insure the quality of the chassis shielding, all joints were overlapped one inch and chassis screws were installed every two inches.

Table II. Effective Electromagnetic Shielding of 1 mm Thick Aluminum (24:85).

Frequency	Shielding Effectiveness	Absorption	Reflection
10 kHz	136 dB	10 dB	126 dB
100 kHz	149 dB	33 dB	116 dB
1 MHz	211 dB	105 dB	106 dB
10 MHz	429 dB	332 dB	96 dB

To reduce the impact of noisy connections to the microsensor, the connections were made using a zero-insertion-force 64-pin dual-in-line socket. The socket used gold plated contacts at the microsensor interface which is contained completely within the stainless steel test chamber (Figure 16). All external connections were made using BNC connectors at the test cell front panel. All interconnect cables (RG-174) inside the test cell chassis had a 50Ω impedance and the shielding was grounded to the chassis at both cable ends.

The test chamber top was sealed in place using 0.125 inch silver-filled conductive gasket material (Teknit, Model #85-10506 Compound 856, 129 Dermody St, Cranford, NJ 07016) to provide a gas tight seal and EMI shielding. The zero-insertion force 64-pin socket was attached to the bottom of the test chamber with a double-sided fiberglass circuit card containing a large ground plane for shielding. All connections were soldered to insure gas tight seals. The circuit card was then attached to the bottom of the test chamber using screws, and sealed using a conductive RTV adhesive.

Cross-talk minimization was accomplished by designing the test chamber interface circuit card with minimum length bonding pads using the maximum amount of separation facilitated by the inter-electrode spacing of the 64-pin dual-in-line socket (inter-electrode spacing is 0.1 inch). The length of the unshielded RG-174 at the connection interface was kept to a minimum length (one-half inch) that would allow soldering without cable or circuit damage. The inter-electrode capacitance can be estimated using the following equation:

$$C = \frac{\epsilon_r * \epsilon_0 * A}{d} \qquad (3)$$

where C is the inter-electrode capacitance in picofarads (pF), ϵ_r is the relative permittivity of the dielectric material (no units), ϵ_0 is the permittivity of vacuum (pF/cm), A is the cross-sectional area (cm^2), and d is the inter-electrode separation (cm). The particular values for ϵ_r, ϵ_0, A, and d are:

$A = 1\ cm^2$ (based on drawing dimensions)

d = 0.2 cm (based on drawing dimensions)

ϵ_r = 1.6 (based on averaging the values for air = 1.0, fiberglass = 3.2, and polyethylene = 2.3 and their percentage effect (26))

$\epsilon_0 = 8.854 \times 10^{-2}$ pF/cm (27:733),

yielding C = 0.70 pF, which compares favorably with the measured capacitance of the test cell's inter-electrode capacitance (Table III).

Table III. Measured Inter-Electrode Capacitance Between Selected Test Cell Pins.

Electrode A	Electrode B	Capacitance
1	2	0.81 pF
5	6	0.89 pF
10	11	0.75 pF
32	33	0.80 pF
63	64	0.90 pF

Test Chamber Volume Reduction. Measuring the microsensor's response time to a challenge gas required minimizing the internal volume of the test chamber. For example, when three parts-per-million (ppm) of the diisopropyl fluorophosphate (DFP) challenge gas was introduced into the test chamber, the flow rate was 14 milliliters per minute. Completely exchanging ten volumes of gas in the prior test cell would have

required three hours and fifty seven minutes. Determining the microsensor's response time, which is typically on the order of seconds, would be impossible using the old test cell design.

The test chamber in the new test cell configuration was designed to minimize the internal gas volume while still allowing the challenge gas to flow freely over the microsensor. The test chamber was sized to accommodate a non-interference fit with the microsensor, IC socket, heater strip, thermocouple, and wiring connections (Figure 16). A plug was connected to the inside face of the test chamber's top to allow flexibility in testing, such as mounting custom wiring to the top of the microsensor.

When the plug is inserted inside the test chamber, and a microsensor is installed, the gas volume in the test chamber is approximately 65 milliliters. When the plug is removed, the internal volume increases to approximately 100 milliliters. With this volume, the corresponding time required to exchange ten volumes of gas requires less than five minutes. Additionally, since gas flow is across the length of the test chamber, and the unfilled cross-sectional area is less than 6 cm^2, only three volumes of gas are required to exchange the test chamber's atmosphere, which reduces the ideal gas stabilization time to less than two minutes. For the challenge gases delivered at the concentrations used in this investigation, gas stabilization in the test cell was achieved in less than 20 seconds.

For the interested reader, Appendix D contains copies of the drawings used to fabricate the test cell, complete with test chamber, assembly instructions, and the photolithographic masks used to produce the test chamber interface circuit card.

Summary

This chapter presented a brief discussion on the redesign of the IGEFET and the rational for the current configuration. The rest of the chapter contained a discussion on the redesign of the test cell used in this research effort. The need for a new test cell was discussed as well as the major considerations that led to the new test cell design as implemented. The new test cell was designed to increase reliability, reduce electromagnetic interference, and reduce the required challenge gas flow rate.

IV. Chemically-Sensitive Thin Film Deposition and Experimental Evaluation Procedures

The microsensor thin film deposition and experimental evaluation are presented in this chapter. The first section describes the methods and procedures used to deposit the chemically-sensitive thin films to the microsensor. The evaluation and performance comparisons of chemically-sensitive thin film deposition methods are discussed. The second section presents the experimental measurement and data reduction methods used in this research.

Chemically-Sensitive Thin Film Application

Eleven packaged devices were used to conduct the microsensor's performance evaluation in this investigation. Two devices, along with three surplus devices remaining from Captain Shin's thesis, were separated from the test lot for initial evaluation and testing of the chemically-sensitive thin film deposition methods. Two different methods, vacuum evaporation and airbrush spraying, were used to deposit the chemically-sensitive thin films to the interdigitated gate electrode field-effect transistor (IGEFET) microsensors. This process was accomplished by masking all but the desired application area of the microsensor (Figure 17). The IGE location of the chemically-sensitive thin films are shown in Table IV. The vacuum evaporation process was used to deposit the copper phthalocyanine thin film on to two electrode structures on each microsensor. L-histidine dihydrochloride, succinylcholine chloride, succinyl chloride, 2-naphthol(β), and DFPase were deposited using the airbrush technique.

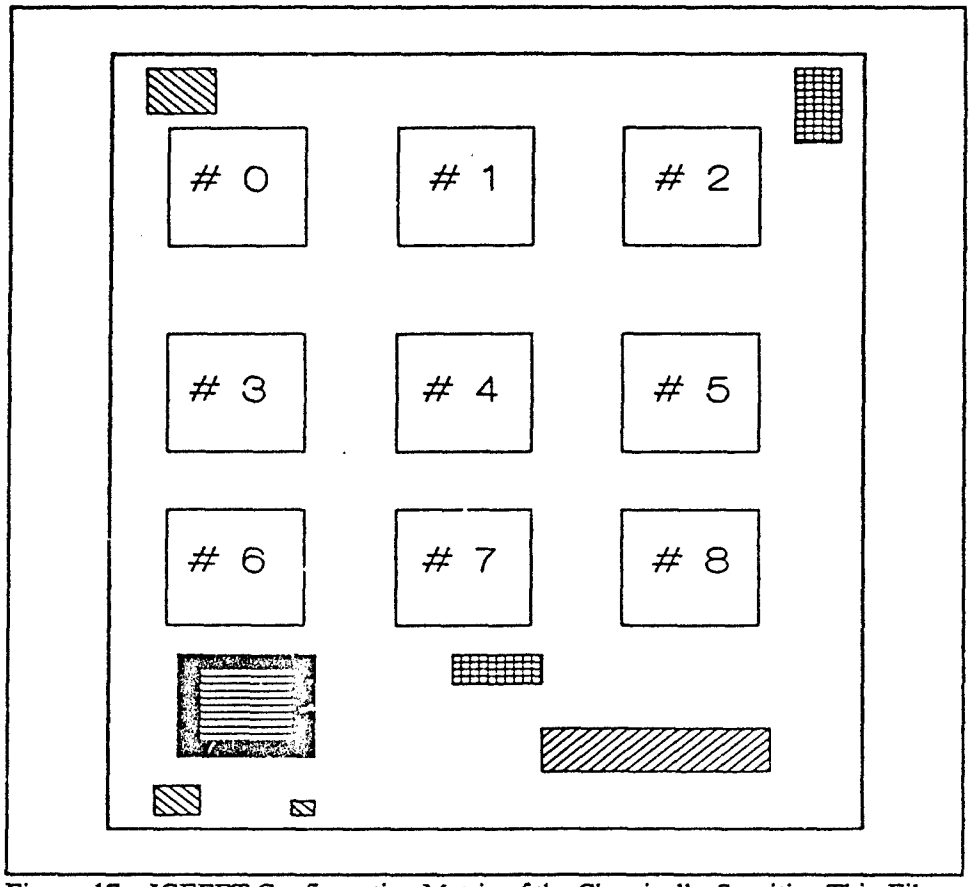

Figure 17. IGEFET Configuration Matrix of the Chemically-Sensitive Thin Films.

Since there are nine independent interdigitated gate electrodes (IGE)s and field-effect transistors (IGEFETs), the device must be masked so the chemically-sensitive thin film candidate will be deposited only to the desired electrode or electrodes. The masks used in this thesis were produced using a hard steel punch to cut a hole to the proper dimensions in a two inch by three inch piece of aluminum foil. With a few practice attempts, it was possible to cut two or more holes in the mask and maintain the desired alignment. A punch plate composed of 20 or more sheets of paper was necessary to produce a clean cut in the aluminum foil mask material.

Table IV. Chemically-Sensitive Thin film Location on Each IGEFET.

IGE	IGEFET#1	IGEFET#2	IGEFET#3	IGEFET#4	IGEFET#5
0	CuPc	CuPc	CuPc	CuPc	CuPc
1	CuPc	CuPc	CuPc	CuPc	CuPc
2	DFPase	L-Hist	L-Hist	L-hist	L-Hist
3	L-Hist	SuClCh	SuClCh	DFPase	DFPase
4	L-Hist	Naphth	Naphth	L-Hist	L-Hist
5	DFPase	DFPase	DFPase	DFPase	DFPase
6	Naphth	SuCh	SuCh	L-Hist	DFPase
7	SuClCh	SuCh	Naphth	DFPase	
8	SuCh		DFPase		

IGE	IGEFET#6	IGEFET#7	IGEFET#8	IGEFET#9
0	CuPc	CuPc	CuPc	CuPc
1	CuPc	CuPc	CuPc	CuPc
2	SuClCh	SuClCh	SuClCh	SuClCh
3	Naphth	Naphth	Naphth	Naphth
4	DFPase	DFPase	DFPase	DFPase
5	SuCh	SuCh	SuCh	SuCh
6				
7				
8				

CuPc - Copper Phthalocyanine L-Hist - L-Histidine Dihydrochloride
Naphth - 2-Naphthol(β) SuClCh - Succinylcholine Chloride
SuCh - Succinyl Chloride DFPase - DFPase

The past research efforts of Capt Jenny Shin and others, used a photolithographic etching process to fabricate the mask (3:C). Using the hard steel punch to cut the mask produced three benefits. The first benefit was faster mask fabrication because a new mask with any desired pattern could be fabricated in just a few minutes. This fabrication process saved hours of labor as compared with the photolithographic process used by Captain Jenny Shin and others, especially when a pattern change was desired. Since succinyl chloride is very corrosive, a fresh mask was required for each film

deposition, due to the problems incurred in handling the mask once it was contaminated with the corrosive film.

The second benefit was better mask edges because cutting the mask with a hard steel punch provided a cleaner edge than was typically obtained using the photolithographic process masks (3). The third benefit of using the hard steel punch to fabricate the mask was less over-spray because cutting the mask with a punch slightly depressed the cut edges of the mask. This feature facilitated positioning the mask edge closer to the surface of the IGEFET microsensor than is possible to attain with a flat mask. The advantage of this feature is that it reduced the amount of over-spray on the IGEFET's surface. By using a sacrificial IGEFET microsensor for fit testing a mask, verification that the mask's edge flair would not physically touch the microsensor's surface was accomplished before the mask was actually used.

The vacuum deposition process used for the copper phthalocyanine was modified from the procedures used by Captain John Wiseman, Captain Jenny Shin, and Captain Thomas Jenkins to obtain more consistent and uniform thickness films (2; 3; 4). The majority of the effort required to develop the current vacuum deposition procedures was accomplished by Captain Anthony Moosey in support of his thesis research. The primary modifications involved moving the target closer to the evaporation boat which contained the copper phthalocyanine, and heating the evaporation boat to the temperature where the copper phthalocyanine was deposited at a rate of approximately one angstrom per second. All the devices used in this investigation were positioned 10 centimeters directly above the evaporation boat. Copper phthalocyanine was deposited on two

devices with an approximate thickness of 1000 angstroms, and to the other nine devices with a thickness of 2000 angstroms, plus or minus 15 percent.

The other chemically-sensitive thin film candidates used in this investigation, 2-naphthol(β), L-histidine dihydrochloride, succinylcholine chloride, succinyl chloride, and DFPase, were deposited using an external mix airbrush (Paasche Airbrush Co., Model H-Set, Harwood Heights, IL 60656) using dry nitrogen as the propellant. Each chemically-sensitive thin film candidate required a slightly different technique to obtain an acceptable film on the interdigitated gate electrode structure.

Initial testing was conducted on 2-naphthol(β) using several different combinations of propellant pressure and needle orifice openings. The best films were produced when the propellant pressure was set to 10 psig, and the orifice was opened 180 degrees from the full-closed position using the number-one tip. Higher propellant pressure produced craters in the film as the highly energetic droplets impacted the film's surface. Wider orifice openings caused the 2-naphthol(β) film to grow into large singular crystals which were widely spaced on the IGE structure. Using the favorable orifice and pressure settings discussed above, and spraying from a distance of eight to ten inches, yielded a fairly uniform surface of crystals where planar features are on the order of one micron in diameter (Figure 18). It was observed that during the deposition process the 2-naphthol(β) sublimes at room temperature at an apparent rate of 500 to 2000 angstroms per hour, depending upon the air currents near the film. This phenomena was observed using a microscope (Wild Heerbrugg Ltd., Model M20, CH-9435 Heerbrugg, Switzerland) with the interferometer attachment (Wild Heerbrugg Ltd., Model 255 574, CH-9435 Heerbrugg, Switzerland).

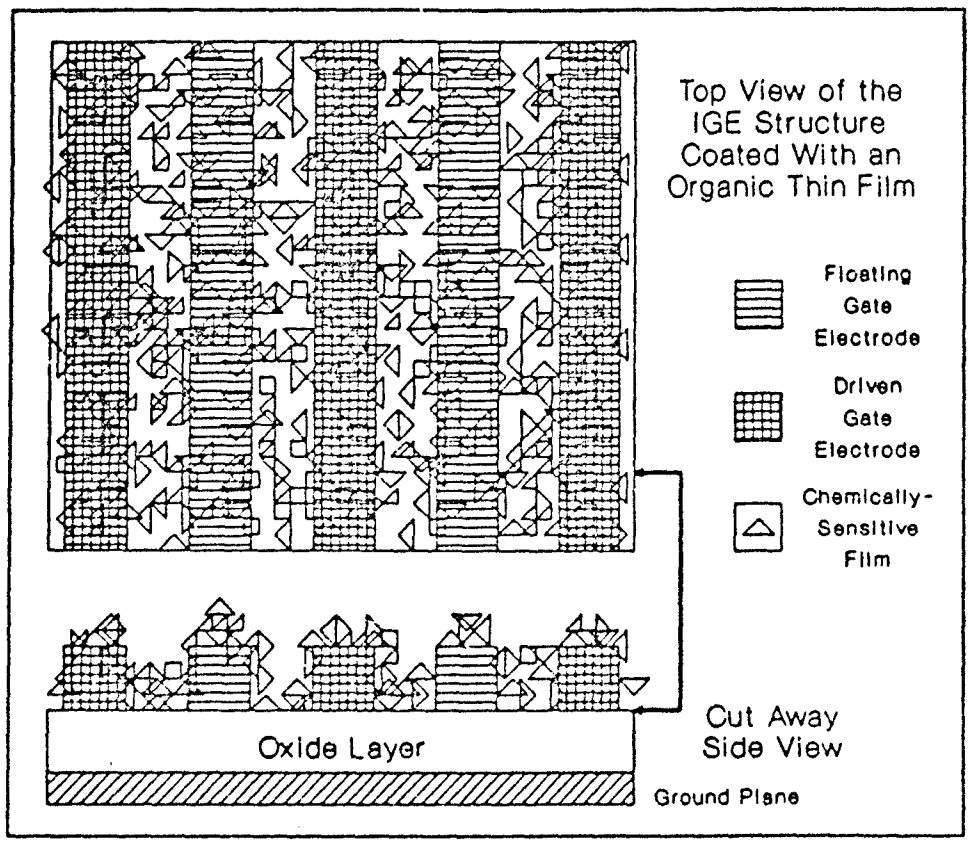

Figure 18. 2-Naphthol(β) Applied to an IGE Structure.

Next, L-histidine dihydrochloride was evaluated to identify a useful deposition technique. Figure 19 shows how the L-histidine dihydrochloride thin film accumulates on the IGE structure on the microsensor. Producing the best quality L-histidine dihydrochloride thin films required the airbrush propellant pressure to be set to 25 psig and the needle orifice to be opened to 120 degrees from the full-closed position using the number-one tip. A larger opening or lower delivery pressure caused the material to accumulate in spheres that were several microns wide. The deposited L-histidine

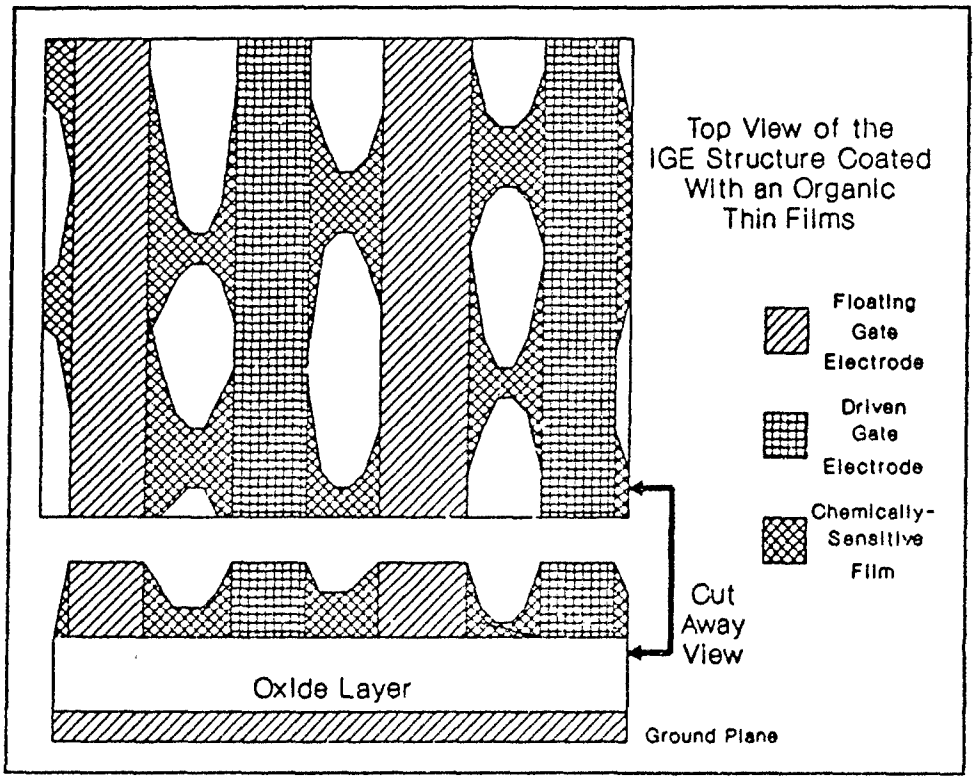

Figure 19. L-Histidine Dihydrochloride Thin Film on the IGE Structure.

dihydrochloride formed a nice bridge between each electrode without having any noticeable chemical reaction with the substrate.

Succinylcholine chloride, DFPase, and succinyl chloride each had similarly appearing film morphologies when applied to the IGE structure. The structure of the films were manifested as small flattened spheroids that coated over the IGE structure, but they did not appear to wick to the electrode surface as was observed with the L-histidine dihydrochloride thin film (Figure 20). Several different pressures and orifice openings were evaluated, but the same settings used for the application of L-histidine dihydrochloride provided the best results. One special note regarding the airbrush --

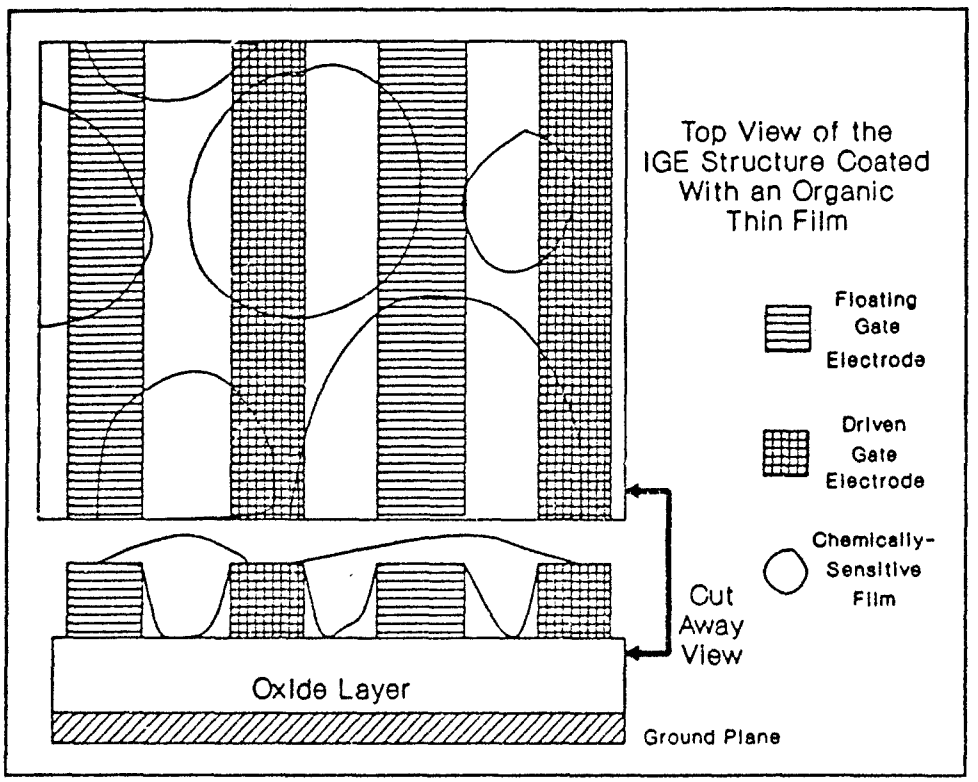

Figure 20. Appearance of Succinylcholine Chloride, DFPase, and Succinyl Chloride as Applied to an IGE Structure.

succinyl chloride was very corrosive, and the airbrush solution reservoir and tip was cleaned and polished after each deposition to insure consistent results.

Experimental Evaluation Techniques

During the IGEFET microcircuit evaluation, an electrical problem with the demultiplexer and multiplexer was discovered. Baseline testing of the IGEFETs was initially conducted using the demultiplexer and multiplexer to switch between the various electrodes. This procedure was abandoned after repeated failures of the demultiplexer circuit by shorting, sinking one ampere of current, which increased the temperature of

the IGEFET at a rate greater than 20° C per minute. This problem irreversibility damaged two IGEFET microsensors by overheating the circuits in the demultiplexer. If the excessive current draw was observed and power turned off before the IGEFET case reached a temperature of 60 to 70° C, it was possible to recover the device after allowing the IGEFET to cool to room temperature. It was also observed that by the time the IGEFET case temperature reached 70° C, the power supply lines on the IGEFET near the demultiplexer suffered permanent damage.

All signals in subsequent tests were measured at either the floating gate or the sense-element amplifier output on each device, bypassing the multiplexer. Switching between the individual IGEFETs on the microsensor was accomplished manually, using the front panel of the test cell as a patch panel. The test equipment and controlling computer was connected as shown in Figure 21.

After several occurrences of the IGEFET circuit shorting it was decided that the demultiplexer circuits would no longer be used. All electrode selection and device switching was accomplished off chip using the patch panel of the test cell.

Each performance evaluation was accomplished immediately after the deposition of the organic chemically-sensitive thin films. The IGEFET microsensor was sealed in the test chamber, and 90% relative humidity filtered laboratory air was passed through the test chamber with a flow rate of 100 milliliters per minute. The air flow continued for a period spanning 30 to 45 minutes to stabilize the microsensor and test chamber for challenge gas exposure testing.

A complete set of baseline data was collected for the microsensor. The baseline test measurements included: DC resistance, AC impedance, gain/phase, spectrum

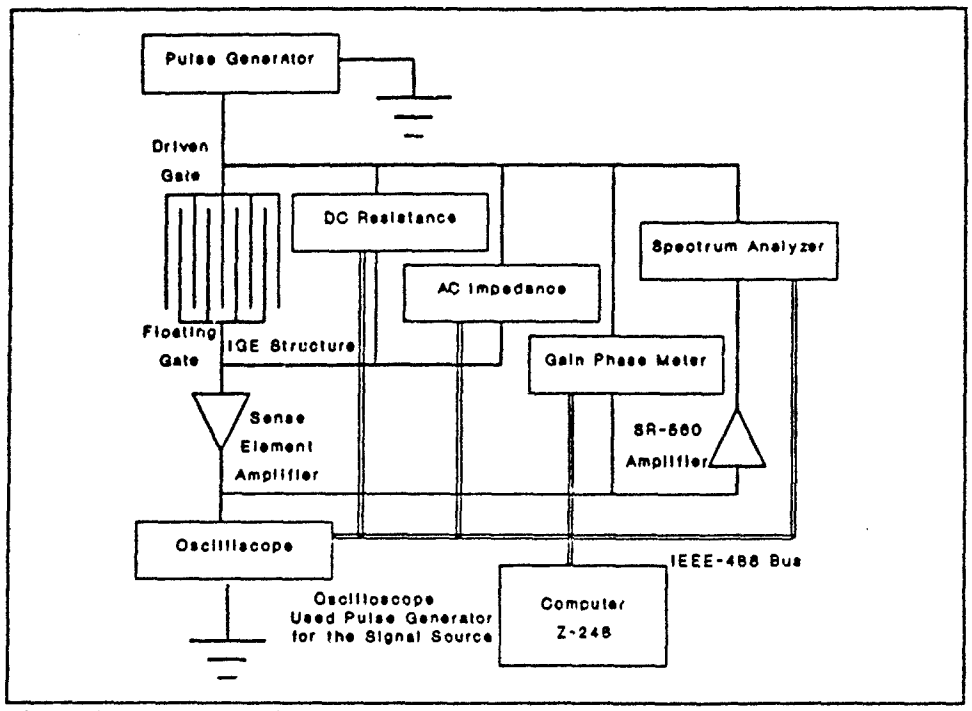

Figure 21. Configuration of the Test Equipment Connections.

analysis, and the time-domain response due to an applied pulse excitation. Immediately after collecting the baseline data, a challenge gas was introduced, and the complete measurement set was repeated. This process was repeated for each test combination in Table V.

The DC resistance measurements were collected using an electrometer (Keithley Instruments, Model 617, Cleveland, OH 44139), in the (V/I)-mode to measure the anticipated very large resistances of the thin films. The voltage applied to the IGE driven electrode was fixed at 2.5 volts to ensure that the demultiplexer would not short. Even though the demultiplexer circuit was not used, any voltage applied to an IGE

Table V. IGEFET Microsensor Evaluation Matrix.

Challenge Gas and Concentration	Temperature in Degrees Centigrade 30	50	70
DIMP 100 ppb	X	X	X
DIMP 1 ppm	X	X	X
DIMP 10 ppm	X	X	X
DMMP 100 ppb	X	X	X
DMMP 1 ppm	X	X	X
DMMP 10 ppm	X	X	X
DFP 100 ppb	X	X	X
DFP 1 ppm	X	X	X
DFP 3 ppm	X	X	X
DIMP / DMMP	X		
DIMP / DFP	X		
DMMP / DFP	X		

driven electrode greater than +5 volts (V_{DD}) would cause the demultiplexer circuit to avalanche and sink one ampere of current from the power supply.

The AC impedance measurements were collected using an impedance/gain-phase analyzer (Hewlett-Packard, Model HP 4194A, Palo Alto, CA 94304). To collect the impedance measurements, the frequency was swept from 100 Hz to 1 MHz. After the parasitic cable and test fixture impedance calibration was accomplished, the microsensor's performance measurement data was collected. Details of the instrument initialization and measurement parameters are summarized in Appendix C.

The gain-phase measurements were collected using an HP 4194A impedance/gain-phase analyzer. The HP 4194A was configured for the gain-phase mode, and the frequency was swept from 10 Hz to 1 MHz. After a calibration measurement of the wiring configuration was performed, the microsensor's performance data was collected.

The spectrum analyzer measurements were collected using a spectrum analyzer equipped with a tracking generator (Hewlett-Packard, Model HP 4195A, Palo Alto, CA 94304). All spectral analysis measurements were made over two frequency ranges, one from 0.001 Hz to 10 kHz, and the other from 0.001 Hz to 1 MHz. The tracking generator was set to 0 dBM, and it was connected to the driven-electrode of the IGEFET under evaluation. By collecting two sweeps, finer detail of the low-frequency behavior of the IGEFET microsensor was obtained while gathering data to a frequency of 1 MHz.

Since the output impedance of the sense-element amplifier is large (on the order of 100 kΩ) and sensitive to capacitance of a load, a low-noise amplifier (Stanford Research Systems, Model SR-560, 1290-D Reamwood Avenue, Sunnyvale, CA 94089) was connected between the output of the sense-element amplifier and the input of the spectrum analyzer. Figure 22 shows the gain-phase response of the SR-560 amplifier.

Time-domain measurements were accomplished using a pulse generator (Hewlett-Packard, Model HP 8082A, Palo Alto, CA 94304) to generate the input signal to the IGEFET being evaluated and a digital storage oscilloscope (Hewlett-Packard, Model HP 54100A Palo Alto, CA 94304) to capture the output signal. The pulse generator was initialized to generate 10 microsecond wide, three volt amplitude pulses, with a period of one millisecond. The three volt 10 microsecond pulse used as the excitation pulse is shown in Figure 23.

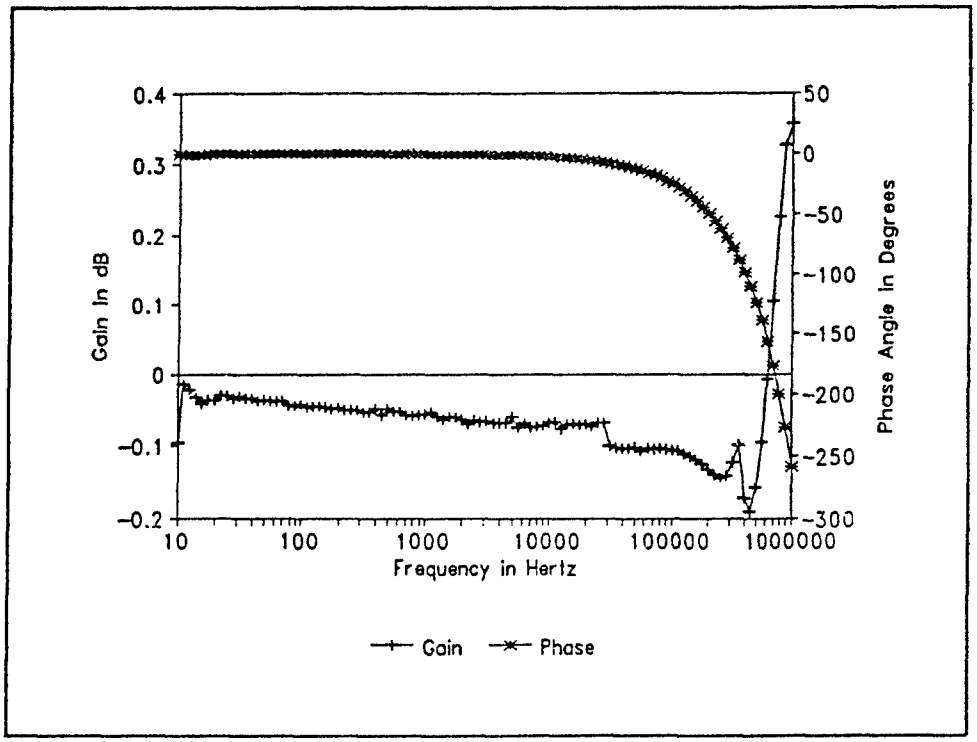

Figure 22. Gain-Phase Response of the SR-560 Low-Noise Amplifier.

The test instrumentation output was captured for storage using a microcomputer (Zenith Data Systems, Model Z-248, St. Joseph, MI 49085) using the BASIC program listed in Appendix C.

The complete evaluation test procedures were conducted on each IGEFET for each challenge gas (DIMP, DMMP, DFP, and their binary combinations) as follows:

1. Copper Phthalocyanine was deposited to IGE 0 and 1 on every IGEFET.
2. The organic chemically-sensitive thin films were deposited on IGE structures.
3. The IGEFET was placed into the test chamber.
4. The test chamber was purged with filtered laboratory air for 30 to 45 minutes.

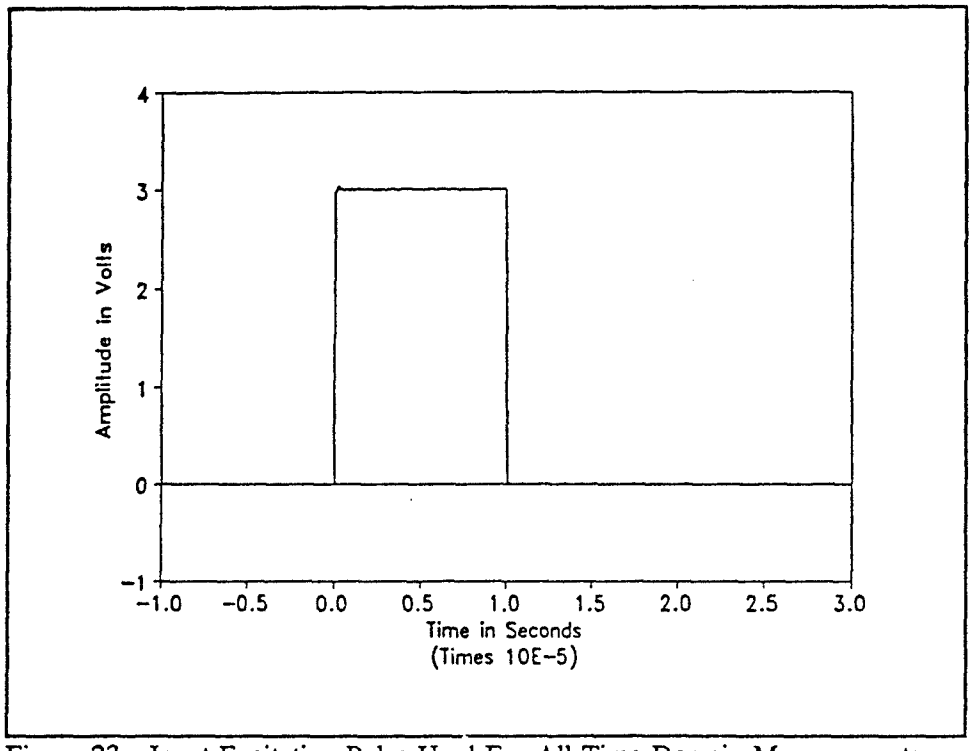

Figure 23. Input Excitation Pulse Used For All Time-Domain Measurements.

5. Evaluation measurements were made on the IGEFET; DC resistance, AC impedance, frequency-domain gain, and time-domain response to the pulse excitation.

6. The lowest concentration (100 ppb) of challenge gas was introduced into the test chamber; then the evaluation measurements were repeated.

7. The challenge gas was stopped and the test chamber purged with filtered laboratory air for 30 to 45 minutes; then the evaluation measurements were repeated to measure for reversibility.

8. Steps 6 and 7 were repeated for the larger concentrations of challenge gas, 1 ppm and then 10 ppm (3 ppm for DFP).

Summary

The location of all chemically-sensitive thin films was listed for each IGEFET. The chemically-sensitive thin film deposition techniques were described. The mask fabrication process was described in detail. The vacuum evaporation deposition method for the copper phthalocyanine chemically-sensitive thin film was described. The airbrush application technique used for depositing the organic chemically-sensitive thin films was depicted. The experimental measurement procedures were explained as well as the measurement limits and test equipment configuration.

V. Results and Discussion

Chapter V presents the results of the performance evaluation of nine interdigitated gate electrode field-effect transistor (IGEFET) microsensors, each which contained six different chemically-sensitive thin films. Evaluation of each chemically-sensitive thin film was accomplished for three different challenge gases and their binary combinations. The first section contains the performance results associated with the IGEFET baseline testing. The second section reports the results for copper phthalocyanine, which was used as a reference chemically-sensitive thin film due to its extensive characterization when exposed to various challenge gases (2; 3; 4). Subsequent sections report the observations for each organic chemically-sensitive thin film evaluated in this research, which includes: succinyl chloride, succinylcholine chloride, 2-naphthol(β), L-histidine dihydrochloride, and DFPase. The final section contains a summary of the results and significant findings.

Baseline Results

Initial measurements were conducted on each IGEFET to establish baseline data to facilitate a comparison of the changes in each device's performance before and after exposure of a chemically-sensitive thin film to a specific challenge gas. After the baseline data was collected, the measurements were repeated after introducing the challenge gases. Table VI contains the initial average DC resistance values for each of the nine IGE structures. The measurements were taken with power supplied to the

IGEFET and the demultiplexer/multiplexer combination set to select element 15 (a nonexistent element). An interesting result noted from taking these measurements was that the DC resistance values for element numbered zero were consistently larger than the values obtained for the other electrodes. This trend is also manifested for the coated electrodes, since electrodes numbered zero and one were coated with the same thickness of copper phthalocyanine.

Table VI. Uncoated Interdigitated Gate Electrode Element Resistance Values.

Device Number	Element 0	1	2	3	4	5	6	7	8
1	3.1	1.7	1.3	1.4	1.3	0.8	1.3	1.3	1.1
2	3.0	1.5	1.5	1.6	1.4	1.4	1.4	1.3	1.3
3	2.5	1.3	1.6	1.4	1.6	1.7	0.9	1.5	1.2
4	2.1	1.5	1.5	1.8	1.8	1.6	1.1	1.3	1.2
5	2.4	1.2	1.7	1.4	1.9	1.4	1.2	1.4	1.5
6	3.0	1.9	1.3	1.3	1.2	1.3	1.4	1.5	1.4
7	2.7	1.8	1.9	1.6	1.1	1.5	1.5	1.2	1.3
8	2.0	1.4	1.4	1.5	1.6	1.7	1.5	1.3	1.3
9	1.9	1.6	1.7	1.4	1.9	0.9	1.6	1.4	1.5

All values in $T\Omega = 1 \times 10^{12}\Omega$

Temperature testing of the sense-element amplifiers was also accomplished (Figure 24). It was also noted that the low-frequency gain of the sense-element amplifier at 30° C corresponds to 15.5 dB. All the sense-element amplifiers evaluated had a gain which spanned 13.5 to 15.5 decibels at low-frequencies (<10 kHz) at a thermostated temperature of 30° C. For all the amplifiers tested, the gain decreased by

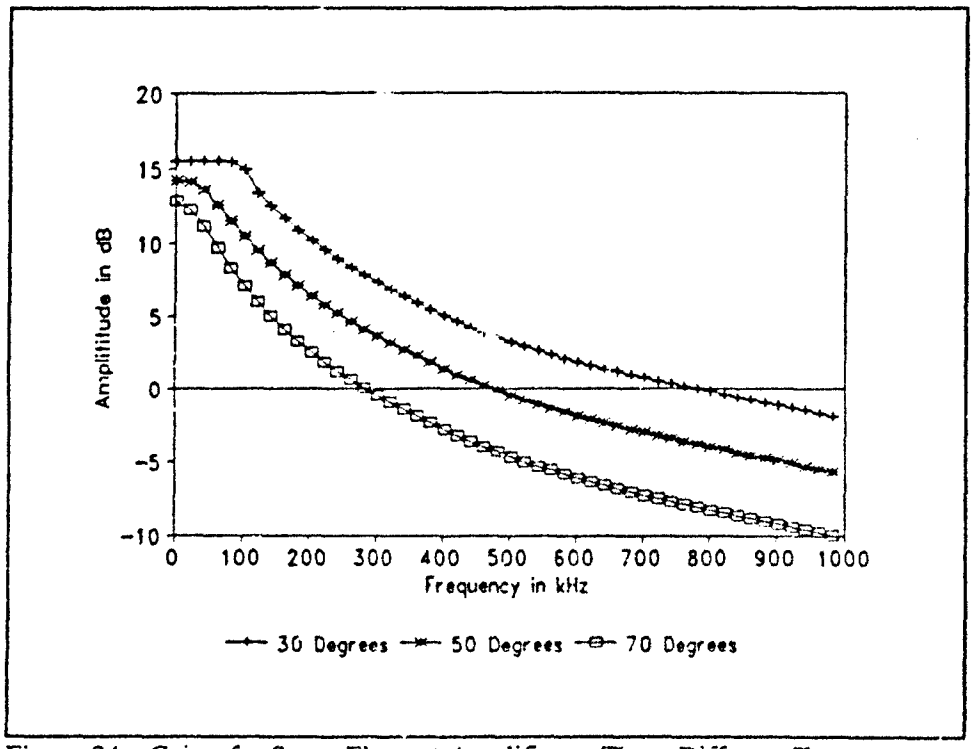

Figure 24. Gain of a Sense-Element Amplifier at Three Different Temperatures.

approximately 3 dB at low frequencies (< 10 kHz), to approximately 10 dB at 10 MHz when the IGEFET was heated to 70° C. All amplifiers evaluated had a similar frequency response.

The decrease in sense element amplifier's gain as the temperature increased is completely explainable. The sense element amplifier is composed of a three stage inverting class A, NMOS transistor amplifier which incorporates diffused load resistors. Since the load resistors are fabricated from p-type diffusion regions in the integrated circuit, their resistance decreases measurably as the temperature increases. As the load resistance decreases, the amplifier gain decreases, as expected.

Copper Phthalocyanine Response

Copper phthalocyanine was used as a chemically-sensitive thin film on the IGEFET microsensor in this research to verify the measurement methods, techniques, and to collect gas-sensitivity data when exposed to diisopropyl fluorophosphate (DFP). The data collected was compared with the data previously collected by Captain John Wiseman, Captain Jenny Shin, and Captain Thomas Jenkins (2; 3; 4). The data in this research indicates that copper phthalocyanine is sensitive to all three challenge gases used in this thesis research: DFP, diisopropyl methylphosphonate (DIMP), and dimethyl methylphosphonate (DMMP) at concentrations as low as 100 parts-per-billion (ppb). An IGEFET using copper phthalocyanine as the chemically-sensitive thin film may be sensitive to challenge gas concentrations lower than 100 ppb, but testing was limited to using challenge gas concentrations of 100 parts per billion and larger, due to time constraints in conducting this investigation.

The copper phthalocyanine film's response was evaluated by measuring DC and AC performance parameters. DC resistance measurements indicated that a 2000Å thick copper phthalocyanine thin film coated IGE structure had a resistance of 300 to 750 GΩ when exposed to 90% relative humidity filtered laboratory air. The resistance decreased measurably when the IGEFET was exposed to each of the three different challenge gases (Figure 25). Figure 25 shows the response of IGEFET element numbered one before and after it was challenged with DIMP, DMMP, and DFP. While the results for element numbered zero are not shown, a similar result with higher resistance values were obtained for the element numbered zero for all the measurements. That is, the element numbered one manifests the same trends as the element numbered zero, and in all cases,

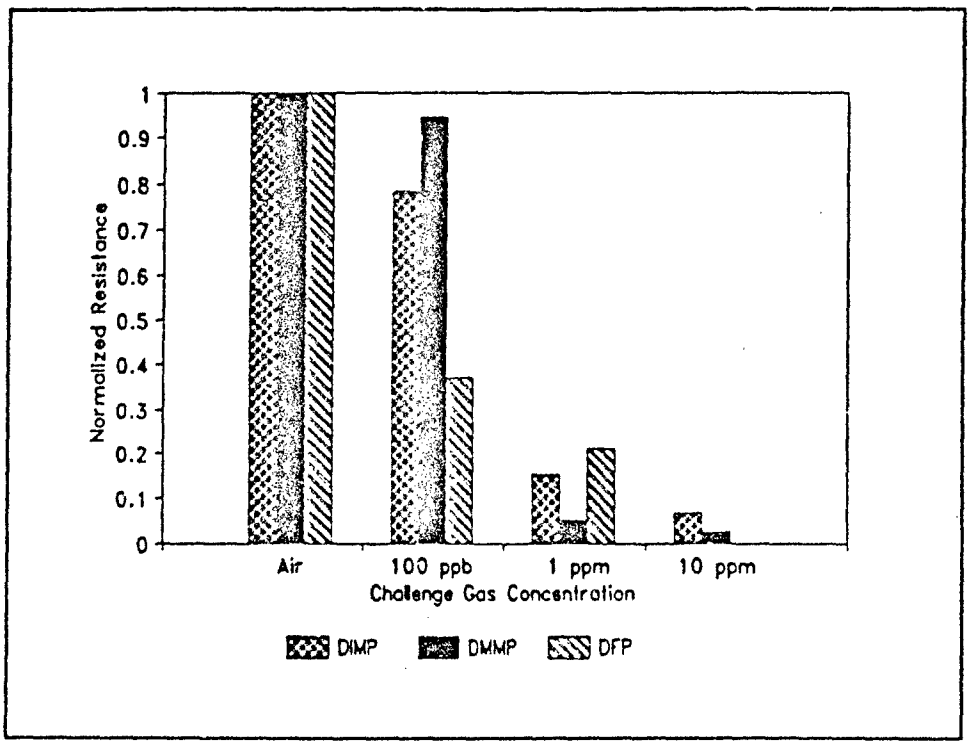

Figure 25. Copper Phthalocyanine Thin Film on Element #1, 2000Å Thick, Normalized DC Resistance Response at 30° C.

the resistance measurements are lower for the element numbered one compared to the element numbered zero.

These DC resistance changes compare favorably for DIMP exposures with the results reported by Captain Thomas Jenkins and Captain Jenny Shin, and for DMMP exposures with the results obtained by Captain Jenny Shin (3; 4). Additionally, the copper phthalocyanine DC resistance decreases as the DFP challenge gas concentration increases. This data is consistent with the results obtained by previous researchers at the Air Force Institute of Technology (2; 3; 4). It is important to note that the DC resistance changes were noted for a challenge gas concentration of 100 ppb for all three

challenge gases. This data agrees with the DIMP test results obtained by Captain John Wiseman and Captain Thomas Jenkins (2; 4). Testing conducted by Captain Jenny Shin noted no sensitivity to DIMP or DMMP at low concentrations (3). The measured DC resistance values indicate that copper phthalocyanine is more sensitive to DFP at a 100 ppb concentration compared to the other two challenge gases used in this investigation.

Reversibility was noted during the 70° C testing, as shown in Figure 26. The reversibility observed was not complete, since only approximately one half the magnitude of the initial change in the copper phthalocyanine response for any gas concentration was observed. The reversibility rate of the copper phthalocyanine was also very slow compared to the rate of the initial response. At 70° C, all recorded reversibility was on the order of hours for DIMP, DMMP, and DFP. All reversibility evaluations were only accomplished for a single cycle. That is, the microsensor test chamber is purged with filtered laboratory air followed by the test challenge gas and finally the challenge gas is purged with filtered laboratory air.

The time-domain response of an IGEFET using copper phthalocyanine as a chemically-sensitive thin film with DIMP as the challenge gas is shown in Figure 27. The input excitation pulse for the time-domain response, is a three volt ten microsecond pulse generated by a pulse generator (Hewlett-Packard, Model HP 8082A, Palo Alto, CA 94304). The frequency response of the copper phthalocyanine coated IGEFET using DIMP as the challenge gas is shown in Figure 28.

The lower sensitivity to DIMP is also reflected in the time-domain and frequency-domain data over the entire frequency range. The spectral analysis and time-domain

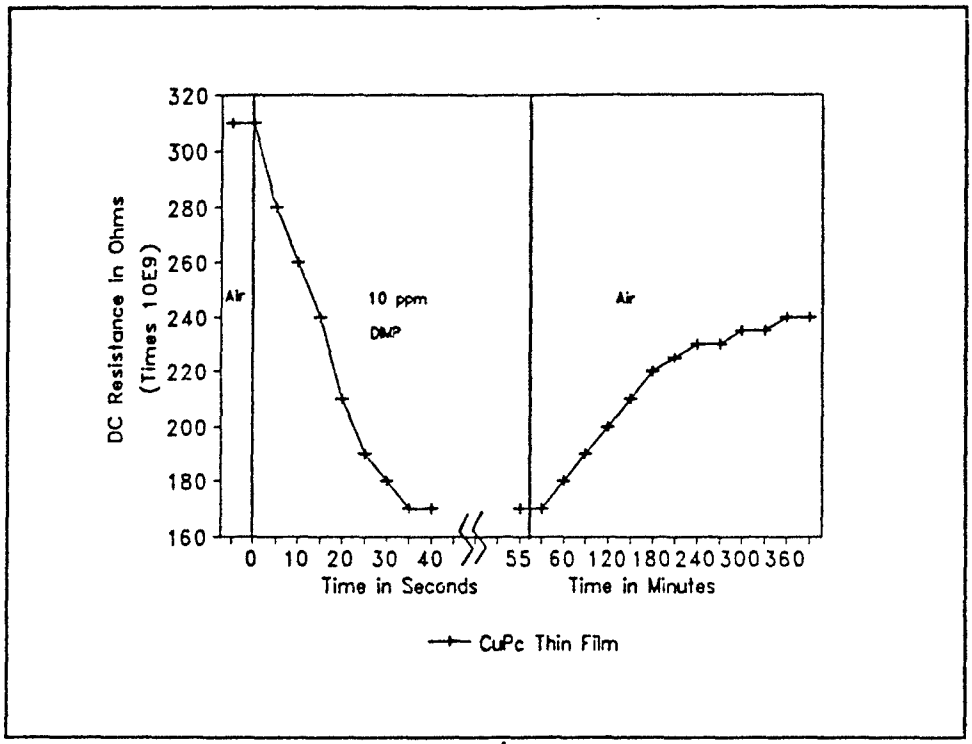

Figure 26. Copper Phthalocyanine, 2000Å Thick, DC Resistance Reversibility to 10 ppm DIMP Challenge Gas Exposure at 70° C.

response of the IGEFET using copper phthalocyanine as the chemically-sensitive thin film reflect the DC resistance changes for DIMP.

The spectral response of copper phthalocyanine when exposed to the DMMP challenge gas indicates a decrease in conduction at all measured frequencies when compared with the response obtained when copper phthalocyanine is exposed to filtered laboratory air. Comparing the results obtained using DMMP as the challenge gas to the results obtained by Captain Jenny Shin are inconclusive. Captain Shin's data indicates an initial decrease in electrical conductivity for a DMMP concentration of 500 ppb, and then an increase in electrical conductivity for a concentration of 3 ppm. Future research

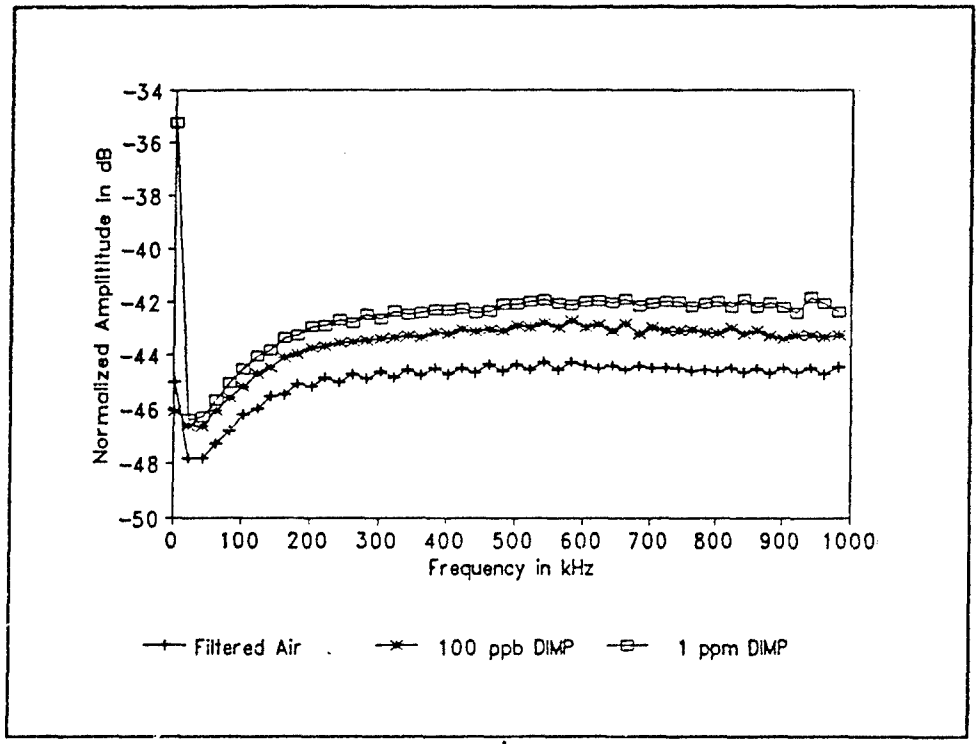

Figure 27. Copper Phthalocyanine, 2000Å Thick, Frequency-Domain Response to DIMP at 30° C.

should repeat the test exposing copper phthalocyanine to DMMP to verify the reaction of an IGEFET microsensor using copper phthalocyanine as the chemically-sensitive thin film. The set of data collected in this investigation contradicts the data collected by Caption Jenny Shin.

Changes in the response of copper phthalocyanine to DFP are similar to the responses observed for DIMP, only the changes in magnitude are smaller. The entire frequency response change for copper phthalocyanine when exposed to DFP is less than 0.5 dB at 100 ppb, and 1 dB at 3 ppm (the largest DFP challenge gas concentration

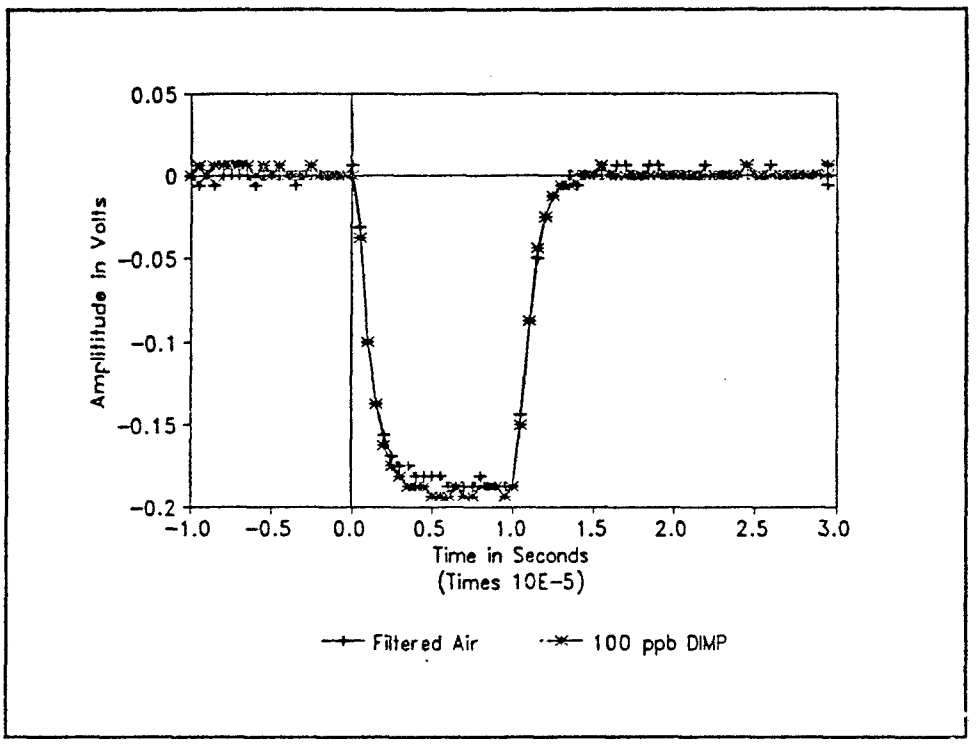

Figure 28. Copper Phthalocyanine Time-Domain Voltage-Pulse Response to DIMP at 30° C.

used). Copper phthalocyanine demonstrated no evidence of reversibility for any of the gas concentrations when tested at 30° C.

IGEFETs using copper phthalocyanine were also evaluated for their performance at elevated temperatures. Tests were conducted at 50° C and 70° C using all three challenge gases. At 50° C, the test results were nearly identical as those obtained at 30° C for copper phthalocyanine. Changes in DC resistance, time-domain response, and frequency-domain response were all comparable to the results obtained at 30° C and varied by only a few percent. No significant reversibility was noted when the copper phthalocyanine coated IGEFET was evaluated at 50° C.

When testing was conducted at 70° C, the sensitivity of the copper phthalocyanine coated IGEFET decreased significantly. Changes observed in the DC resistance were evaluated to be approximately one half those observed at 30° C. Similar results were observed in the frequency-domain data at 70° C. No observable changes were noted in the time-domain data obtained.

Individual gas testing of copper phthalocyanine indicated that DIMP, DMMP, and DFP all behaved similarly. Binary gas testing of copper phthalocyanine yielded very little useful data. The observed selectivity of copper phthalocyanine was very poor. This behavior was also reflected in the binary gas combination testing using all three challenge gases (DIMP with DMMP, DIMP with DFP, and DMMP with DFP).

DFPase Response

DFPase, an squid enzyme, was evaluated for its suitability as a chemically-sensitive thin film. The DFPase was deposited as a very thin film onto one or two elements of each IGEFET microsensor evaluated in this investigation (Chapter IV). DFPase reacted with all three challenge gases tested in this thesis. In every case, when the DFPase was exposed to one of the challenge gases (DIMP, DMMP, or DFP), the DC resistance decreased and the AC conductance increased.

The DFPase chemically-sensitive thin film is very sensitive to the DIMP challenge gas. The DC response of the DFPase thin film demonstrated a significant decrease in DC resistance when exposed to 100 ppb DIMP (Figure 29). Very little additional change was manifested when the DFPase was exposed to higher concentrations of DIMP. The time- and frequency-domain results of the DFPase thin film challenge gas

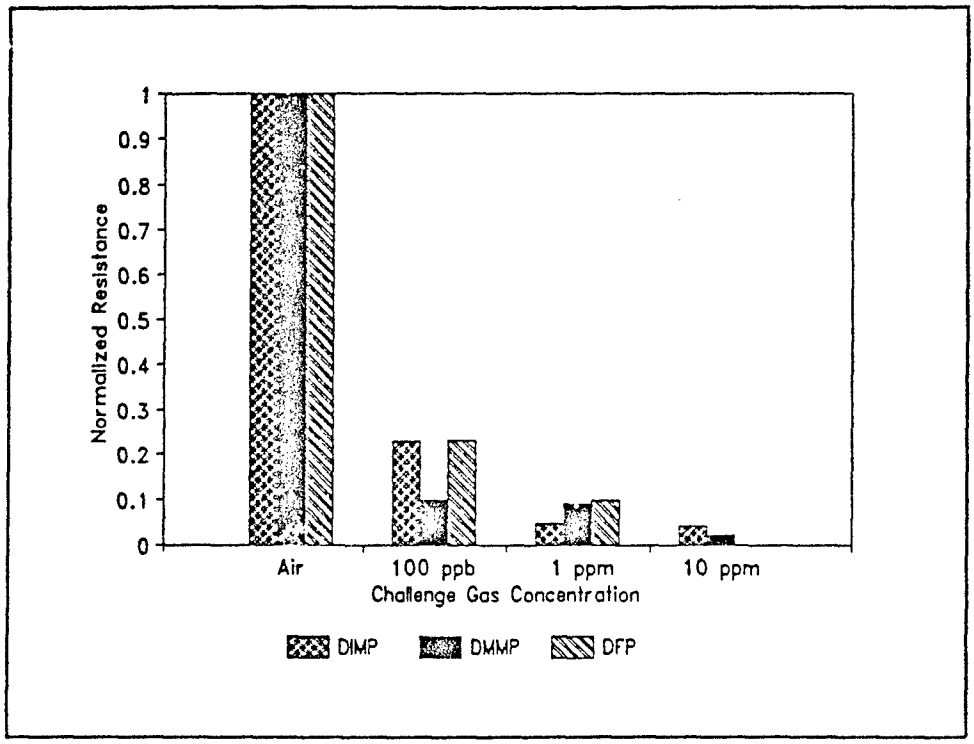

Figure 29. DFPase Normalized DC Resistance Response to the Three Challenge Gases at 30° C.

exposure reflected this trend in the plots for DFPase exposed to the DIMP challenge gas delivered at 100 ppb; they nearly exactly overlay the plots for the DIMP challenge gas delivered at one and ten ppm. The amplitude change for the frequency-domain plots were all two to three decibels higher when DFPase was challenged with the DIMP challenge gas. The time-domain pulse response magnitude only increased by approximately 10 millivolts relative to the unexposed response.

The DFPase thin film was not observed to be reversible for any of the tests conducted in this investigation. The lack of reversibility combined with the long

response time when the DFPase thin film was exposed to the challenge gases indicate that DFPase may bond with the challenge gas by absorption.

Time response testing was conducted with the chemically-sensitive DFPase thin film. The test was conducted by purging the test chamber with filtered laboratory for 45 minutes to allow the system to stabilize. The test chamber purge gas flow was terminated when the DIMP challenge gas concentration was established at 100 ppb. After the challenge gas concentration stabilized, it was directed through the test chamber containing the IGEFET microsensor (Figure 30). The DC resistance values were collected every ten seconds, and the challenge gas flow rates were sufficient to exchange three volumes of gas in 10 seconds. The response time of the chemically-sensitive thin film was approximately 50 seconds, a much slower response than that observed for some of the other chemically-sensitive thin films evaluated in this investigation.

The DFPase chemically-sensitive thin film reacted with the DMMP challenge gas with a more gradual response. When exposed to 100 ppb of DMMP, the DC resistance change was less than half the change observed for the DIMP challenge gas (Figure 30). The time-domain response for the three volt excitation pulse facilitated differentiating between the different concentrations of the DMMP challenge gas (Figure 31). This relative separation is apparent in both the DC resistance values and the maximum amplitude of the time-domain voltage pulse responses.

The frequency-domain data of the DFPase chemically-sensitive thin film is particularly of interest. There is a 5 to 10 decibel amplitude difference between the DFPase characteristic response to filtered laboratory air and when the DFPase thin film is exposed to 10 ppm DMMP. The DFPase thin film, exposed to 10 ppm DMMP, is

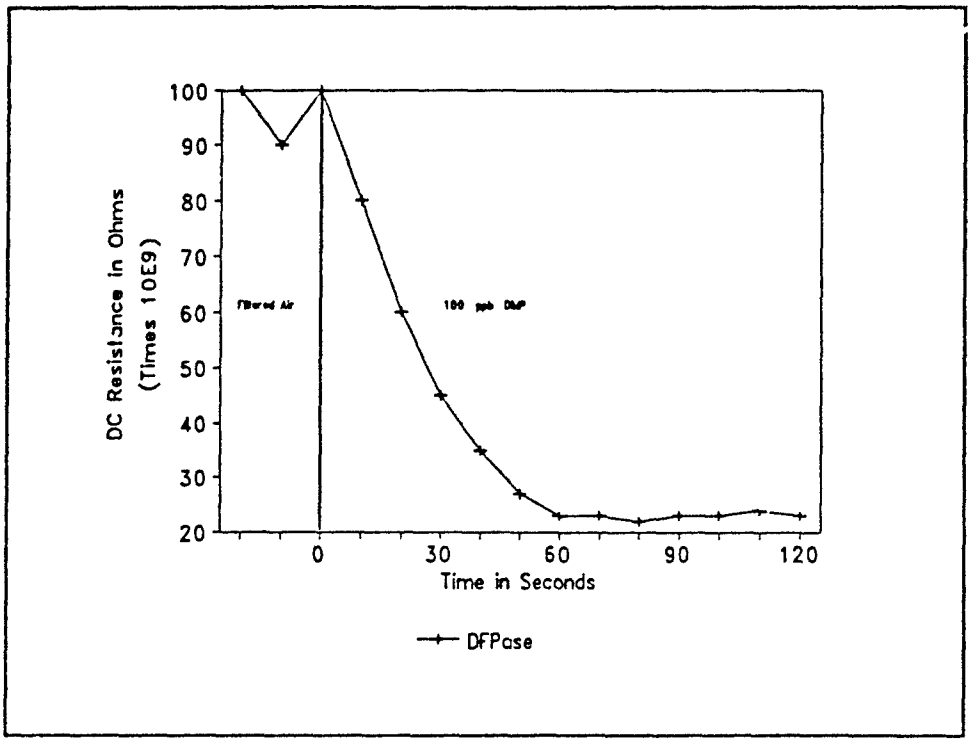

Figure 30. DFPase DC Resistance Change With Respect to Time for a 100 ppb DIMP Challenge at 30° C.

more conductive across the measured frequency range. When the DFPase thin film was exposed to 100 ppb DMMP, the AC conduction was essentially that in air for the low frequencies, and near the response level for the 10 ppm DMMP gas concentration challenge at the higher frequencies (Figure 32). The frequency-domain response observed for the DFPase thin film exposed to one ppm of the DMMP challenge gas is nearly identical to the frequency-domain response observed when the DFPase thin film was exposed to 10 ppm DMMP.

The chemically-sensitive DFPase thin film responded to the DFP challenge gas nearly the same as it did to the DMMP challenge gas. The observed change in DC

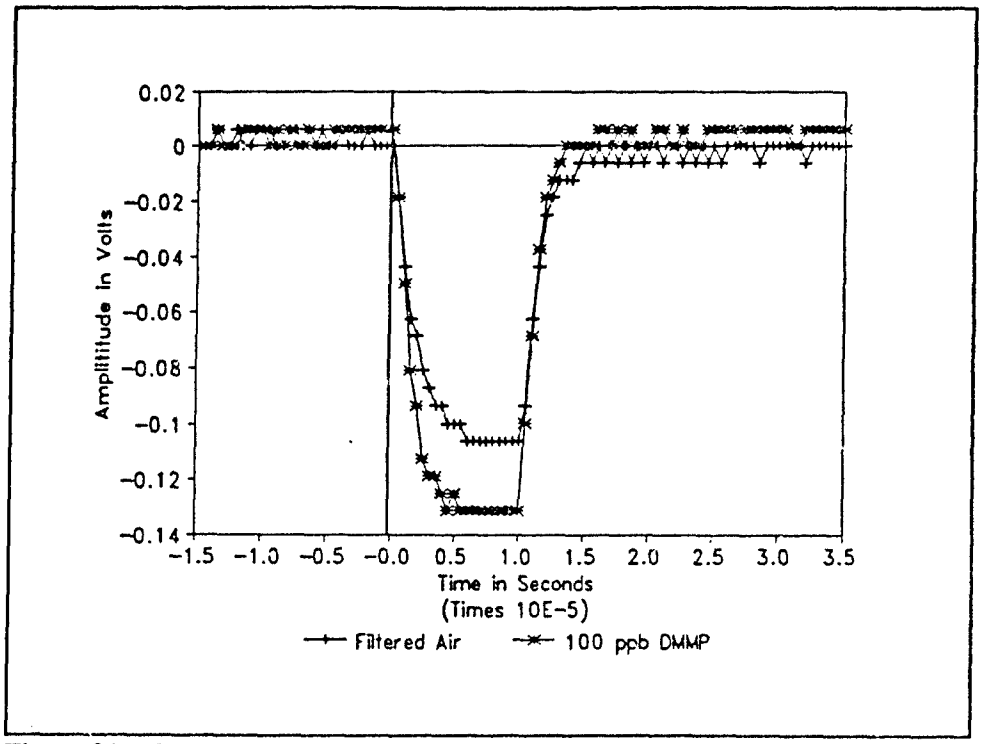

Figure 31. DFPase Time-Domain Voltage-Pulse Response to DMMP at 30° C.

resistance was almost identical. The frequency-domain response was within one decibel for the challenge gas concentration of one ppm and larger. One significant difference was manifested in the sensitivity of DFPase to the DFP challenge gas concentration of 100 ppb. DFPase was less sensitive to DFP at 100 ppb compared to the DMMP challenge gas at 100 ppb.

DFPase was tested at elevated temperatures of 50 and 70° C. The results of the elevated temperature testing indicated that DFPase ceased to be an effective chemically-sensitive thin film. Visual inspection indicated that the liquid carrier for the DFPase enzyme evaporated rapidly at the elevated temperatures. While there were some minor differences in the responses observed for the different challenge gases, the differences

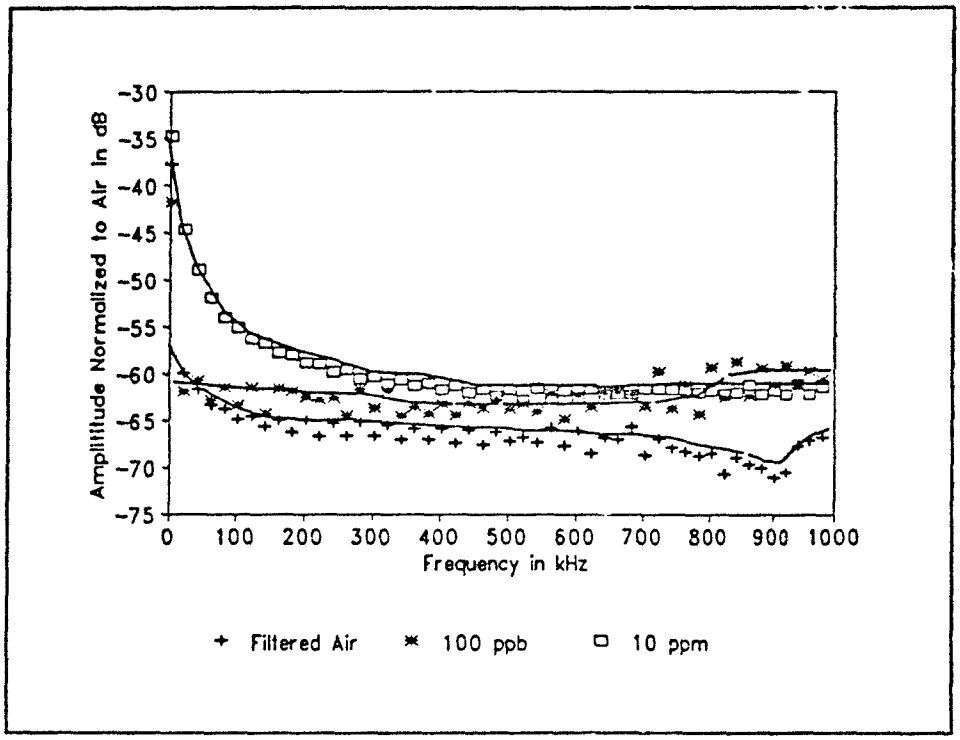

Figure 32. DFPase High-Frequency Response to DMMP at 30° C.

were too small to quantify selectivity. When the IGEFET microsensor coated with the DFPase thin film was exposed to the binary combinations of the challenge gas, no significant selectivity features were observed.

Succinyl Chloride Response

Succinyl chloride was found to be the most selective of the six different chemically-sensitive thin films evaluated. Succinyl chloride was observed to be sensitive to all three different challenge gases tested (DIMP, DMMP, and DFP); succinyl chloride behaved similarly to DIMP and DMMP, but completely different to DFP. The difference is evident in the DC resistance data for succinyl chloride (Figure 33).

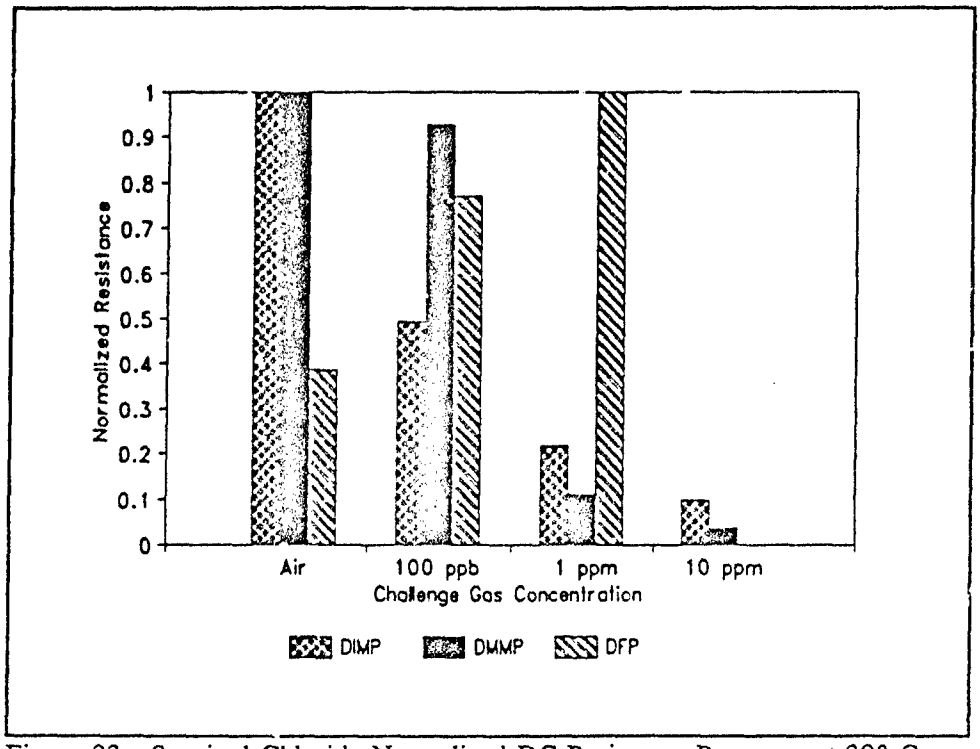

Figure 33. Succinyl Chloride Normalized DC Resistance Response at 30° C.

Whenever, the DIMP or DMMP challenge gas was supplied, the IGEFET microsensor element displayed a decrease in its DC resistance. The magnitude of the change was nearly the same for 1 ppm concentrations of both challenge gases, with the DC resistance decreasing by 80% from the response to filtered laboratory air. The differences in the resistance observed for the different elements containing succinyl chloride when exposed to air is due the variance in the thin film morphologies of the succinyl chloride material as deposited on the different IGEFET microsensor elements.

Time reversibility response testing of succinyl chloride was conducted for a DIMP challenge gas exposure at a concentration of one ppm, and then to laboratory air (Figure 34). The reversibility response observed was only approximately half the

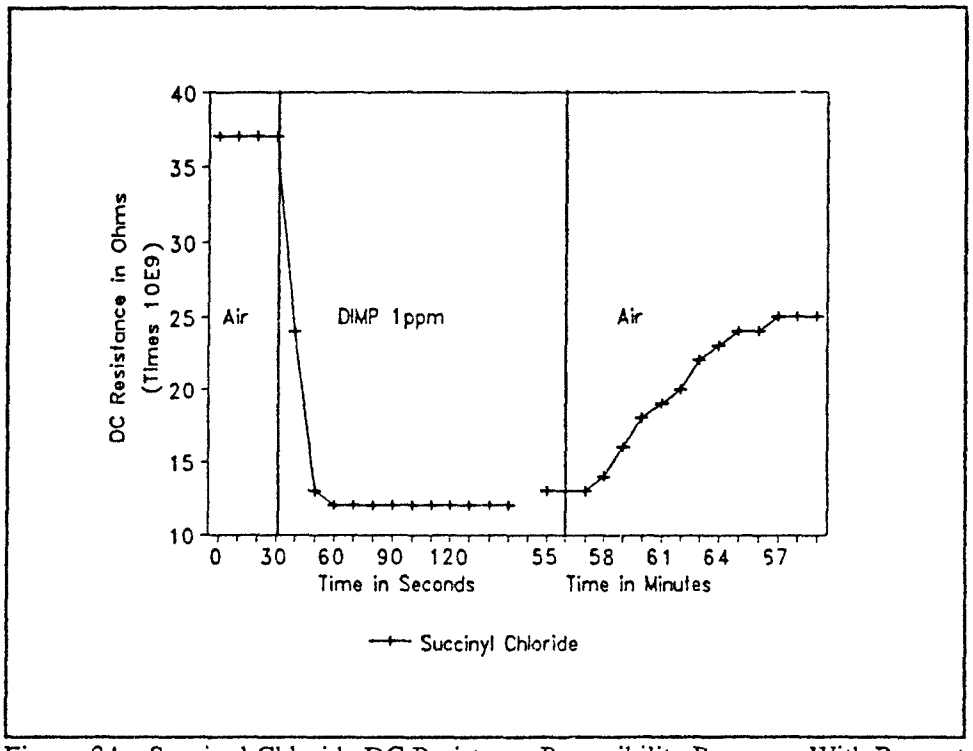

Figure 34. Succinyl Chloride DC Resistance Reversibility Response With Respect to Time for DIMP Challenge at 30° C.

original change in resistance observed when the challenge gas was introduced. The incomplete reversibility of the succinyl chloride thin film may be due to its observed evaporation. That is, the challenge gas may not be desorbing from the succinyl chloride thin film, but some of the succinyl chloride material may be evaporating, leaving an unexposed surface of succinyl chloride on the IGEFET microsensor.

The time-domain voltage pulse response for the succinyl chloride thin film is shown in Figure 35. Similar results are observed for the 100 ppb and 10 ppm values. The high-frequency response is shown in Figure 36. The response of succinyl chloride at one ppm is indistinguishable from the response for 100 ppb and 10 ppm. The only

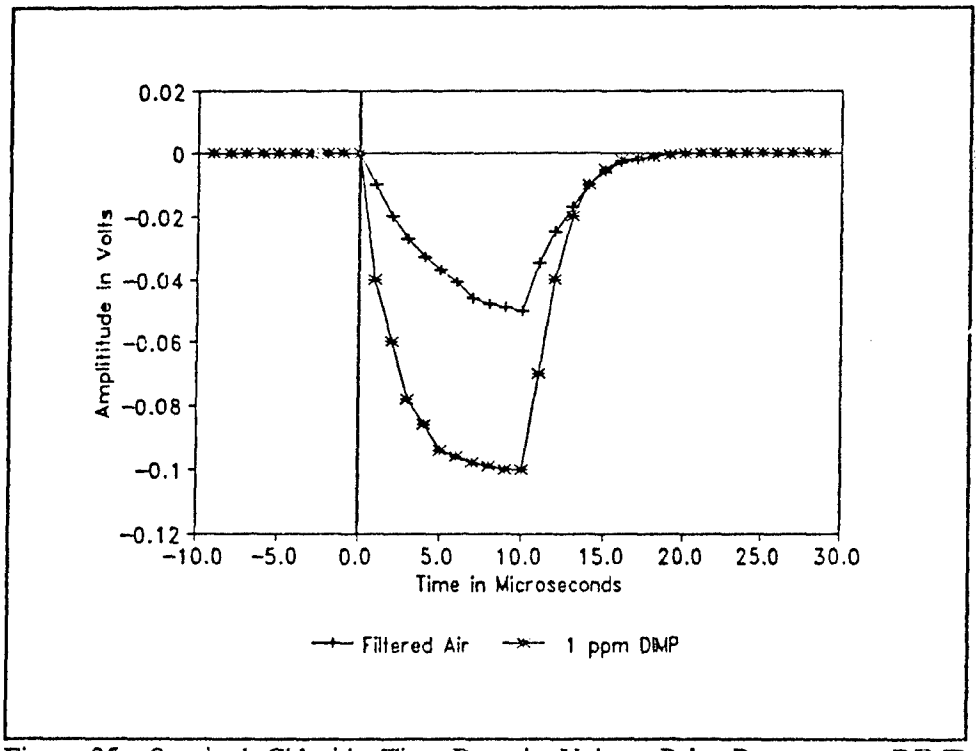

Figure 35. Succinyl Chloride Time-Domain Voltage-Pulse Response to DIMP Challenge at 30° C.

change observed for the different concentrations of the DIMP challenge gas are the changes observed in the film's DC resistance. Succinyl chloride responded to DMMP almost identically as it did to DIMP. The only detectable difference was observed in the DC resistance versus time responses (Figure 34). The time-domain and frequency-domain responses were the same as those observed for the DIMP challenge gas.

The selectivity of succinyl chloride became apparent when succinyl chloride was exposed to DFP as the challenge gas. As can be observed in Figure 34, the DC resistance increases when succinyl chloride is exposed to DFP. The corresponding time-domain response is shown in Figure 37. Both the DC resistance and the AC

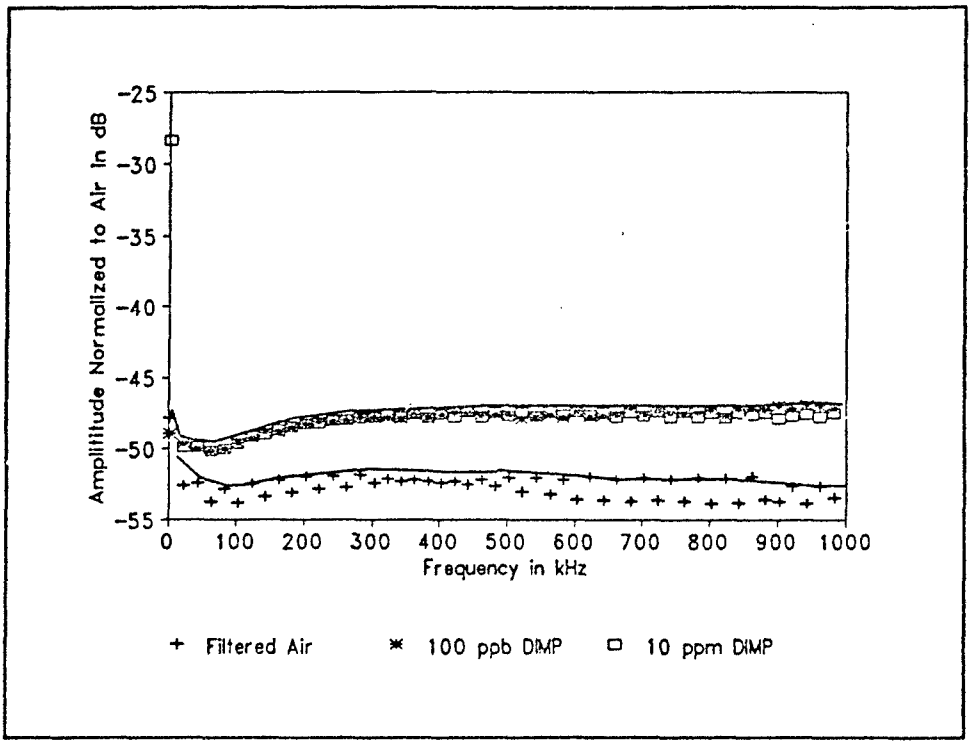

Figure 36. Succinyl Chloride Frequency-Domain Response to DIMP at 30° C.

conductance portion of the waveform were attenuated when succinyl chloride was exposed to DFP. Some change in the DC amplitude was observed at the larger DFP challenge gas concentrations.

The AC conductances were constant for the succinyl chloride thin film for the different challenge gas concentrations, indicating that the portion of the response signal that is determined by the AC conductance of the thin film is constant after the initial exposure to the DFP challenge gas.

The succinyl chloride film's frequency response is depicted in two different figures. Figure 38 depicts the low-frequency response of the succinyl chloride film to the DFP challenge gas. The conductance of the succinyl chloride chemically-sensitive

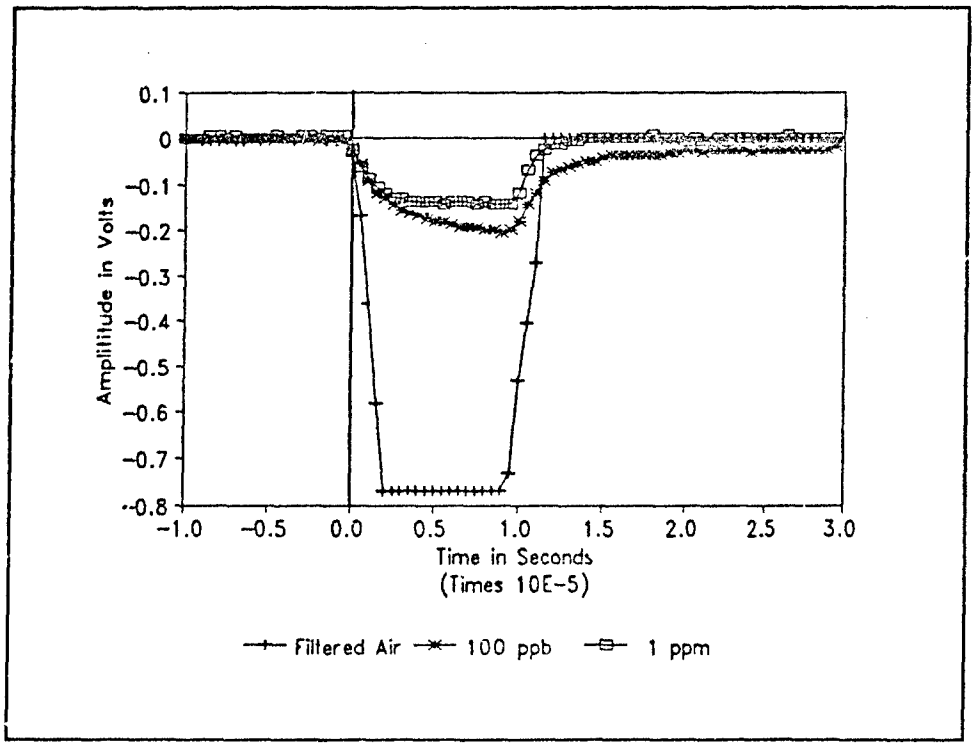

Figure 37. Succinyl Chloride Time-Domain Voltage-Pulse Response to DFP at 30° C.

thin film to laboratory air is clearly larger compared to when the DFP challenge gas is present. However, the response differentiation to different concentrations of DFP are essentially indistinguishable.

The high-frequency response of the succinyl chloride chemically-sensitive thin film is shown in Figure 39. Similar to the low-frequency response, differentiation between the filtered laboratory air response and the DFP challenge gas response is clearly visible. The response differential spans 10 to 15 dB over the measured frequency range. However, the change in the film's response for different challenge gas concentrations

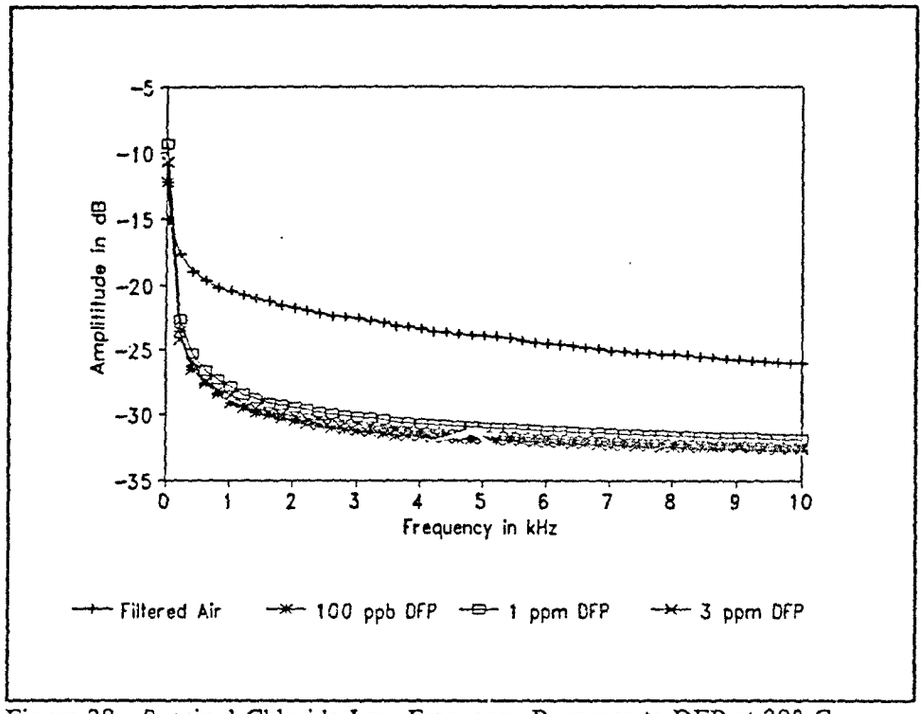

Figure 38. Succinyl Chloride Low-Frequency Response to DFP at 30° C.

is unmeasurable. The noise level in the response signals are more significant compared to the observed changes in the responses.

Elevated temperature testing was attempted using succinyl chloride as a chemically-sensitive thin film. The results of the elevated temperature testing suggested that the succinyl chloride evaporated so fast that detailed test results were unattainable at 50 or 70° C. However measurements that were rapidly accomplished with succinyl chloride films at 50° C indicated that the response was similar to its response at 30° C. (Insufficient time was available to collect a full data set to verify these measurements).

Binary combinations of DIMP, DMMP, and DFP were also evaluated during the testing of IGEFET microsensors containing succinyl chloride as the chemically-sensitive

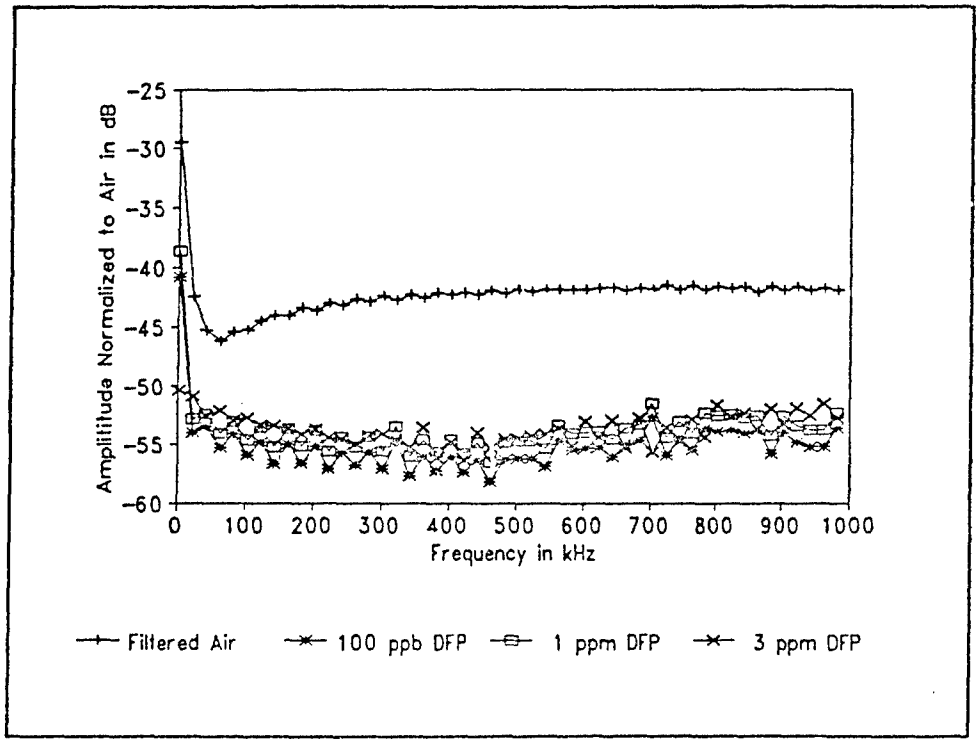

Figure 39. Succinyl Chloride High-Frequency Response to DFP at 30° C.

thin film. Due to physical limitations of the gas generation system, only constant ratios of the challenge gas could be generated. The ratio of DMMP to DFP is 1000 to 230; that is, when DMMP is delivered at one ppm the DFP must be delivered at 230 ppb. Similarly, the ratio of deliverable DIMP to DFP is 500 ppb DIMP to 230 ppb DFP.

When the mixture of the DIMP and DMMP challenge gases was evaluated, the results mimicked the individual challenge gas results for DIMP and DMMP. These results were anticipated since both the DIMP and DMMP reactions with succinyl chloride were nearly identical. The response of succinyl chloride when exposed to the combination of one ppm DMMP combined with 230 ppb DFP was very similar to the results observed for the challenge gas combination of DIMP with DFP. Whenever DFP

was present in the binary challenge gas mixture, the AC conductance decreased by approximately 5 dB. Figure 40 depicts the high-frequency response of succinyl chloride when exposed to a challenge gas mixture of 500 ppb DIMP and 230 ppb DFP. Whenever the binary challenge gas combination contained DFP, the measured frequency-domain amplitude also decreased, which mimicked the response of the film when exposed only to the DFP challenge gas. The exposure to the DFP gas component dominated the response when present in the binary gas mixture since the AC conduction decreased; however, the change in magnitude was approximately one decibel less than the change in magnitude observed when the challenge gas was exclusively DFP.

The DC resistance response of the binary challenge gas testing of succinyl chloride yielded the expected results. The chemically-sensitive succinyl chloride thin film exposed to the binary gas combination of DIMP and DMMP decreased in resistance. Since succinyl chloride reacted to both DIMP and DMMP singularly in a similar manner, the results of the binary gas combination were completely as expected. When the IGEFET microsensor element containing succinyl chloride was exposed to a binary gas combination containing DFP, the DC resistance increased, indicating that the succinyl chloride response to DFP was the dominate reaction of the three challenge gases. The magnitude of the DFP dominance is even more evident than depicted in the data because the DFP response represented the smaller percentage challenge gas in the binary gas mixture for the two of the three binary gas combinations tested where DFP was present.

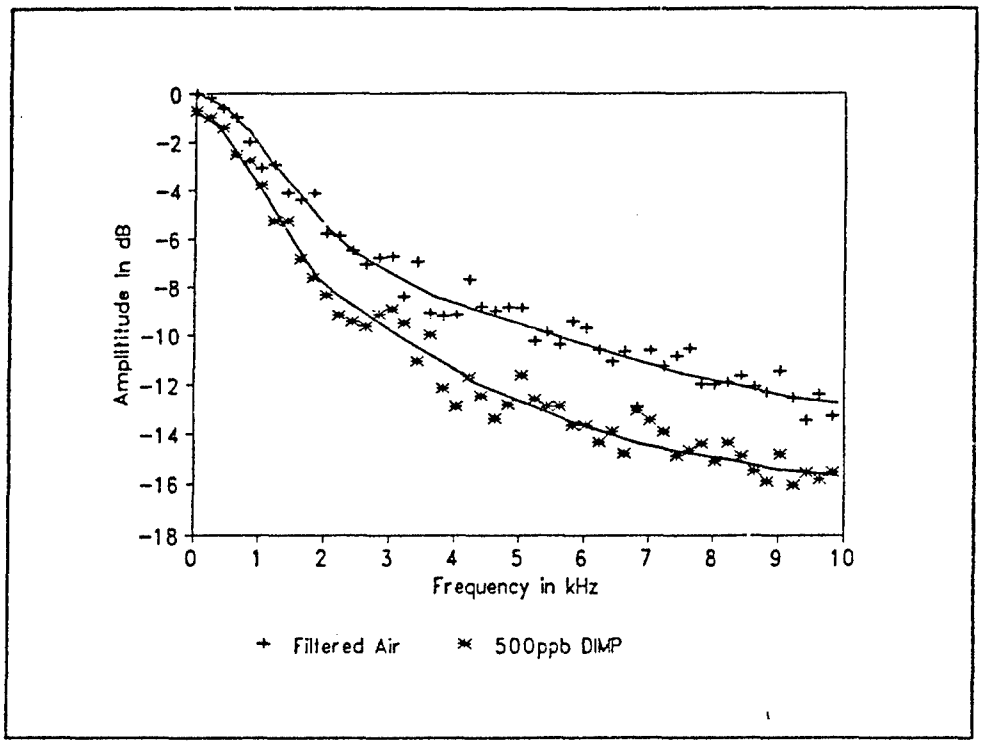

Figure 40. Succinyl Chloride High Frequency Response to 500 ppb of DIMP and 230 ppb of DFP at 30° C.

Succinylcholine Chloride Response

Evaluation of the IGEFET microsensors coated with succinylcholine chloride indicated moderate sensitivity, excellent DFP selectivity, and only partial reversibility. Succinylcholine chloride was sensitive to all three challenge gases. The DC resistance values decreased for all of the challenge gases used to expose an IGEFET microsensor element coated with the succinylcholine chloride chemically-sensitive thin film (Figure 41). The observed DC resistance response was similar for DIMP, DMMP, and DFP.

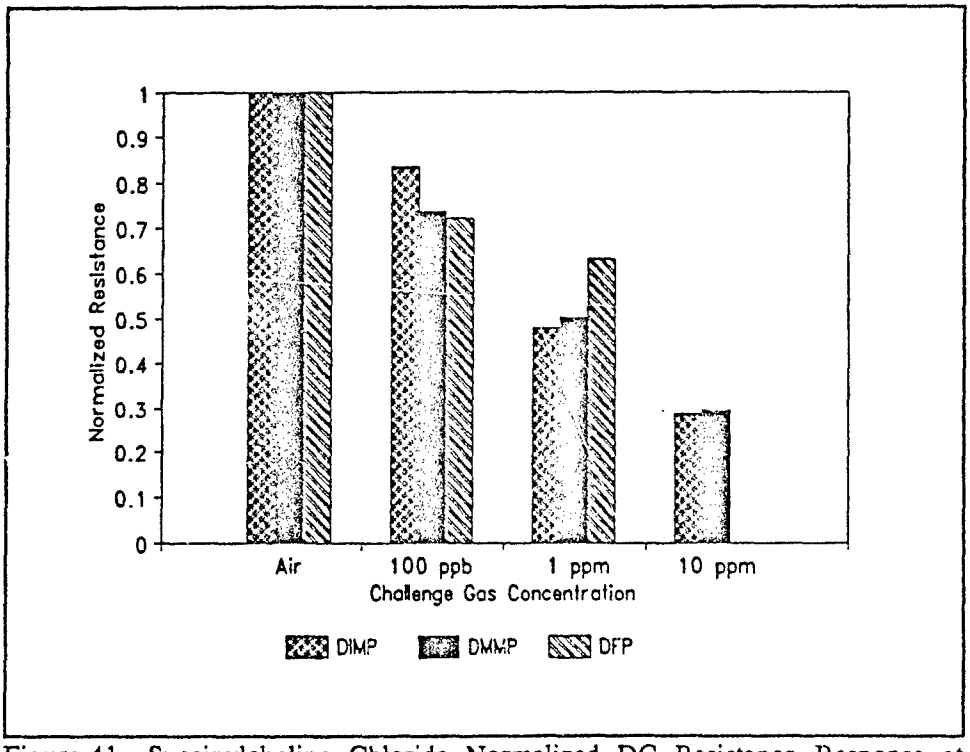

Figure 41. Succinylcholine Chloride Normalized DC Resistance Response at 30° C.

The reversibility of the succinylcholine chloride coated IGEFETs were only partial. Measurable increases in DC resistance were observed after the challenge gas was purged from the test chamber. The increase in the DC resistance was approximately one fourth the observed decrease in the DC resistance measured when the succinylcholine chloride thin film was exposed to the challenge gas. This change was observed for both the DIMP and DMMP challenge gases. There was no observable change in the AC conduction for succinylcholine chloride thin film in either the time- or frequency-domains.

No reversibility was noted after the succinylcholine chloride thin film was exposed to the DFP challenge gas. The notch filter response associated with the succinylcholine chloride thin film was still present 18 hours after the DFP challenge gas exposure had been discontinued.

The succinylcholine chloride thin film reacted to DIMP with an increase in the AC conductance over the measured frequency which extended to 1 MHz. Captain Jenny Shin's initial evaluation of the succinylcholine chloride thin film coating indicated a decrease in the DC resistance when the succinylcholine chloride thin film was exposed to DIMP. The frequency response plot of the succinylcholine chloride thin film coating, when exposed to the DIMP challenge gas, is shown in Figure 42. As depicted in the plot, the succinylcholine chloride thin film coating demonstrated a 5 dB increase in conduction when exposed to a DIMP challenge gas concentration of 100 ppb. When larger concentrations of DIMP were used to expose the IGEFET element coated with the succinylcholine chloride thin film material a small increase in the AC amplitude of approximately 2 dB was achieved when a 100 ppb DIMP challenge gas was used to expose the IGEFET.

The time-domain response of the IGEFET microsensor element coated with the succinylcholine chloride chemically-sensitive thin film when exposed to a DIMP challenge of 100 ppb is shown in Figure 43. The time-domain response was very similar for three DIMP challenge gas concentrations: 100 ppb, 1 ppm, and 10 ppm.

The frequency- and time-domain response of an IGEFET microsensor element using the succinylcholine chloride chemically-sensitive thin film when exposed to the DMMP challenge gas was very similar to the responses observed when the microsensor

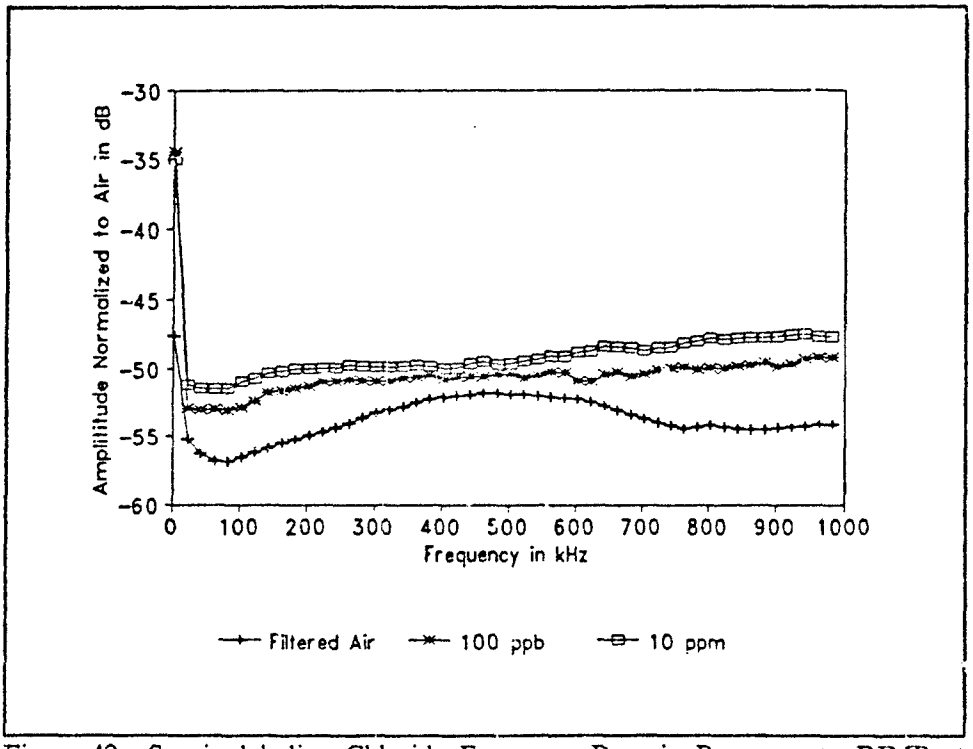

Figure 42. Succinylcholine Chloride Frequency-Domain Response to DIMP at 30° C.

element was exposed to the DIMP challenge gas. The succinylcholine chloride thin film coating's DC resistance change observed when exposed to the DMMP challenge gas in the frequency- and time-domain responses were almost identical to the responses observed when the succinylcholine chloride thin film was challenged with DIMP. The small differential between the two different challenge gas responses could be attributed to the differences in the thin film morphologies and the errors in the measurement process.

The IGEFET microsensor element coated with succinylcholine chloride demonstrated a unique selectivity signature when exposed to the DFP challenge gas. A

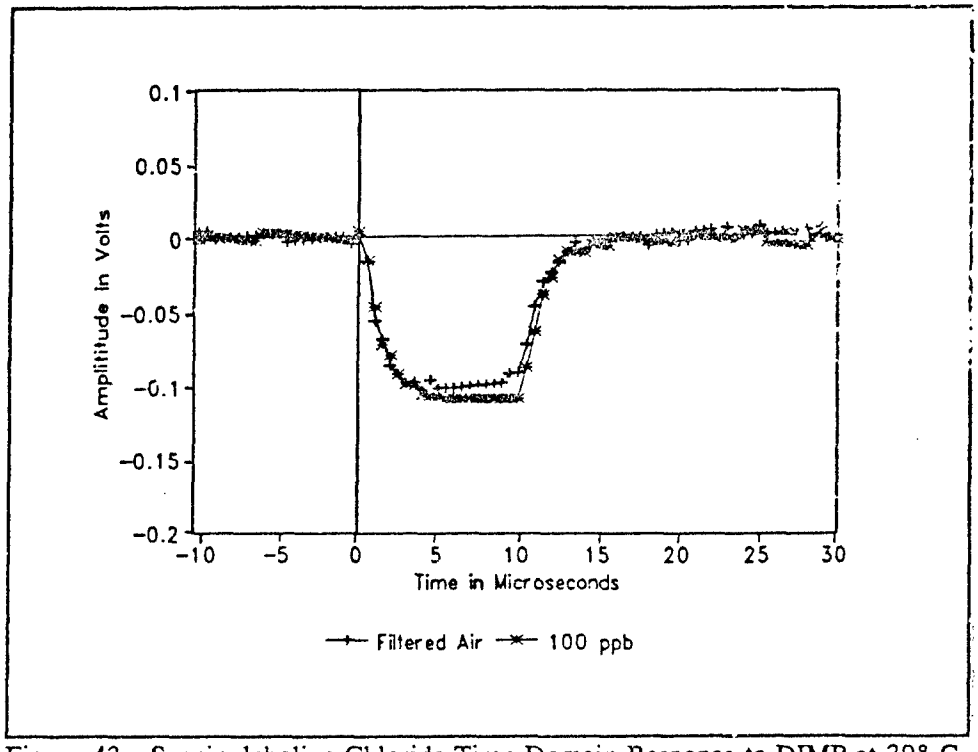

Figure 43. Succinylcholine Chloride Time-Domain Response to DIMP at 30° C.

very obvious band-reject (notch) filter response was observed whenever the IGEFET microsensor element was coated with the succinylcholine chloride thin film and exposed to the DFP challenge gas (Figure 44). The observed notch depth was greater than 10 dB for all exposure concentrations of the DFP challenge gas.

The frequency shift of the notch filter response appears to be an artifact of the challenge gas flow rate in the test chamber, and not attributed to the challenge gas concentration (Figure 45). The frequency shift associated with the notch depth was initially observed with the DFP challenge gas concentration of three ppm. The unique nature of the notch filter response warranted additional investigation. A π resistance

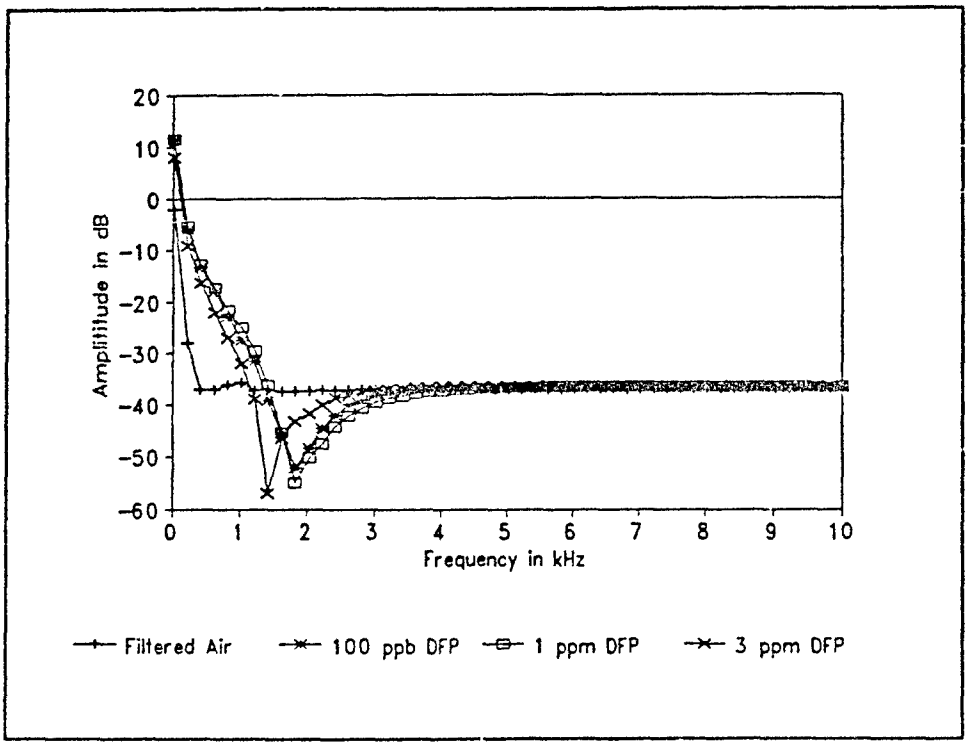

Figure 44. Succinylcholine Chloride Low-Frequency Response to DFP at 30° C.

capacitance model of the IGE structure response to succinylcholine chloride is presented in Appendix G.

Additional testing was then conducted to determine the source of the variations in the notch filter frequency. The evaluations demanded that only one parameter be varied at a time to determine the source of the observed results. Holding the challenge gas concentration constant and varying the challenge gas flow rate, the result was the observed shift in the notch filter's frequency. Next, the test was repeated by holding the challenge gas flow rate constant and varying the challenge gas concentration. The observed result displayed no appreciable change in notch filter's frequency. The change in the notch filter's frequency could be due to surface cooling of the microsensor since

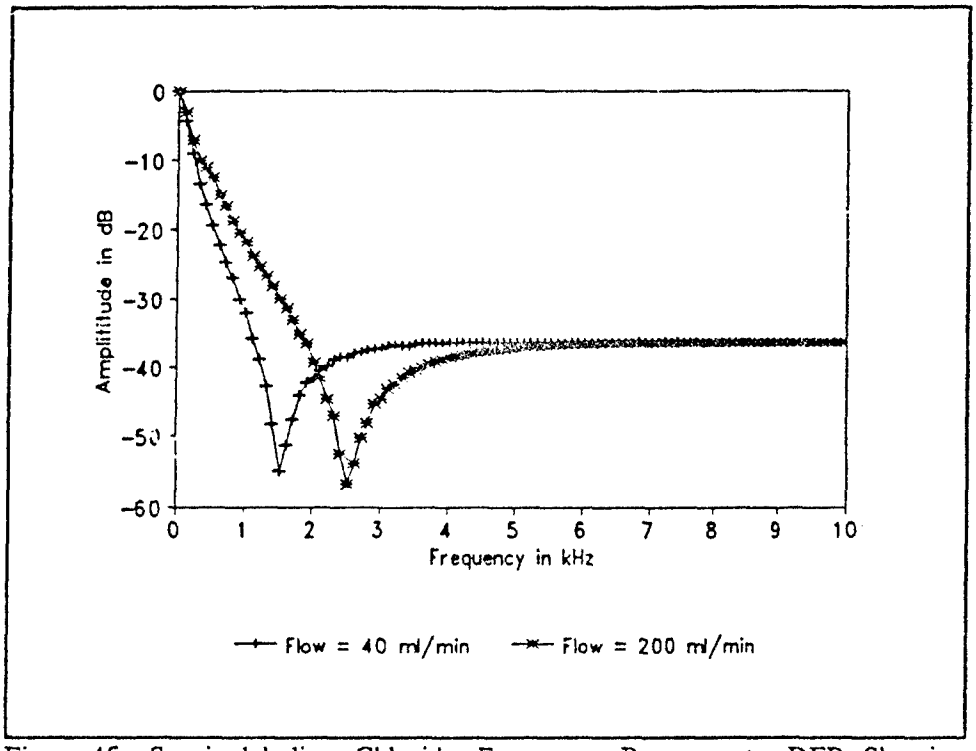

Figure 45. Succinylcholine Chloride Frequency Response to DFP Showing Frequency Shift Due to Challenge Gas Flow Rate Changes.

it was heated to 30° C, as measured by the *in situ* thermocouple, and the challenge gas was delivered to the test chamber at a temperature of 23°C, as measured by the combined hygrometer/thermometer (Thunder Scientific Corp., Model HS-ICHDT-2A, Albuquerque, NM 87123). Changes in the test chamber pressure probably would not account for the notch filter's frequency change observed since the total change in the test chamber pressure was less than 0.5 pounds-per-square-inch-gauge.

Elevated temperature testing of the succinylcholine chloride thin film provided no useful results because the succinylcholine chloride thin film ceased to be sensitive to any challenge gas after the IGEFET microsensor was heated to 50° C.

Testing binary gas mixtures of DIMP, DMMP, and DFP provided some interesting results. When the succinylcholine chloride thin film was exposed to a combination of the DIMP and DMMP challenge gas, the changes in DC resistance and AC conductance were identical to the changes observed when this chemically-sensitive thin film was individually exposed to DIMP and DMMP.

When DFP was one of the gases in the binary combination of challenge gases, the notch filter frequency response was observed (Figure 46). The characteristic notch filter response was manifested for both binary combinations of the challenge gases containing DFP. In Figure 46, when DMMP was delivered at a concentration of one ppm, DFP was delivered at a concentration of 230 ppb. Additionally, when DMMP was delivered at a concentration of ten ppm, DFP was delivered at a concentration of 2.3 ppm.

The notch filter response observed for the binary gas combination of DMMP and DFP occurred at seven kilohertz instead of the 1.3 to 1.9 kHz frequency observed when the microsensor was exposed to the DFP challenge gas, and it may be attributable to a difference in the thin film thickness. The frequency shift noted for changes in gas flow rate, for the change in the notch filter frequency was not responsible for the frequency difference noted during the binary gas testing, since the gas flow rate was controlled to 100 milliliters per minute. The chemically-sensitive thin film of succinylcholine chloride on the IGEFET microsensor element was slightly thicker for the test conducted using the binary gas combination of DMMP and DFP. This finding was verified by coating two elements of an IGEFET microsensor with different thicknesses of succinylcholine chloride. The thinner the coating, the lower the observed notch filter frequency. The magnitude of the notch did not appear to be affected. This data indicates a need for

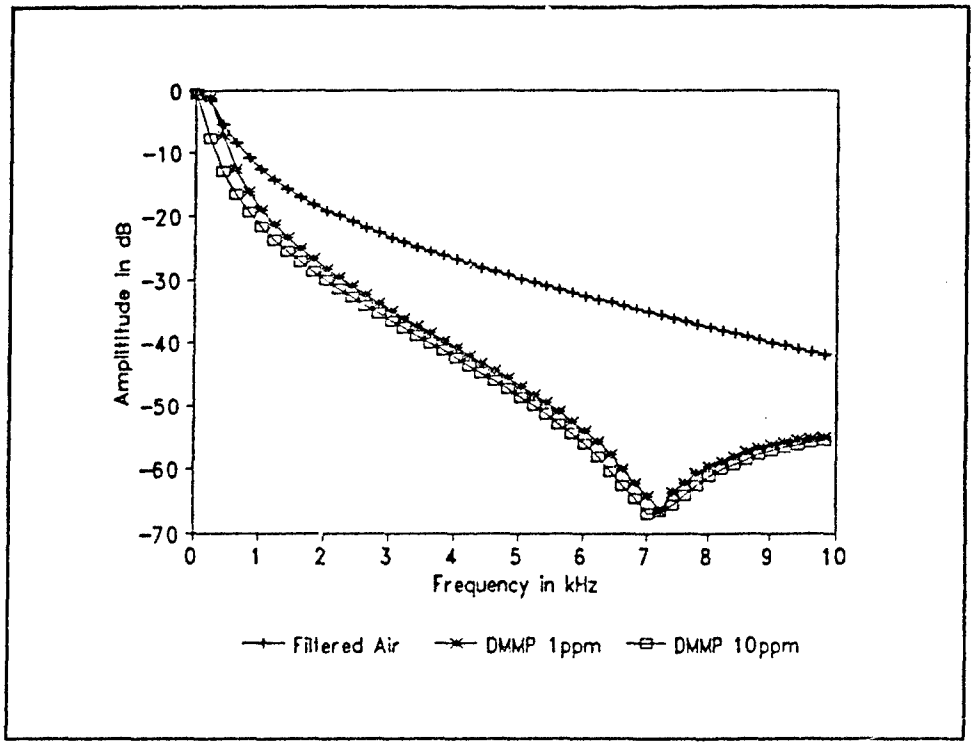

Figure 46. Succinylcholine Chloride Low-Frequency Response to the Binary Combination of (1 ppm DMMP and 230 ppb DFP) and (10 ppm DMMP and 2.3 ppm DFP) at 30° C.

developing a method that will more accurately control the applied film thicknesses of the organic films used in this research.

2-Naphthol(β) Response

Evaluation of IGEFET microsensor elements coated with 2-Naphthol(β) as the chemically-sensitive thin film indicated sensitivity to all three challenge gases (DIMP, DMMP, and DFP). The observed changes in DC resistance and AC conductance were very significant. The response of 2-Naphthol(β) was completely reversible within a period of approximately 10 minutes. The selectivity of 2-Naphthol(β) was very poor

because there were very minimal variations between the responses associated with the three different challenge gases.

All measurements collected for the 2-Naphthol(β) chemically-sensitive thin film required that the measurements be taken rapidly since 2-Naphthol(β) sublimes at a fairly rapid rate, even at 30° C (the lowest temperature at which testing was conducted). Several tests using 2-Naphthol(β) as the chemically-sensitive thin film were repeated due to its rapid sublimation. The reasonable limit for completing the measurements for a 2-Naphthol(β) thin film was approximately 90 minutes. Significant changes in the film's performance after 90 minutes would seriously influence the real data trends. To insure the data's integrity, the 2-Naphthol(β) thin film was reapplied, and the challenge gas exposure evaluations were repeated for 2-Naphthol(β) whenever the total IGEFET microsensor testing consumed more than 90 minutes.

The 2-Naphthol(β) thin film reacted to DIMP with a significant increase in the DC resistance (Figure 47). This behavior agrees with the data collected by Captain Jenny Shin (3). The time-domain data reveals that the signal level is highly attenuated when 2-Naphthol(β) is exposed to the DIMP challenge gas (Figure 48). When larger concentrations of the DIMP challenge gas are exposed to the microsensor, the results manifest more significant attenuation of the response signal. Since the signal levels of the exposed time-domain response of the 2-Naphthol(β) thin film are so small, it is impractical to derive the AC conductance from the time-domain response.

The IGEFET microsensor coated with the 2-Naphthol(β) chemically-sensitive thin film was evaluated for reversibility. In each trail, the 2-Naphthol(β) thin film would completely reverse its response within ten minutes of the challenge gas flow being

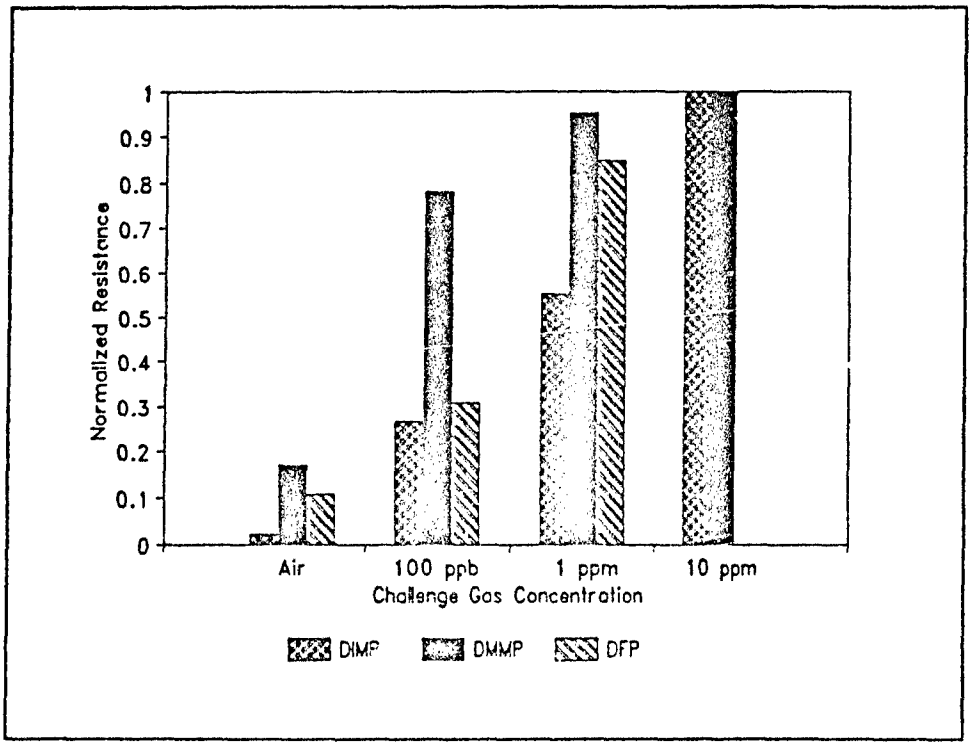

Figure 47. 2-Naphthol(β) Normalized DC Resistance Response at 30° C.

terminated, and a purge gas flow of 90% relative humidity laboratory air was allowed to flow through the test chamber. The observed reversibility may be due to the surface of the 2-Naphthol(β) thin film subliming and leaving an unexposed surface of 2-Naphthol(β). This occurrence seems probable since the rate of observed sublimation was fairly high at several hundred angstroms per hour (as estimated by observing the 2-Naphthol(β) through a microscope with an interferometer installed).

The frequency-domain response of the chemically-sensitive 2-Naphthol(β) thin film yields the same results as the time-domain response (Figure 49). As depicted in Figure 49, the conductance of the chemically-sensitive 2-Naphthol(β) thin film is several decibels less when exposed to 100 ppb of the DIMP challenge gas. The electrical

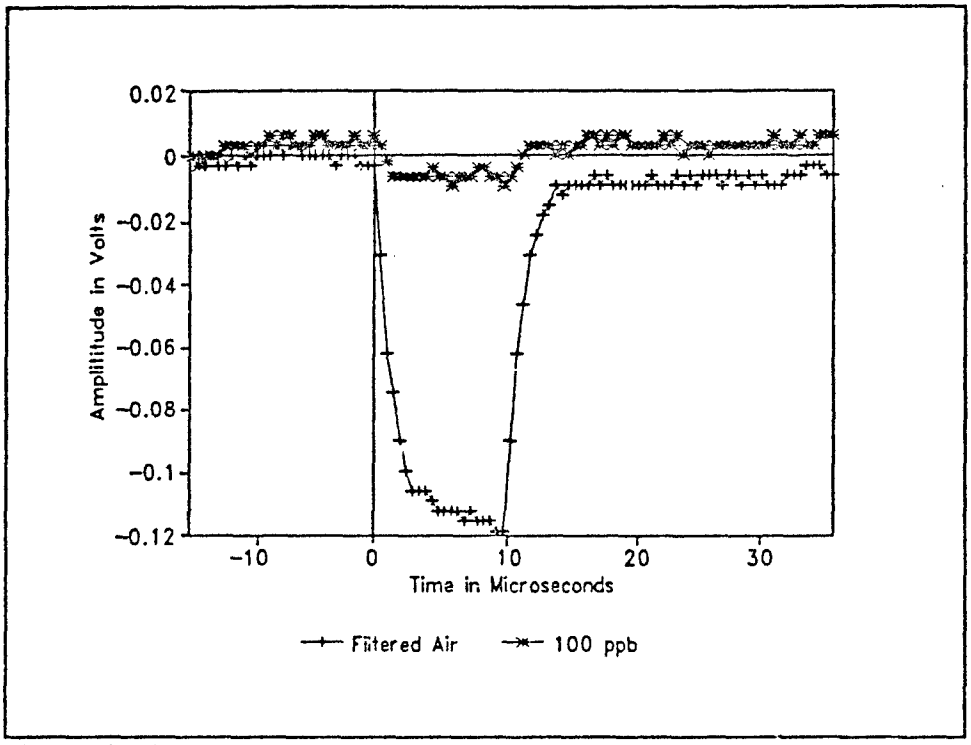

Figure 48. 2-Naphthol(β) Time-Domain Voltage-Pulse Response to DIMP at 30° C.

conductance was further reduced when the DIMP challenge gas concentration was increased to 1 and 10 ppm. When the challenge gas concentration was increased to 10 ppm, the response signal level was so small that it became indistinguishable from the instrumentation noise level. The frequency-domain response for the low-frequency range (1 to 10 kilohertz), yielded results.

The results for challenging the IGEFET microsensor with the DMMP challenge gas paralleled the results obtained when the 2-Naphthol(β) thin film was exposed to the DIMP challenge gas. The observed change in the DC resistance increased by a factor of two over the that was indicative of the DMMP challenge gas response. The changes

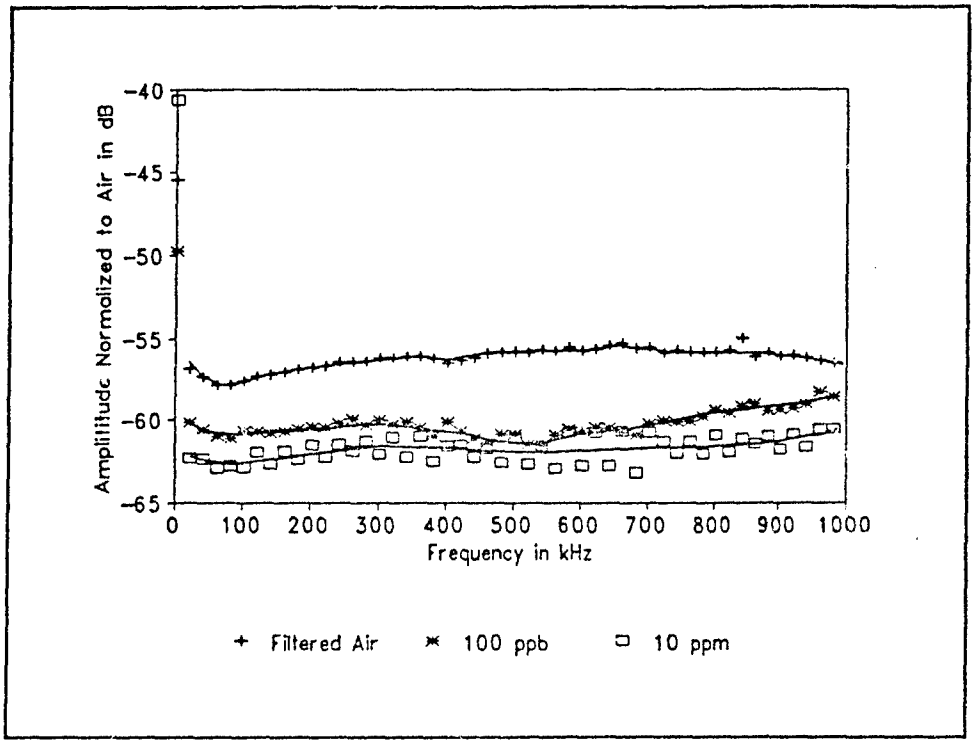

Figure 49. 2-Naphthol(β) Frequency-Domain Response to DIMP at 30° C.

in the 2-Naphthol(β) thin film time-domain response, when challenged with DMMP, was also observed to be similar to the results for the DIMP challenge gas.

Time-domain response testing was conducted on the 2-Naphthol(β) thin film with a one ppm DMMP challenge gas concentration. The IGEFET microsensor element using 2-Naphthol(β) as the chemically-sensitive thin film changed its resistance to 95% of the final resistance value 15 seconds after the DMMP challenge gas was introduced into the test chamber. The actual response time of the 2-Naphthol(β) thin film may be faster than that observed since it requires nearly 40 seconds to exchange three volumes of the challenge gas in the microsensor's test chamber.

The IGEFET microsensor using 2-Naphthol(β) as the chemically-sensitive thin film was evaluated for its response to the DFP challenge gas at concentrations of 100 ppb, 1 ppm and 3 ppm. The change in DC resistance for the 2-Naphthol(β) thin film exposed to DFP was nearly identical to the changes observed when 2-Naphthol(β) was exposed to the DIMP challenge gas. The observed time- and frequency-domain responses were nearly the same as for the DFP challenge gas exposure responses indicative of the DIMP and DMMP challenge gases.

Given the problems observed with the 2-Naphthol(β) thin film subliming in a few hours at room temperature, the success of elevated temperature testing seemed unlikely. A thin film of 2-Naphthol(β) was applied to an IGEFET element, and then the IGEFET was placed under a microscope. A heater strip was connected to the back of the microsensor, and ten watts of heat were applied. By the time the microsensor's temperature reached 42° C, the 2-Naphthol(β) thin film had completely sublimed.

The 2-Naphthol(β) thin film was also evaluated for its response to binary combinations of the DIMP, DMMP, and DFP challenge gases. The results of testing 2-Naphthol(β) when exposed to the three different binary challenge gas combinations (DIMP with DMMP, DIMP with DFP, and DMMP with DFP) were identical to the results obtained when 2-Naphthol(β) was tested with the individual challenge gases.

L-Histidine Dihydrochloride Response

L-histidine dihydrochloride was also used as a chemically-sensitive thin film on the IGEFET microsensors in this research. The data collected indicated that L-histidine dihydrochloride is sensitive to all three of the challenge gases (DIMP, DMMP, and

DFP). The L-histidine dihydrochloride thin film was sensitive to the smallest concentration of the challenge gases tested (100 ppb). No selectivity of L-histidine dihydrochloride was observed during testing with the different challenge gases. Reversibility of the L-histidine dihydrochloride thin film's exposure response was not observed. Sensitivity of the L-histidine dihydrochloride thin film decreased dramatically as the temperature of the IGEFET microsensor was increased.

The L-histidine dihydrochloride thin film reacted with the DIMP challenge gas and manifested a decrease in its DC resistance. (Figure 50). The magnitude of the DC resistance change was most significant when the microsensor was challenged with a 100 ppb concentration of DIMP, with the DC resistance decreasing by over 60% from the value obtained for exposure to filtered laboratory air. The DC resistance change for larger concentrations of the DIMP challenge gas were also tested, but they only produced small increments in relation to the initial change in the film's DC resistance.

No reversibility of the chemically-sensitive L-histidine dihydrochloride thin film was observed for any of the challenge gases. The DC resistance change response to exposure of the DFP challenge gas was similar to that observed for copper phthalocyanine and succinyl chloride (Figure 51). The DFP flow rate was such that this measurement required approximately 50 seconds to exchange three volumes of the challenge gas in the test chamber containing the IGEFET microsensor. Even with the slow test chamber's gas volume turnover, 90% of the resistance change occurred in the first 30 seconds after the challenge gas was introduced.

The time-domain response of the L-histidine dihydrochloride thin film exposed to DIMP is shown in Figure 52. The time-domain response for the L-histidine

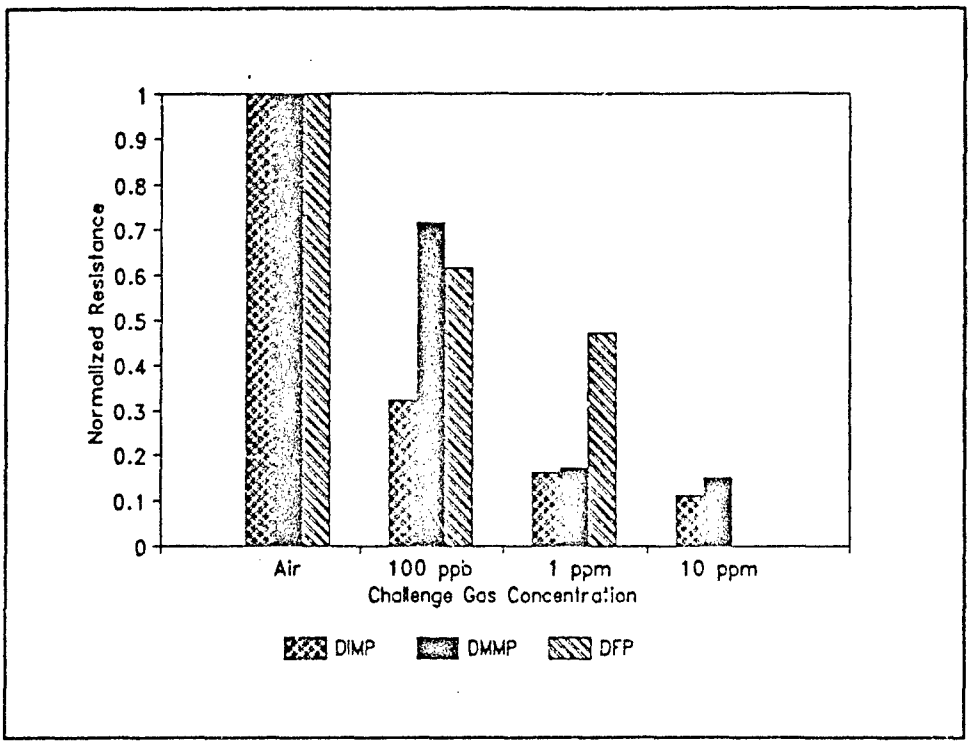

Figure 50. L-Histidine Dihydrochloride Normalized DC Resistance Response at 30° C.

dihydrochloride thin film exposed to the DIMP challenge gas indicates both an increase in the DC and AC conductance. The time-domain response for the L-histidine dihydrochloride thin film when exposed to larger concentrations of the DIMP challenge gas was similar to the waveform observed for the 100 ppb concentration of DIMP. The total variation in the time-domain pulse response was measured for three concentrations (100 ppb, 1 ppm, and 10 ppm); it was less than 5 millivolts.

The frequency-domain response for an IGEFET microsensor element coating with the L-histidine dihydrochloride thin film exposed to the DIMP challenge gas is shown in Figure 53. Figure 53 demonstrates that the L-histidine dihydrochloride thin film is

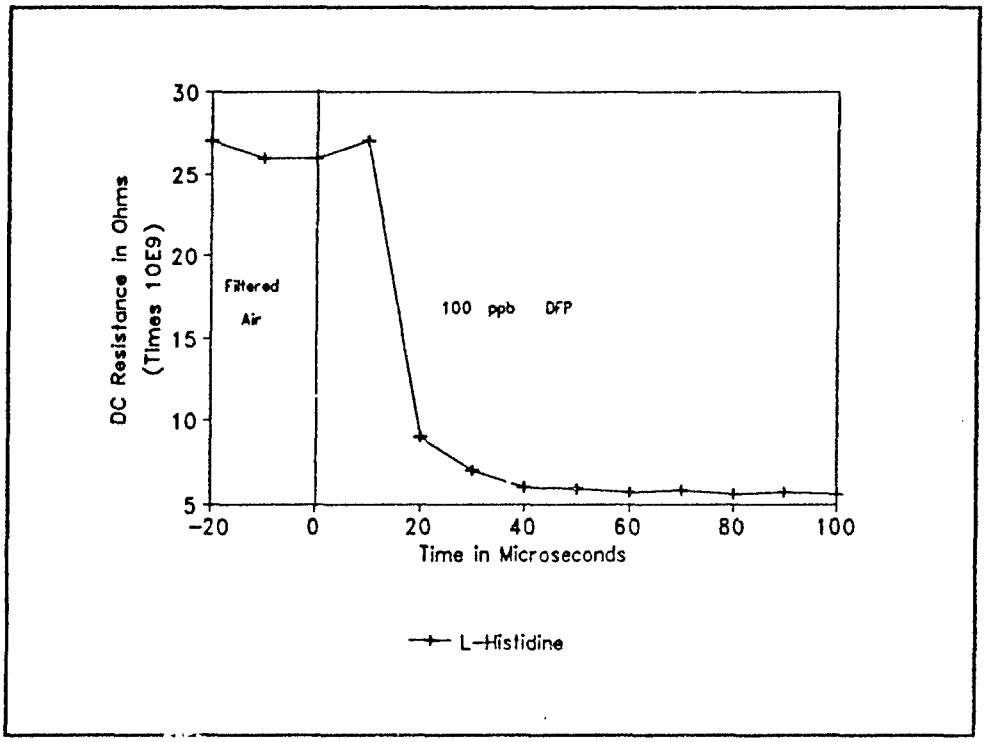

Figure 51. L-Histidine Dihydrochloride DC Resistance Change With Respect to Time due to a 100 ppb DFP Challenge at 30° C.

very sensitive to the DIMP challenge gas, indicated by the same response for 100 ppb as for a 10 ppm DIMP exposure. The change in electrical conductance is approximately 10 decibels across the measured frequency range -- a strong, easily recognizable signal difference.

The L-histidine dihydrochloride thin film's reaction to DMMP was very similar to the reaction observed with the DIMP challenge gas. The change in resistance was slightly smaller for the DMMP challenge gas compared to that observed for DIMP. The time-domain response to the three volt 10 microsecond duration excitation pulse was nearly identical to the response obtained when DIMP was the challenge gas. The

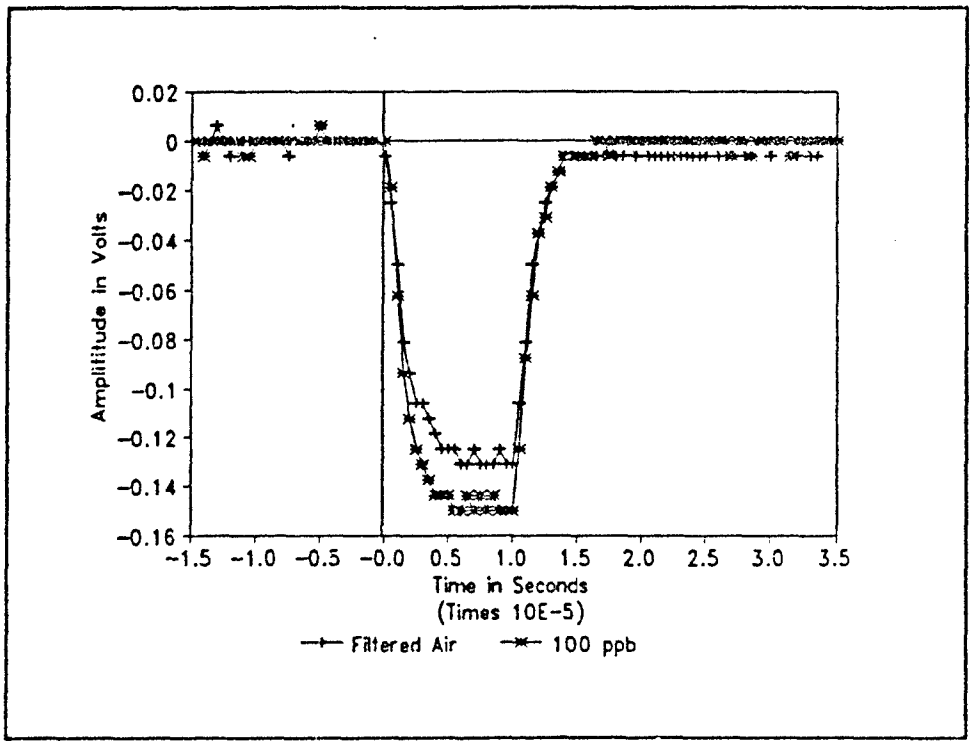

Figure 52. L-Histidine Dihydrochloride Time-Domain Voltage-Pulse Response to DIMP at 30° C.

observed change in the time-domain response was less than 10 millivolts relative to the response measured for the 100 ppb DIMP challenge gas for all the concentrations of DMMP tested (100 ppb, 1 ppm, and 10 ppm).

The L-histidine dihydrochloride thin film's frequency response to DMMP was slightly smaller in magnitude compared to the frequency response results obtained for DIMP. The total change in the magnitude of the L-histidine dihydrochloride thin film's frequency response when exposed to DMMP was only approximately 7 decibels. The observed change in the frequency response was 10 decibels when the L-histidine dihydrochloride thin film was exposed to the DIMP challenge gas.

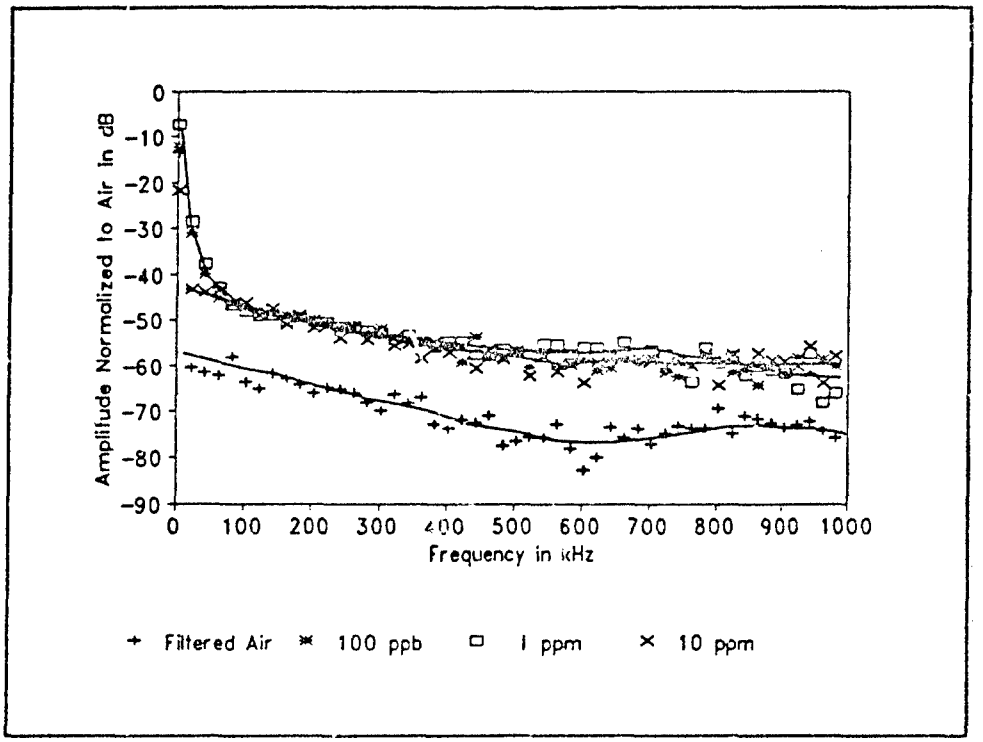

Figure 53. L-Histidine Dihydrochloride Frequency-Domain Response to DIMP at 30° C.

An IGEFET microsensor element coated with the L-histidine dihydrochloride thin film was also tested for its response to the DFP challenge gas. The results were similar to those observed for DIMP and DMMP. The L-histidine dihydrochloride thin film was less-sensitive to DFP compared to the other two challenge gases. The DC resistance changes were nearly identical to those observed for the DIMP challenge gas. The changes in AC conductance were slightly different though. The change in magnitude for the frequency response data was smaller when DFP was the challenge gas (Figure 54). For example, the L-histidine dihydrochloride thin film is much less sensitive to DFP at 100 ppb. At very low frequencies, the L-histidine dihydrochloride

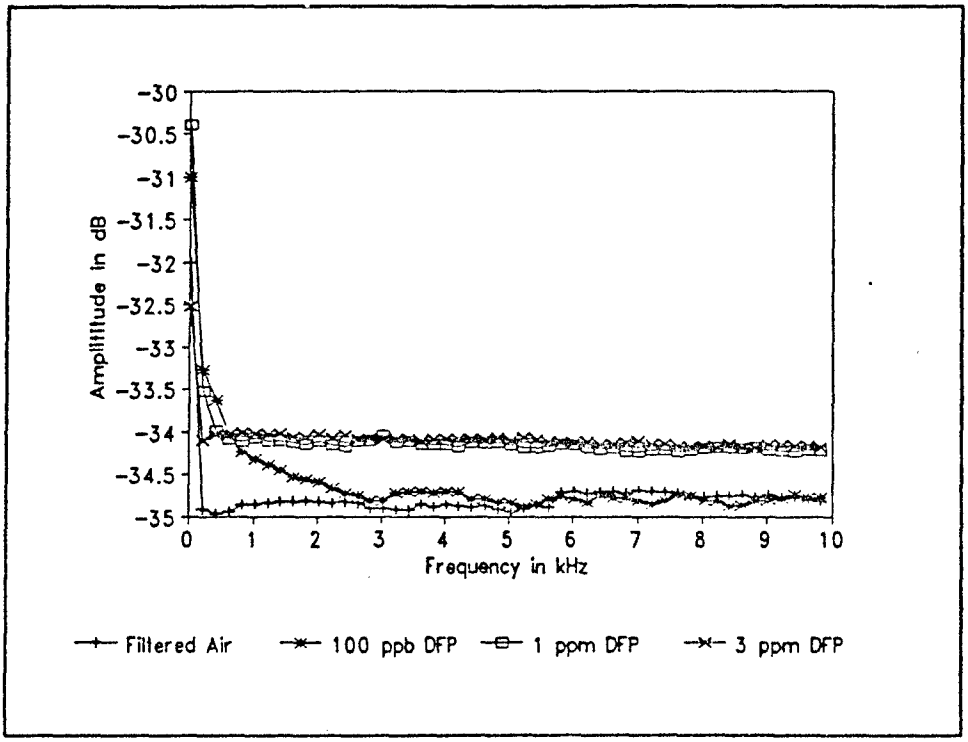

Figure 54. L-Histidine Dihydrochloride Low-Frequency Response To DFP at 30° C.

thin film is sensitive to DFP, but at frequencies above three kilohertz, the L-histidine dihydrochloride thin film is not sensitive to DFP.

Elevated temperature testing was conducted using the L-histidine dihydrochloride thin film, but no useful results were obtained. When the IGEFET was heated to 50° C, the L-histidine dihydrochloride thin film lost most of its sensitivity and reacted only very weakly with the challenge gases. The largest change in the frequency response data was a one decibel change in AC conductance when the L-histidine dihydrochloride thin film was exposed to a one ppm concentration of the DIMP challenge gas. The observed

changes in the DC resistance were so small, that the results were within the measurement system's noise margin.

Testing the L-histidine dihydrochloride thin film using binary combinations of the challenge gases reinforced the earlier data which indicated a lack of selectivity. This data is as expected since the response of the L-histidine dihydrochloride thin film was very similar for the three challenge gases. That is, all the binary challenge gas test results mimicked the results obtained for the individual challenge gases.

Chemically-Sensitive Thin Film Response by Challenge Gas

The data in this section will be presented for each challenge gas with respect to the six different chemically-sensitive thin film candidates. In each subsection, the normalized DC resistance data for copper phthalocyanine and DFPase will be presented first, followed by the four organic thin films (succinylcholine chloride, succinyl chloride, 2-naphthol(β), and L-histidine dihydrochloride).

Response to DIMP. The normalized DC resistance response of copper phthalocyanine is the similar to the results that have been observed by previous investigators (2; 3; 4). The observed DC response is quite noticeable for even the smallest concentration evaluated (100 ppb) as shown in Figure 55. The normalized DC resistance response for copper phthalocyanine indicates a decrease in resistance of approximately 20% when exposed to a 100 ppb DIMP challenge. The normalized DC resistance response of the copper phthalocyanine thin film indicates that it is sensitive to DIMP at concentrations as small as 100 ppb; however, the relative change in

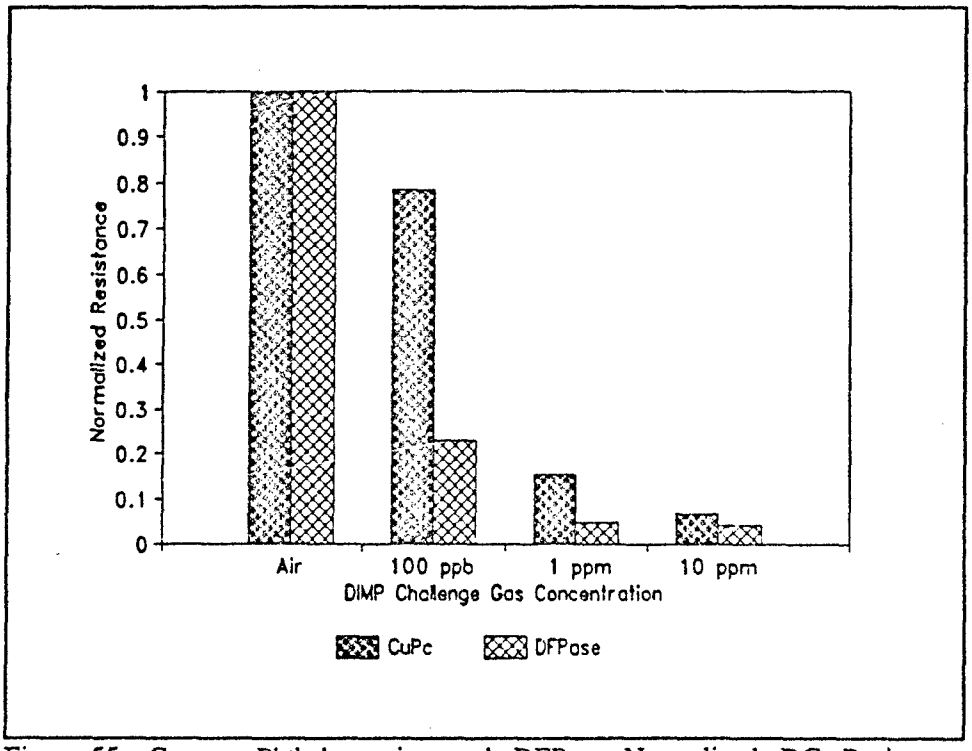

Figure 55. Copper Phthalocyanine and DFPase Normalized DC Resistance Response to DIMP at 30° C.

resistance is relatively small. Copper phthalocyanine's DC resistance response is sensitive to the concentration of the DIMP challenge gas that is delivered to the test chamber. The DFPase is very sensitive to the DIMP challenge gas. DFPase's normalized DC resistance response changes quite dramatically to the 100 ppb gas concentration, with the DC resistance decreasing over 75% when exposed to the challenge gas. Challenge gas concentrations greater than one ppm have no additional effect on the DC resistance response of the DFPase.

The normalized DC resistance response to DIMP of the four organic chemically-sensitive thin film candidates (succinylcholine chloride, succinyl chloride, 2-naphthol(β),

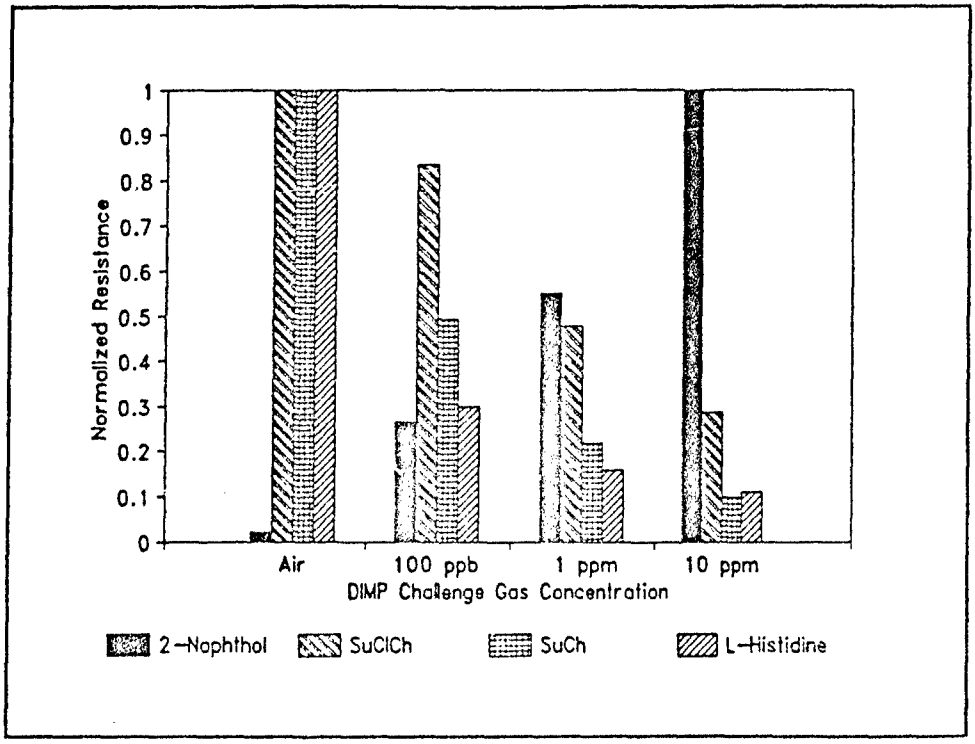

Figure 56. 2-Naphthol(β), Succinylcholine Chloride (SuClCh), Succinyl Chloride (SuCh), and L-Histidine Dihydrochloride Normalized DC Resistance Responses to DIMP at 30° C.

and L-histidine dihydrochloride) are presented in Figure 56. The response of the 2-naphthol(β) chemically-sensitive thin film is displayed with the values normalized with respect to the DC resistance values obtained when the 2-naphthol(β) was exposed to 10 ppm DIMP challenge gas. Succinylcholine chloride, succinyl chloride, L-histidine dihydrochloride are all normalized with respect to their respective DC resistance responses obtained when exposed to filtered laboratory air. With respect to normalized the DC resistance responses, L-histidine dihydrochloride and succiryl chloride DC resistance decreased over 50% when exposed to 100 ppb challenge gas concentration, making them the most sensitive to DIMP. Succinylcholine chloride DC resistance

decreased less than 20% when exposed to 100 ppb DIMP challenge gas making it the smallest relative response of the four organic thin films evaluated.

The normalized frequency response of copper phthalocyanine and DFPase using their response to filtered laboratory air as the reference level is shown in Figure 57. The observed normalized frequency response is very similar to the results observed for their normalized DC resistance response. The normalized frequency response for copper phthalocyanine when exposed to 100 ppb DIMP indicates approximately a one decibel increase in conductance across the measured frequency band.

DFPase increases its electrical conductance by aproximately two decibels when exposed to 100 ppb DIMP challenge gas. Very little increase in electrical conductance was noted when DFPase was exposed to higher concentrations of the challenge gas.

The four organic chemically-sensitive thin films candidates (succinylcholine chloride, succinyl chloride, 2-naphthol(β), and L-histidine dihydrochloride) are presented with respect to their normalized frequency response to DIMP in Figure 58. Succinyl chloride and 2-naphthol(β) are the most responsive to 100 ppb the DIMP challenge gas. The results for succinyl chloride and 2-naphthol(β) are both in close agreement with the results obtained for the normalized DC resistance responses. Succinylcholine chloride is somewhat less responsive to the 100 ppb DIMP challenge gas compared to the succinyl chloride. L-histidine dihydrochloride has no significant frequency response when exposed to the 100 ppb DIMP challenge gas compared to its response exposed to filtered laboratory air. This data does not agree with the data obtained for the DC resistance response. At concentrations equal to or larger than one ppm of the DIMP

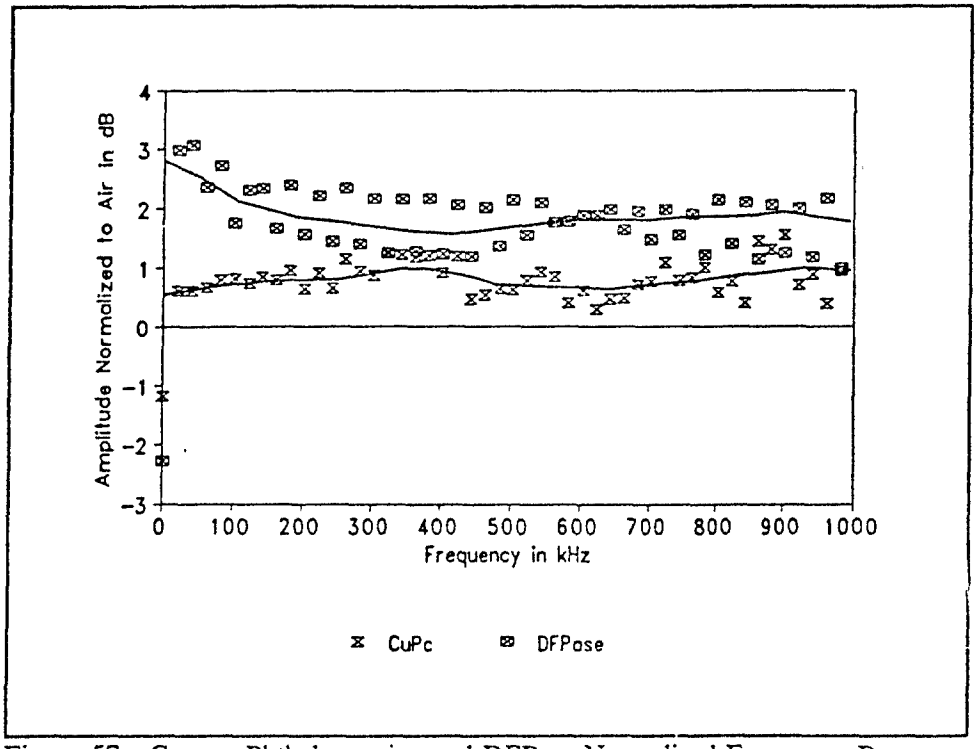

Figure 57. Copper Phthalocyanine and DFPase Normalized Frequency Response to 100 ppb DIMP at 30° C.

challenge gas, the L-histidine dihydrochloride's AC conduction increases to about three decibels above the conduction observed when exposed to filtered laboratory air.

Response to DMMP. The normalized DC resistance response of copper phthalocyanine is the similar to the results that have been observed by Captain Jenny Shin (3). The observed normalized DC resistance response is just measurable for the 100 ppb concentration of the DMMP challenge gas as shown in Figure 59. Copper phthalocyanine's DC resistance response is sensitive to a 100 ppb concentration of the DMMP challenge gas. The DFPase is very sensitive to the DMMP challenge gas;

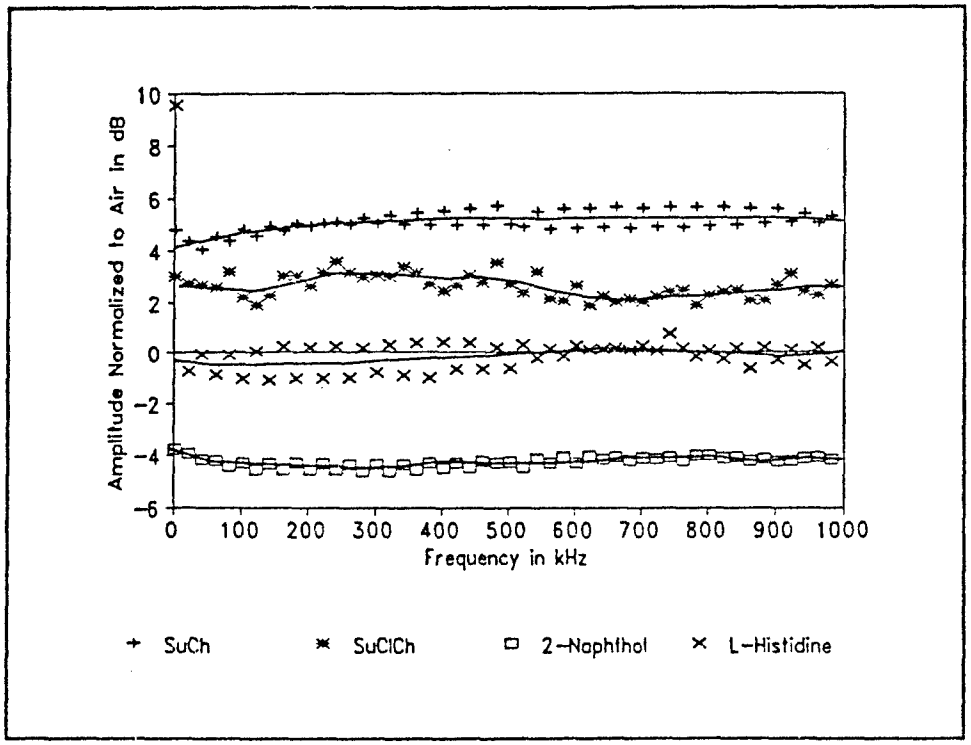

Figure 58. 2-Naphthol(β), Succinylcholine Chloride (SuClCh), Succinyl Chloride (SuCh), and L-Histidine Dihydrochloride Normalized Frequency Responses to 100 ppb DIMP at 30° C.

DFPase's normalized DC resistance response decreases by 90% when exposed to the 100 ppb gas concentration, making the change quite dramatic. DMMP challenge gas concentrations greater than one ppm had little additional effect on the DC resistance response of the DFPase.

The four organic chemically-sensitive thin film candidate's (succinylcholine chloride, succinyl chloride, 2-naphthol(β), and L-histidine dihydrochloride) normalized DC resistance response to DMMP are shown in Figure 60. The chemically-sensitive thin film, 2-naphthol(β), is displayed with values normalized against the DC resistance values obtained with 10 ppm DMMP challenge gas. The normalization for the

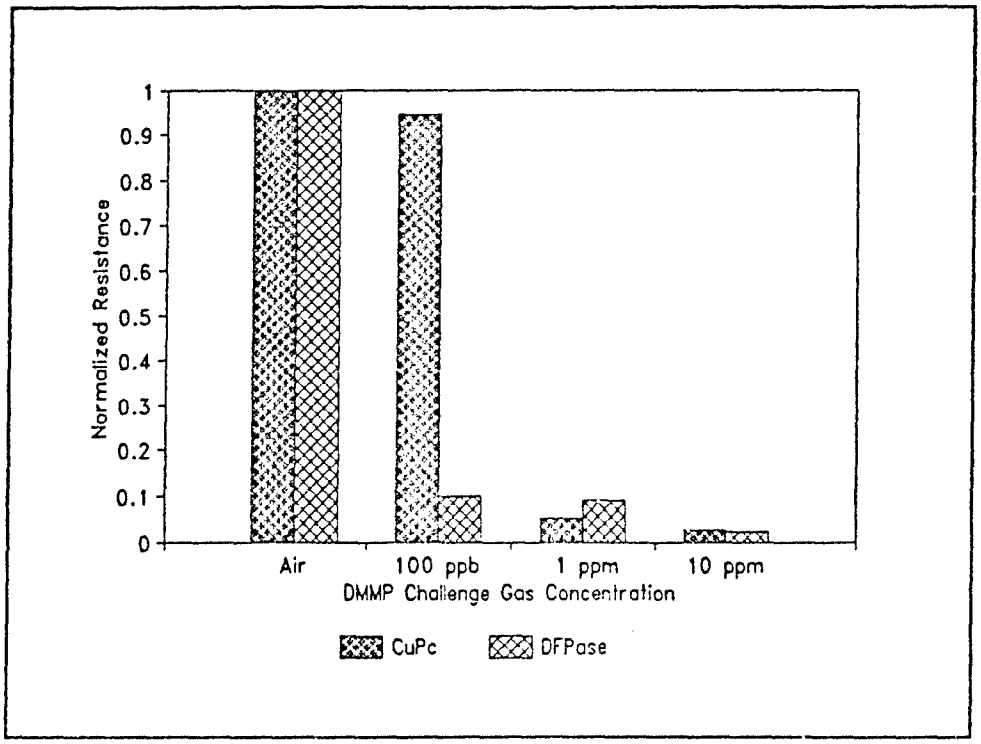

Figure 59. Copper Phthalocyanine and DFPase Normalized DC Resistance Response to DMMP at 30° C.

2-naphthol(β) was done this way to keep the normalized DC resistance scale limited to a range of 0 to 1, with 1 being the normalized value. Succinylcholine chloride, succinyl chloride, L-histidine dihydrochloride are all normalized to their respective DC resistance values obtained when exposed to filtered laboratory air. With respect to the normalized DC resistance responses shown, L-histidine dihydrochloride and succinyl chloride are the most sensitive to DMMP.

Copper phthalocyanine reacts unusually when exposed to DMMP; that is, the AC conduction decreases even though the DC resistance decreases, implying that there are independent complex impedance parameters effecting the overall conduction. The

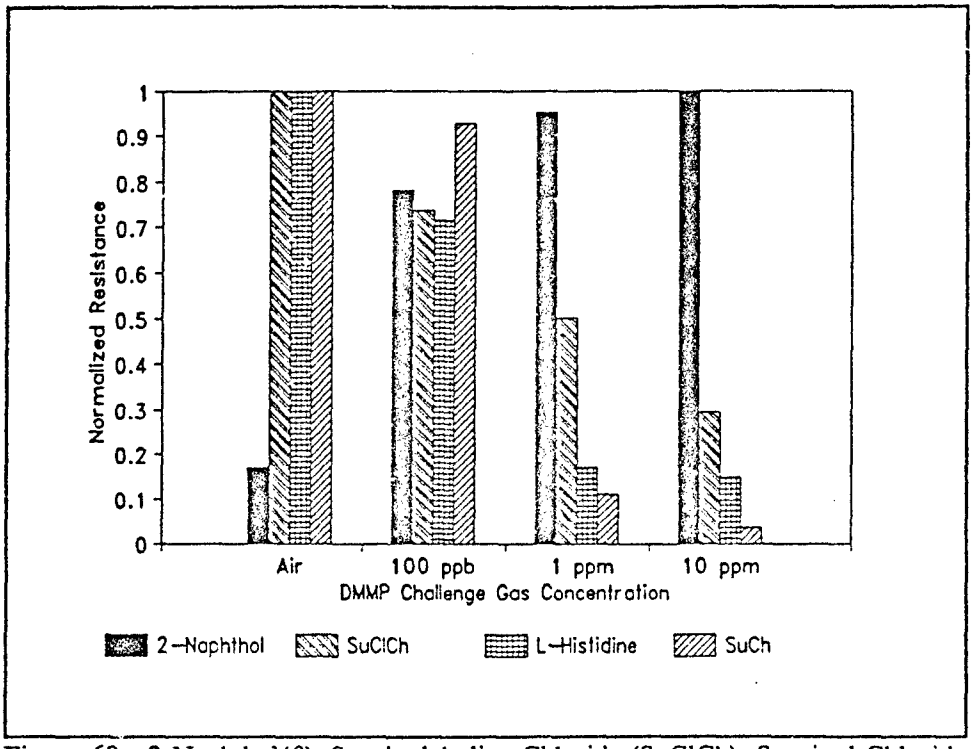

Figure 60. 2-Naphthol(β), Succinylcholine Chloride (SuClCh), Succinyl Chloride (SuCh), and L-Histidine Dihydrochloride Normalized DC Resistance Responses to DMMP at 30° C.

normalized frequency responses for copper phthalocyanine and DFPase are shown in Figure 61. DFPase increases up to seven decibels in AC conductance when exposed to the 100 ppb DIMP challenge gas, as shown in the normalized frequency response. The chemically-sensitive thin film DFPase AC conductance does not significantly increase relative to the 100 ppb level when DFPase is exposed to higher concentrations of the DMMP challenge gas. This result is expected since there is very little additional change in the normalized DC resistance response when DFPase is exposed to higher concentrations of the DMMP challenge gas, as shown in Figure 60.

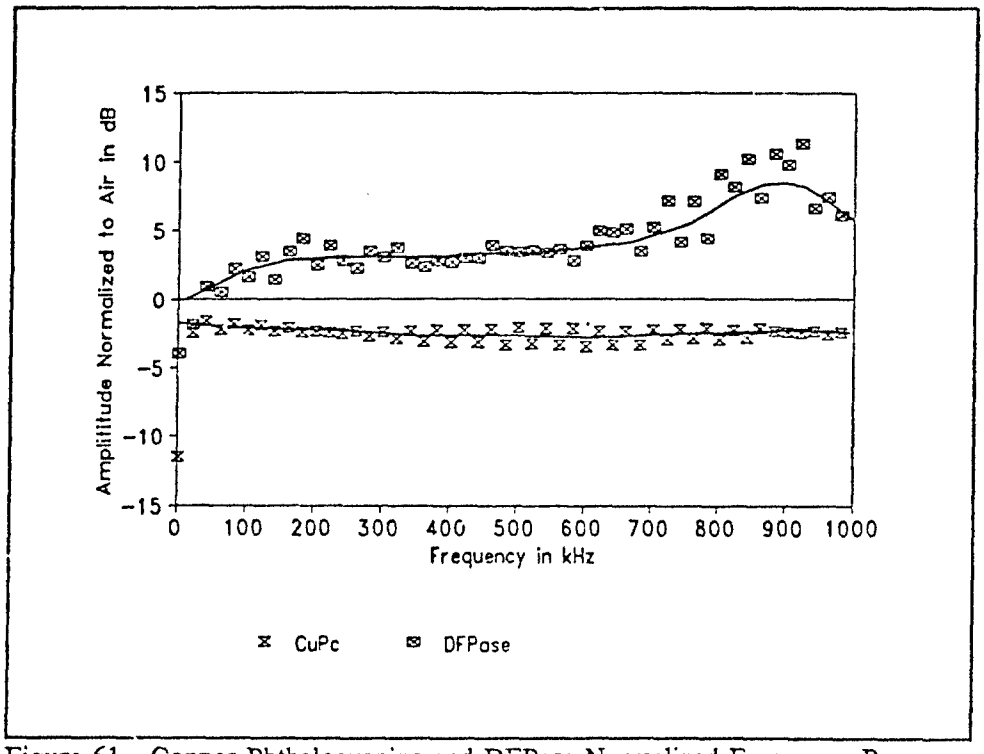

Figure 61. Copper Phthalocyanine and DFPase Normalized Frequency Response to 100 ppb DMMP at 30° C.

The normalized frequency response to the 100 ppb DMMP challenge gas for the four organic chemically-sensitive thin films candidates, 2-naphthol(β), succinylcholine chloride, L-histidine dihydrochloride, and succinyl chloride are shown with their in Figure 62. 2-naphthol(β), succinylcholine chloride, succinyl chloride, and L-histidine dihydrochloride were all normalized using the respective frequency responses obtained when they were exposed to filtered laboratory air. In the normalized frequency responses, succinylcholine chloride and 2-naphthol(β) are the most sensitive to DMMP. Succinyl chloride has a smaller relative response to the DMMP challenge gas compared

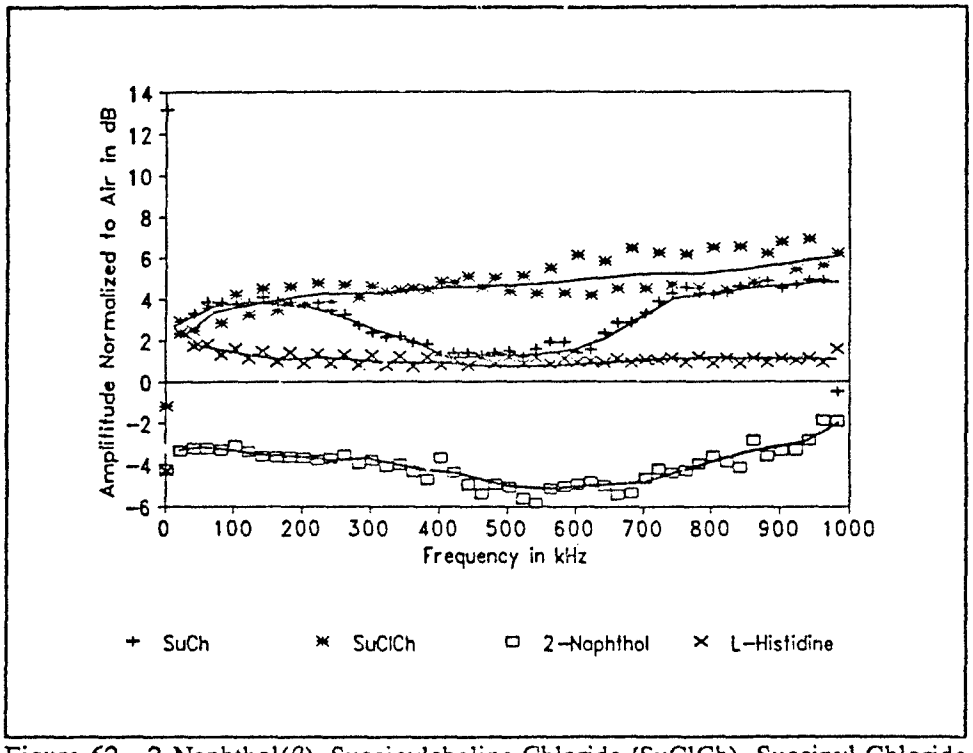

Figure 62. 2-Naphthol(β), Succinylcholine Chloride (SuClCh), Succinyl Chloride (SuCh), and L-Histidine Dihydrochloride Normalized Frequency Responses to 100 ppb DMMP at 30° C.

to succinyl chloride from 200 to 700 kHz, but, is similar to succinyl chloride at the other frequencies measured.

L-histidine dihydrochloride has a very small (about one decibel) normalized frequency response when exposed to 100 ppb of the DMMP challenge gas. This data has only a weak correlation with the data obtained for the DC resistance, since L-histidine dihydrochloride changes significantly in their DC resistance response when exposed to the DMMP challenge gas. At concentrations greater than one ppm of the DMMP challenge gas, L-histidine dihydrochloride's AC conductance increases to

approximately four decibels above the conductance level observed when exposed to filtered laboratory air.

Response to DFP. The observed normalized DC resistance response is less than 40 percent of the value observed for filtered laboratory air, compared to for the 100 ppb concentration of the DFP challenge gas (Figure 63). Copper phthalocyanine's DC resistance values are not sensitive to the concentrations of the DFP challenge gas greater than 100 ppb. The DFPase is very sensitive to the DFP challenge gas; DFPase's normalized DC resistance changed by 80% compared to the filtered laboratory air resistance value, for a 100 ppb gas concentration exposure. Challenge gas concentrations greater than one ppm continued to reduce the DC resistance of the DFPase, unlike the results observed for DIMP challenge gas.

The normalized DC resistance response to DFP for the four organic chemically-sensitive thin film candidates (succinylcholine chloride, succinyl chloride, 2-naphthol(β), and L-histidine dihydrochloride) is shown in Figure 64. The 2-naphthol(β) chemically-sensitive thin film's response is displayed with the values normalized to the DC resistance response normalized to the values obtained with the DFP challenge gas delivered at 10 ppm, to keep the displayed resistance values in the range from 0 to 1, with 1 representing the normalized value. The succinylcholine chloride, succinyl chloride, and L-histidine dihydrochloride responses were all normalized with respect to their respective DC resistance values obtained when exposed to filtered laboratory air. Normalized DC resistance responses for L-histidine dihydrochloride and succinyl chloride were only moderately sensitive to DFP, since the DC resistance decreased less

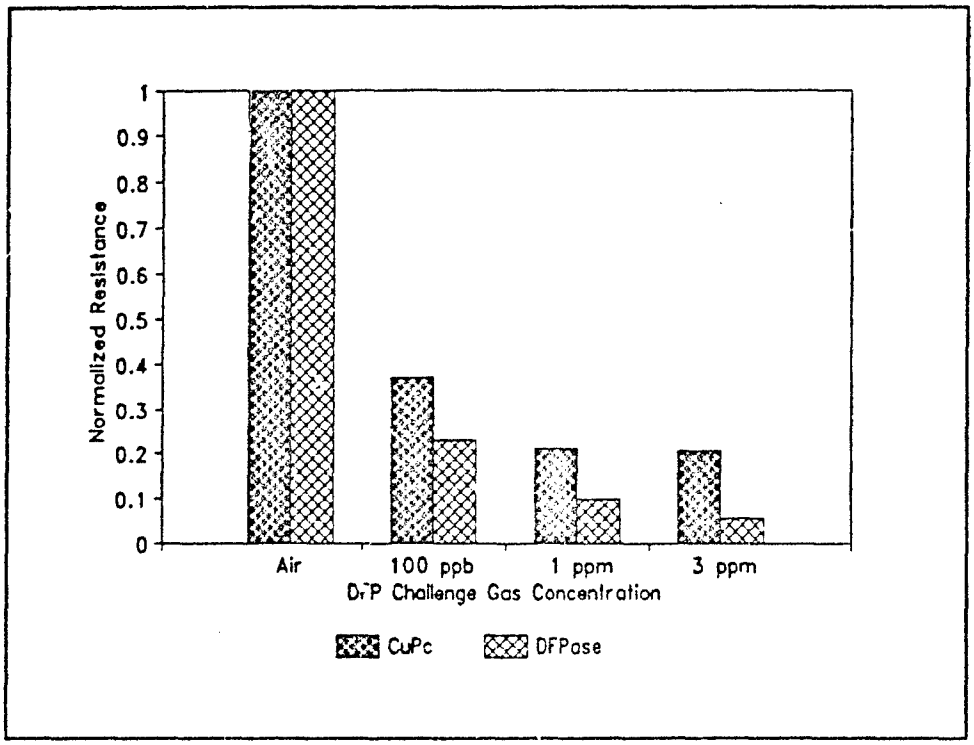

Figure 63. Copper Phthalocyanine and DFPase Normalized DC Resistance Response to DFP at 30° C.

than 40% for a 100 ppb challenge gas concentration as compared to the DC resistance value when exposed to filtered laboratory air.

The normalized frequency response of copper phthalocyanine and DFPase when exposed to 100 ppb DFP, using their response to filtered laboratory air as the reference level, is shown in Figure 65. DFPase increases its AC conductance by more than two decibels when exposed to 100 ppb DFP, as seen from the normalized frequency response. The chemically-sensitive thin film DFPase AC conductance increases to four decibels when DFPase is exposed to larger concentrations of the DFP challenge gas.

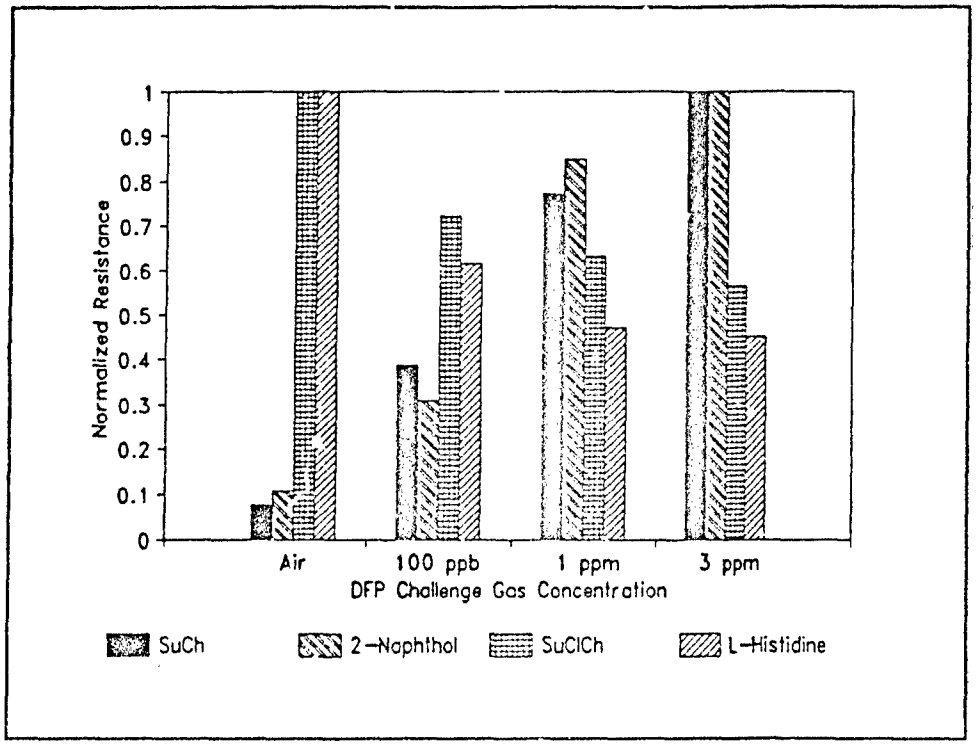

Figure 64. 2-Naphthol(β), Succinylcholine Chloride (SuClCh), Succinyl Chloride (SuCh), and L-Histidine Dihydrochloride Normalized DC Resistance Responses to DFP at 30° C.

This res is expected since there are very significant changes in the normalized DC resistance when DFPase is exposed to larger concentrations of the DFP challenge gas.

The normalized frequency response to DFP for the four organic chemically-sensitive thin film candidates (succinyl chloride, 2-naphthol(β), succinylcholine chloride, and L-histidine dihydrochloride) are displayed with respect to their normalized responses in Figure 66. The succinyl chloride, 2-naphthol(β), succinylcholine chloride, and L-histidine dihydrochloride chemically-sensitive thin films are displayed with the values normalized to the frequency-domain response obtained when the thin film was exposed to filtered laboratory air. With respect to normalized frequency responses

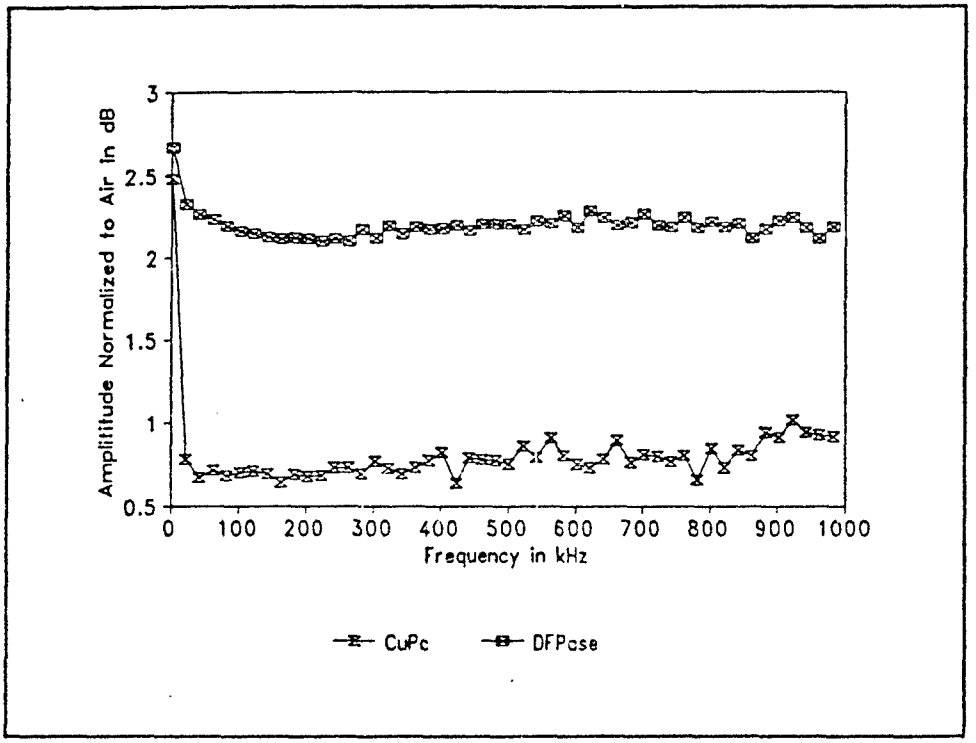

Figure 65. Copper Phthalocyanine and DFPase Normalized Frequency Response to 100 ppb DFP at 30° C.

succinylcholine chloride and 2-naphthol(β) are the most sensitive to DFP. Both succinyl chloride and 2-naphthol(β) exhibit an increase in DC resistance and a decrease in AC conductance when exposed to 100 ppb DFP challenge gas.

Summary

In this chapter, each of the six chemically-sensitive thin film candidates (copper phthalocyanine, DFPase, succinylcholine chloride, succinyl chloride, 2-naphthol(β), and L-histidine dihydrochloride) were evaluated for their response to three challenge gases. Each thin film candidate was evaluated for its response to DIMP, DMMP, and DFP

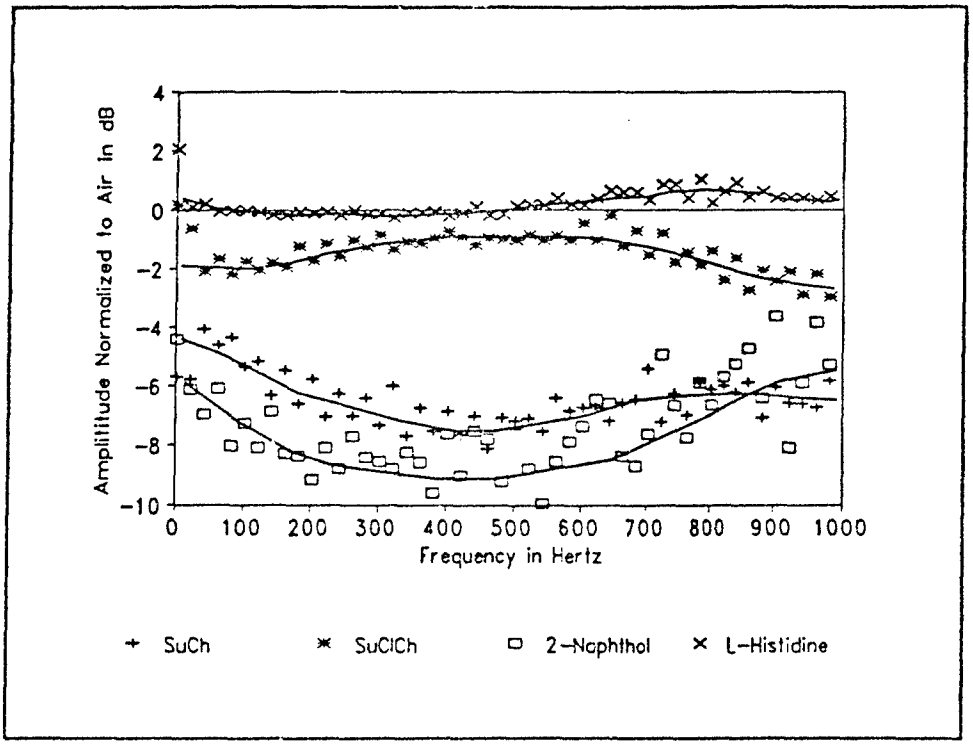

Figure 66. 2-Naphthol(β), Succinylcholine Chloride (SuClCh), Succinyl Chloride (SuCh), and L-Histidine Dihydrochloride Normalized Frequency Responses to 100 ppb DFP at 30° C.

challenge gas concentrations of 100 ppb, 1 ppm, and 10 ppm (DFP at 3 ppm). All performance evaluations were conducted using 90% relative humidity filtered laboratory air as the purge gas and the carrier for the challenge gases. The performance evaluation of each chemically-sensitive thin film was conducted with the IGEFET microsensors isothermally thermostated to 30° C, 50° C, and 70° C.

The performance of the each chemically-sensitive thin film candidate was discussed for each test parameter (DC resistance, time-domain response to an pulse excitation, and AC conductance). The performance and reversibility of each thin film candidate was evaluated with respect to the results obtained for each different thin film measurement

parameter. The performance of each thin film candidate's response to binary challenge gas combinations were compared to the response obtained when the thin films were exposed to the individual challenge gases.

VI. Conclusions and Recommendations

Conclusions

Each of the six chemically-sensitive thin films evaluated in this thesis had unique properties the manifested themselves in their responses to the three challenge gases. Figure 67 shows the response of all six chemically-sensitive thin film candidates when exposed to a 100 ppb concentration of each of the three challenge gases. Figure 68 shows the response of all six chemically-sensitive thin film candidates when exposed to a 1 ppm concentration of each of the three challenge gases.

Rank ordering the six candidate chemically-sensitive thin films depends upon the order of importance and weights assigned to sensitivity, reversibility, and selectivity. The chemically-sensitive thin films will be rank ordered with sensitivity having the greatest weight, reversibility next and selectivity third.

Based on the above criteria, DFPase is ranked number one. The DFPase thin film is very sensitive to even the smallest concentrations of the challenge gases, with the DC resistance decreasing by over 80% for 100 ppb concentrations of each of the three challenge gases. However, the DFPase thin film has two weaknesses; this thin film did not manifest any reversibility and very little selectivity.

The 2-Naphthol(β) thin film ranked number two. The 2-Naphthol(β) thin film was sensitive to all three of the challenge gases, and it was the only completely reversible thin film evaluated in this investigation. The 2-Naphthol(β) thin film was slightly

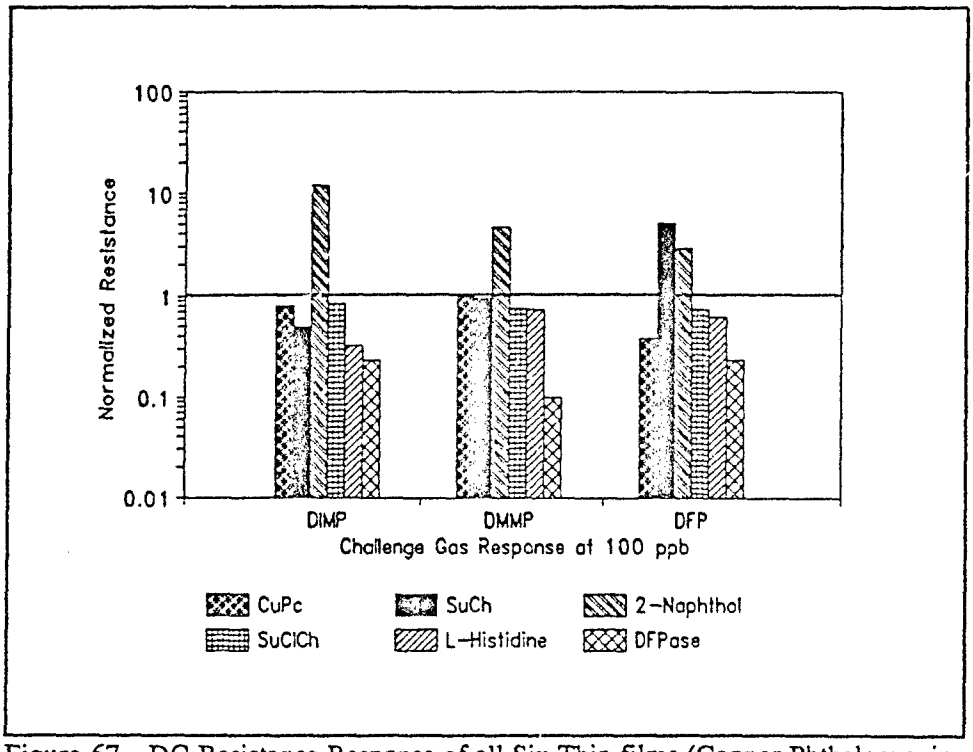

Figure 67. DC Resistance Response of all Six Thin films (Copper Phthalocyanine (CuPc), Succinyl Chloride (SuCh), 2-Naphthol(β), Succinylcholine Chloride (SuClCh), L-Histidine Dihydrochloride, and DFPase) to 100 ppb of the three Challenge Gases at 30° C.

selective since the DC resistance values differed by less than 40% between the three challenge gases.

The succinyl chloride thin film ranked number three. This thin film manifested good sensitivity since the DC resistance changed value by one order of magnitude for exposure to 1 ppm of the challenge gas. The succinyl chloride manifests some reversibility; that is, the DC resistance value returns within 40% of its unexposed resistance value. Selectivity is good since the DC resistance value change to DFP is opposite to those observed for DIMP and DMMP.

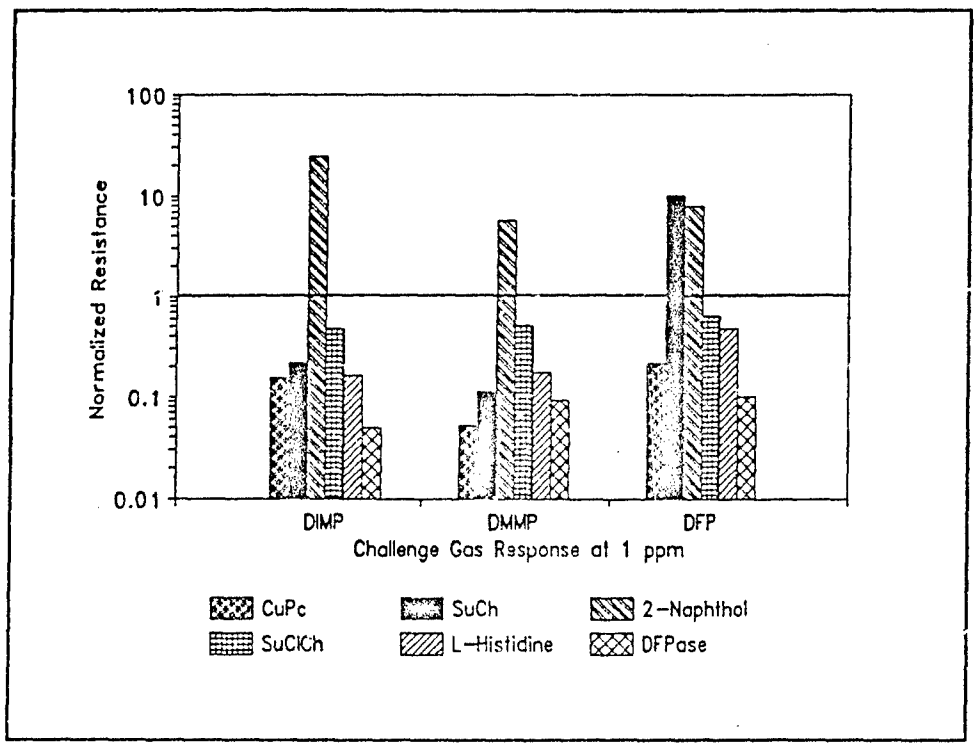

Figure 68. DC Resistance Response of the Six Thin films (Copper Phthalocyanine (CuPc), Succinyl Chloride (SuCh), 2-Naphthol(β), Succinylcholine Chloride (SuClCh), L-Histidine Dihydrochloride, and DFPase) to a 1 ppm of three Challenge Gases at 30° C.

The succinylcholine chloride thin film ranked number four. The film's DC sensitivity was the poorest of the six films measured, and it indicated no reversibility. The succinylcholine thin film manifested a unique 10 dB notch filter response to the DFP challenge gas, ranking it very high in selectivity.

The copper phthalocyanine thin film ranked number five. The copper phthalocyanine thin film was only moderately sensitive to the 100 ppb concentration exposure of the challenge gases evaluated in thesis. The thin film indicated reversibility only at elevated temperatures (70° C), and selectivity was poor with the observed differences in the frequency response to be less than 1 decibel.

The L-histidine dihydrochloride thin film ranked number six. The sensitivity observed in the DC resistance response was measurable, but the change in magnitude was less than that observed for some of the other thin films. The thin film was completely non-reversible. Selectivity was minimal to the three challenge gases measured.

The copper phthalocyanine thin films reacted consistently with the behavior manifested in the prior thesis investigations when challenged with diisopropyl methylphosphonate (DIMP) (2; 3; 4). However, the results measured for the copper phthalocyanine thin film's response when challenged with dimethyl methylphosphonate (DMMP) yielded some unexpected results. While the direct current measurements indicated an increase in resistance, the corresponding high frequency response conduction trends indicated an increase in the film's AC conductance. This behavior was also mimicked for the copper phthalocyanine thin film's evaluation with respect to the DMMP challenge gas testing conducted at 50° C and 70° C. The copper phthalocyanine thin film's response to diisopropyl fluorophosphate (DFP) was similar to DIMP, but the magnitude of the observed change was smaller than the change observed when similar concentrations of the DIMP challenge gas were used to expose the IGEFET microsensor.

DFPase manifested a very significant sensitivity to the three challenge gases investigated. The response of the DFPase enzyme was nearly saturated when a 100 ppb challenge gas concentration of DIMP, DMMP, or DFP was used to expose the microsensor. The response of DFPase was complete within 10 to 20 seconds, indicating a very rapid response to any challenge gas at the concentrations evaluated. No

reversibility was noted for the DFPase enzyme for any of the challenge gases. The DFPase enzyme provided no useful sensitivity data at elevated temperatures (50° C or 70° C). Since the DFPase enzyme was very sensitive to all three challenge gases the reactions were similar. However, the DFPase enzyme demonstrated very poor selectivity to the different challenge gases.

Succinyl chloride appeared to manifest a good overall blend of sensitivity, reversibility, and selectivity. The reaction to DIMP and DMMP was almost identical because similar changes in DC resistance were evaluated with respect to corresponding in changes in the concentrations of the challenge gases. The reaction to DFP manifested the opposite behavior compared to that observed for the DIMP and DMMP challenge gases. That is, the DC resistance of succinyl chloride increased, and the AC conductance decreased whenever the DFP challenge gas was present. The effect of the DFP challenge gas also appeared to dominate the response when a binary combination of DIMP and DFP, or DMMP and DFP, were used to expose an IGEFET microsensor element coated with succinyl chloride. The succinyl chloride thin film was partially reversible, though not completely reversible, since its DC resistance returns to within 40% of its unexposed value.

The succinylcholine chloride thin film candidate demonstrated sensitivity and a significant selectivity to DFP. Whenever an IGEFET microsensor element was coated with succinylcholine chloride as the chemically-sensitive thin film, and it was exposed to the DFP challenge gas, the frequency response yielded a unique and very prominent notch filter effect. The notch filter's depth was on the order of 10 decibels. The notch filter effect of the succinylcholine chloride thin film was not reversible. Additionally,

succinylcholine chloride was not functional as a chemically-sensitive thin film at elevated temperatures.

The 2-Naphthol(β) thin film was sensitive to the three challenge gases (DIMP, DMMP, and DFP) at the lowest concentrations tested. The 2-Naphthol(β) thin film was also completely reversible in approximately ten minutes. However, the 2-Naphthol(β) thin film sublimed quickly and the performance measurements had to be accomplished rapidly (in less than 120 minutes after deposition). The 2-Naphthol(β) thin film was not selective, and its response was very similar for all three challenge gases.

Used as a chemically-sensitive thin film, L-histidine dihydrochloride was sensitive to all three challenge gases. The film's DC resistance decreased by 20% when the L-histidine dihydrochloride thin film was exposed to 100 ppb of DIMP, DMMP, or the DFP challenge gases as well as the binary combination of these gases. The AC conductance increased significantly for each of the challenge gases. Selectivity of the L-histidine dihydrochloride thin film was poor since its response was similar for all three challenge gases. The performance evaluation discovered no evidence of reversibility for the L-histidine dihydrochloride thin film.

Recommendations

While this thesis is a continuation of previous studies, further study should take place in specific areas to improve the operation of the interdigitated gate electrode field-effect transistor (IGEFET) microsensor.

1. To determine the sensitivity level of the DFPase enzyme, further testing should be conducted at much lower concentrations of challenge gas. If linearity is preserved

to smaller concentrations, DFPase may be capable of sensing challenge gas concentrations as low as 10 ppb.

2. The succinyl chloride thin film deserves further study to investigate the increased electrical conductance when it is exposed to DIMP and DMMP versus the decreased electrical conductance observed when the film is exposed to DFP. Further understanding of this conduction change will assist in using the succinyl chloride as a selective chemically-sensitive thin film.

3. The succinylcholine chloride thin film deserves further study to completely characterize the notch filter response. The resistance capacitance model of the thin film applied to the IGE structure requires additional characterization.

4. The demultiplexer and multiplexer should be removed from the IGEFET microsensor until well-isolated and transient-protected circuits are developed. Repeated failures occurred with the demultiplexer during logic switching due to switching voltage transients on the select lines. Additionally, any voltage transients greater than V_{dd} impressed on the driven gate of the IGE caused the demultiplexer to short circuit, sinking excessive current.

5. The sense element amplifiers should be retained for their output impedance matching capability. However, the sense element amplifiers should be modified to operate with 10 volt power supply voltages. This would increase the output signal levels and the linear region of the amplifiers.

6. The operational amplifiers and the voltage-follower amplifier should be removed from the microsensor design since they are not needed if the demultiplexer and multiplexer are removed. All voltage and current amplification greater than that

provided by the sense-element amplifiers may be obtained using an off-chip, low-noise amplifier such as the SR 560 (Stanford Research Systems, 1290-D Reamwood Avenue, Sunnyvale, CA 94089).

7. The nine IGEs on the IGEFET microsensor are adequate for evaluating multiple film candidates. The current separation distance between each interdigitated gate electrode (IGE) is also adequate for isolating each electrode response. However, the surface area of each IGE should be increased to enhance the measurable conductance and noise margin of the thin film semiconductor material. This could readily be accomplished by removing the demultiplexer, multiplexer, operational amplifiers, and voltage-follower amplifier, without increasing the overall die size.

8. To reduce 60 Hertz noise in the instrumentation scheme, the chassis of all test equipment used should be grounded to the case of the test cell. Additionally, power for the heater strip should be well shielded and filtered for 60 Hertz noise by insuring that ground loops are eliminated. To further reduce the potential for 60 Hertz noise in the measurements, all power supplied to the microsensor circuit could be supplied with a rechargeable battery pack that is well shielded and capable of supplying one ampere of current for continuous periods of eight hours or more.

9. The gas delivery system should be modified to accommodate two requirements. First, dry and humidified laboratory air stability and flow are difficult to control with the current arrangement. This section of the gas delivery system should be redesigned to facilitate accurately setting the humidified and dry air flow rates. Second, the challenge gas mixing section requires a redesign to accommodate various challenge gas ratios to be delivered to the test chamber.

10. The airbrush deposition of DFPase, succinyl chloride, succinylcholine chloride, 2-naphthol(β), and L-histidine dihydrochloride, all need to be improved to insure constant thickness coverage of the IGE structures. Succinyl chloride is the most difficult to deal with since its corrosive nature is very destructive to the airbrush's metering needle.

Appendix A

Equipment List

Semiconductor Parameter Analyzer
Hewlett-Packard, Model HP 4145B
Palo Alto, CA 94304

Impedance/Gain-Phase Analyzer
Hewlett-Packard, Model HP 4194A
Palo Alto, CA 94304

Pulse Generator
Hewlett-Packard, Model HP 8082A
Palo Alto, CA 94304

Spectrum Analyzer
Hewlett-Packard, Model HP 4195A
Palo Alto, CA 94304

Digital Storage Oscilloscope
Hewlett-Packard, Model HP 54100A
Palo Alto, CA 94304

DC Power Supply
Hewlett-Packard, Model HP 6205B
Palo Alto, CA 94304

Matrix Switch
Wave-Tek Corp., Model 604
9045 Balboa Avenue
San Diego, CA 92123

Low-Noise Amplifier
Stanford Research Systems, Model SR560
1290-D Reamwood Avenue
Sunnyvale, CA 94089

Thermocouple
Omega Engineering Inc., Model SAI-K
One Omega Drive
Stamford, CT 06907-0047

6 Volt Battery
Burgess Inc., Model F4M
Freeport, IL 61032

IEEE-488 Interface Plug-in Card
Capitol Equipment Corp., Model 01000-60300
Burlington, MA 01803

Microcomputer
Zenith Data Systems, Model Z-248
St. Joseph, MI 49085

Kapton Strip Heater
Watlow Inc., Model K005020C5
St. Louis, MO 63146

Electron Beam Vacuum Deposition System
Denton Vacuum Corp., Model DV-6O2
Cherry Hill, NJ 08003

Digital Hygrometer/Thermometer
Thunder Scientific Corp., Model HS-lCHDT-2A
Albuquerque, NM 87123

Micromanipulator Probe Station
Micromanipulator Co., Model 6200
Carson City, NV 89701

Active Probe
Micromanipulator Co., Model FET-l
Carson City, NV 89701

FET Probe Power Supply
Micromanipulator Co., Model FET PS4
Carson City, NV 89701

Power Supply
KEPCO, Model CK4O-O.8M
Flushing, NY 11241

Gas Flow Meters
Gilmont Instruments, Model F-7660
401 Great Neck Road
Great Neck, NY 11021

N_2 Pressure Regulator
Cincinnati Valve & Fitting Co., Model 41910-53
3710 Southern Avenue
Cincinnati, OH 45227

Ball Valves
Cincinnati Valve & Fitting Co., Model 43S4-316
3710 Southern Avenue
Cincinnati, OH 45227

Stainless Steel Connectors and Fittings
Cincinnati Valve & Fitting Co., Series 316
3710 Southern Avenue
Cincinnati, OH 45227

Stainless Steel Tubing
Williams, Co., Quarter Inch Diameter, 316 Stainless
7640 Reinhold Drive
Roselawn, OH 45237

Electrometer
Keithley Instruments, Model 617
Cleveland, OH 44139

Oscilloscope
Tektronix, Model 475
P. O. Box 500
Beaverton, OR 97077

Curve Tracer
Tektronix, Model 577
P. O. Box 500
Beaverton, OR 97077

Sputter Deposition System
Structure Probe Inc., Model SPI Sputterer
West Chester, PA 19380

Digital Multimeter
John Fluke Mfg. Co., Model 77/AN
Everett, WA 98206

Airbrush, External Mix
Paasche Airbrush Co., Model H-Set
Harwood Heights, IL 60656

Wild Microscope
Wild Heerbrugg Ltd., Model M20
CH-9435 Heerbrugg, Switzerland

Wild Interference Attachment
Wild Heerbrugg Ltd., Model 255-574
CH-9435 Heerbrugg, Switzerland

Test Cell

Appendix B

Materials List

Copper Phthalocyanine
Fluka Chemical Corp., Stock # 147-14-8
Ronkonkoma, NY 11779

L-Histidine Dihydrochloride
Fluka Chemical Corp., Stock # 36440-588
Ronkonkoma, NY 11779

Succinyl Chloride
Fluka Chemical Corp., Stock # 35808-887
Ronkonkoma, NY 11779

Succinylcholine Chloride
Fluka Chemical Corp., Stock # 255529-987
Ronkonkoma, NY 11779

2-Naphthol(β)
Fluka Chemical Corp., Stock # 249465-988
Ronkonkoma, NY 11779

DFPase
Chemical Division
IIT Research Institute,
10 West 35th Street
Chicago, IL 60616

DIMP Gas Permeation Tube
G. C. Industries, Inc., Model 23-7392
8967 Oso Avenue
Chatsworth, CA 91311

DMMP Gas Permeation Tube
G. C. Industries, Inc., Model 23-7082
8967 Oso Avenue
Chatsworth, CA 91311

DFP Gas Permeation Tube
G. C. Industries, Inc., Model 23-7432
8967 Oso Avenue
Chatsworth, CA 91311

Appendix C

Data Acquisition Programs

The programs listed in this section were used to record numerical data from the Hewlett Packard oscilloscope, model HP 54100, spectrum analyzer, model HP 4195A, and gain phase/impedance analyzer, model HP 4194B. Data is saved with ascii header information delimited with quote marks, and the numerical data is delimited with commas for direct importation into Lotus or Quattro Pro.

```
1000 REM************************************************************
1010 REM** PROGRAM TO COLLECT DATA FROM THREE HEWLETT PACKARD     **
1020 REM** PIECES OF TEST EQUIPMENT USING THE IEEE-488 BUS.       **
1030 REM** HP-54100 OSCILLOSCOPE                                  **
1040 REM** HP-4195A SPECTRUM ANALYZER                            **
1050 REM** HP-4194b GAIN PHASE/IMPEDANCE ANALYZER                **
1060 REM**                                                       **
1070 REM** Charles P. Brothers Jr.                               **
1080 REM** GE-90D                                               **
1090 REM** NOTES:  The data collection subroutines are a         **
1100 REM**   collection of routines written by Capt Thomas      **
1110 REM**   Jenkins and the author.                            **
1120 REM**                                                       **
1130 REM************************************************************
1140 '
1150 REM -------------- INITIALIZE PROGRAM ------------------
1160 DEF SEG=&HC400                  'PC-488 MEMORY ADDRESS
1170 INIT%=0                         'INITIALIZATION CODE
1180 TRANSMIT%=3                     'TRANSMIT CODE
1190 RECEIVE%=6                      'RECEIVE CODE
1200 SEND%=9                         'SEND CODE
1210 SPOLL%=12                       'SERIAL POLL CODE
1220 PPOLL%=15
1230 ENTER%=21
1240 TARRAY%=200
1250 RARRY%=203
1260 DMA2=206
1270 BUSADDRS%=21                    'IEEE-488 BUS ADDRESS
1280 SYSCONT%=0                           'SYSTEM CONTROLLER
1290 '
1300 REM --------------- INITIALIZE ARRAYS ------------------
1310 DIM A(401)
1320 DIM X(401)
1330 DIM D%(2048)
1340 DIM VPOINT(1300)
1350 DIM MAG(400)
1360 DIM PHS(400)
1370 DIM GFREQ(400)
1380 '
1390 REM ------------- INITIALIZE CONTROLLER ----------------
1400 CALL INIT% (BUSADDRS%,SYSCONT%)
1410 CHRFILE$ = "BLANK"
1420 '
1430 REM --------------------- TRANSMIT ---------------------
1440 S$="UNL UNT"                    'INITIALIZE BUS
1450 CALL TRANSMIT% (S$,STATUS%)
1460 IF STATUS%<>0 THEN GOTO 8900
1470 '
```

```
1480 REM -------------------- SCREEN MENU ---------------------
1490 CLS : PRINT " "
1500 PRINT "          SYSTEM MENU - Choose one "
1510 PRINT " "
1520 PRINT "      (0)  Enter experiment data header information."
1530 PRINT "      (1)  Retrieve Data from HP-54100 Oscilloscope"
1540 PRINT "      (2)  Retrieve Data from HP-4194B in Gain/Phase Mode"
1550 PRINT "      (3)  Retrieve Data from HP-4194B in Impedance Mode"
1560 PRINT "      (4)  Retrieve Data from HP-4195A from 1HZ to 10KHZ"
1570 PRINT "      (5)  Retrieve Data from HP-4195A from 1HZ to 1MHZ"
1580 PRINT "      (6)  EXIT TO DOS"
1590 PRINT " "
1600 PRINT "" :INPUT "ENTER CHOICE:  ",MENU
1610 '
1620 S$="UNL UNT"                  'INITIALIZE BUS
1630 CALL TRANSMIT% (S$,STATUS%)
1640 IF STATUS%<>0 THEN GOTO 8900
1650 '
1660 IF MENU=0 THEN GOSUB 1780
1670 IF MENU=1 THEN GOSUB 2080
1680 IF MENU=2 THEN GOSUB 3690
1690 IF MENU=3 THEN GOSUB 5170
1700 IF MENU=4 THEN GOSUB 6560
1710 IF MENU=5 THEN GOSUB 7770
1720 IF MENU=6 THEN GOTO 8780
1730 '
1740 GOTO 1490
1750 REM -------------------- END MENU ----------------------
1760 '
1770 REM ------------------ GENERATE FILE HEADERS -------------------
1780 CLS
1790 PRINT " "
1800 INPUT "ENTER FIVE CHARACTER CODE NAME TO STORE DATA:  ", CHRFILE$
1810 INPUT "ENTER FILE HEADER:  ",EXPERIMENT$
1820 INPUT "ENTER    CHALLENGE GAS:  ",GAS$
1830 INPUT "ENTER BATH TEMPERATURE:  ",BATH$
1840 INPUT "ENTER         FLOW RATE:  ",FLOWR$
1850 INPUT "ENTER CHIP TEMPERATURE:  ",CHIPTEMP$
1860 INPUT "ENTER     GAS HUMIDITY:  ",VHUMD$
1870 RETURN
1880 '
1890 '
1900 '
1910 '
1920 '
1930 REM*****************************************************************
1940 REM** SUBROUTINE TO COLLECT OSCILLOSCOPE DATA FROM THE HP   **
1950 REM** 54100 DIGITAL OSCILLOSCOPE                           **
1960 REM**                                                     **
1970 REM** WRITTEN BY: Capt Thomas Jenkins                     **
1980 REM**                                                     **
1990 REM** Modified by: Charles P. Brothers Jr.                **
2000 REM**               GE-90D                                **
2010 REM**                                                     **
2020 REM** NOTES: The HP-4194A is set to run SINGLE SWEEP MODE  **
2030 REM**   measurements from the IGEFET electrodes.          **
2040 REM**                                                     **
2050 REM**                                                     **
2060 REM*****************************************************************
2070 '
2080 CLS
2085 CHOPT = 0
2090 PRINT "    ROUTINE TO CAPTURE SCOPE DISPLAY IN PC FILE"
```

```
2100 PRINT "
2110 PRINT "(1) FOR CHAN1, (2) FOR CHAN2, OR ANY OTHER KEY--BOTH"
2120 REM KEY POLL
2130 A$=INKEY$:IF A$="" THEN 2130
2140 IF A$="1" THEN CHOPT=1
2150 IF A$="2" THEN CHOPT=2
2160 K=1  'CHANNEL 1
2170 IF CHOPT <>0 THEN K= CHOPT
2180 '
2190 MY.ADDR%=21
2200 SYS.CONTROL%=0     ' initialize as system ctrlr
2210 CALL INIT%(MY.ADDR%,SYS.CONTROL%)
2220 S$="UNL UNT"              'INITIALIZE BUS
2230 CALL TRANSMIT%(S$,STATUS%)
2240 IF STATUS%<>0 THEN GOTO 8900
2250 ADDR%=15                        ' HP-54100 Oscilloscope address
2260 '
2270 REM ---------------------- Send --------------------------
2280 CLS:LOCATE 1,1
2290 PRINT"SCOPE GRABBER NOW GRABBING CHANNEL ";K
2300 'S$="CLEAR"
2310 'CALL SEND% (ADDR%,S$,STATUS%)
2320 'IF STATUS%<>0 THEN 2320
2330 'S$="HEADER OFF"
2340 'CALL SEND% (ADDR%,S$,STATUS%)
2350 'IF STATUS%<>0 THEN 2320
2360 REM ---------------------- Send --------------------------
2370 'N$=RIGHT$(STR$(K),1)
2380 'S$="CHANNEL "+N$+";
2390 'CALL SEND% (ADDR%,S$,STATUS%)
2400 'IF STATUS%<>0 THEN 8900
2402 'S$="DISPLAY FORMAT SINGLE"
2404 'CALL SEND% (ADDR%,S$,STATUS%)
2406 'IF STATUS%<>0 THEN 8900
2410 REM ---------------------- Send --------------------------
2420 'S$="ACQUIRE TYPE AVERAGE COUNT 1 COMPLETE 90 POINTS 1024;"
2430 'CALL SEND% (ADDR%,S$,STATUS%)
2440 'FOR SCOPEW=1 TO 10000: NEXT SCOPEW 'WAIT FOR SCOPE TO SETTLE
2450 'IF STATUS%<>0 THEN 8900
2460 REM ---------------------- Send --------------------------
2470 S$="DIGITIZE CHANNEL"+N$+"
2480 CALL SEND% (ADDR%,S$,STATUS%)
2490 IF STATUS%<>0 THEN 8900
2500 REM ---------------------- Send --------------------------
2510 S$="WAVEFORM POINTS?"
2520 CALL SEND% (ADDR%,S$,STATUS%)
2530 IF STATUS%<>0 THEN 8900
2540 REM ---------------------- Enter -------------------------
2550 R$=SPACE$(13)              'allocate receive buffer
2560 CALL ENTER% (R$,LENGTH%,ADDR%,STATUS%)
2570 IF STATUS%<>0 THEN 8900
2580 POINTS=VAL(R$):PRINT "THE NUMBER OF WAVE POINTS=";POINTS,
2590 PTMOD=INT(POINTS/100)
2600 PRINT "PTMOD =";PTMOD
2610 IF (PTMOD < 1) THEN PTMOD=1
2620 IF POINTS>1300 THEN PRINT"WARNING: EXCESS POINTS (MAX 1300)"
2630 REM ---------------------- Send --------------------------
2640 S$="WAVEFORM XINC?"
2650 CALL SEND% (ADDR%,S$,STATUS%)
2660 IF STATUS%<>0 THEN 8900
2670 R$=SPACE$(30)              'allocate receive buffer
2680 CALL ENTER% (R$,LENGTH%,ADDR%,STATUS%)
2690 IF STATUS%<>0 THEN 8900
```

```
2700 XINC=VAL(R$):'---------- Send --------------------------
2710 S$="WAVEFORM XOR?"
2720 CALL SEND% (ADDR%,S$,STATUS%)
2730 IF STATUS%<>0 THEN 8900
2740 R$=SPACE$(30)              'allocate receive buffer
2750 CALL ENTER% (R$,LENGTH%,ADDR%,STATUS%)
2760 IF STATUS%<>0 THEN 8900
2770 XORG=VAL(R$):'---------- Send --------------------------
2780 S$="WAVEFORM YREF?"
2790 CALL SEND% (ADDR%,S$,STATUS%)
2800 IF STATUS%<>0 THEN 8900
2810 R$=SPACE$(13)              'allocate receive buffer
2820 CALL ENTER% (R$,LENGTH%,ADDR%,STATUS%)
2830 IF STATUS%<>0 THEN 8900
2840 YREF=VAL(R$):'---------- Send --------------------------
2850 S$="WAVEFORM YINC?"
2860 CALL SEND% (ADDR%,S$,STATUS%)
2870 IF STATUS%<>0 THEN 8900
2880 R$=SPACE$(13)              'allocate receive buffer
2890 CALL ENTER% (R$,LENGTH%,ADDR%,STATUS%)
2900 IF STATUS%<>0 THEN 8900
2910 YINC=VAL(R$):'---------- Send --------------------------
2920 S$="WAVEFORM YOR?"
2930 CALL SEND% (ADDR%,S$,STATUS%)
2940 IF STATUS%<>0 THEN 8900
2950 REM ---------- Enter --------------------------
2960 R$=SPACE$(13)              'allocate receive buffer
2970 CALL ENTER% (R$,LENGTH%,ADDR%,STATUS%)
2980 IF STATUS%<>0 THEN 8900
2990 YOR=VAL(R$)
3000 S$="WAVEFORM FORMAT ASCII;WAVEFORM DATA? "
3010 CALL SEND% (ADDR%,S$,STATUS%)
3020 IF STATUS%<>0 THEN 8900
3030 REM ---------- TRANSMIT ----------
3040 S$="MLA TALK 15"
3050 CALL TRANSMIT% (S$,STATUS%)
3060 IF STATUS%<>0 THEN 8900
3070 TRACE$ = +CHRFILE$+"SCP.PRN"
3080 OPEN "O",#1, TRACE$
3090 WRITE #1, TRACE$
3100 WRITE #1, EXPERIMENT$
3110 WRITE #1, DATE$
3120 WRITE #1, TIME$
3130 WRITE #1,
3140 WRITE #1, "TEST GAS=";GAS$
3150 WRITE #1, "BTH TEMP=";BATH$
3160 WRITE #1, "FLW RATE=";FLOWR$
3170 WRITE #1, "CHP TEMP=";CHIPTEMP$
3180 WRITE #1, "HUMIDITY=";VHUMD$
3190 WRITE #1, "
3200 WRITE #1, "HP-54100A OSCILLOSCOPE DUMP "
3210 WRITE #1, "
3220 WRITE #1, "   TIME          VOLTAGE"
3230 WRITE #1,
3240 PRINT " "
3250 PRINT "(INDEX)                TIME                  VOLTAGE"
3260 PRINT "-----------------------------------------------------"
3270 FOR I=1 TO POINTS
3280    REM ---------- Receive ----------
3290    R1$=SPACE$(32)              ' allocate receive buffer
3300    IF STATUS%<>0 THEN 8900
3310    TPOINT=XINC*I+XORG
3320    CALL RECEIVE% (R1$,LENGTH%,STATUS%)
```

```
3330     IF STATUS%<>0 THEN 8900
3340     VPOINT(I)=((VAL(R1$)-YREF)*YINC)+YOR
3350     IF (I MOD 100)=0 THEN PRINT "(";I;")",TPOINT;",",VPOINT(I)
3360     IF (I MOD PTMOD)=0 THEN PRINT#1, USING "+#.#####^^^^,";
    TPOINT;VPOINT(I)
3370 NEXT I
3380 CLOSE #1
3390 X=K+1 : IF CHOPT<>0 THEN K=3
3400 IF K<3 THEN 2270
3410 '
3420 S$="LOCAL"
3430 CALL SEND% (ADDR%,S$,STATUS%)
3440 S$="UNL UNT"
3450 CALL TRANSMIT% (S$,STATUS%)
3460 IF STATUS%<>0 THEN 8900
3470 PRINT"FINISHED"
3480 RETURN
3490 '
3500 '
3510 '
3520 '
3530 '
3540 REM*****************************************************************
3550 REM** ROUTINE TO COLLECT GAIN PHASE DATA FROM THE HP-4194B  **
3560 REM** GAIN PHASE ANALYZER.                                  **
3570 REM**                                                      **
3580 REM** WRITTEN BY: Capt Thomas Jenkins                      **
3590 REM**                                                      **
3600 REM** Modified by: Charles P. Brothers Jr.                 **
3610 REM**                GE-90D                                **
3620 REM**                                                      **
3630 REM** NOTES: The HP-4194A is set to run GAIN PHASE         **
3640 REM**   measurements from the IGEFET electrodes.          **
3650 REM**                                                      **
3660 REM**                                                      **
3670 REM*****************************************************************
3680 '
3690 CLS
3700 PRINT,"  HP4194A GAIN PHASE DATA TRANSFER "
3710 '
3720 '------------- GP-IB ADDRESSES OF INSTRUMENTS ------------------
3730 HP4194%=17: HP4192%=9: PRINTER%=1: MY.ADDR%=21: K617%=27
3740 SWITCH%=28
3750 '
3760 SYSCON%=0                          'PC488 ACTS AS CONTROLLER
3770 CALL INIT%(MY.ADDR%,SYSCON%)
3780 '
3790 PRINT " "
3800 PRINT "SETTING-UP 4194 FOR GAIN PHASE MEASUREMENTS -- WAIT..."
3810 '
3820 S$="RST"                         'INITIALIZE 4194 TO POWER ON SETTING
3830 CALL SEND%(HP4194%,S$,STATUS%)
3840 S$="RQS2"                         'UNMASK AND ENABLE BIT1 FOR SRQ
3850 CALL SEND%(HP4194%,S$,STATUS%)
3860 S$="FNC2"                         'SET 4194 TO GAIN PHASE MODE
3870 CALL SEND%(HP4194%,S$,STATUS%)
3880 S$="PHS2"                         'SET PHASE SCALE TO EXPANSION MODE
3890 CALL SEND%(HP4194%,S$,STATUS%)
3900 S$="SWM2"                         'SET SWEEP MODE TO SINGLE
3910 CALL SEND%(HP4194%,S$,STATUS%)
3920 S$="SWT2"                         'SET TO LOG SWEEP
3930 CALL SEND%(HP4194%,S$,STATUS%)
3940 S$="OSC=0.5V"                     'SET SWEEP OSCILLATOR TO .5 VOLT
```

```
3950 CALL SEND%(HP4194%,S$,STATUS%)
3960 S$="MCF1"                          'TURN MARKERS ON
3970 CALL SEND%(HP4194%,S$,STATUS%)
3980 S$="ZIT1"                          'TEST CHANNEL TO 1 MOHMS
3990 CALL SEND%(HP4194%,S$,STATUS%)
4000 'S$="ATR2"                         'REFERENCE CHANNEL 20DB
4010 'CALL SEND%(HP4194%,S$,STATUS%)
4020 S$="START=10HZ"                    'STRT SWEEP AT 10HZ
4030 CALL SEND%(HP4194%,S$,STATUS%)
4040 S$="STOP=1000000HZ"                'SWEEP TO 1MHz
4050 CALL SEND%(HP4194%,S$,STATUS%)
4060 '
4070 INPUT "PERFORM THE OFFSET REF STORE, THEN RETURN", NULL$
4080 '
4090 CALL INIT%(MY.ADDR%,SYSCON%)
4100 CALL SPOLL%(HP4194%,POLL%,STATUS%)   'MAKE SURE SRQ NOT SET
4110 S$="OSC=0.1V"                      'SET SWEEP OSCILLATOR TO 0.1 VOLT
4120 CALL SEND%(HP4194%,S$,STATUS%)
4130 S$="ITM2"                          'SET INTEGRATION TIME TO 10 mSEC
4140 CALL SEND%(HP4194%,S$,STATUS%)
4150 S$="X?"                            'READ IN FREQUENCY POINTS
4160 CALL SEND%(HP4194%,S$,STATUS%)
4170 IF STATUS%<>0 THEN 8900
4180 S$="MLA TALK 17"                   '4194 TO OUTPUT
4190 CALL TRANSMIT%(S$,STATUS%)
4200 TEMP$=SPACE$(15)
4210 FOR I=0 TO 400
4220    CALL RECEIVE%(TEMP$,LENGTH%,STATUS%)
4230    GFREQ(I)=VAL(LEFT$(TEMP$,12))
4240 NEXT I
4250 '
4260 CLS
4270 INPUT "NUMBER OF ELECTRODES TO BE SAMPLED:  ",NELECT
4280 GAINPHS = +CHRFILE$+"GPA.PRN"
4290 OPEN "O",#2, GAINPH$
4300 WRITE #2, GAINPH$
4310 WRITE #2, EXPERIMENT$
4320 WRITE #2, DATE$
4330 WRITE #2, TIME$
4340 WRITE #2,
4350 WRITE #2, "TEST GAS=";GAS$
4360 WRITE #2, "BTH TEMP=";BATH$
4370 WRITE #2, "FLW RATE=";FLOWR$
4380 WRITE #2, "CHP TEMP=";CHIPTEMP$
4390 WRITE #2, "HUMIDITY=";VHUMD$
4400 WRITE #2, "
4410 WRITE #2, "HP-4194A GAIN PHASE DUMP
4420 WRITE #2, "
4430 WRITE #2, "ELECTRODE    FREQUENCY    Z-MAG       PHASE"
4440 WRITE #2, "
4450 CLS
4460 INPUT "CONNECT 4194 ACROSS GATE.   HIT RETURN ", NULL$
4470 FOR N=0 TO (NELECT-1)     'LOOP THROUGH THE NUMBER OF ELECTRODES
4480     PRINT "CONNECT ELECTRODE ";N,
4490     INPUT "HIT RETURN ",NULL$
4500     GOSUB 4650     ' GO GET DATA
4510     '
4520     FOR I= 0 TO 400
4530 IF (I MOD 4)=0 THEN PRINT#2, USING "+#.####^^^^,";
     N;GFREQ(I);MAG(I);PHS(I)
4540     IF (I MOD 100) = 0 THEN PRINT N,GFREQ(I),MAG(I),PHS(I)
4550     NEXT I
4560 NEXT N    ' LOOP THROUGH THE ELECTRODE
```

```
4570 CLOSE #2
4580 S$="UNL UNT"            'INITIALIZE BUS
4590 CALL TRANSMIT% (S$,STATUS%)
4600 IF STATUS%<>0 THEN GOTO 8900
4610 RETURN
4620 '
4630 '-------------------- HP4194 DATA INPUT ROUTINE ----------------
4640 '
4650 CALL SPOLL%(HP4194%,POLL%,STATUS%)  'MAKE SURE SRQ IS NOT SET
4660 S$="SWTRG"                          'PERFORM SINGLE SWEEP
4670 CALL SEND%(HP4194%,S$,STATUS%)
4680 CALL SPOLL%(HP4194%,POLL%,STATUS%)  'IS SWEEP COMPLETE?
4690 IF ((POLL% AND 64) <> 64) THEN 4680 'IF NOT CONTINUE POLL
4700 '
4710 S$="AUTOA"                          'AUTOSCALE DISPLAY A
4720 CALL SEND%(HP4194%,S$,STATUS%)
4730 S$="AUTOB"                          'AUTOSCALE DISPLAY B
4740 CALL SEND%(HP4194%,S$,STATUS%)
4750 S$="A?"                             'READ IN MAG VALUE
4760 CALL SEND%(HP4194%,S$,STATUS%)      'FROM THE ARRAY REG A
4770 '
4780 S$= "MLA TALK 17"
4790 CALL TRANSMIT%(S$,STATUS%)
4800 TEMP$= SPACE$(13)
4810 FOR I = 0 TO 400
4820     CALL RECEIVE%(TEMP$,LENGTH%,STATUS%)
4830     MAG(I)=VAL(LEFT$(TEMP$,12))     'EXTRACT MAG VALUE
4840 NEXT I
4850 '
4860 S$="B?"                 'READ IN PHASE FROM ARRAY REGISTER B
4870 CALL SEND%(HP4194%,S$,STATUS%)
4880 S$= "MLA TALK 17"
4890 CALL TRANSMIT%(S$,STATUS%)
4900 FOR I= 0 TO 400
4910     CALL RECEIVE%(TEMP$,LENGTH%,STATUS%)
4920     PHS(I)= VAL(LEFT$(TEMP$,12))     'EXTRACT PHASE VALUE
4930 NEXT I
4940 '
4950 CALL SPOLL%(HP4194%,POLL%,STATUS%)   'MAKE SURE SRQ NOT SET
4960 RETURN
4970 '
4980 '
4990 '
5000 '
5010 '
5020 REM*****************************************************************
5030 REM** ROUTINE TO COLLECT IMPEDANCE DATA FROM THE HP-4194B   **
5040 REM** IMPEDANCE / GAIN PHASE ANALYZER.                     **
5050 REM**                                                     **
5060 REM** WRITTEN BY: Capt Thomas Jenkins                     **
5070 REM**                                                     **
5080 REM** Modified by: Charles P. Brothers Jr.                **
5090 REM**               GE-90D                                **
5100 REM**                                                     **
5110 REM** NOTES: The HP-4194A is set to run IMPEDANCE         **
5120 REM**   measurements from the IGEFET electrodes.          **
5130 REM**                                                     **
5140 REM**                                                     **
5150 REM*****************************************************************
5160 '
5170 CLS
5180 PRINT,"  HP4194A IMPEDANCE DATA TRANSFER "
5190 '
```

```
5200 '------------ GP-IB ADDRESSES OF INSTRUMENTS -------------------
5210 HP4194%=17
5220 HP4192%=9
5230 PRINTER%=1
5240 K617%=27
5250 SWITCH%=28
5260 '
5270 PRINT " "
5280 PRINT "SETTING-UP 4194 FOR IMPEDANCE MEASUREMENTS -- WAIT..."
5290 '
5300 S$="RST"                          'INITIALIZE 4194 TO POWER ON SETTING
5310 CALL SEND%(HP4194%,S$,STATUS%)
5320 S$="RQS2"                         'UNMASK AND ENABLE BIT1 FOR SRQ
5330 CALL SEND%(HP4194%,S$,STATUS%)
5340 S$="FNC1"                         'SET 4194 TO IMPEDANCE MODE
5350 CALL SEND%(HP4194%,S$,STATUS%)
5360 S$="PHS2"                         'SET PHASE SCALE TO EXPANSION MODE
5370 CALL SEND%(HP4194%,S$,STATUS%)
5380 S$="SWM2"                         'SET SWEEP MODE TO SINGLE
5390 CALL SEND%(HP4194%,S$,STATUS%)
5400 S$="SWT2"                         'SET TO LOG SWEEP
5410 CALL SEND%(HP4194%,S$,STATUS%)
5420 S$="OSC=0.1V"                     'SET SWEEP OSCILLATOR TO 0.1 VOLT
5430 CALL SEND%(HP4194%,S$,STATUS%)
5440 S$="MCF1"                         'TURN MARKERS OFF
5450 CALL SEND%(HP4194%,S$,STATUS%)
5460 S$="ITM2"                         'SET INTEGRATION TIME TO 5 mSEC
5470 CALL SEND%(HP4194%,S$,STATUS%)
5480 S$="START=100HZ"                   'STRT SWEEP AT 100 HZ
5490 CALL SEND%(HP4194%,S$,STATUS%)
5500 S$="STOP=1000000HZ"               'SWEEP TO 1MHz
5510 CALL SEND%(HP4194%,S$,STATUS%)
5520 '
5530 INPUT "PERFORM THE OFFSET REF STORE, THEN RETURN", NULL$
5540 '
5550 S$="X?"                           'READ IN FREQUENCY POINTS
5560 CALL SEND%(HP4194%,S$,STATUS%)
5570 IF STATUS%<>0 THEN 8900
5580 S$="MLA TALK 17"                  '4194 TO OUTPUT
5590 CALL TRANSMIT%(S$,STATUS%)
5600 TEMP$=SPACE$(15)
5610 FOR I=0 TO 400
5620    CALL RECEIVE%(TEMP$,LENGTH%,STATUS%)
5630    GFREQ(I)=VAL(LEFT$(TEMP$,12))
5640 NEXT I
5650 '
5660 CLS
5670 INPUT "NUMBER OF ELECTRODES TO BE SAMPLED:  ",NELECT
5680 GATEIMP$ = +CHRFILE$+"IMP.PRN"
5690 OPEN "O",#2, GATEIMP$
5700 WRITE #2, GATEIMP$
5710 WRITE #2, EXPERIMENT$
5720 WRITE #2, DATE$
5730 WRITE #2, TIME$
5740 WRITE #2,
5750 WRITE #2, "TEST GAS=";GAS$
5760 WRITE #2, "BTH TEMP=";BATH$
5770 WRITE #2, "FLW RATE=";FLOWR$
5780 WRITE #2, "CHP TEMP=";CHIPTEMP$
5790 WRITE #2, "HUMIDITY=";VHUMD$
5800 WRITE #2, "
5810 WRITE #2, "HP-4194A IMPEDANCE DUMP"
5820 WRITE #2, "
```

```
5830 WRITE #2, "ELECTRODE    FREQUENCY    Z-MAG       PHASE"
5840 WRITE #2,
5850 CLS
5860 INPUT "CONNECT 4194 ACROSS GATE,   HIT RETURN ", NULL$
5870 FOR N=0 TO (NELECT-1)     'LOOP THROUGH THE NUMBER OF ELECTRODES
5880      PRINT "CONNECT ELECTRODE ";N,
5890      INPUT "HIT RETURN ",NULL$
5900      GOSUB 6050     ' GO GET DATA
5910      '
5920      FOR I= 0 TO 400
5930 IF (I MOD 4)=0 THEN PRINT#2, USING "+#.####^^^^,";
     N;GFREQ(I);MAG(I);PHS(I)
5940      IF (I MOD 100) = 0 THEN PRINT N,GFREQ(I),MAG(I),PHS(I)
5950      NEXT I
5960 NEXT N    ' LOOP THROUGH THE ELECTRODE
5970 CLOSE #2
5980 S$="UNL UNT"            'INITIALIZE BUS
5990 CALL TRANSMIT% (S$,STATUS%)
6000 IF STATUS%<>0 THEN GOTO 8900
6010 RETURN
6020 '
6030 '---------------------- HP4194 DATA INPUT ROUTINE ----------------
6040 '
6050 CALL SPOLL%(HP4194%,POLL%,STATUS%)  'MAKE SURE SRQ IS NOT SET
6060 S$="SWTRG"                          'PERFORM SINGLE SWEEP
6070 CALL SEND%(HP4194%,S$,STATUS%)
6080 CALL SPOLL%(HP4194%,POLL%,STATUS%)  'IS SWEEP COMPLETE?
6090 IF ((POLL% AND 64) <> 64) THEN 6080 'IF NOT CONTINUE POLL
6100 '
6110 S$="AUTOA"                          'AUTOSCALE DISPLAY A
6120 CALL SEND%(HP4194%,S$,STATUS%)
6130 S$="AUTOB"                          'AUTOSCALE DISPLAY B
6140 CALL SEND%(HP4194%,S$,STATUS%)
6150 S$="A?"                             'READ IN MAG VALUE
6160 CALL SEND%(HP4194%,S$,STATUS%)      'FROM THE ARRAY REG A
6170 '
6180 S$= "MLA TALK 17"
6190 CALL TRANSMIT%(S$,STATUS%)
6200 TEMP$= SPACE$(13)
6210 FOR I = 0 TO 400
6220      CALL RECEIVE%(TEMP$,LENGTH%,STATUS%)
6230      MAG(I)=VAL(LEFT$(TEMP$,12))     'EXTRACT MAG VALUE
6240 NEXT I
6250 '
6260 S$="B?"                  'READ IN PHASE FROM ARRAY REGISTER B
6270 CALL SEND%(HP4194%,S$,STATUS%)
6280 S$= "MLA TALK 17"
6290 CALL TRANSMIT%(S$,STATUS%)
6300 FOR I= 0 TO 400
6310      CALL RECEIVE%(TEMP$,LENGTH%,STATUS%)
6320      PHS(I)= VAL(LEFT$(TEMP$,12))     'EXTRACT PHASE VALUE
6330 NEXT I
6340 '
6350 CALL SPOLL%(HP4194%,POLL%,STATUS%)   'MAKE SURE SRQ NOT SET
6360 RETURN
6370 '
6380 '
6390 '
6400 '
6410 '
6420 '
6430 REM*****************************************************************
6440 REM** PROGRAM TO COLLECT SPECTRUM DATA FROM THE HP 4195A    **
```

```
6450 REM** SPECTRUM ANALYZER.                                          **
6460 REM**                                                             **
6470 REM** Charles P. Brothers Jr.                                     **
6480 REM** GE-90D                                                      **
6490 REM**                                                             **
6500 REM** NOTES: The HP-4195A is set to run in one pass               **
6510 REM**   from 0.001HZ to 10 KHZ.                                   **
6520 REM**                                                             **
6530 REM**                                                             **
6540 REM*****************************************************************
6550 '
6560 CLS
6570 HPADDR%=18                          'HP-4195A ADDRESS
6580 REM ---------------------- TRANSMIT ----------------------
6590 S$="UNL UNT"              'INITIALIZE BUS
6600 CALL TRANSMIT% (S$,STATUS%)
6610 IF STATUS%<>0 THEN GOTO 8900
6620 CLS : PRINT " "
6630 PRINT "          HP4195A (SPECTRUM ANALYZER) Control Software"
6640 '
6650 REM ------------------ GENERATE FILE HEADER --------------------
6660 CLS
6670 PRINT " "
6680 FILENAM$=+CHRFILE$+"SPL.PRN"
6690 OPEN "O",#1, FILENAM$
6700 WRITE #1, FILENAM$
6710 WRITE #1, EXPERIMENT$
6720 WRITE #1, DATE$
6730 WRITE #1, TIME$
6740 WRITE #1,
6750 WRITE #1, "TEST GAS=";GAS$
6760 WRITE #1, "BTH TEMP=";BATH$
6770 WRITE #1, "FLW RATE=";FLOWR$
6780 WRITE #1, "CHP TEMP=";CHIPTEMP$
6790 WRITE #1, "HUMIDITY=";VHUMD$
6800 WRITE #1, "
6810 WRITE #1, "HP-4195A LOW FREQ SWEEP,  0.001 HZ TO 10 KHZ"
6820 WRITE #1,
6830 WRITE #1, " ELECTRODE    FREQUENCY    AMPLITUDE"
6840 WRITE #1,
6850 '
6860 '
6865 INPUT "ENTER NUMBER OF ELECTRODES TO BE MEASURED: ",ELECT
6870 REM ---------- BEGIN DATA COLLECTION PASS ----------------------
6890 REM CAPTURE DATA AND TRANSFER TO 1EEE-488 BUS
6900 '
6910 CLS                         'CLEAR PC SCREEN
6920 PRINT "PLEASE WAIT, CAPTURING DATA . . ."
6940 REM SETUP HP4195A
6950 S$="FNC2;START=.001HZ;STOP=10KHZ;NOP=401;SAP1;SWP1;SWT1;PORT1;PWR1"
6960 CALL SEND% (HPADDR%,S$,STATUS%)
6970 S$="SWM1;FMT1"
6980 CALL SEND% (HPADDR%,S$,STATUS%)
7002 FOR COUNT = 0 TO (ELECT - 1)
7004   PRINT "CONNECT ELECTRODE ";COUNT,
7006   INPUT "HIT RETURN", NULL$
7008   INPUT " WAIT FOR DISPLAY TO STABILIZE,  HIT RETURN ",NULL$
7010   S$="SWM2;FMT1"
7012   CALL SEND% (HPADDR%,S$,STATUS%)
7014   IF STATUS%=0 THEN GOTO 7080
7020   PRINT "A LONG SWEEP TIME IS HOLDING UP SYSTEM"
7030   IF STATUS%<>8 OR (STATUS%=8 AND SWEEP < 10) THEN GOTO 8900
7040   CALL SPOLL% (HPADDR%,POLL%,STATUS%)
```

```
7050   GOTO 7020
7060   '
7070   REM ---------------------- TRANSMIT ----------------------
7080   S$="X?"
7090   CALL SEND%(HPADDR%,S$,STATUS%)
7100   S$="MLA TALK 18"
7110   CALL TRANSMIT% (S$,STATUS%)
7120   IF STATUS%<>0 THEN GOTO 8900
7130   REM ---------------------- RECEIVE ----------------------
7140   X$=SPACE$(15)                ' allocate RECEIVE buffer
7150   FOR I=0 TO 400
7160     CALL RECEIVE% (X$,LENGTH%,STATUS%)
7170     IF STATUS%<>0 THEN GOTO 8900
7180     X(I)=VAL(X$)
7190   NEXT I
7200   REM ---------------------- TRANSMIT ----------------------
7210   S$="UNL UNT"
7220   CALL TRANSMIT% (S$,STATUS%)
7230   S$="A?"
7240   CALL SEND%(HPADDR%,S$,STATUS%)
7250   S$="MLA TALK 18"
7260   CALL TRANSMIT% (S$,STATUS%)
7270   IF STATUS%<>0 THEN GOTO 8900
7280   REM ---------------------- RECEIVE ----------------------
7290   REM DRESS-UP THE PC SCREEN OUTPUT
7300   CLS:PRINT " FREQUENCY       AMPLITUDE"
7310   '
7320   A$=SPACE$(13)                ' allocate RECEIVE buffer
7330   FOR I=0 TO 400
7340     CALL RECEIVE% (A$,LENGTH%,STATUS%)
7350     IF STATUS%<>0 THEN GOTO 8900
7360     A(I)=VAL(A$)
7370     IF (I MOD 4)=1 THEN PRINT #1, USING "+#.#####^^^^,";
       COUNT,X(I),A(I)
7380     IF (I MOD 40)=0 THEN PRINT X(I);"HZ  ";A(I);"dbM"
7390   NEXT I
7392   '
7393   S$="SWM1"              ' HP-4195A BACK TO CONTINUOUS SWEEP
7394   CALL SEND% (HPADDR%,S$,STATUS%)
7395   IF STATUS%<>0 THEN GOTO 8900
7396 NEXT COUNT
7400 CLOSE #1
7410 PRINT ""
7420 PRINT " DATA TRANSFER TO '";FILENAM$;"' COMPLETE."
7430 '
7440 REM ---------------------- TRANSMIT ----------------------
7450 S$="UNL UNT"
7460 CALL TRANSMIT% (S$,STATUS%)
7470 IF STATUS%<>0 THEN GOTO 8900
7480 '
7490 S$="SWM1"          ' HP-4195A BACK TO CONTINUOUS SWEEP
7500 CALL SEND% (HPADDR%,S$,STATUS%)
7510 IF STATUS%<>0 THEN GOTO 8900
7520 '
7530 REM -----------TERMINATE HP-4195A CONTROL ---------------
7540 S$="UNL UNT"
7550 CALL TRANSMIT% (S$,STATUS%)
7560 '
7570 CLS         'CLEAR SCREEN
7580 RETURN
7590 '
7600 '
7610 '
```

```
7620 '
7630 '
7640 REM*****************************************************************
7650 REM** ROUTINE TO COLLECT SPECTRUM DATA FROM THE HP 4195A     **
7660 REM** SPECTRUM ANALYZER.                                    **
7670 REM**                                                      **
7680 REM** Charles P. Brothers Jr.                              **
7690 REM** GE-90D                                               **
7700 REM**                                                      **
7710 REM** NOTES: The HP-4195A is set to run in one pass        **
7720 REM**   from 0.001HZ to 1.0MHZ.                           **
7730 REM**                                                      **
7740 REM**                                                      **
7750 REM*****************************************************************
7760 '
7770 CLS
7780 HPADDR%=18                              'HP-4195A ADDRESS
7790 '
7800 REM ---------------------- TRANSMIT ----------------------
7810 S$="UNL UNT"            'INITIALIZE BUS
7820 CALL TRANSMIT% (S$,STATUS%)
7830 IF STATUS%<>0 THEN GOTO 8900
7840 '
7850 REM ------------------- GENERATE FILE HEADER -------------------
7860 CLS
7870 PRINT " "
7880 FILENAM$ = +CHRFILE$+"SPH.PRN"
7890 OPEN "O",#1, FILENAM$
7900 WRITE #1, FILENAM$
7910 WRITE #1, EXPERIMENT$
7920 WRITE #1, DATE$
7930 WRITE #1, TIME$
7940 WRITE #1,
7950 WRITE #1, "TEST GAS=";GAS$
7960 WRITE #1, "BTH TEMP=";BATH$
7970 WRITE #1, "FLW RATE=";FLOWR$
7980 WRITE #1, "CHP TEMP=";CHIPTEMP$
7990 WRITE #1, "HUMIDITY=";VHUMD$
8000 WRITE #1, "
8010 WRITE #1, "HP-4195A HIGH FREQ SWEEP,  0.001 HZ TO 1.0 MHZ"
8020 WRITE #1,
8030 WRITE #1, " ELECTRODE    FREQUENCY    AMPLITUDE"
8040 WRITE #1,
8050 '
8052 INPUT "ENTER NUMBER OF ELECTRODES TO BE MEASURED: ",ELECT
8060 REM ---------- BEGIN DATA COLLECTION PASS ----------------------
8070 REM CAPTURE DATA AND TRANSFER TO IEEE-488 BUS
8080 '
8090 CLS                        'CLEAR PC SCREEN
8100 PRINT "PLEASE WAIT, CAPTURING DATA . . ."
8110 REM SETUP HP4195A
8120 S$="FNC2;START=.001HZ;STOP=1MHZ;NOP=401;SAP1;SWP1;SWT1;PORT1;PWR1"
8130 CALL SEND% (HPADDR%,S$,STATUS%)
8140 S$="SWM1;FMT1"
8150 CALL SEND% (HPADDR%,S$,STATUS%)
8161 FOR COUNT = 0 TO (ELECT - 1)
8162   PRINT "CONNECT ELECTRODE ";COUNT,
8163   INPUT "HIT RETURN", NULL$
8164   INPUT " WAIT FOR DISPLAY TO STABILIZE,  HIT RETURN ",NULL$
8165   S$="SWM2;FMT1"
8166   CALL SEND% (HPADDR%,S$,STATUS%)
8170   IF STATUS%=0 THEN GOTO 8240
8180   PRINT "A LONG SWEEP TIME IS HOLDING UP SYSTEM"
```

```
8190   IF STATUS%<>8 OR (STATUS%=8 AND SWEEP < 10) THEN GOTO 8900
8200   CALL SPOLL% (HPADDR%,POLL%,STATUS%)
8210   GOTO 8180
8220   '
8230   REM ---------------------- TRANSMIT ----------------------
8240   S$="X?"
8250   CALL SEND%(HPADDR%,S$,STATUS%)
8260   S$="MLA TALK 18"
8270   CALL TRANSMIT% (S$,STATUS%)
8280   IF STATUS%<>0 THEN GOTO 8900
8290   REM ---------------------- RECEIVE -----------------------
8300   X$=SPACE$(15)                ' allocate RECEIVE buffer
8310   FOR I=0 TO 400
8320     CALL RECEIVE% (X$,LENGTH%,STATUS%)
8330     IF STATUS%<>0 THEN GOTO 8900
8340     X(I)=VAL(X$)
8350   NEXT I
8360   REM ---------------------- TRANSMIT ----------------------
8370   S$="UNL UNT"
8380   CALL TRANSMIT% (S$,STATUS%)
8390   S$="A?"
8400   CALL SEND%(HPADDR%,S$,STATUS%)
8410   S$="MLA TALK 18"
8420   CALL TRANSMIT% (S$,STATUS%)
8430   IF STATUS%<>0 THEN GOTO 8900
8440   REM ---------------------- RECEIVE -----------------------
8450   REM DRESS-UP THE PC SCREEN OUTPUT
8460   CLS:PRINT " FREQUENCY       AMPLITUDE"
8470   '
8480   A$=SPACE$(13)                ' allocate RECEIVE buffer
8490   FOR I=0 TO 400
8500     CALL RECEIVE% (A$,LENGTH%,STATUS%)
8510     IF STATUS%<>0 THEN GOTO 8900
8520     A(I)=VAL(A$)
8530     IF (I MOD 4)=1 THEN PRINT #1, USING "+#.#####^^^^,";
       COUNT,X(I),A(I)
8540     IF (I MOD 40)=0 THEN PRINT X(I);"HZ  ";A(I);"dbM"
8550   NEXT I
8552   '
8553   S$="SWM1"             ' HP-4195A BACK TO CONTINUOUS SWEEP
8554   CALL SEND% (HPADDR%,S$,STATUS%)
8555   IF STATUS%<>0 THEN GOTO 8900
8556 NEXT COUNT
8560 CLOSE #1
8570 PRINT ""
8580 PRINT " DATA TRANSFER TO '";FILENAM$;"' COMPLETE."
8590 '
8600 REM ---------------------- TRANSMIT ----------------------
8610 S$="UNL UNT"
8620 CALL TRANSMIT% (S$,STATUS%)
8630 IF STATUS%<>0 THEN GOTO 8900
8640 '
8650 S$="SWM1"          ' HP-4195A BACK TO CONTINUOUS SWEEP
8660 CALL SEND% (HPADDR%,S$,STATUS%)
8670 IF STATUS%<>0 THEN GOTO 8900
8680 '
8690 REM -----------TERMINATE HP-4195A CONTROL ---------------
8700 S$="UNL UNT"
8710 CALL TRANSMIT% (S$,STATUS%)
8720 RETURN
8730 '
8740 '
8750 '
```

```
8760 '
8770 '
8780 REM ------------------- TERMINATE PROGRAM -----------------
8790 '
8800 S$="UNL UNT"
8810 CALL TRANSMIT% (S$,STATUS%)
8820 CLS         'CLEAR SCREEN
8830 SYSTEM
8840 '
8850 '
8860 '
8870 '
8880 '
8890 REM -------------------- ERROR MESSAGE ---------------------
8900 PRINT "COMM PROBLEM -- CHECK IEEE-488 CONNECTIONS,
8910 PRINT "                MAKE SURE EQUIPMENT IS ON AND CONNECTED
8920 PRINT "                THEN RESTART PROGRAM."
8930 STOP
```

Appendix D

Test Cell Drawings and Assembly Instructions

The test cell consists of two major assemblies, the aluminum patch panel box and the stainless steel test chamber. The aluminum patch panel box is assembled from 1/16th inch thick aluminum sheet cut and folded to shape. The test chamber is assembled from machined soft stainless steel stock.

Construct the test cell by following the following steps outlined below:

1. Cut one sheet of aluminum (Sheet A) to the dimensions given in Figure 69. Drill or punch 3/8" holes in the sheet of aluminum.
2. Fold Sheet A according to drawing specifications given in Figure 70.
3. Cut one sheet of aluminum (Sheet B) to the dimensions given in Figure 71.
4. Fold Sheet B according to drawing specifications given in Figure 72.
5. Insert the test cell bottom (Sheet B) into the test cell top (Sheet A). Drill 1/16th inch pilot holes every two inches centered along the one inch overlap joints (Figure 77).
6. Machine 1.5" by 3.5" by 6.5" stainless steel stock according the specifications given in the primary chamber drawing (Figure 74).
7. Machine 0.25" by 3.5" by 6.5" stainless steel stock according the specifications given in the chamber top and insert drawing (Figure 75). Drill six holes in the top to align with the holes in the primary chamber (Figure 74). Drill and tap two centered holes in the chamber top (Figure 75).

8. Machine 0.5" by 1.4" by 4.4" stainless steel stock according the specifications given in the chamber top and insert drawing (Figure 75). Drill and countersink two holes to align with the two centered holes in the chamber top (Figure 75).

9. Drill six holes in the test cell top (Sheet A) that align centered with the primary chamber bottom.

10. Build and etch a printed circuit board according to the full size pattern in drawing in Figure 76. Drill 0.050" holes centered in all the circular pads.

11. File the corners of the printed circuit board, allowing it to fit into the bottom of the primary chamber.

12. Drill eight holes in the printed circuit board, that align with the holes in the bottom of the primary chamber.

13. Solder the 64-pin zero-insertion-force socket to the printed circuit board.

14. Solder two feed through pins into two of the feed-through holes in the printed circuit board. Then plug all but one feed-through with a solder plug.

15. Apply a 1/16th inch bead of conductive RTV adhesive along the edge of the 1.5" by 4.5" opening in the bottom of the primary chamber. Next using eight nylon 8 × 32 screws attach the printed circuit board to the bottom of the primary chamber. The Final appearance of the primary chamber should look like Figure 78.

16. Apply a 1/16th inch bead of conductive RTV adhesive along the edge of the 2.5" by 5.5" opening in the test cell top (Sheet A). Attach the primary chamber to the test cell top using six 8 × 32 screws (Figure 77).

17. Install 64 chassis mount female BNC connectors in the test chamber top (Sheet A), with the BNC connectors facing outward.

18. Wire RG-174 from each socket pin on the printed circuit board to a BNC connector. Solder the shielding to the BNC connector ground lug.

19. Drill three 3/8th inch holes in the top of test chamber for the heater strip power supply leads and the thermocouple feed-through. Install female banana connectors into to of the holes. Install a nylon feed-through in the third hole.

20. Solder two wires from the printed circuit feed-through pins to the banana plug connectors.

21. Install a thermocouple sensor running the sensor lead thorough the open printed circuit board and then through the test chamber feed-through. The thermocouple sensor should be placed on top of the socket 0.5" from one end. Seal the feed-through with conductive RTV.

22. Insert the test cell bottom into the test cell top. Attach using the bottom and top using 3/16th inch sheet metal screws.

23. Install 1/8th conductive gasket material into the groove in the top of the primary chamber.

24. Install a heater strip into the primary chamber with the wiring connected to the feed-through pins and heater strip placed over the center of the socket. The heater strip must remain at least 1/2" from the thermocouple sensor.

At this point the test cell is ready for use. To allow easy use and connections to each pin of the integrated circuit, it may be helpful to place labels near each BNC connector indicating which pin it is connected to.

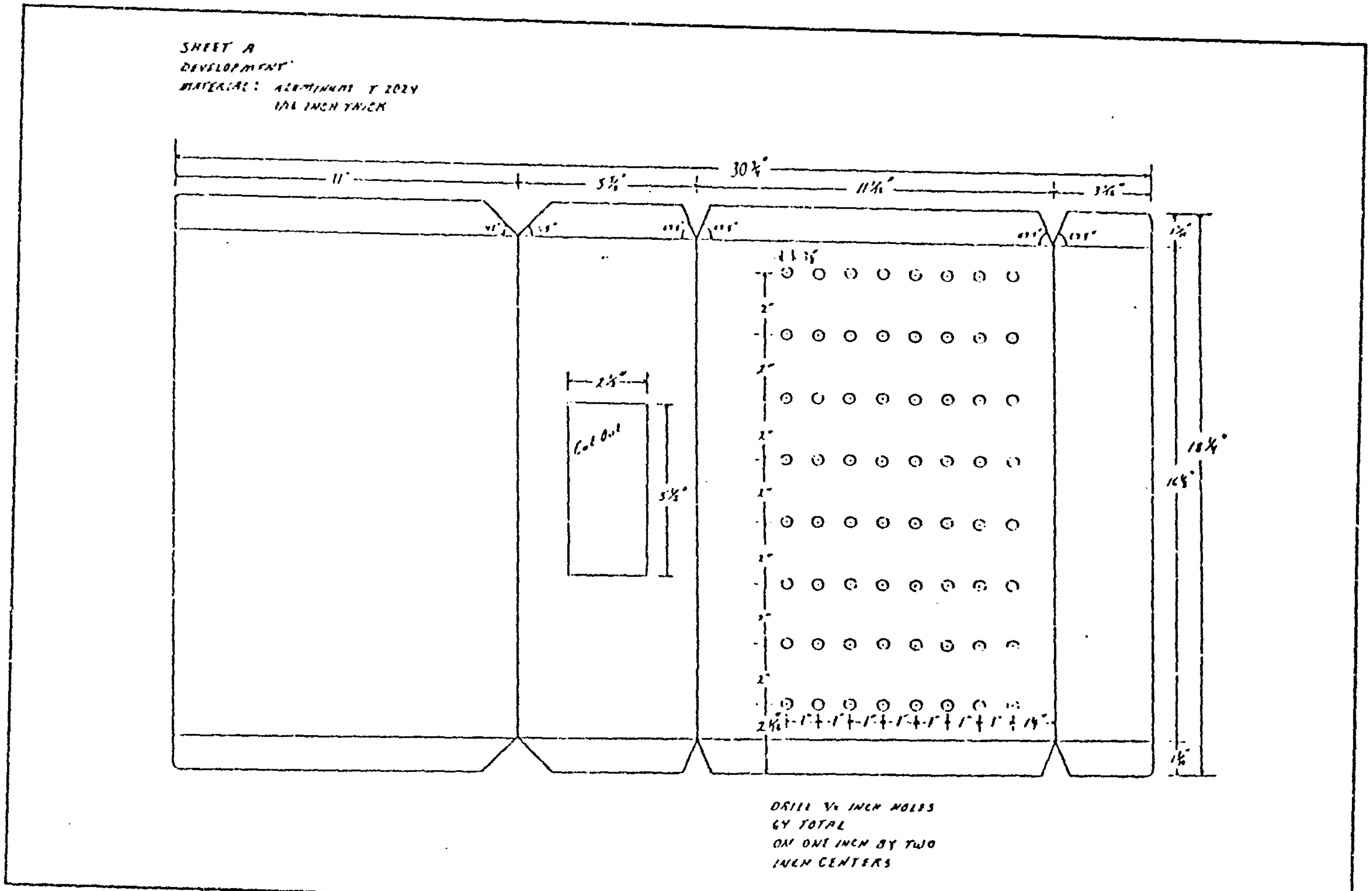

Figure 69. Test Cell Top Half, Sheet A, Development Drawing

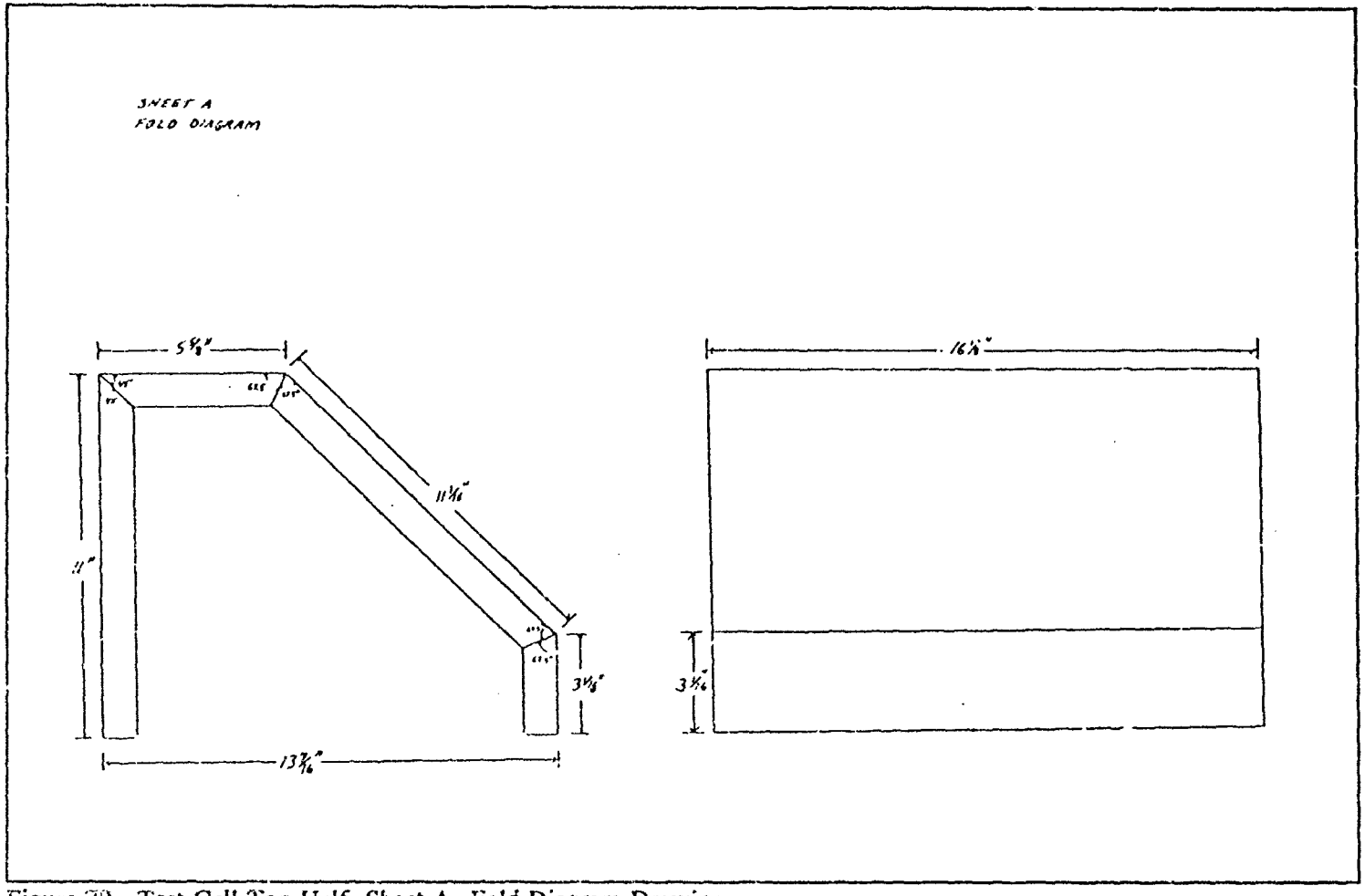

Figure 70. Test Cell Top Half, Sheet A, Fold Diagram Drawing.

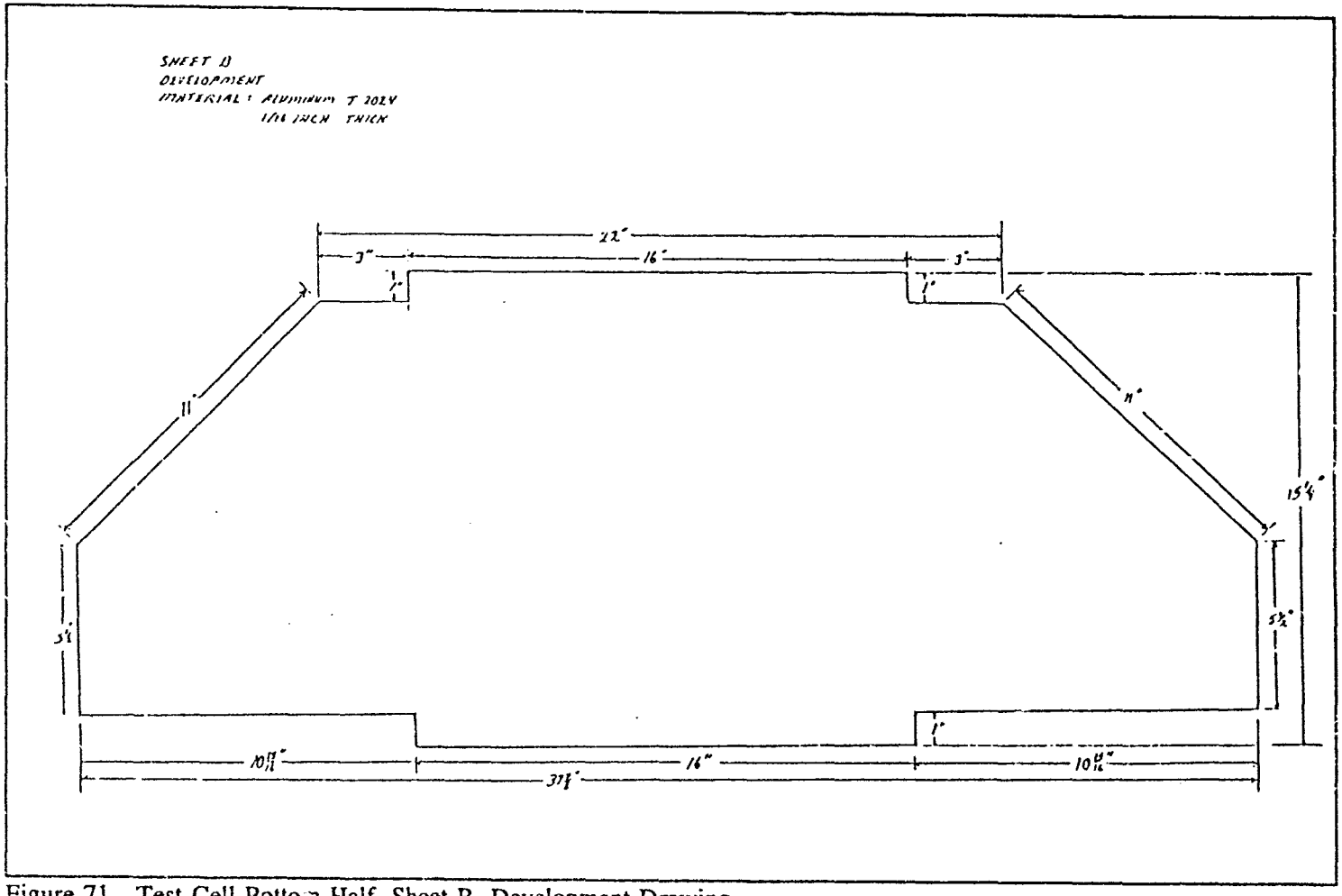

Figure 71. Test Cell Bottom Half, Sheet B, Development Drawing.

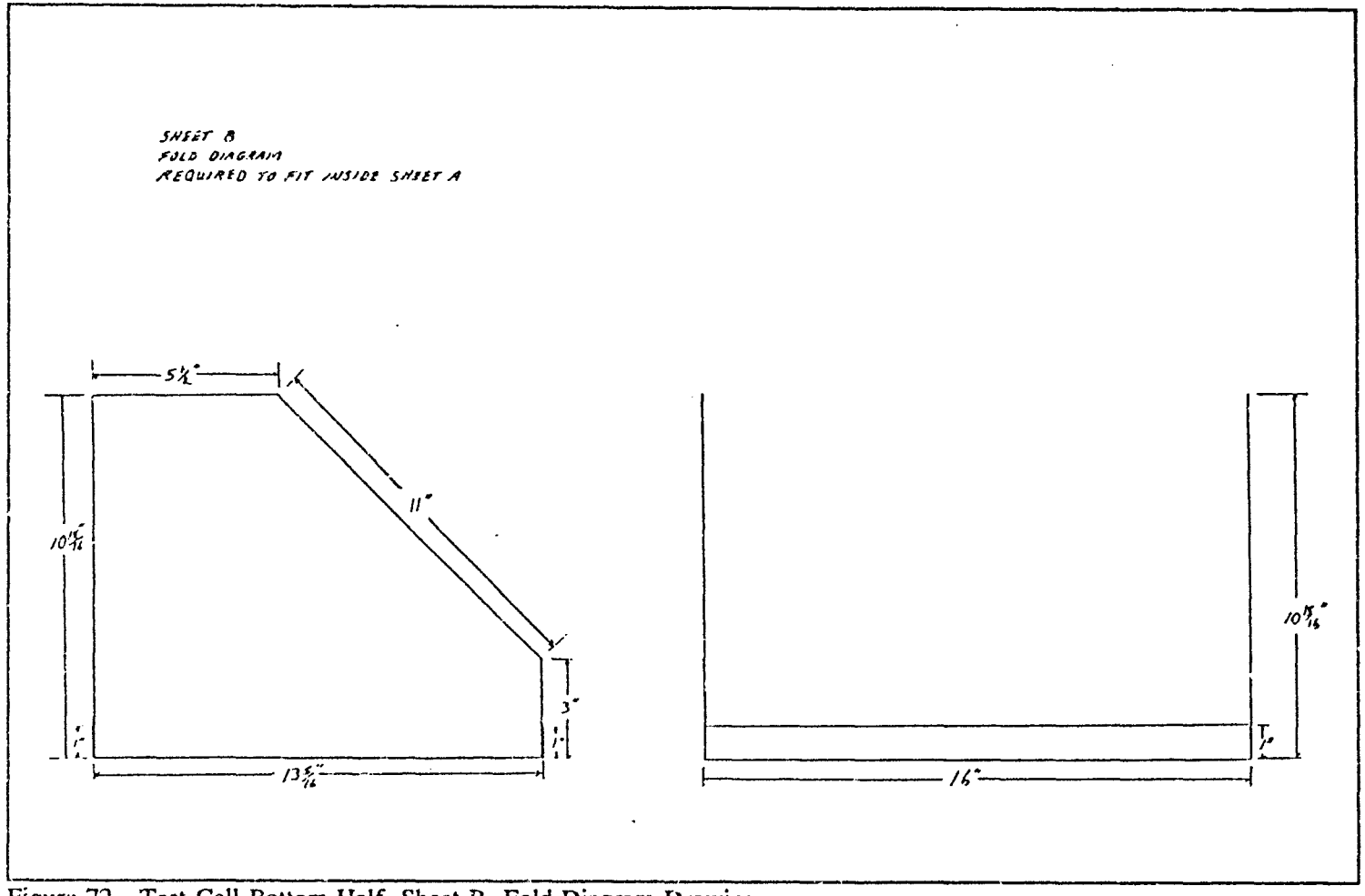

Figure 72. Test Cell Bottom Half, Sheet B, Fold Diagram Drawing.

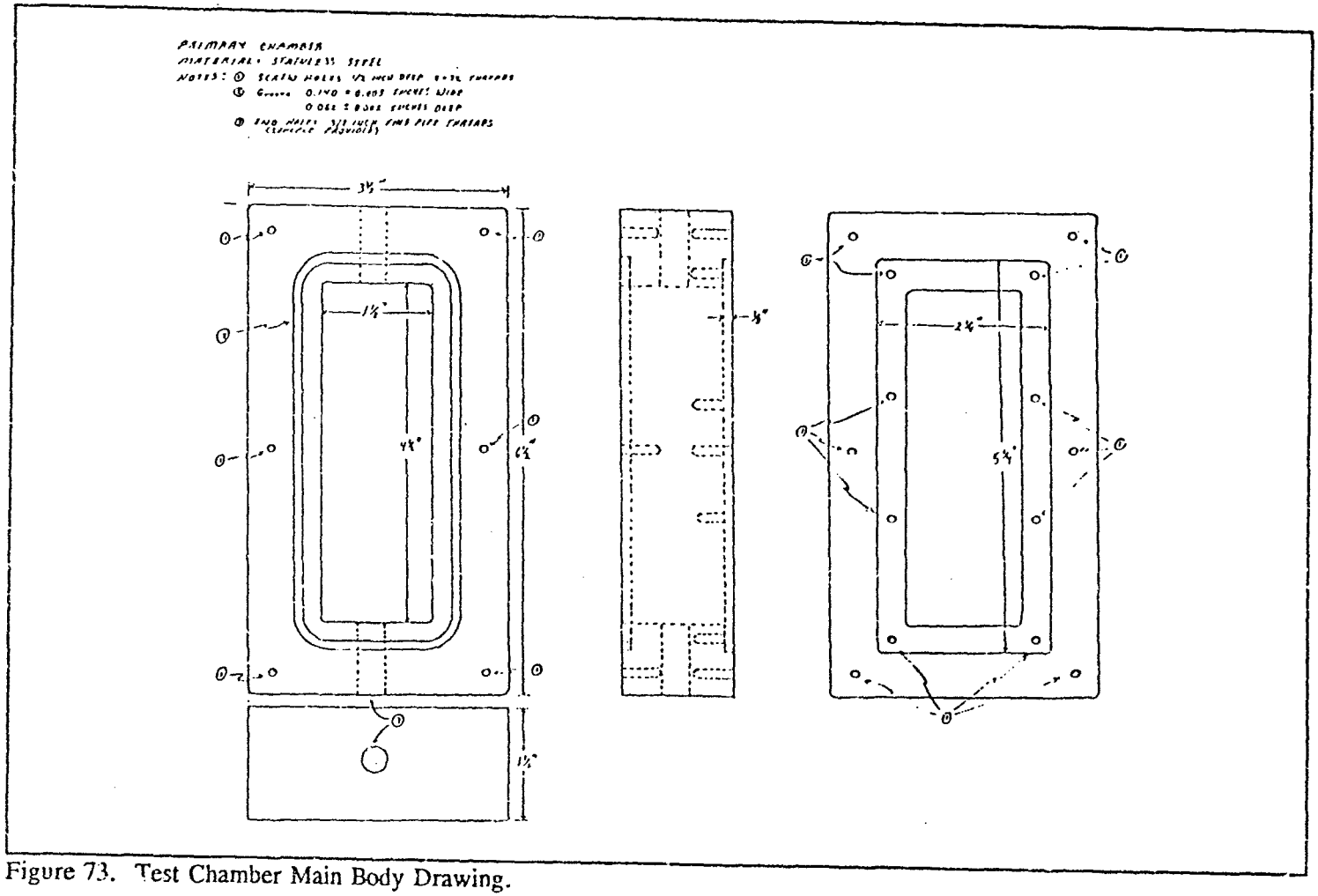

Figure 73. Test Chamber Main Body Drawing.

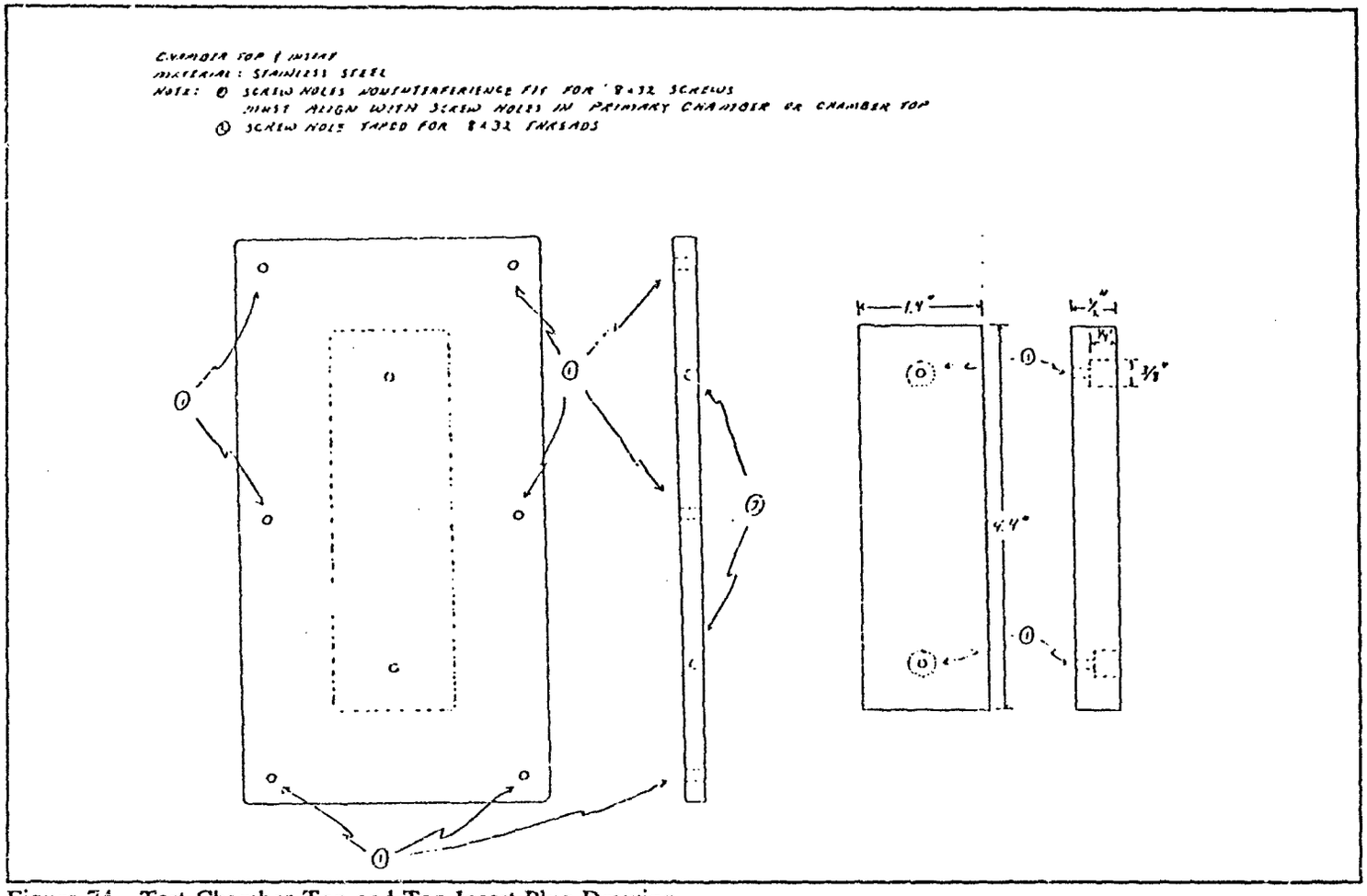

Figure 74. Test Chamber Top and Top Insert Plug Drawing.

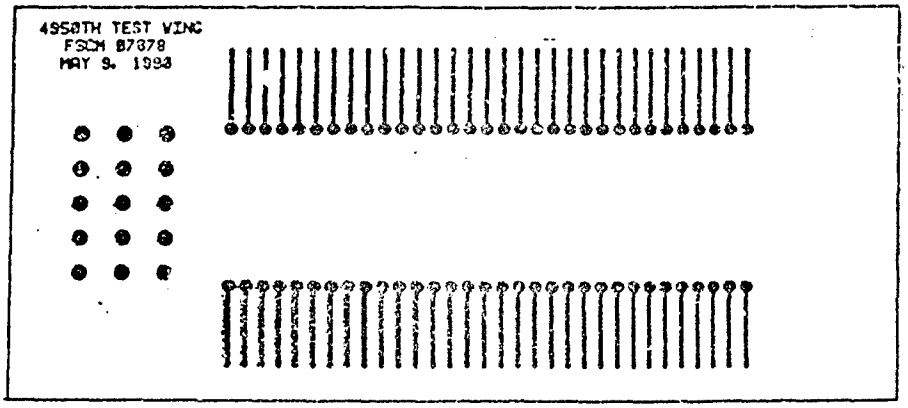

Circuit card photo mask, full size. Bottom side faces toward the test cell for wiring the connections between the socket and the RG-174.

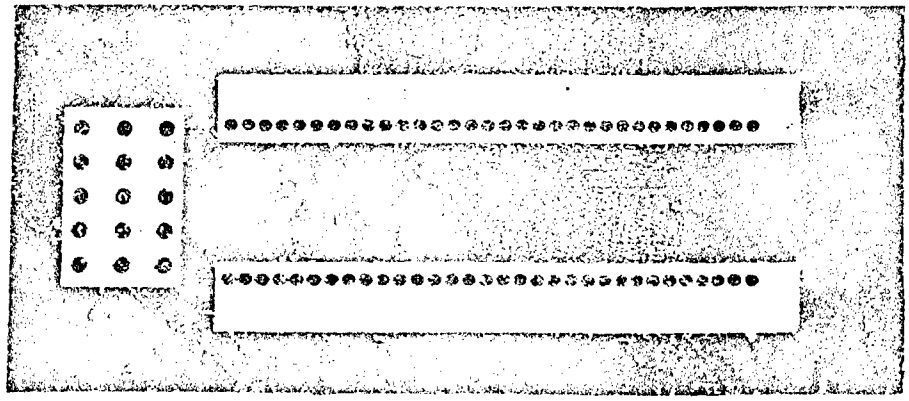

Circuit card photo mask, full size. Top side ground plane, faces upward toward the primary test chamber.

Figure 75. Circuit Card Photolithographic Mask.

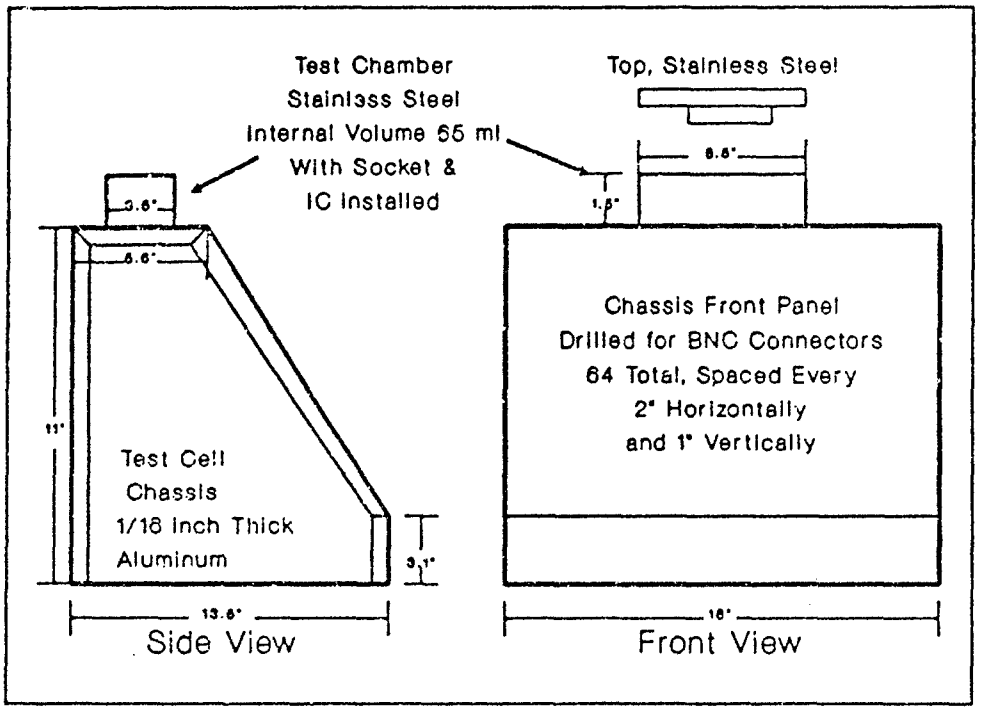

Figure 76. Test Cell Final Assembly Appearance.

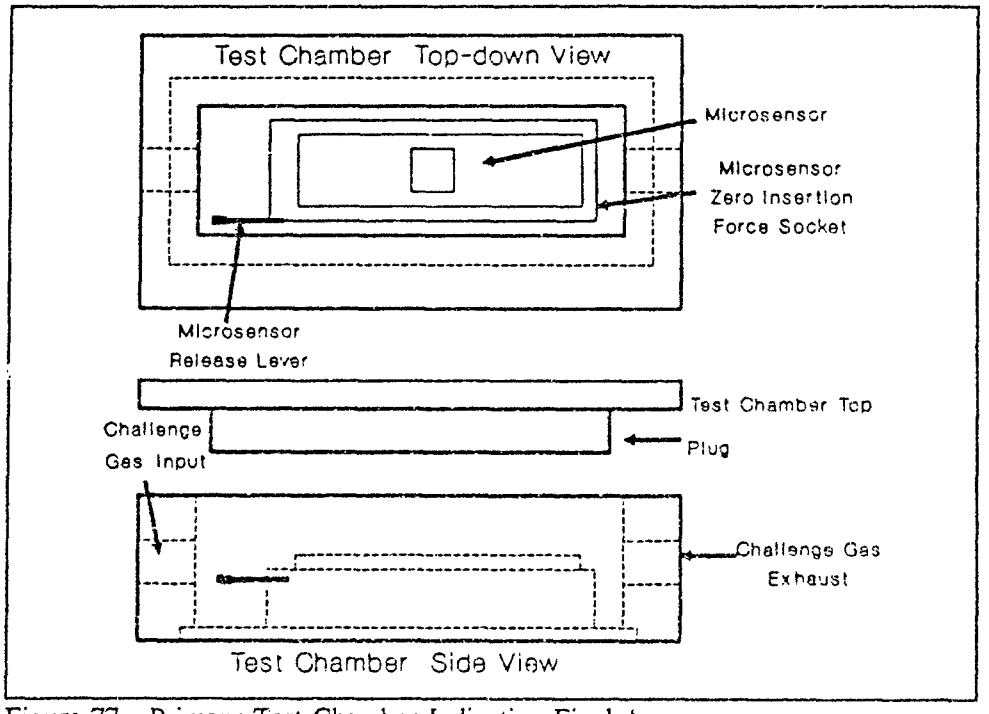

Figure 77. Primary Test Chamber Indicating Final Appearance.

Appendix F

Challenge Gas Delivery System

The challenge and purge gases delivered to the IGEFET microsensor were controlled as shown in Figure 78. Laboratory air was supplied to the gas delivery system with an input pressure of eight pounds-per-square-inch-gauge (psig). The air was then plumbed through a one gallon container filled with activated charcoal which acted as an organic contaminate filter. Next the filtered air was passed through a one gallon container filled with silica gel to remove the moisture from the filtered air. The dried and filtered air was then sent through a splitter with some of the air being routed through a bubbler filled with deionized water. By controlling the percentage of the air passing through the bubbler, it was possible to accurately control the humidity of the laboratory air supply.

The filtered, controlled-humidity laboratory air was then passed through either the purge air flow meter or the gas delivery flow meters. Gas permeation tubes were placed in a temperature controlled bath to stabilize their permeation rate to provide a gas flow to the delivery lines, and thus, provide a known concentration of the challenge gas.

The challenge and purge gases are then routed to gas delivery mixer, and the excess gas is exhausted through a bleed valve. The gas flow rate through the test chamber containing the IGEFET microsensor is controlled using the test chamber flow control flow meter. For most testing, the flow rate was limited to between 40 and 200 milliliters-per-minute.

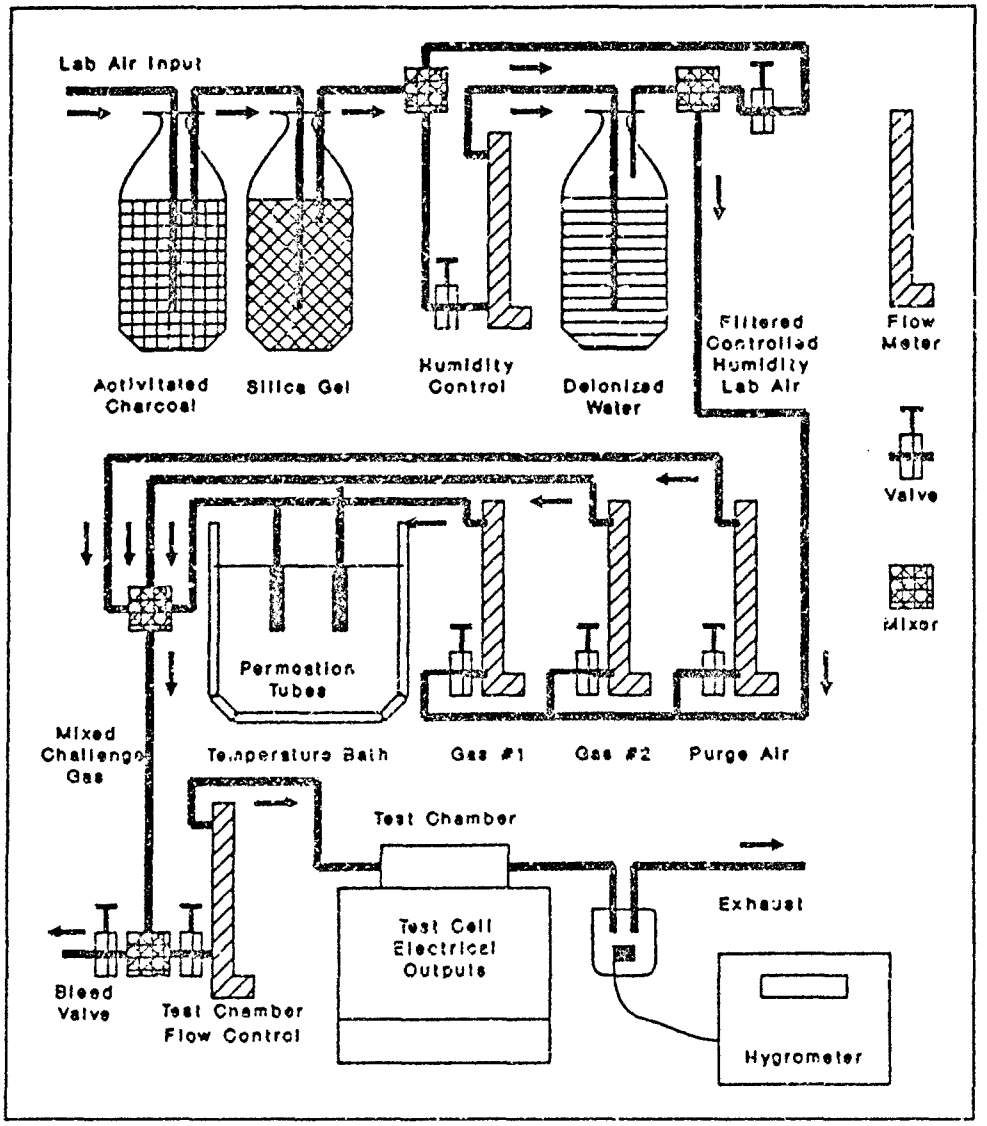

Figure 78. Gas Generation and Delivery System Block Diagram.

Two difficulties were encountered when using the gas generation system. The first problem encountered when using the gas delivery system, was the difficulty in accurately setting the relative humidity level. Once the relative humidity level was established, the setting remained fairly stable, therefore the problem was not insurmountable. The

second difficulty was a limitation in the capability to deliver binary gas combinations. Without the bleed-off capability between the permeation tubes and the challenge gas mix reservoir,, it was impossible to deliver different ratios of two challenge gases. Delivery of different ratios of the challenge gases will require that an additional bleed-valve and flow meter be installed after each permeation tube. This modification would allow exhausting excess gas of each type, and consequently the capability of delivering only the desired gas concentrations to the gas mixture reservoir.

Software to Determine Challenge Gas Concentration

```
1000 REM ************************************************************
1010 REM ** CONCEND.BAS: A PROGRAM THAT CALCULATES THE CONCENTRATION **
1020 REM ** OF THE CHALLENGE GAS IN THE APPLIED AIR STREAM GIVEN;     **
1030 REM ** THE PERMEATION TUBE BATH TEMPERATURE AND THE AIR FLOW     **
1040 REM ** RATE.                                                    **
1050 REM **                                                          **
1060 REM ** WRITTEN BY: Capt Thomas Jenkins                          **
1070 REM ** MODIFIED BY: Capt Anthony Moosey & Capt Charles Brothers **
1080 REM **                                                          **
1090 REM **                                                          **
1100 REM ************************************************************
1110 '
1120 DIM MTR27X(105)     'FLOW RATE ARRAY FOR FLOW METERS #27941 - #28040
1130 MTR27X( 1)= 7.85    'WITH GLASS BALL
1140 MTR27X( 2)= 11.8
1150 MTR27X( 3)= 16.7
1160 MTR27X( 4)= 22.7
1170 MTR27X( 5)= 29.8
1180 MTR27X( 6)= 38.1
1190 MTR27X( 7)= 47.6
1200 MTR27X( 8)= 59.5
1210 MTR27X( 9)= 74.1
1220 MTR27X(10)= 91.1
1230 MTR27X(11)=  108
1240 MTR27X(12)=  124
1250 MTR27X(13)=  140
1260 MTR27X(14)=  157
1270 MTR27X(15)=  174
1280 MTR27X(16)=  191
1290 MTR27X(17)=  209
1300 MTR27X(18)=  227
1310 MTR27X(19)=  245
1320 MTR27X(20)=  264
1330 MTR27X(21)=  284
1340 MTR27X(22)=  303
1350 MTR27X(23)=  324
1360 MTR27X(24)=  344
```

```
1370 MTR27X(25)=  365
1380 MTR27X(26)=  386
1390 MTR27X(27)=  407
1400 MTR27X(28)=  429
1410 MTR27X(29)=  450
1420 MTR27X(30)=  473
1430 MTR27X(31)=  495
1440 MTR27X(32)=  517
1450 MTR27X(33)=  540
1460 MTR27X(34)=  563
1470 MTR27X(35)=  586
1480 MTR27X(36)=  609
1490 MTR27X(37)=  633
1500 MTR27X(38)=  656
1510 MTR27X(39)=  680
1520 MTR27X(40)=  704
1530 MTR27X(41)=  728
1540 MTR27X(42)=  752
1550 MTR27X(43)=  776
1560 MTR27X(44)=  800
1570 MTR27X(45)=  824
1580 MTR27X(46)=  849
1590 MTR27X(47)=  873
1600 MTR27X(48)=  898
1610 MTR27X(49)=  922
1620 MTR27X(50)=  947
1630 MTR27X(51)=  972
1640 MTR27X(52)=  996
1650 MTR27X(53)= 1020
1660 MTR27X(54)= 1050
1670 MTR27X(55)= 1070
1680 MTR27X(56)= 1100
1690 MTR27X(57)= 1120
1700 MTR27X(58)= 1150
1710 MTR27X(59)= 1170
1720 MTR27X(60)= 1200
1730 MTR27X(61)= 1220
1740 MTR27X(62)= 1250
1750 MTR27X(63)= 1270
1760 MTR27X(64)= 1300
1770 MTR27X(65)= 1320
1780 MTR27X(66)= 1350
1790 MTR27X(67)= 1380
1800 MTR27X(68)= 1400
1810 MTR27X(69)= 1430
1820 MTR27X(70)= 1450
1830 MTR27X(71)= 1480
1840 MTR27X(72)= 1510
1850 MTR27X(73)= 1530
1860 MTR27X(74)= 1560
1870 MTR27X(75)= 1590
1880 MTR27X(76)= 1610
1890 MTR27X(77)= 1640
1900 MTR27X(78)= 1670
1910 MTR27X(79)= 1690
1920 MTR27X(80)= 1720
1930 MTR27X(81)= 1750
1940 MTR27X(82)= 1770
1950 MTR27X(83)= 1800
1960 MTR27X(84)= 1830
1970 MTR27X(85)= 1850
1980 MTR27X(86)= 1880
1990 MTR27X(87)= 1910
```

```
2000 MTR27X(88)= 1940
2010 MTR27X(89)= 1960
2020 MTR27X(90)= 1990
2030 MTR27X(91)= 2020
2040 MTR27X(92)= 2050
2050 MTR27X(93)= 2080
2060 MTR27X(94)= 2100
2070 MTR27X(95)= 2130
2080 MTR27X(96)= 2160
2090 MTR27X(97)= 2190
2100 MTR27X(98)= 2220
2110 MTR27X(99)= 2250
2120 MTR27X(100)= 2280
2130 '
2140 CLS '---------------------- SELECT FLOW METER -----------------------
2150 PRINT "     CONCENTRATION OF GASES MENU "
2160 PRINT "     SELECT THE FLOW METER NUMBER"
2170 PRINT "        (1) #25083"
2180 PRINT "        (2) #27941 - #28040"
2190 PRINT "        (0) EXIT TO SYSTEM"
2200 PRINT " "
2210 INPUT "FLOW METER NUMBER? ", FLOWMETER
2220 IF FLOWMETER = 0 THEN GOTO 2760
2230 '----------------------- SELECT PERMEATION TUBE -------------------
2240 PRINT "DIMP, DMMP, & DFP CONCENTRATION USING:"
2250 PRINT "SELECTED FLOW METER WITH THE GLASS FLOAT"
2260 PRINT " "
2270 PRINT "    SELECT THE PERMEATION TUBE:"
2280 PRINT "       (1) S/N G-5645(DIMP)"
2290 PRINT "       (2) S/N G-4942(DIMP)"
2300 PRINT "       (3) S/N G-5646(DMMP)"
2310 PRINT "       (4) S/N G-7101(DFP)"
2320 PRINT "       (0) EXIT TO FLOW METER MENU "
2330 PRINT ""
2340 INPUT "TUBE NUMBER:  ",TUBE
2350 IF TUBE=0 THEN GOTO 2140
2360 PRINT "SELECTED PERMEATION TUBE #";TUBE
2370 PRINT ""
2380 '---------------------- INPUT READINGS ----------------------------
2390 INPUT "BATH TEMPERATURE IN CELSIUS?  ",BATH
2400 IF BATH < -10 OR BATH > 50 THEN PRINT "OUT OF RANGE":GOTO 2390
2410 INPUT "FLOW METER READING NUMBER?  ",F
2420 IF (F<0) OR (F>85) THEN PRINT "OUT OF RANGE, LIMIT 0 TO 85":GOTO 2410
2430 '
2440 '----------------------- CALCULATE PERMEATION RATES --------------
2450 IF TUBE=1 THEN P=10^(9.77656E-03 * BATH + 2.4088)
2460 IF TUBE=2 THEN P=10^(9.893811E-03 * BATH + 3.38612)
2470 IF TUBE=3 THEN P=10^(8.35535E-03 * BATH + 2.62363)
2480 IF TUBE=4 THEN P=10^(9.918379E-03 * BATH + 2.08039)
2490 PRINT "              PERMEATION RATE = ";P;" NANOGRAMS/MINUTE"
2500 '
2510 '------------------------ CALCULATE FLOW RATE --------------------
2520 '5TH DEGREE POLYNOMIAL CURVE FOR FLOW METER #25083 WITH GLASS BALL
2530 FLOW=-2.7204 + 3.3626*F + .74852*F^2 - .014349*F^3
2540 FLOW=FLOW + 1.4982E-04*F^4 - 6.3991E-07*F^5
2550 '
2560 ' ARRAY LOCK-UP FOR FLOW METER #27941 - #28040 WITH GLASS BALL
2570 IF FLOWMETER=2 THEN FLOW=MTR27X(F)
2580 '
2590 PRINT "FLOW RATE FOR METER SELECTED = ";FLOW;" ML/MIN"
2600 '
2610 '------------------------ CALCULATE CONCENTRATION -----------------
2620 IF TUBE=1 THEN K=.136
```

```
2630 IF TUBE=2 THEN K=.136
2640 IF TUBE=3 THEN K=.197
2650 IF TUBE=4 THEN K=.133
2660 C=K*P/FLOW  'THIS IS CONCENTRATION IN PPM
2670 C=C*1000    'SCALE CONCENTRATION TO PPB
2680 IF TUBE=2 OR TUBE=1 THEN PRINT "          DIMP CONCENTRATION = ";C;"
ppb"
2690 IF TUBE=3 THEN PRINT "           DMMP CONCENTRATION = ";C;" ppb"
2700 IF TUBE=4 THEN PRINT "            DFP CONCENTRATION = ";C;" ppb"
2710 PRINT ""
2720 '------------------------ LOOP TO MENUS ----------------------------
2730 INPUT "CALCULATE ANOTHER POINT [Y/N]?  ",ANS$
2740 IF ANS$="Y" OR ANS$="y" THEN GOTO 2370
2750 GOTO 2240
2760 SYSTEM
```

Appendix F

Supplemental Test Results

This appendix contains supplemental data that was collected during the evaluation of the six different chemically sensitive thin films tested in this thesis. The data in this appendix is presented in the same order as discussed in Chapter V. That is, the data is presented in the following order, by subsection: copper phthalocyanine, L-histidine dihydrochloride, succinylcholine chloride, 2-naphthol(β), succinyl chloride, and DFPase. In each subsection, the presented data is organized by the challenge gas tested: DIMP, DMMP, DFP, DIMP/DMMP, DIMP/DFP, and DMMP/DFP.

The data presented in this appendix is not exhaustive or complete, since the presentation of all the data collected would require over 1000 individual graphs.

Copper Phthalocyanine Supplemental Graphs

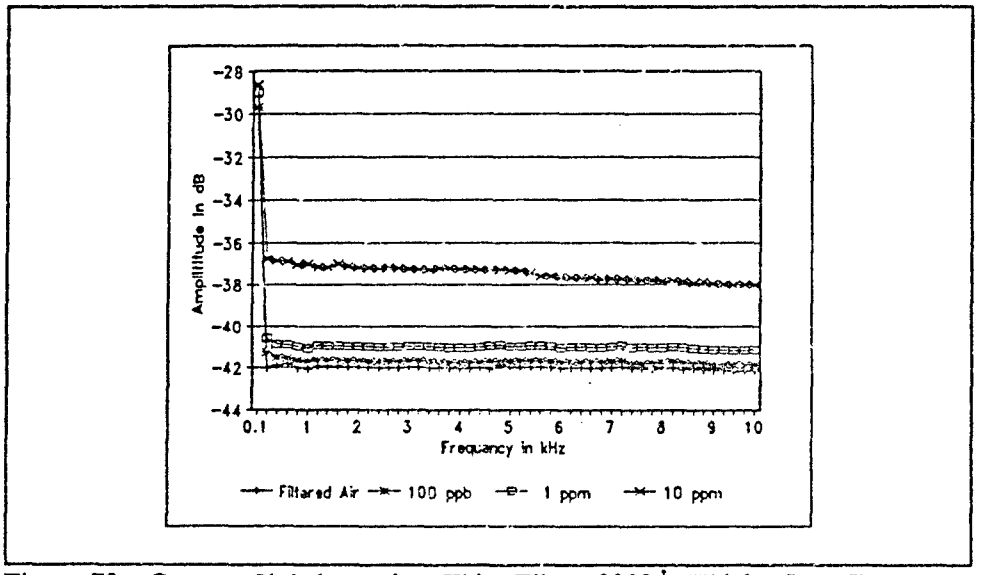

Figure 79. Copper Phthalocyanine Thin Film, 2000Å Thick, Low-Frequency Response to DIMP Challenge Gas at 30° C.

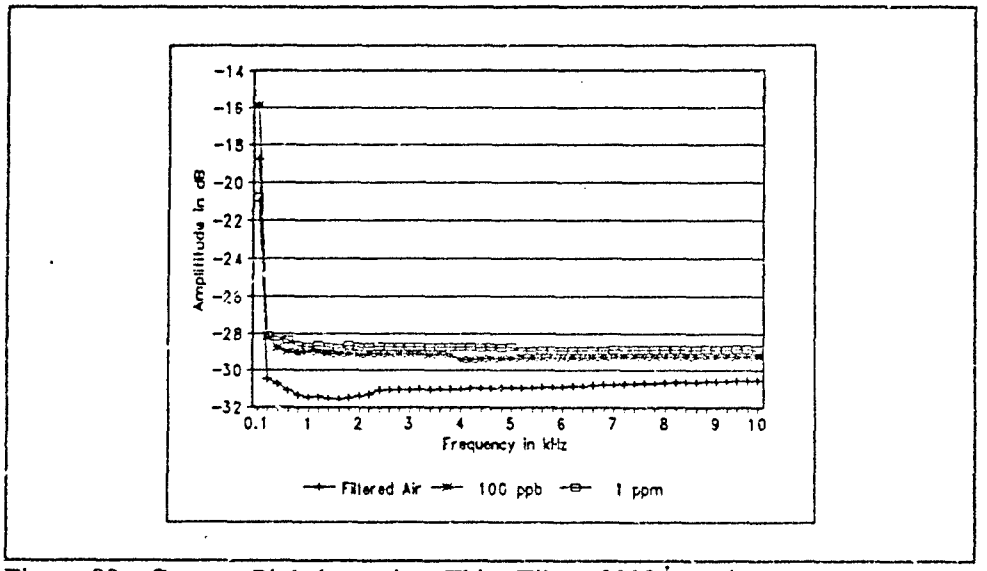

Figure 80. Copper Phthalocyanine Thin Film, 2000Å Thick, Low-Frequency Response to DIMP at 50° C.

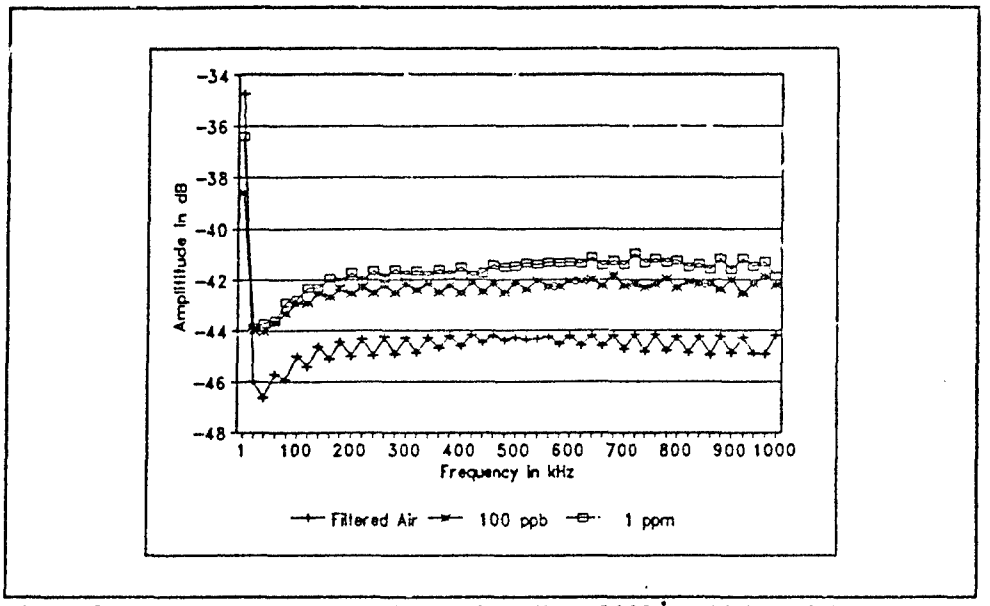

Figure 81. Copper Phthalocyanine Thin Film, 2000Å Thick, High-Frequency Response to DIMP Challenge Gas at 50° C.

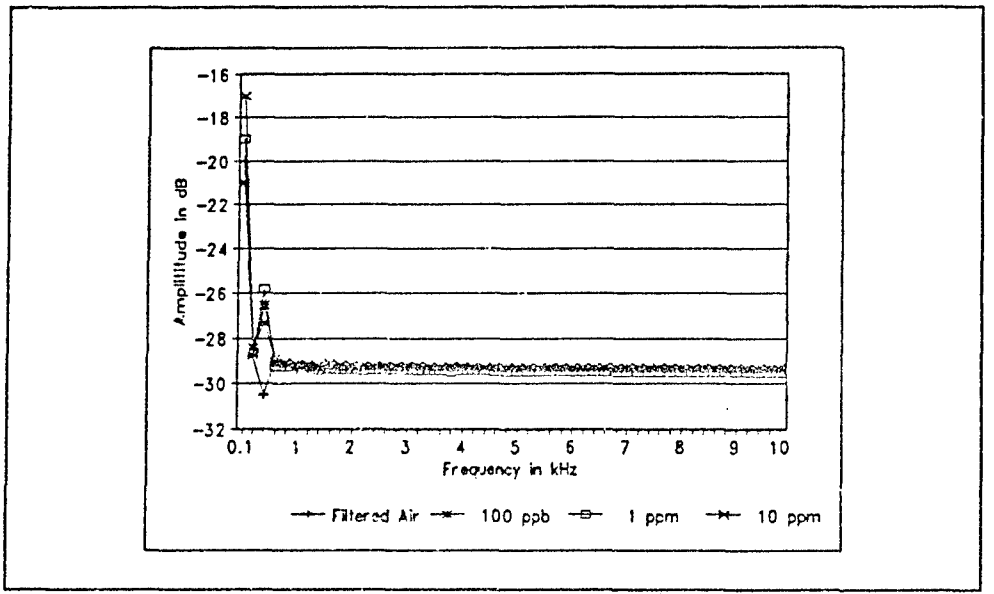

Figure 82. Copper Phthalocyanine Thin Film, 2000Å Thick, Low-Frequency Response to DIMP Challenge Gas at 70° C.

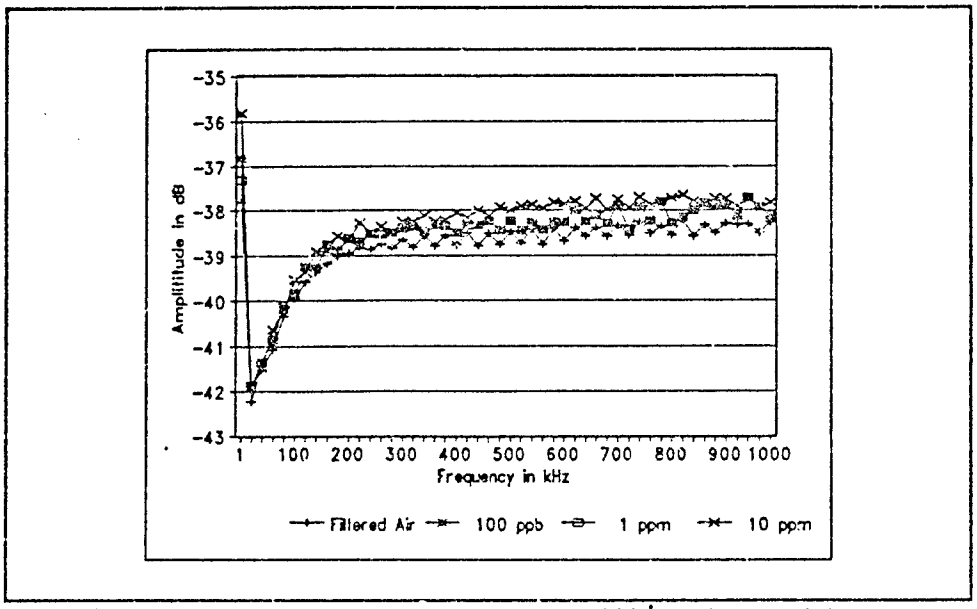

Figure 83. Copper Phthalocyanine Thin Film, 2000Å Thick, High-Frequency Response to DIMP Challenge Gas at 70° C.

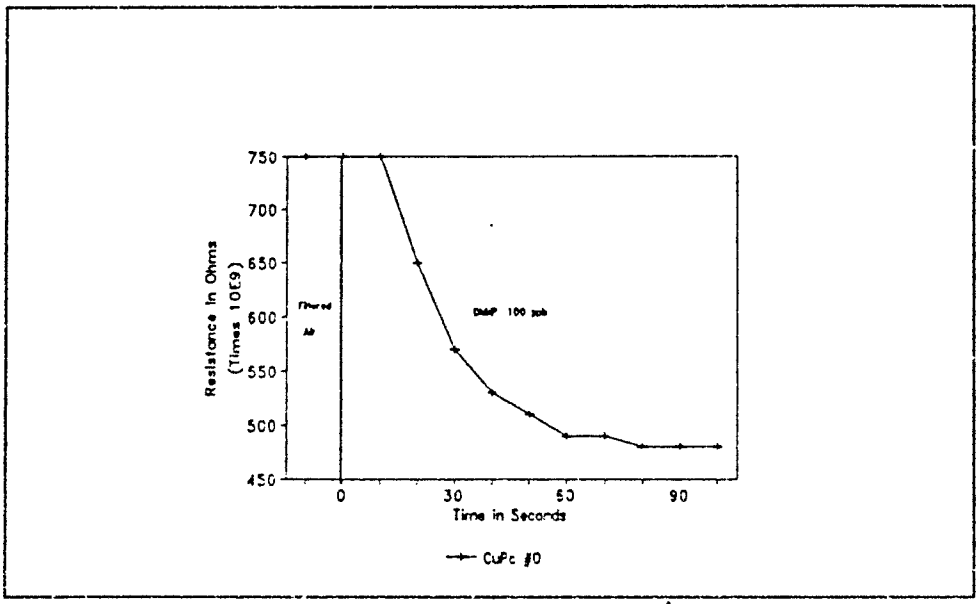

Figure 84. Copper Phthalocyanine Thin Film, 2000Å Thick, DC Resistance Response to the Introduction of DMMP Challenge Gas at 30° C.

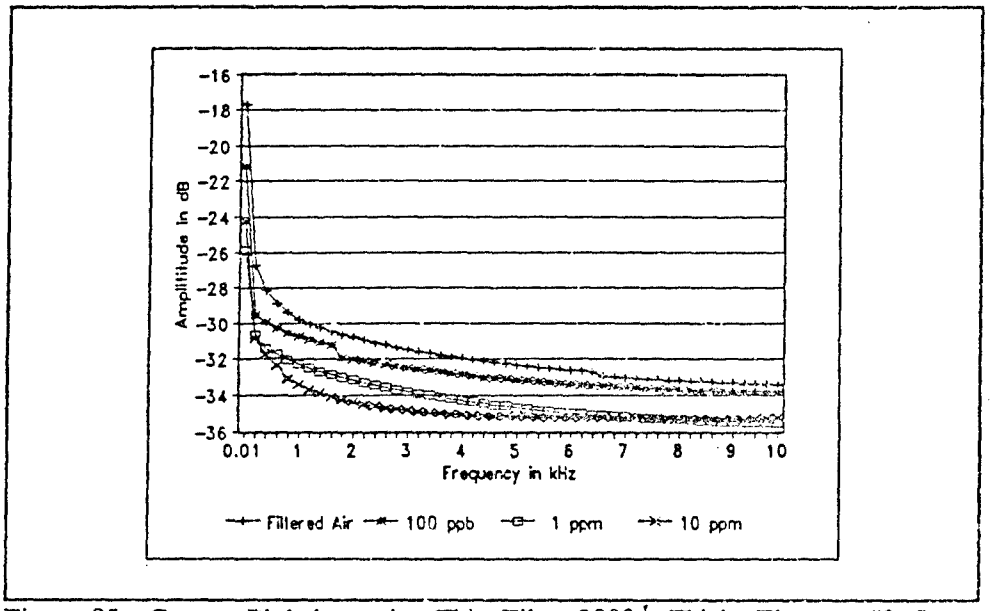

Figure 85. Copper Phthalocyanine Thin Film, 2000Å Thick, Element #0, Low-Frequency Response to DMMP Challenge Gas at 30° C.

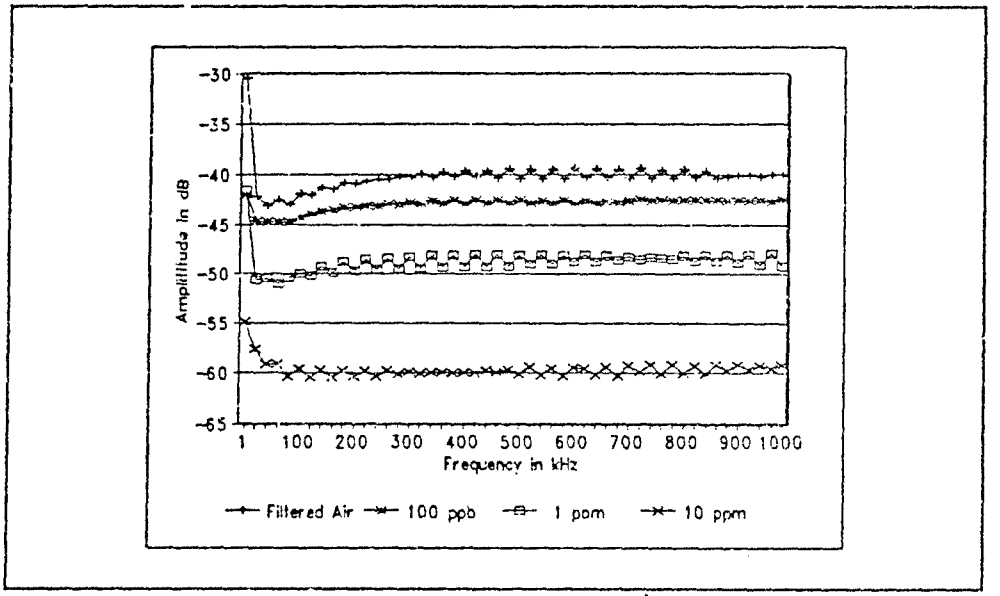

Figure 86. Copper Phthalocyanine Thin Film, 2000Å Thick, Element #0, High-Frequency Response to DMMP Challenge Gas at 30° C.

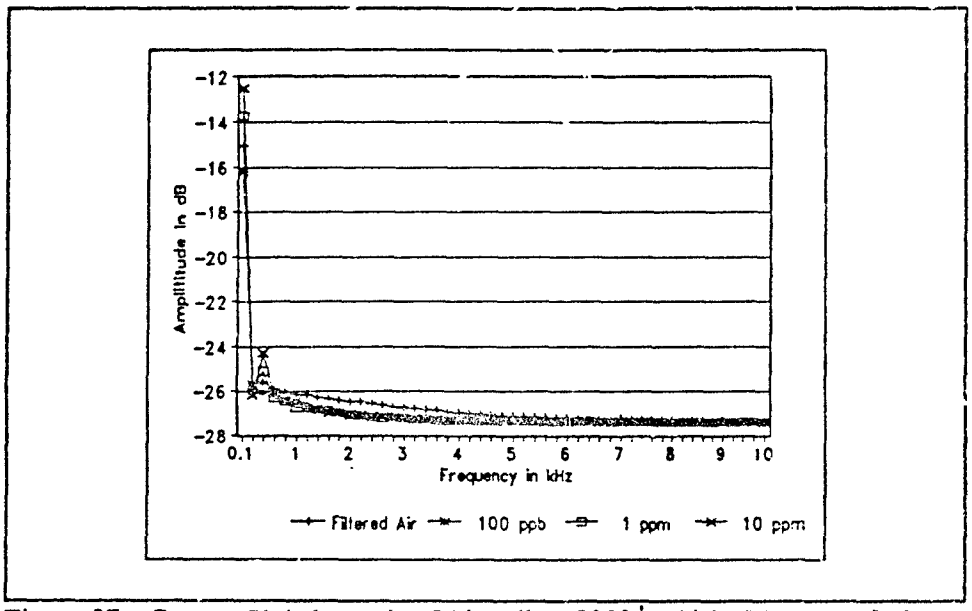

Figure 87. Copper Phthalocyanine Thin Film, 2000Å Thick, Element #0, Low-Frequency Response to DMMP Challenge Gas at 50° C.

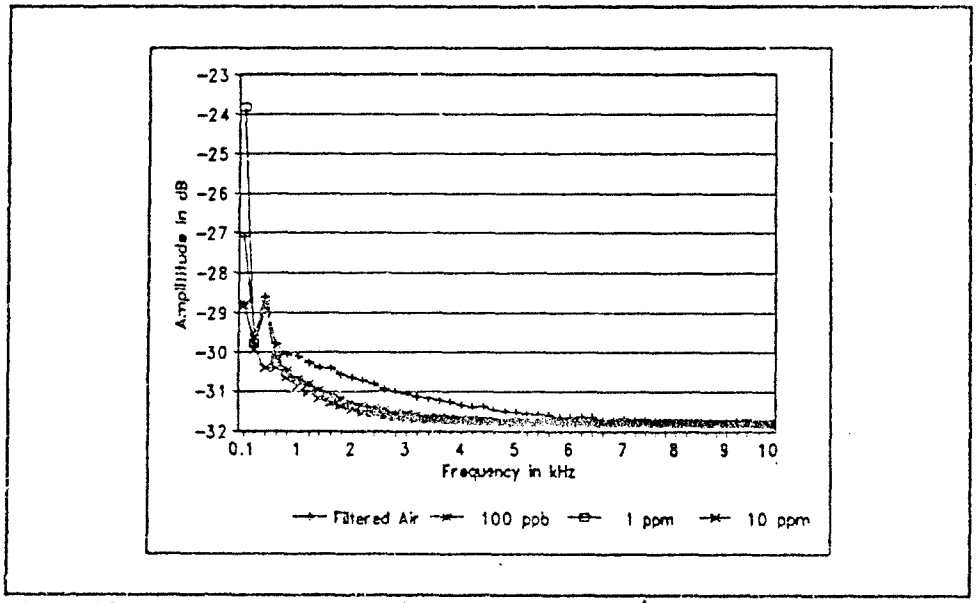

Figure 88. Copper Phthalocyanine Thin Film, 2000Å Thick, Element #1, Low-Frequency Response to DMMP Challenge Gas at 50° C.

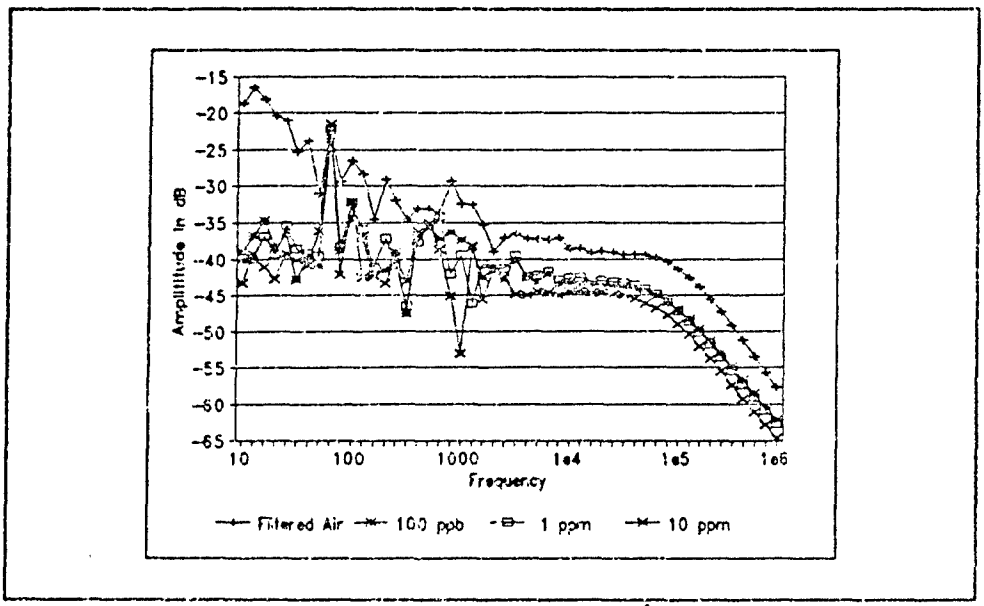

Figure 89. Copper Phthalocyanine Thin Film, 2000Å Thick, Gain Response to DMMP Challenge Gas at 30° C.

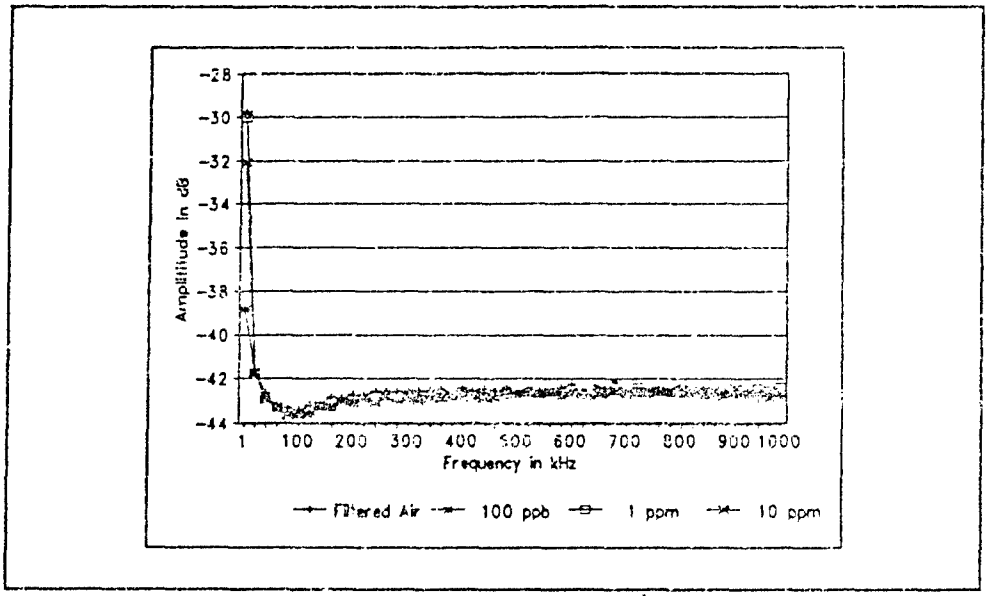

Figure 90. Copper Phthalocyanine Thin Film, 2000Å Thick, Element #0, High-Frequency Response to DMMP Challenge Gas at 50° C.

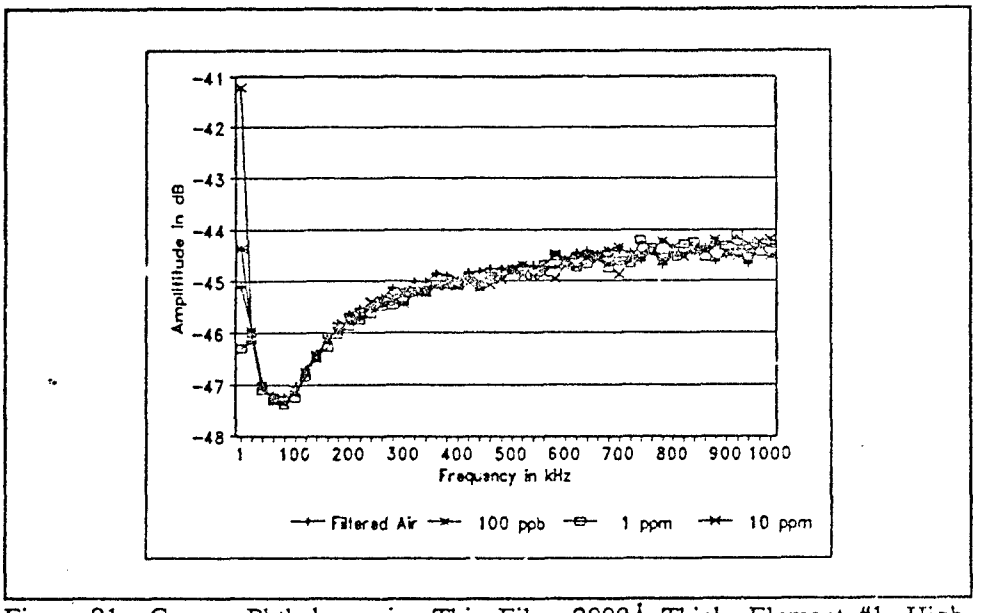

Figure 91. Copper Phthalocyanine Thin Film, 2000Å Thick, Element #1, High-Frequency Response to DMMP Challenge Gas at 50° C.

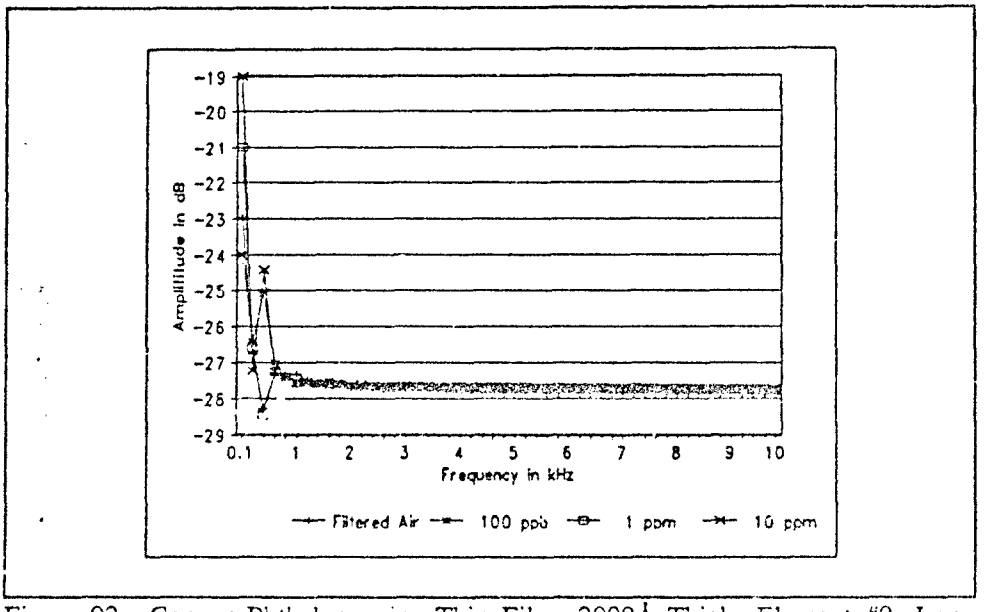

Figure 92. Copper Phthalocyanine Thin Film, 2000Å Thick, Element #0, Low-Frequency Response to DMMP Challenge Gas at 70°C.

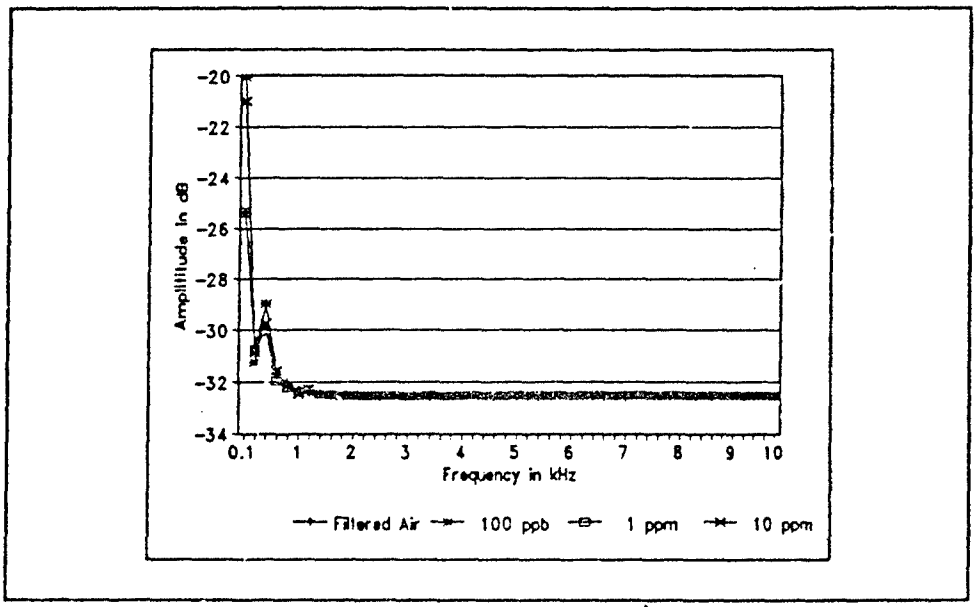

Figure 93. Copper Phthalocyanine Thin Film, 2000Å Thick, Element #1, Low-Frequency Response to DMMP Challenge Gas at 70° C.

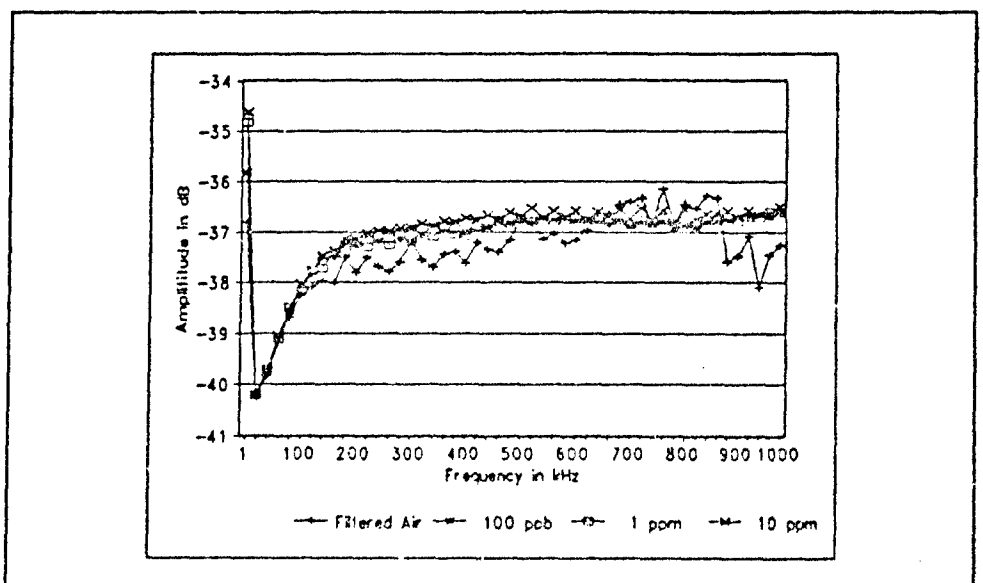

Figure 94. Copper Phthalocyanine Thin Film, 2000Å Thick, Element #0, High Frequency Response to DMMP Challenge Gas at 70° C.

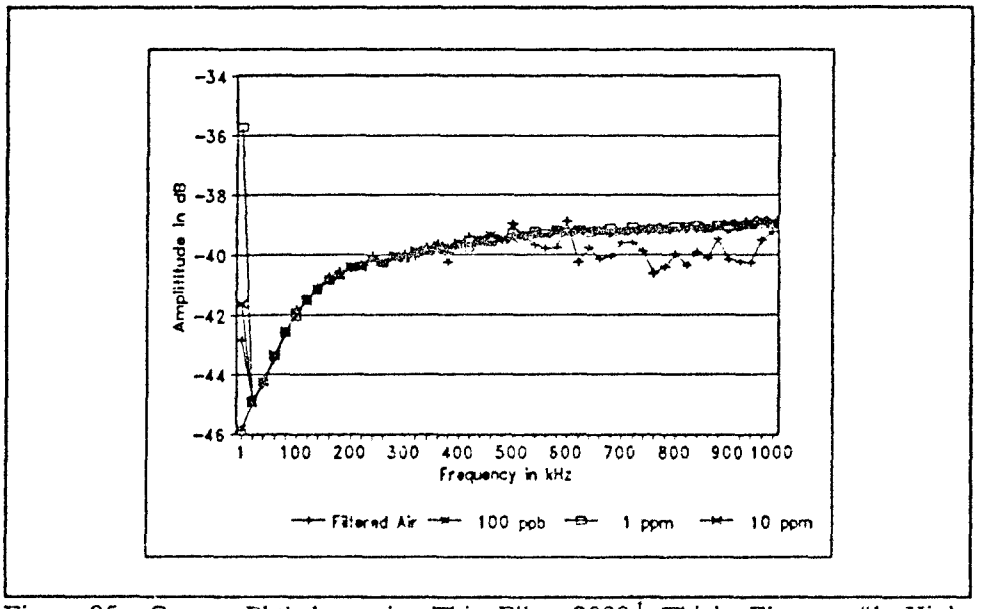

Figure 95. Copper Phthalocyanine Thin Film, 2000Å Thick, Element #1, High-Frequency Response to DMMP Challenge Gas at 70° C.

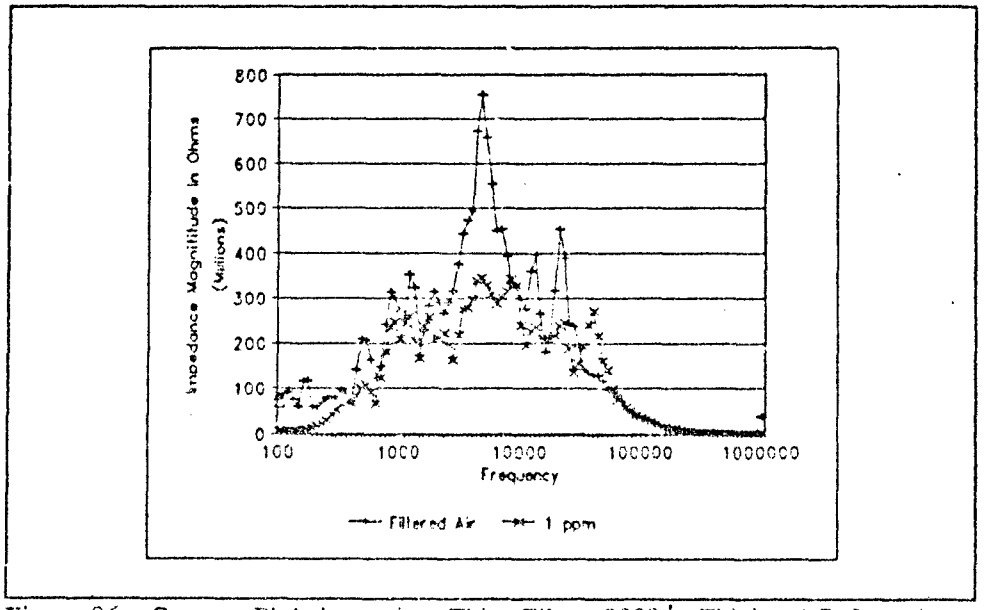

Figure 96. Copper Phthalocyanine Thin Film, 2000Å Thick, AC Impedance Response to DFP Challenge Gas at 30° C.

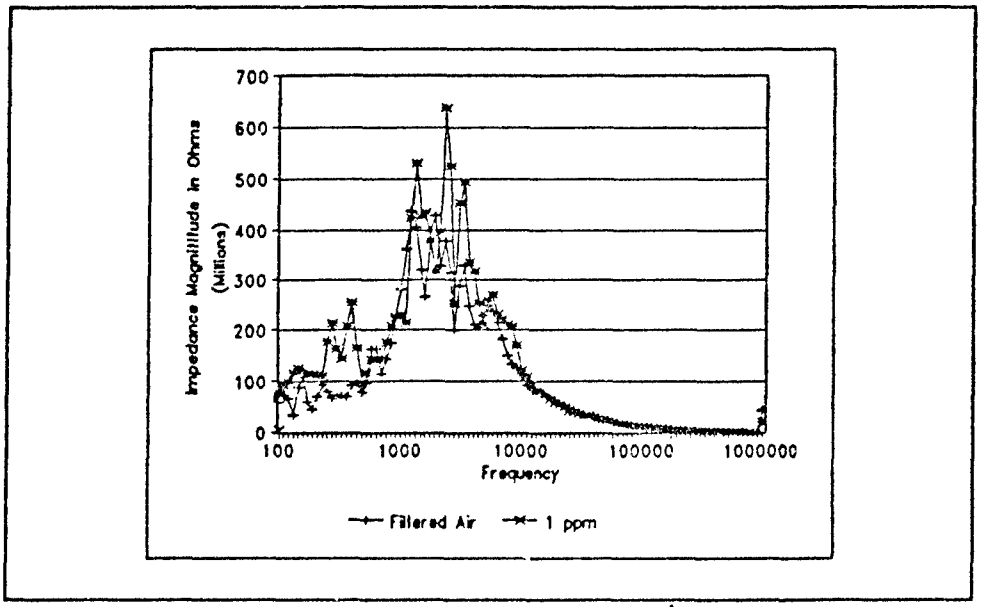

Figure 97. Copper Phthalocyanine Thin Film, 2000Å Thick, AC Impedance Response to DFP Challenge Gas at 30° C.

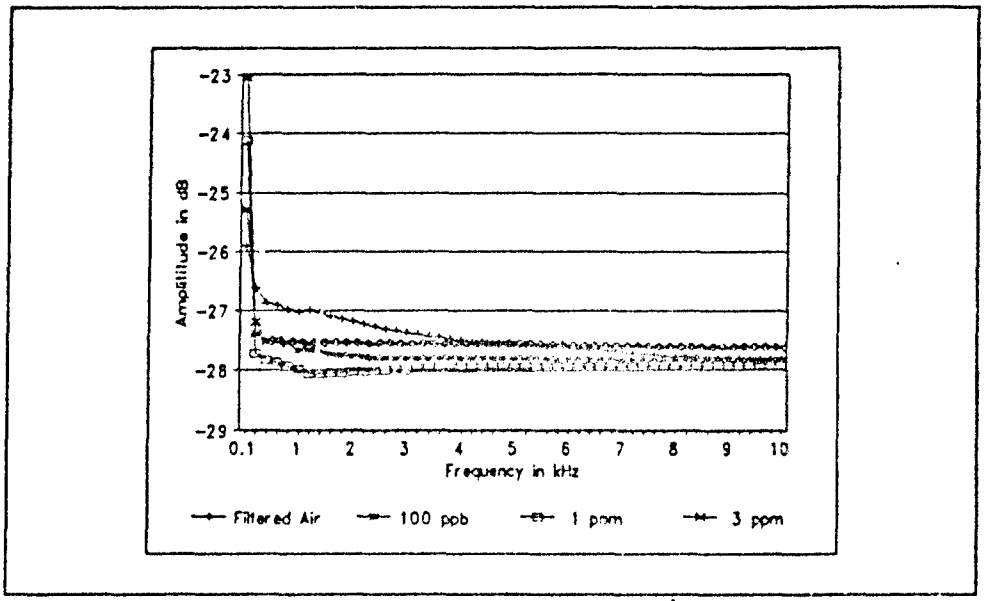

Figure 98. Copper Phthalocyanine Thin Film, 2000Å Thick, Low-Frequency Response to DFP Challenge Gas at 30° C.

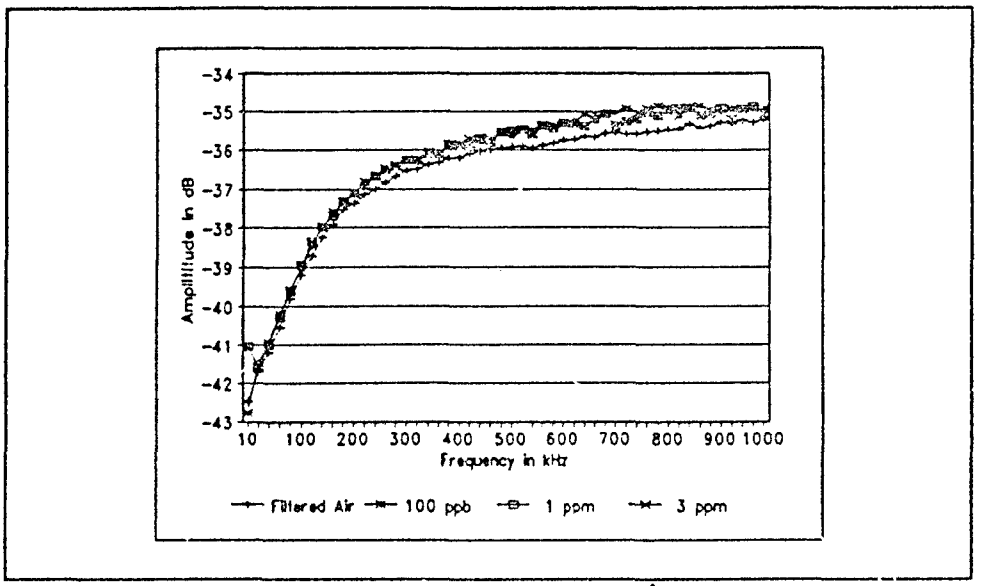

Figure 99. Copper Phthalocyanine Thin Film, 2000Å Thick, High-Frequency Response to DFP Challenge Gas at 30° C.

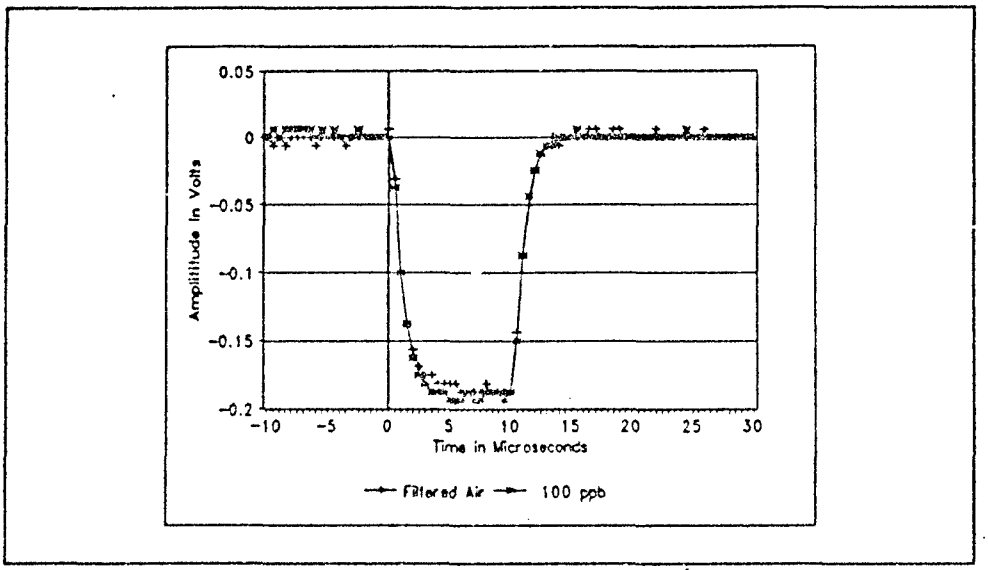

Figure 100. Copper Phthalocyanine Thin Film, 2000Å Thick, Time-Domain Response to a 3 Volt 10 Microsecond Pulse When Exposed to DFP Challenge Gas at 30° C.

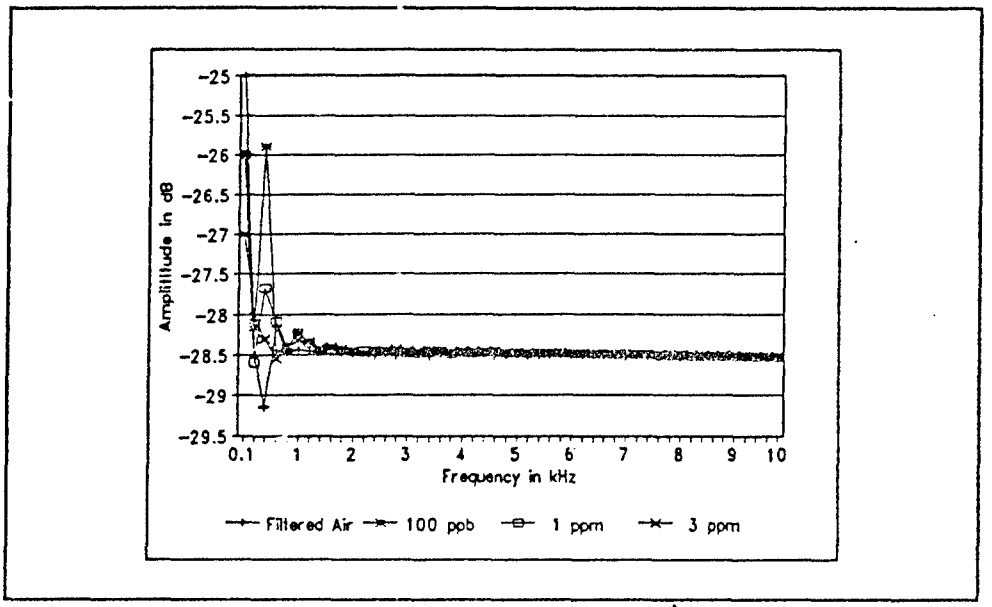

Figure 101. Copper Phthalocyanine Thin Film, 2000Å Thick, Low-Frequency Response to DFP Challenge Gas at 50° C.

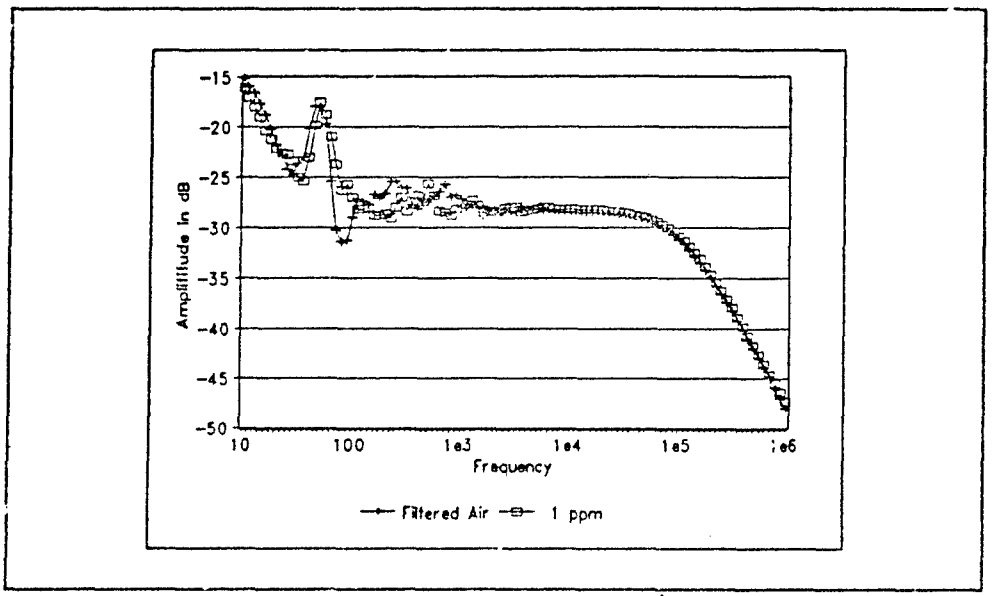

Figure 102. Copper Phthalocyanine Thin Film, 2000Å Thick, Gain Response to DFP Challenge Gas at 30° C.

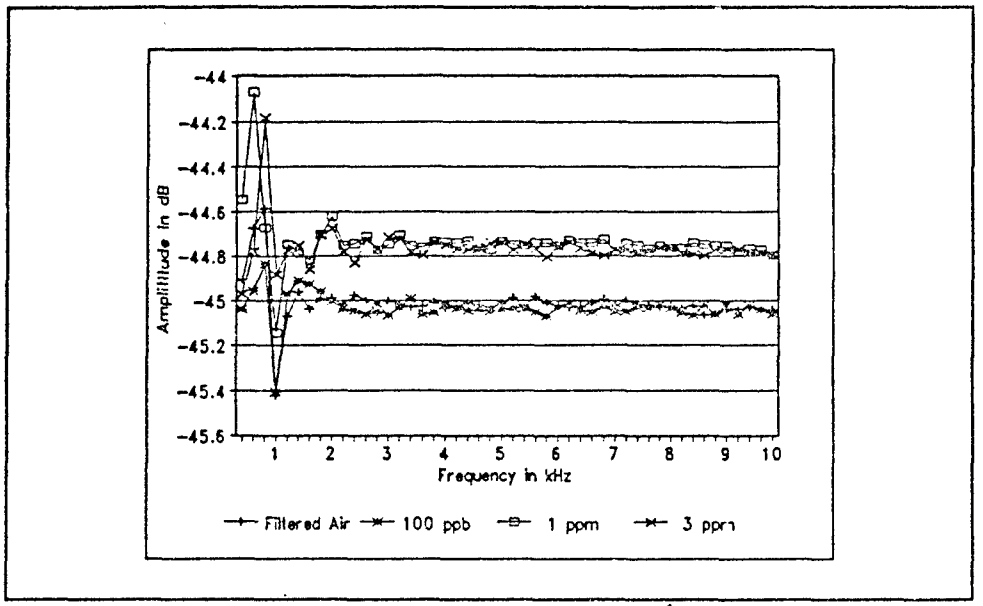

Figure 103. Copper Phthalocyanine Thin Film, 2000Å Thick, Low-Frequency Response to DFP Challenge Gas at 50° C.

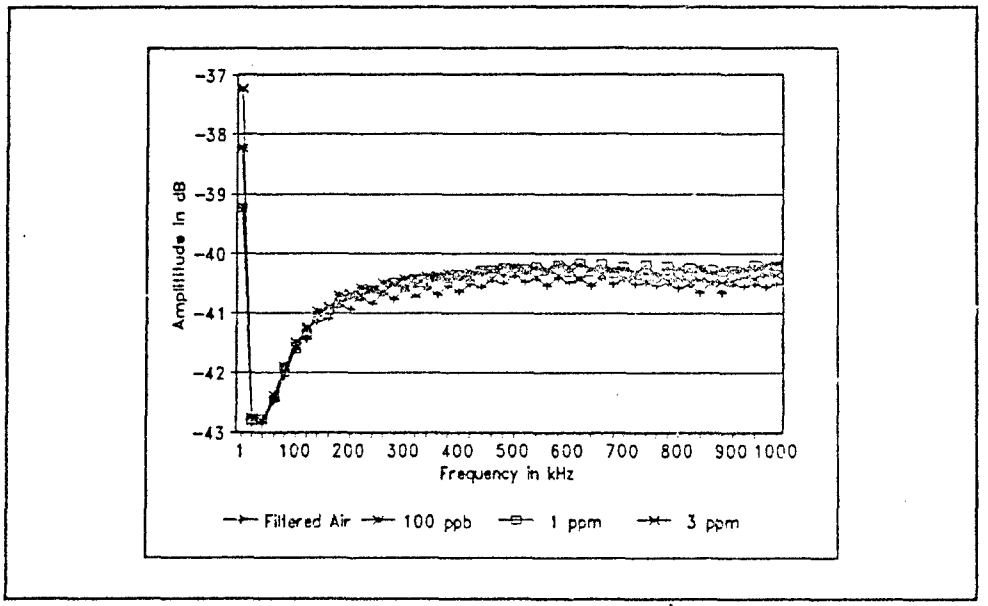

Figure 104. Copper Phthalocyanine Thin Film, 2000Å Thick, High-Frequency Response to DFP Challenge Gas at 50° C.

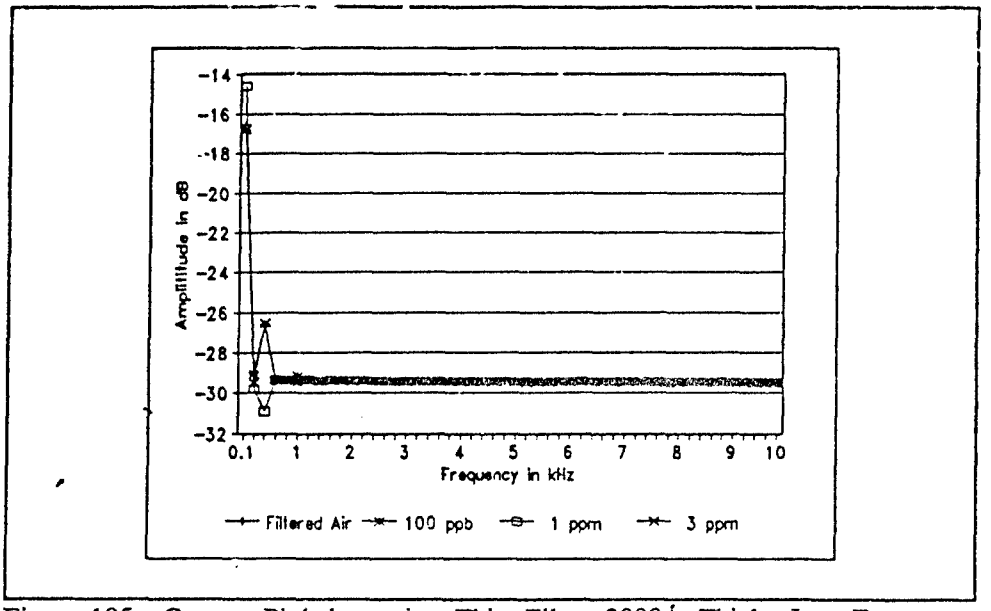

Figure 105. Copper Phthalocyanine Thin Film, 2000Å Thick, Low-Frequency Response to DFP Challenge Gas at 70° C.

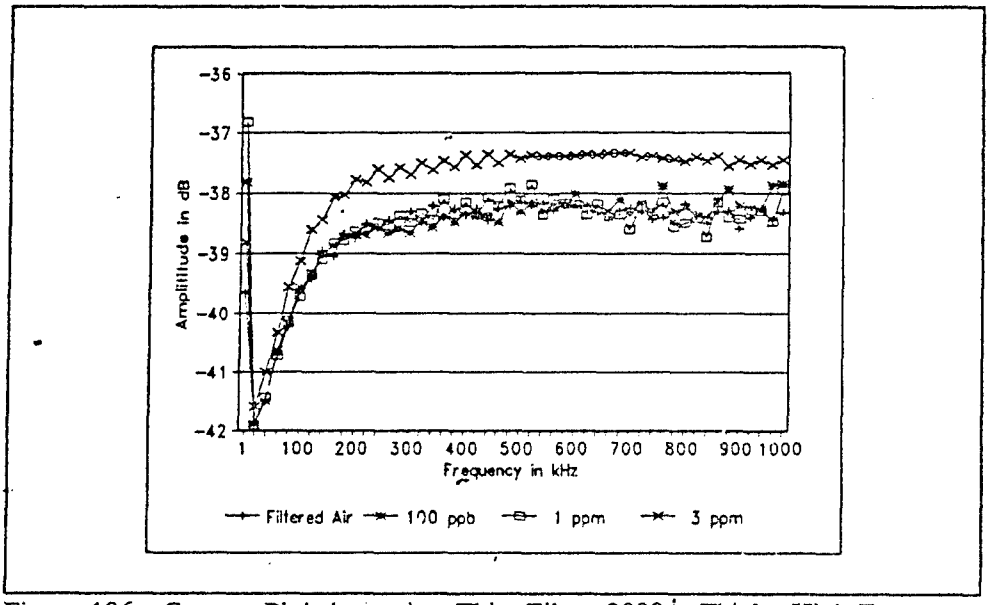

Figure 106. Copper Phthalocyanine Thin Film, 2000Å Thick, High-Frequency Response to DFP Challenge Gas at 70° C.

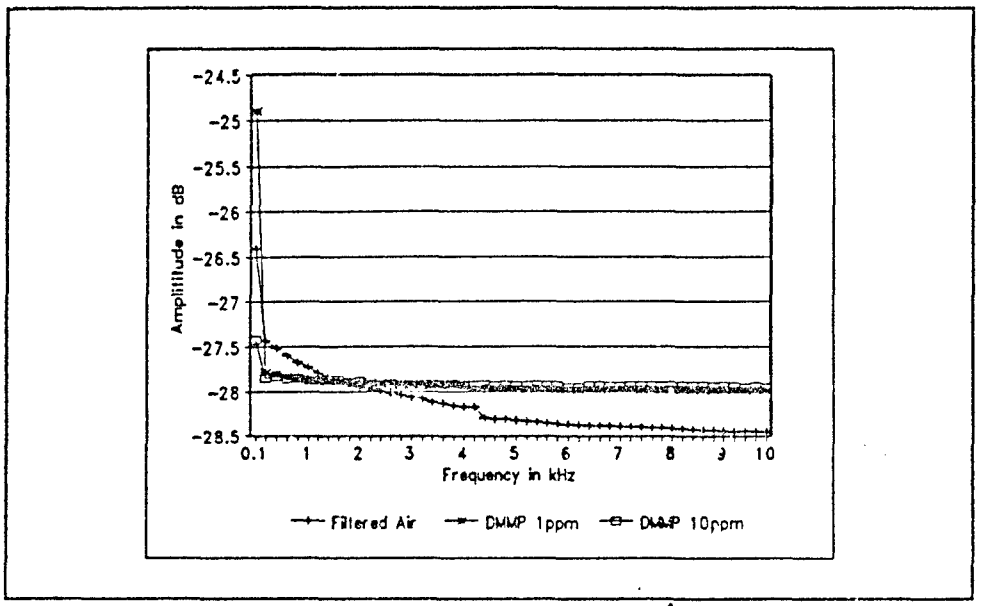

Figure 107. Copper Phthalocyanine Thin Film, 2000Å Thick, Low-Frequency Response to DIMP and DMMP Challenge Gas at 30° C.

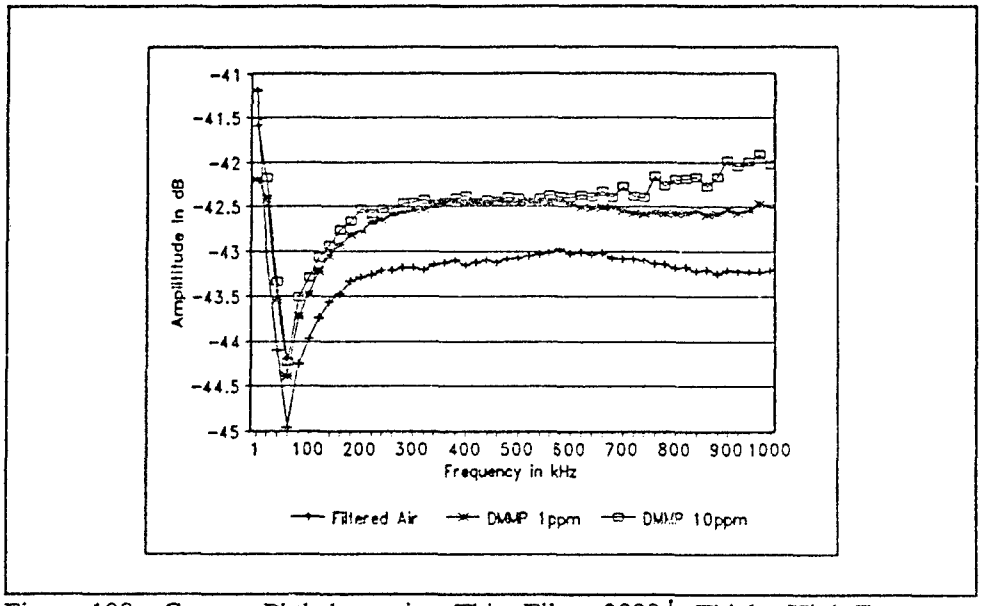

Figure 108. Copper Phthalocyanine Thin Film, 2000Å Thick, High-Frequency Response to DIMP and DMMP Challenge Gas at 30° C.

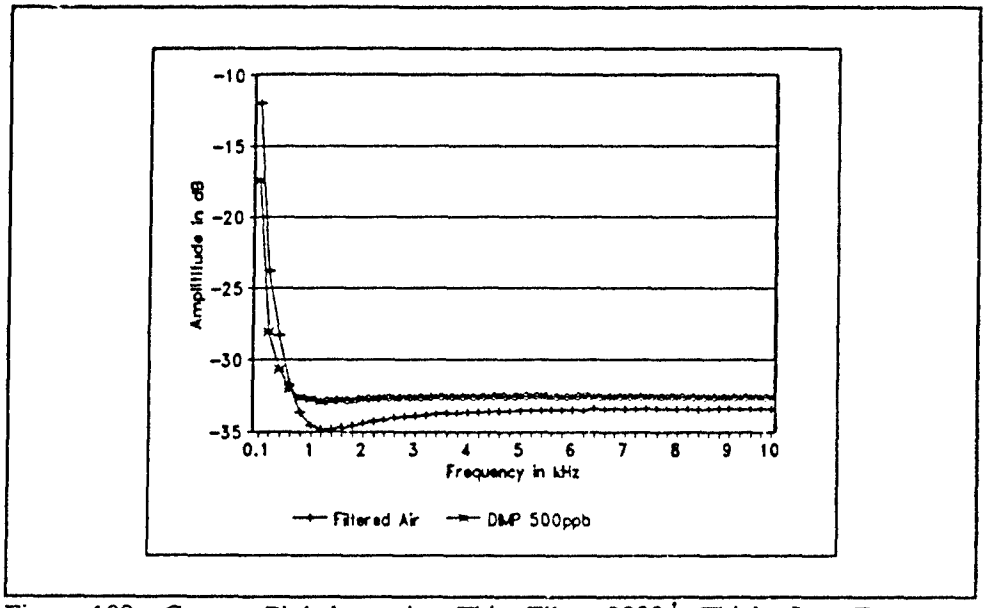

Figure 109. Copper Phthalocyanine Thin Film, 2000Å Thick, Low-Frequency Response to DIMP and DFP Challenge Gas at 30° C.

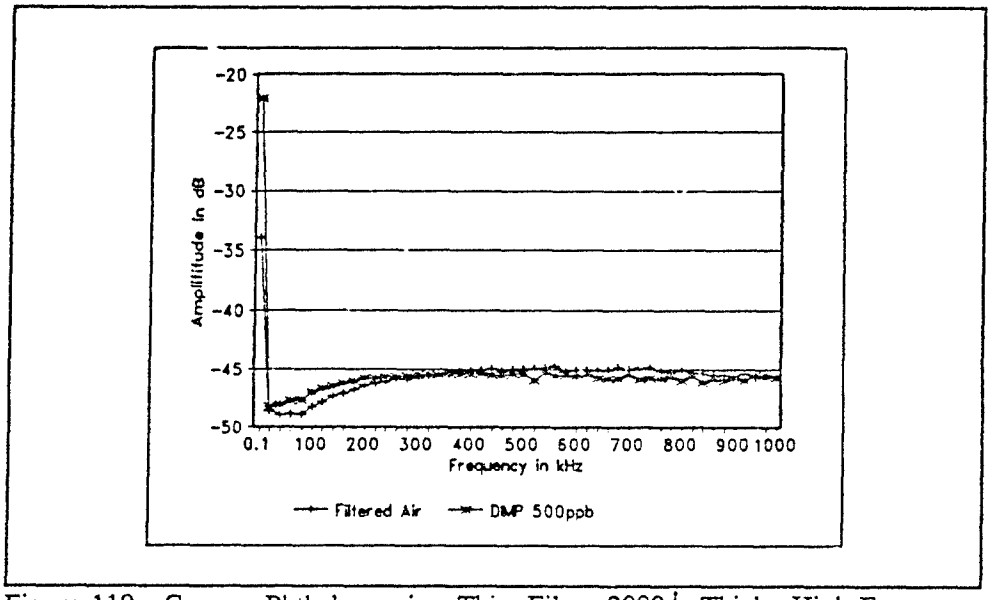

Figure 110. Copper Phthalocyanine Thin Film, 2000Å Thick, High-Frequency Response to DIMP and DFP Challenge Gas at 30° C.

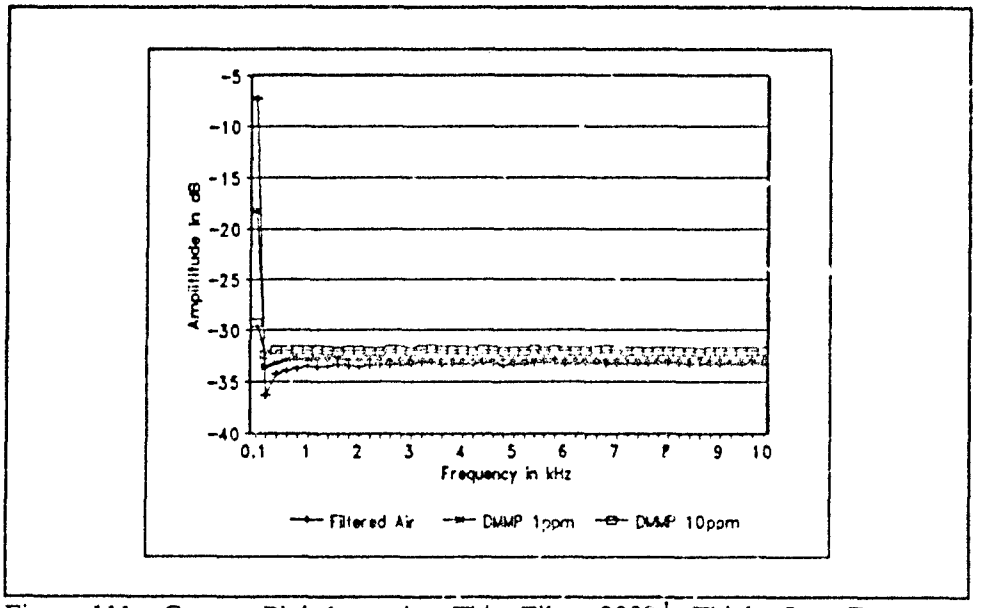

Figure 111. Copper Phthalocyanine Thin Film, 2000Å Thick, Low-Frequency Response to DMMP and DFP Challenge Gas at 30° C.

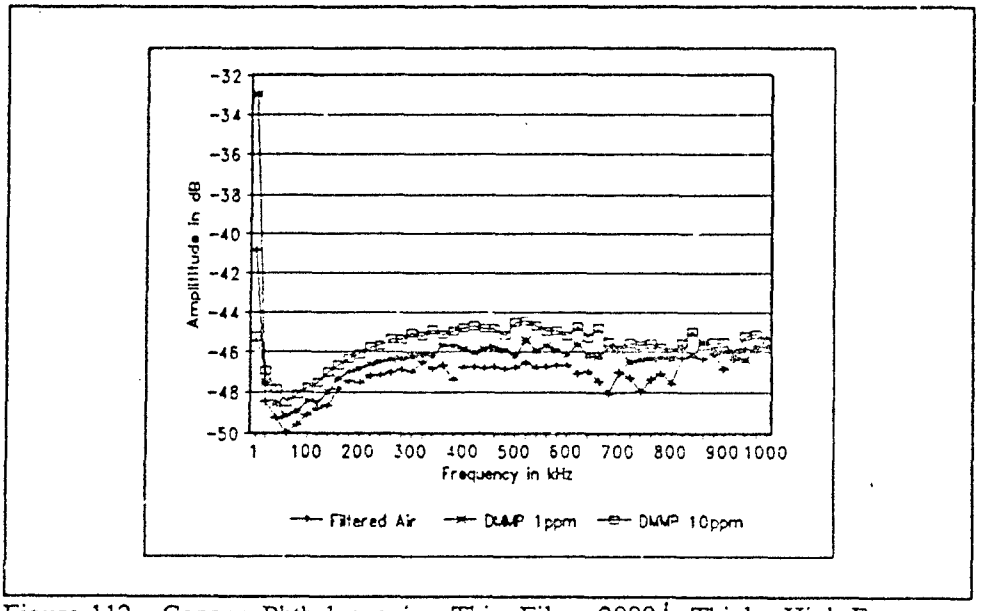

Figure 112. Copper Phthalocyanine Thin Film, 2000Å Thick, High-Frequency Response to DMMP and DFP Challenge Gas at 30° C.

DFPase Supplementary Graphs

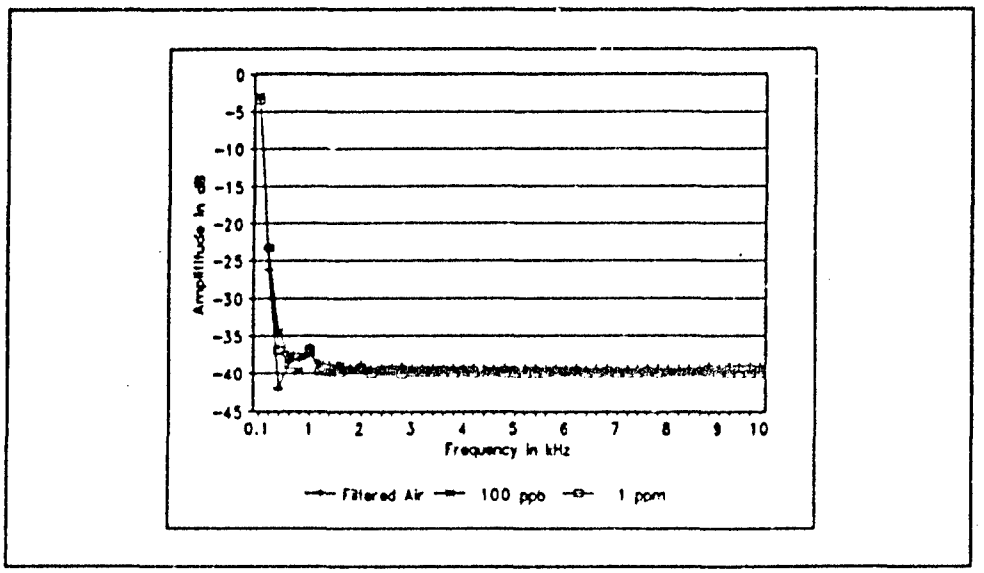

Figure 113. DFPase Thin Film Low-Frequency Response to DIMP Challenge Gas at 50° C.

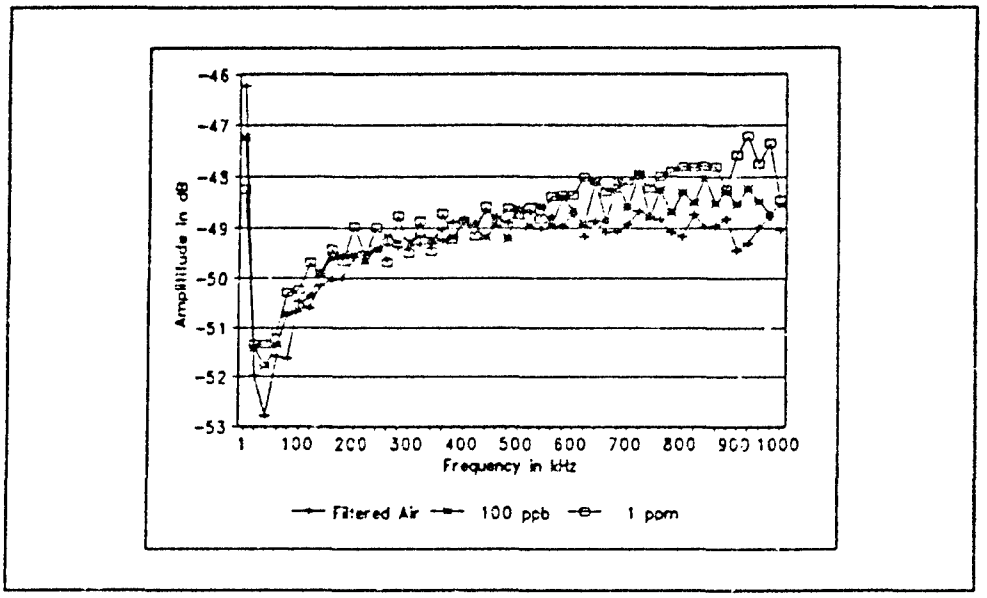

Figure 114. DFPase Thin Film High-Frequency Response to DIMP Challenge Gas at 50° C.

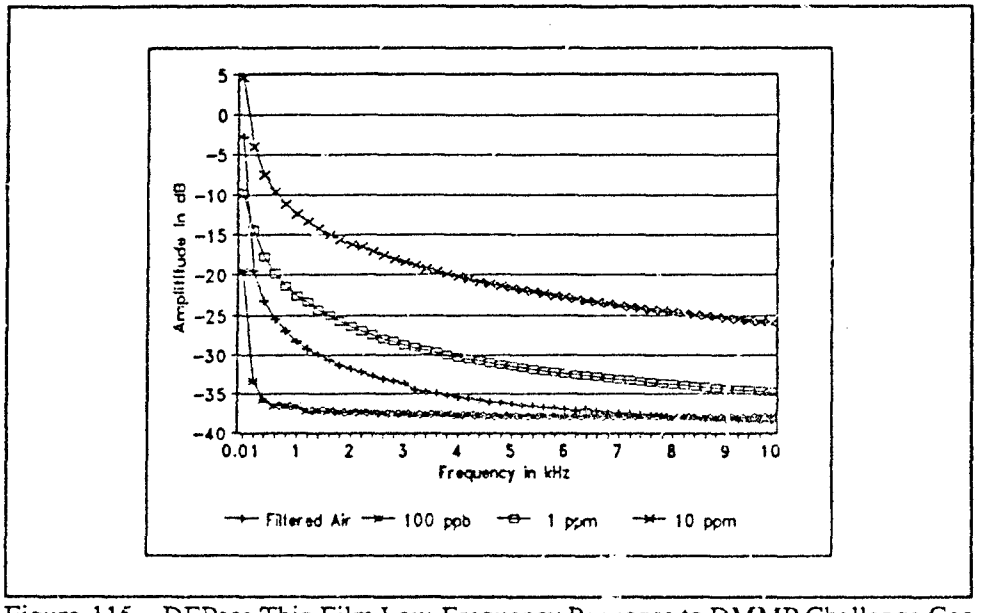

Figure 115. DFPase Thin Film Low-Frequency Response to DMMP Challenge Gas at 30° C.

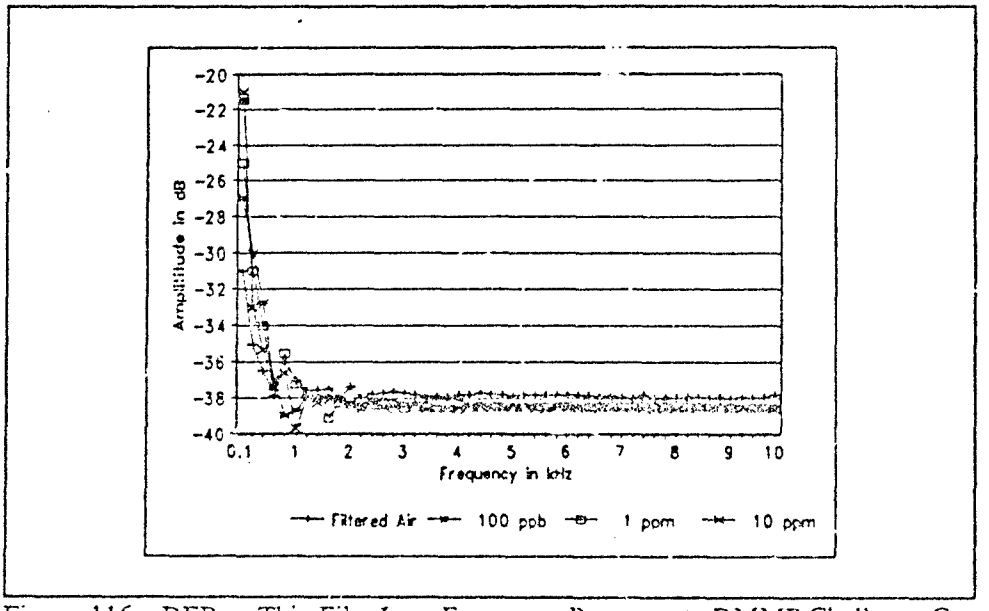

Figure 116. DFPase Thin Film Low-Frequency Response to DMMP Challenge Gas at 50° C.

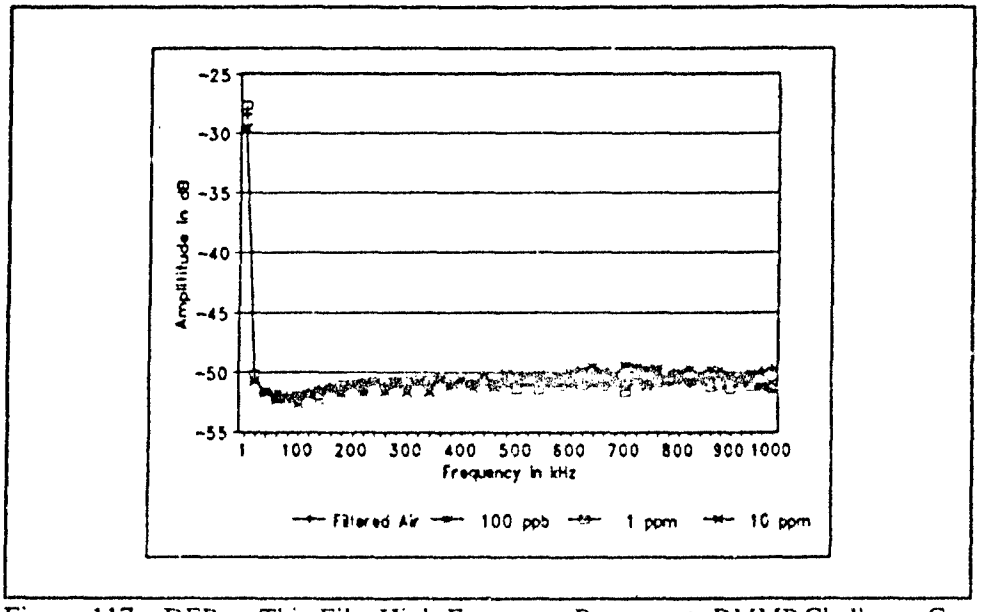

Figure 117. DFPase Thin Film High-Frequency Response to DMMP Challenge Gas at 50° C.

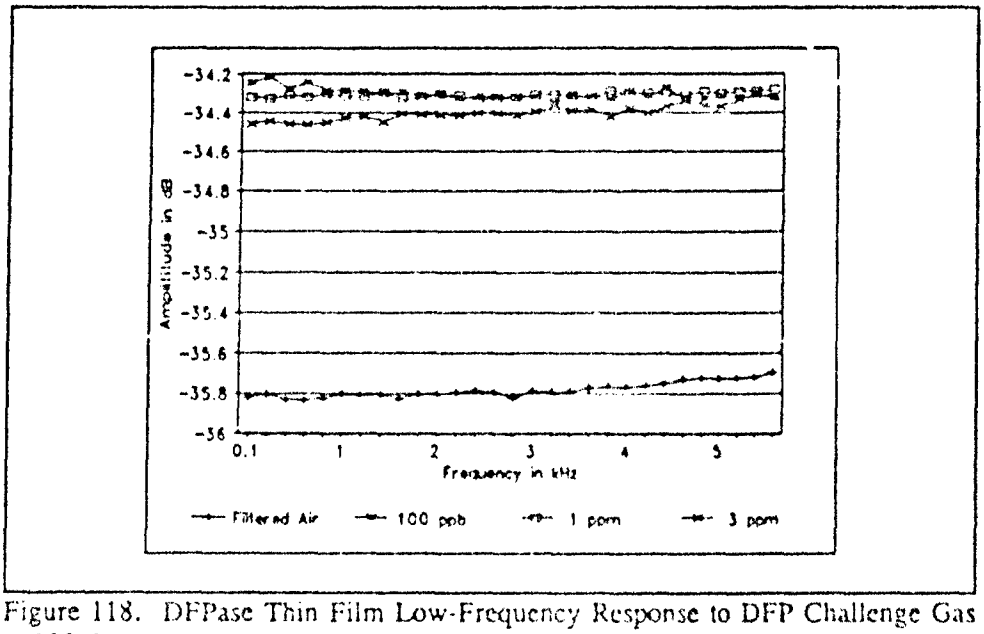

Figure 118. DFPase Thin Film Low-Frequency Response to DFP Challenge Gas at 30° C.

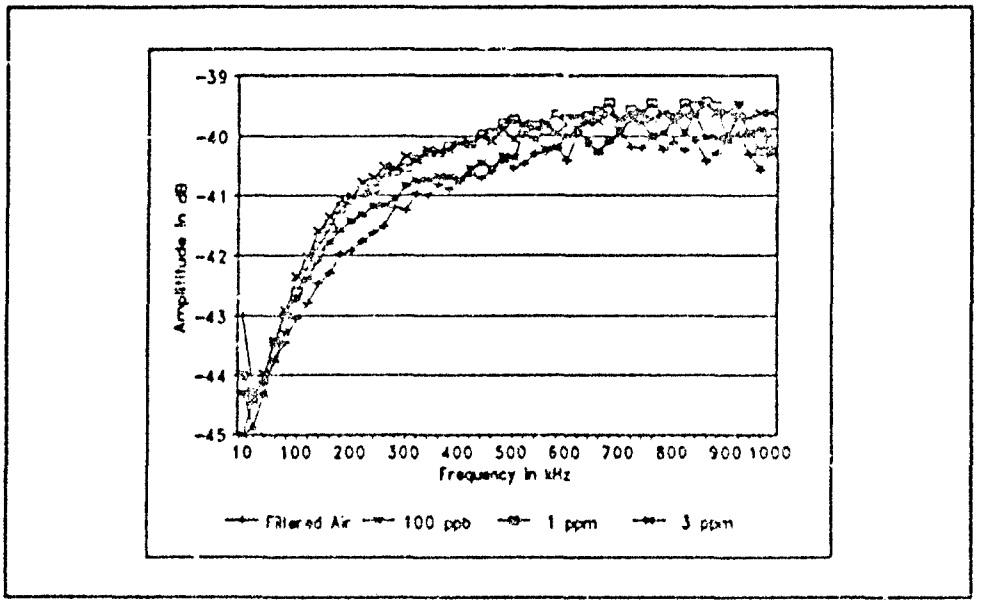

Figure 119. DFPase Thin Film High-Frequency Response to DFP Challenge Gas at 30° C.

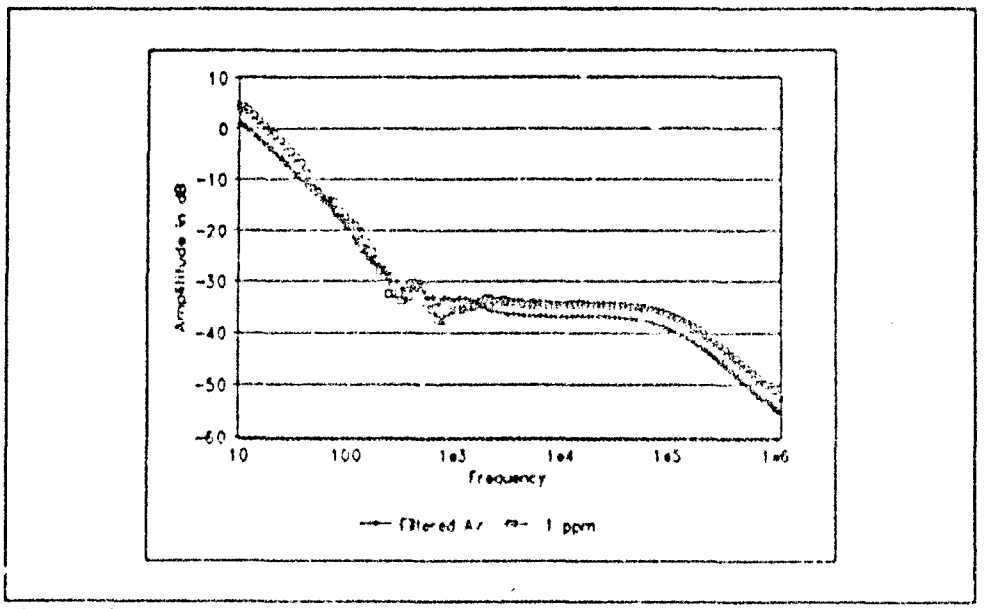

Figure 120. DFPase Thin Film Gain Response to DFP Challenge Gas at 30° C.

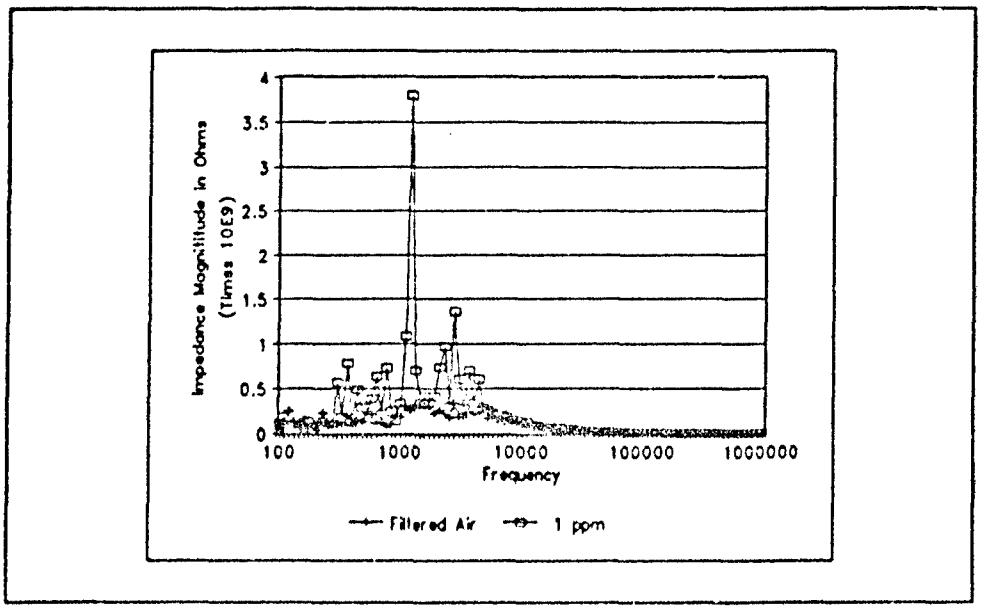

Figure 121. DFPase Thin Film AC Impedance Response to DFP Challenge Gas at 30° C.

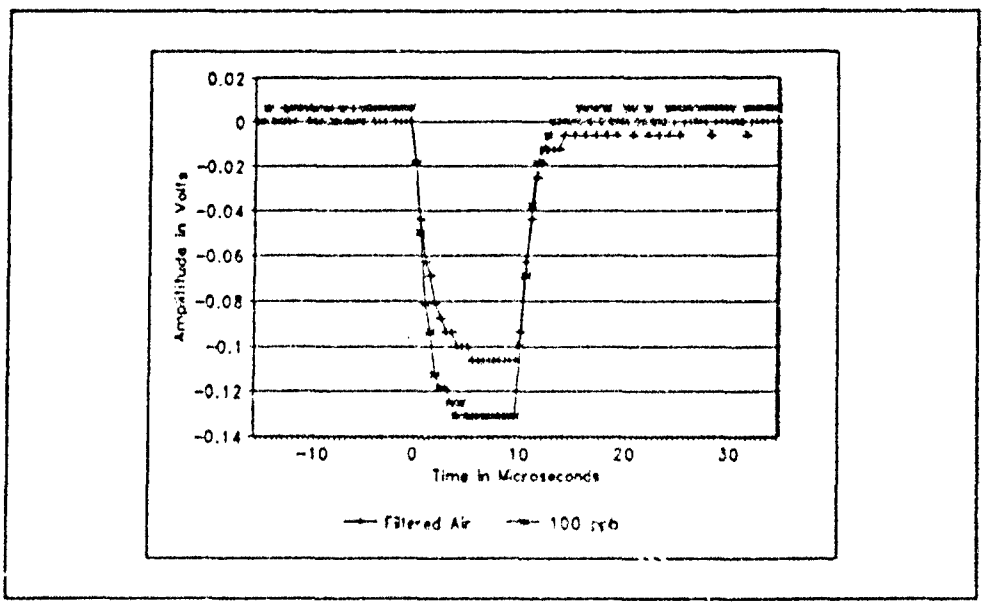

Figure 122. DFPase Thin Film Time-Domain Response to a 3 Volt 10 Microsecond Excitation Pulse With DFP Challenge Gas at 30° C.

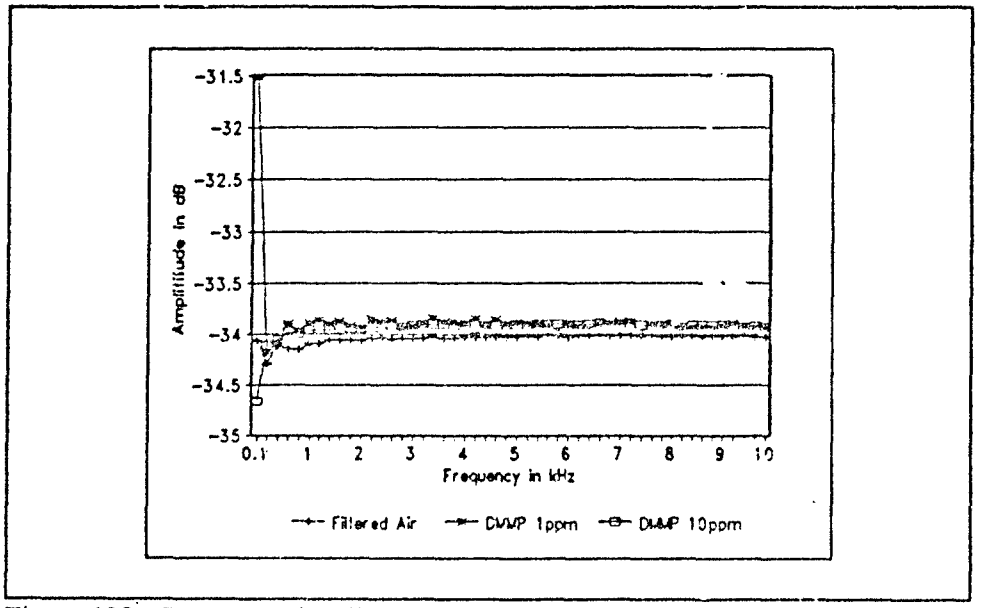

Figure 123. DFPase Thin Film Low-Frequency Response to DIMP and DMMP Challenge Gas at 30° C.

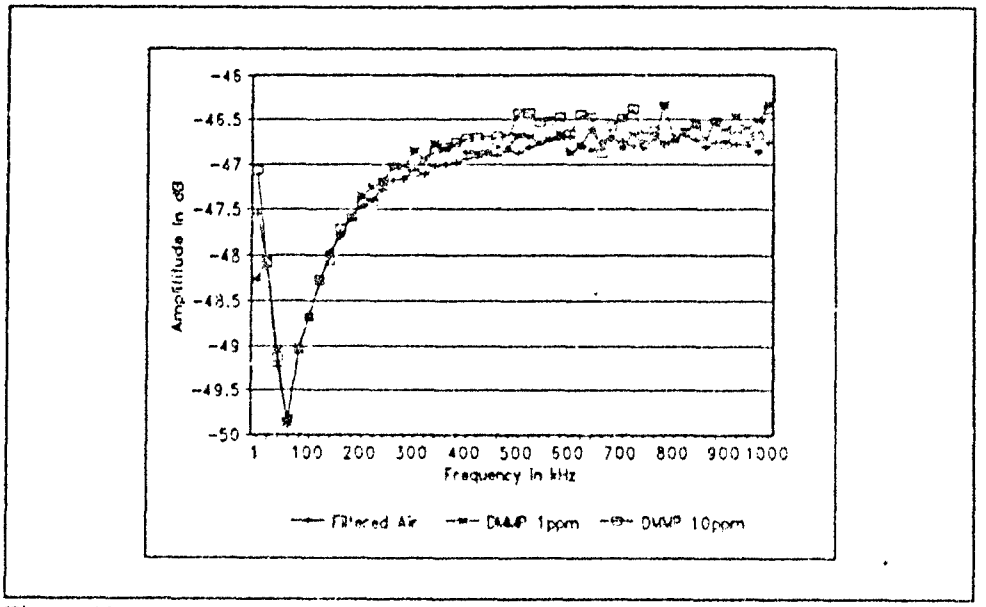

Figure 124. DFPase Thin Film High-Frequency Response to DIMP and DMMP Challenge Gas at 30° C.

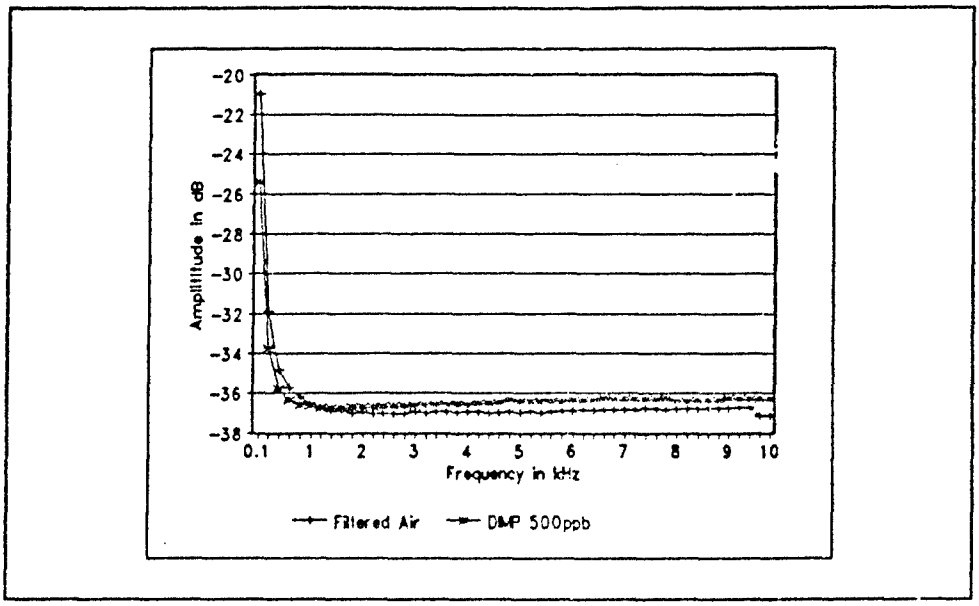

Figure 125. DFPase Thin Film Low-Frequency Response to DIMP and DFP Challenge Gas at 30° C.

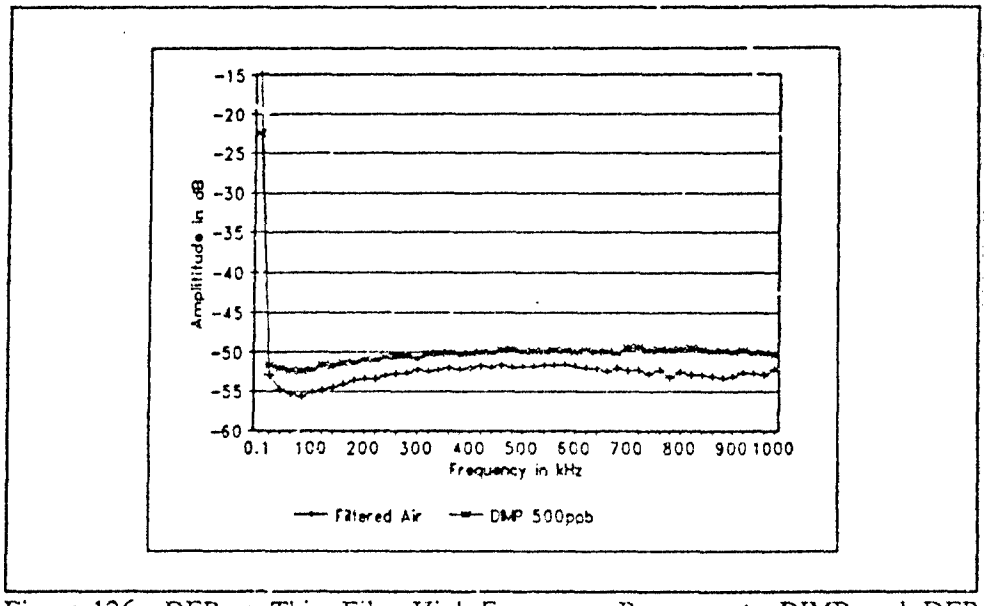

Figure 126. DFPase Thin Film High-Frequency Response to DIMP and DFP Challenge Gas at 30° C.

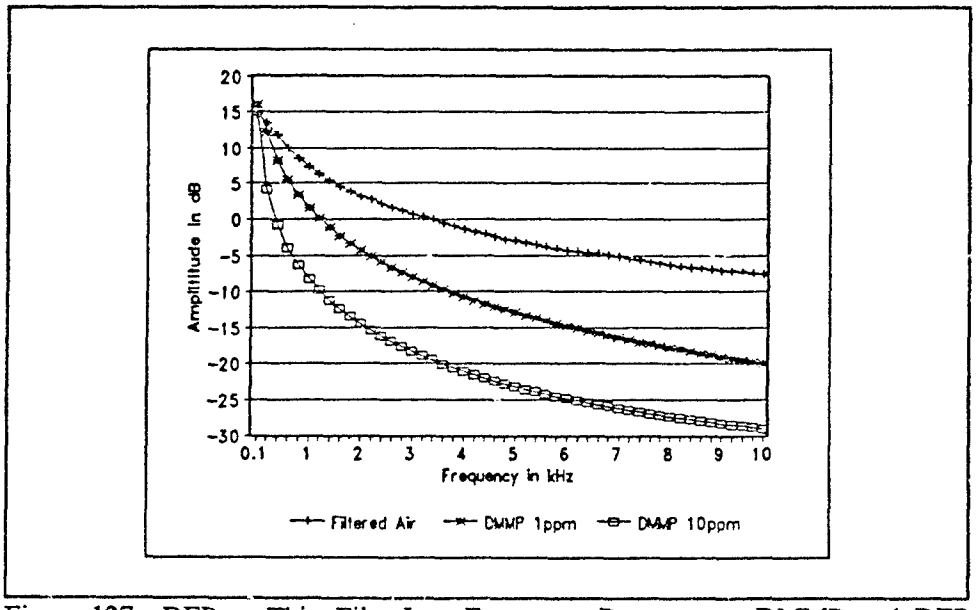

Figure 127. DFPase Thin Film Low-Frequency Response to DMMP and DFP Challenge Gas at 30° C.

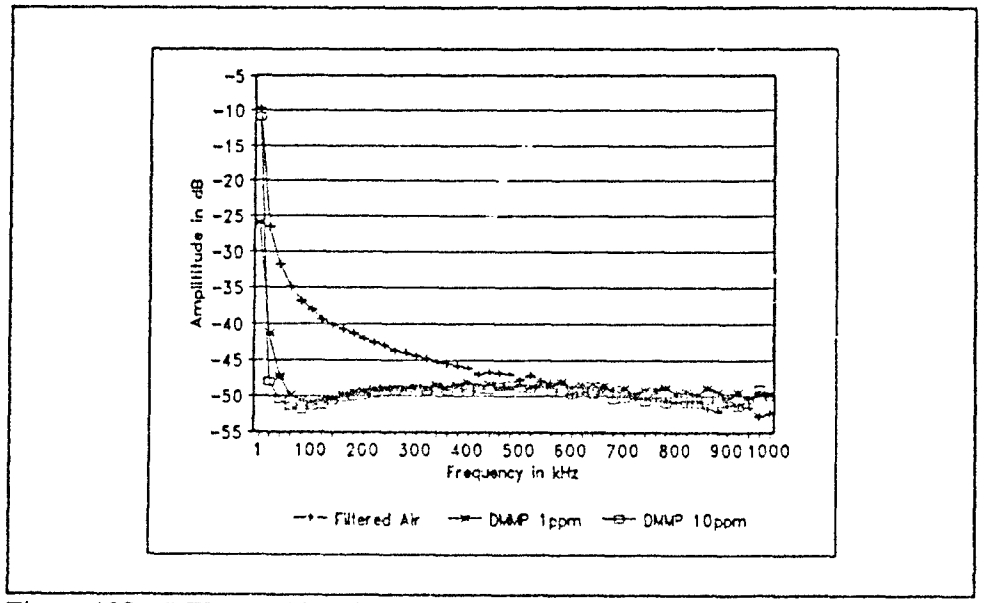

Figure 128. DFPase Thin Film High-Frequency Response to DMMP and DFP Challenge Gas at 30° C.

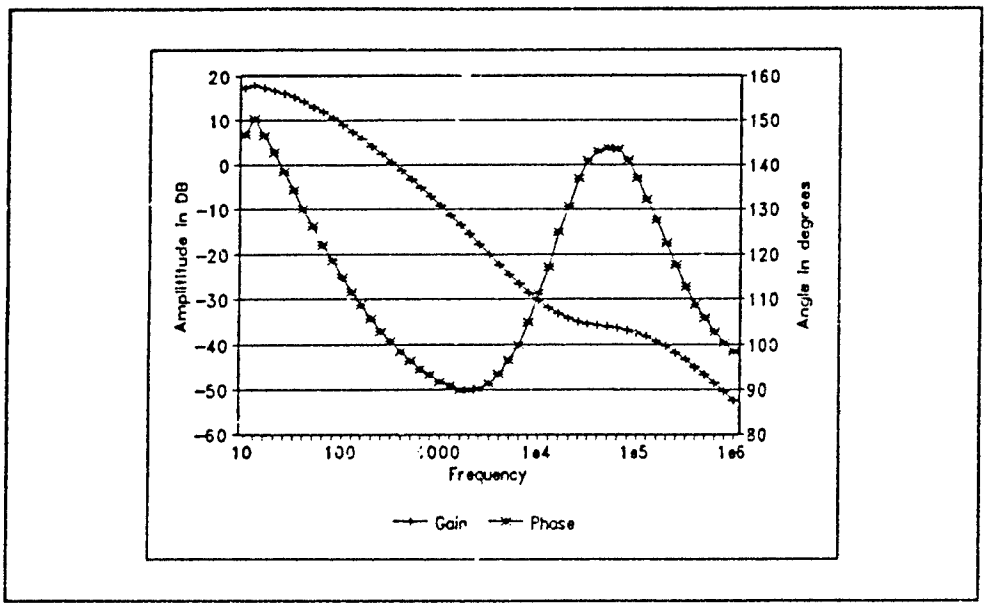

Figure 129. DFPase Thin Film Gain Response to DMMP and DFP Challenge Gas at 30° C.

Succinyl Chloride Supplemental Graphs

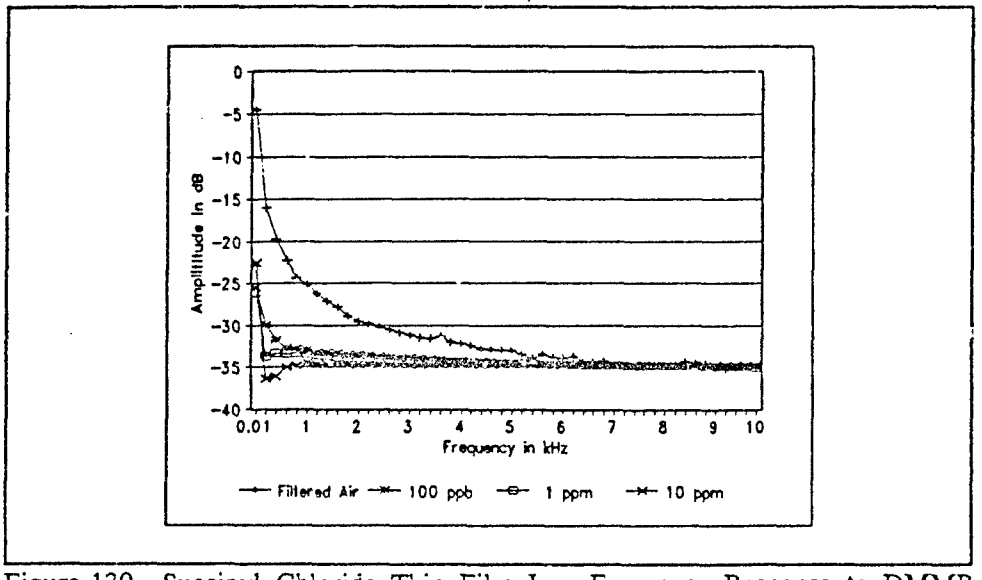

Figure 130. Succinyl Chloride Thin Film Low-Frequency Response to DMMP Challenge Gas at 30° C.

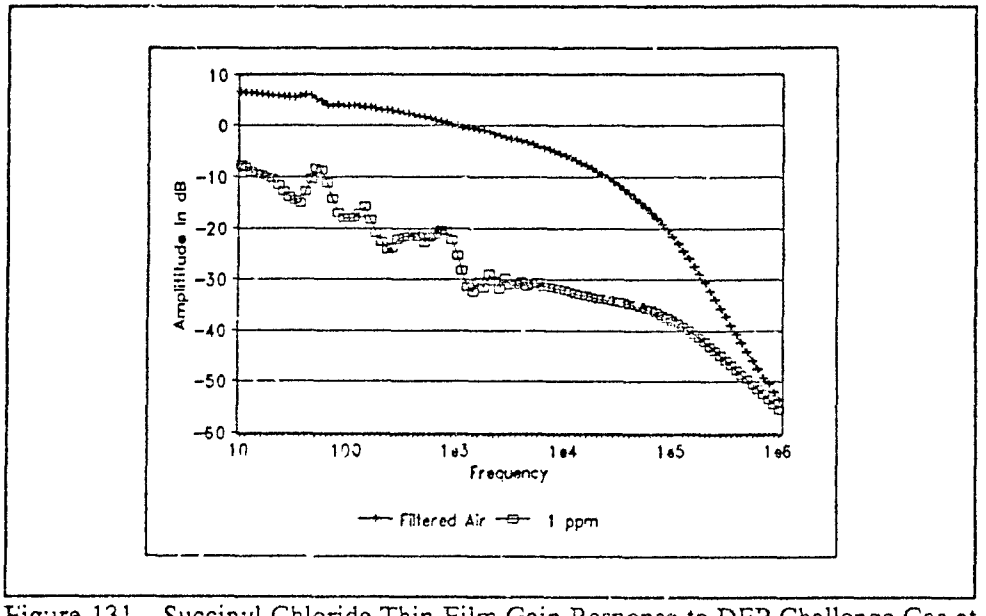

Figure 131. Succinyl Chloride Thin Film Gain Response to DFP Challenge Gas at 30° C.

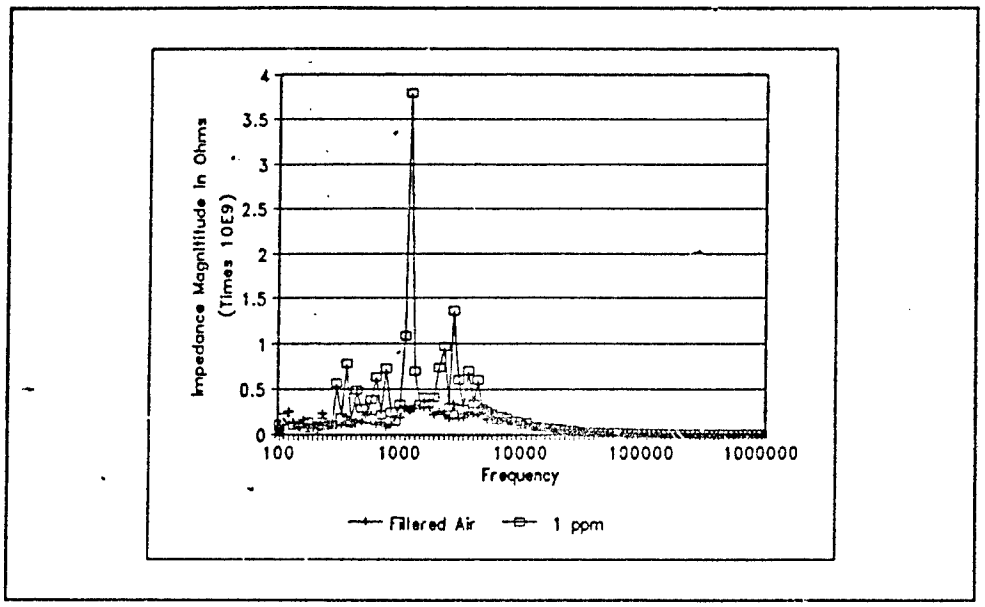

Figure 132. Succinyl Chloride Thin Film AC Impedance Response to DFP Challenge Gas at 30° C.

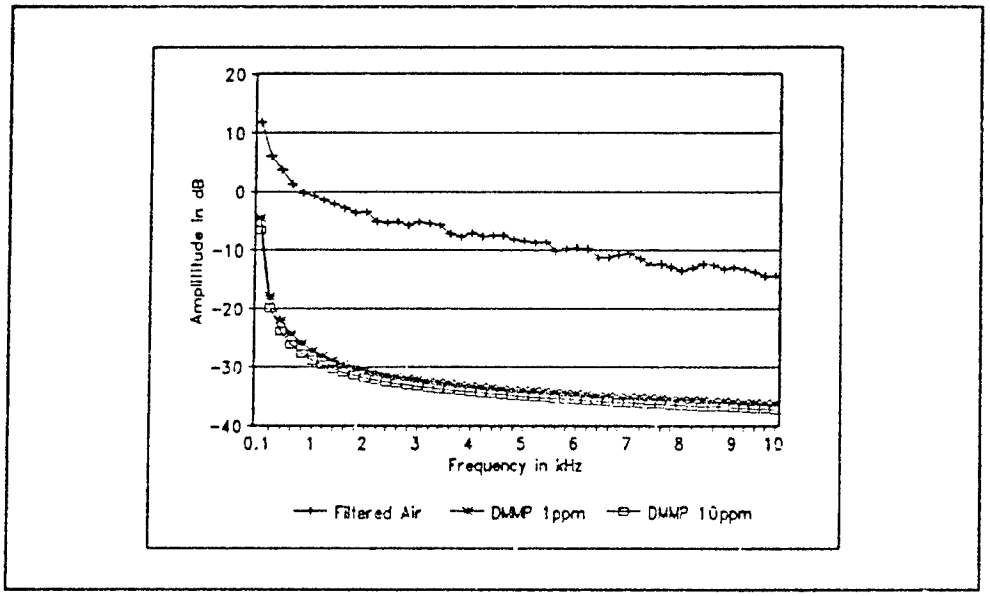

Figure 133. Succinyl Chloride Thin Film Low-Frequency Response to DIMP and DMMP Challenge Gas at 30° C.

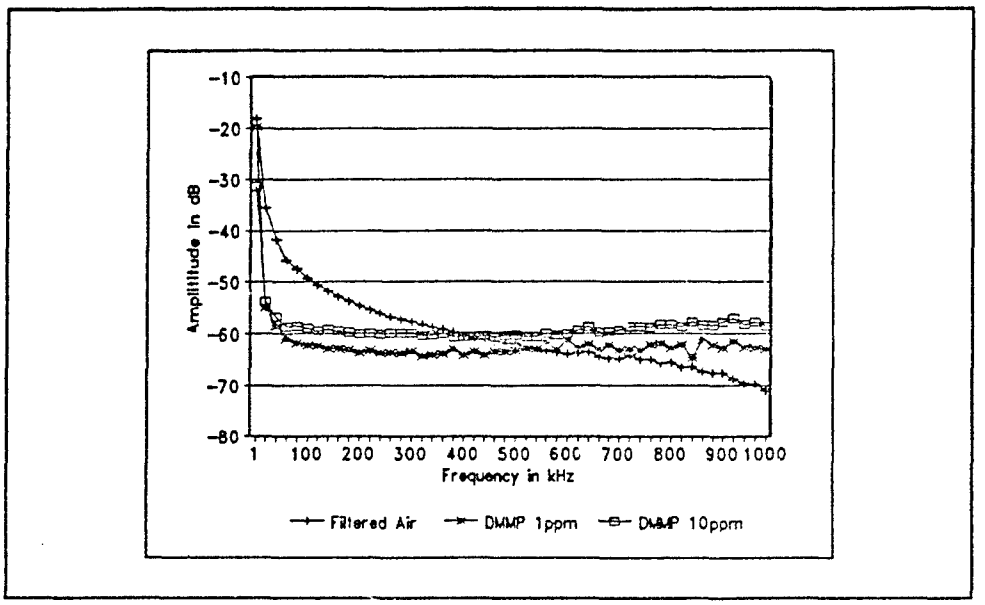

Figure 134. Succinyl Chloride Thin Film High-Frequency Response to DIMP and DMMP Challenge Gas at 30° C.

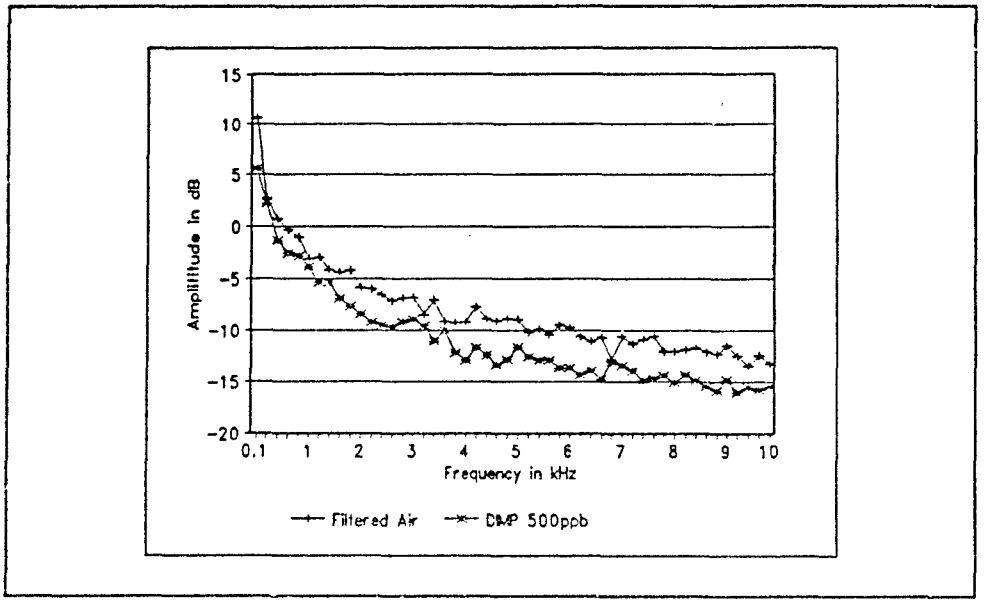

Figure 135. Succinly Chloride Thin Film Low-Frequency Response to DIMP and DFP Challenge Gas at 30° C.

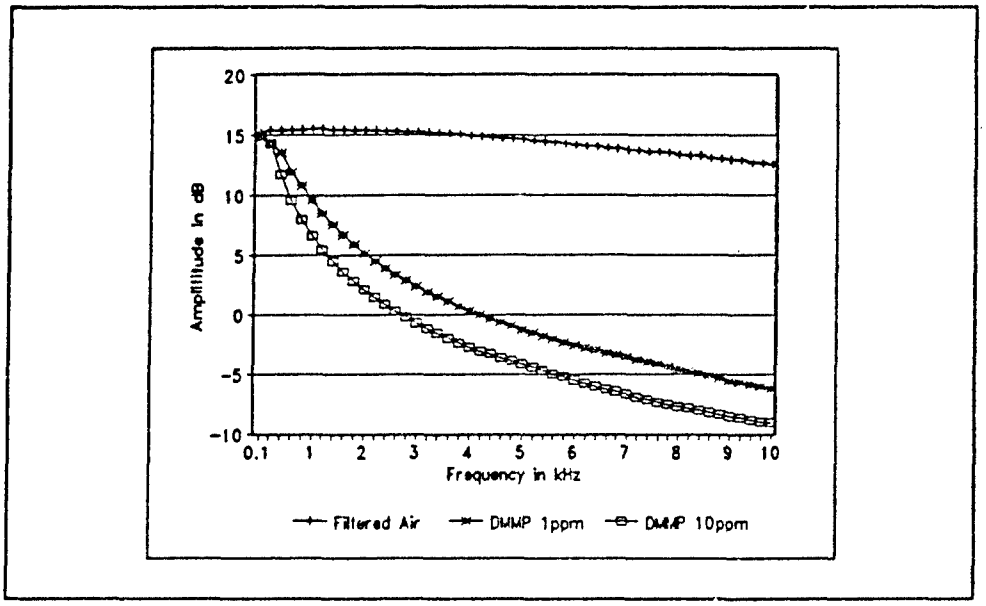

Figure 136. Succinyl Chloride Thin Film Low-Frequency Response to DMMP and DFP Challenge Gas at 30° C.

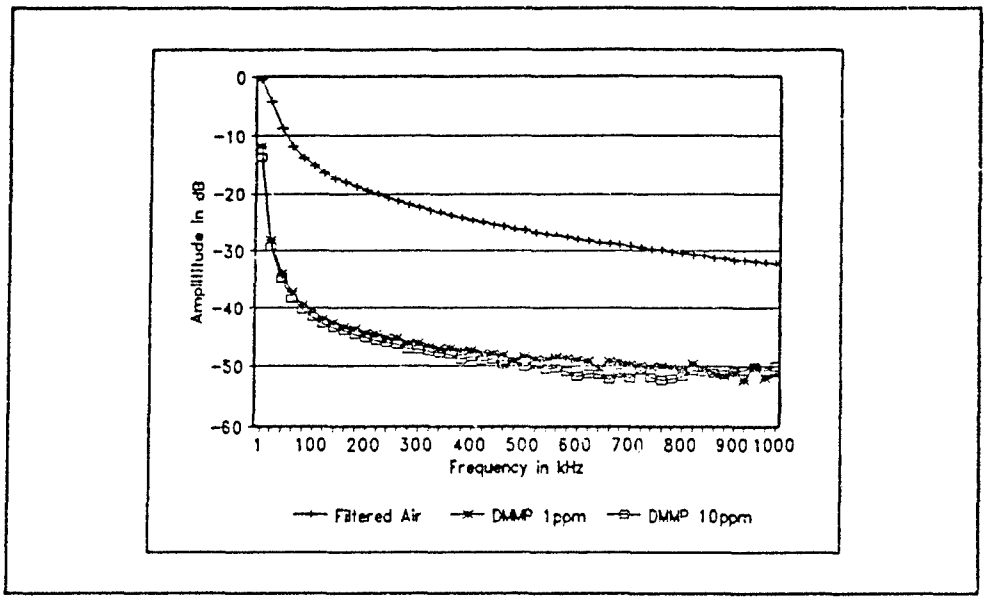

Figure 137. Succinyl Chloride Thin Film High-Frequency Response to DMMP and DFP Challenge Gas at 30° C.

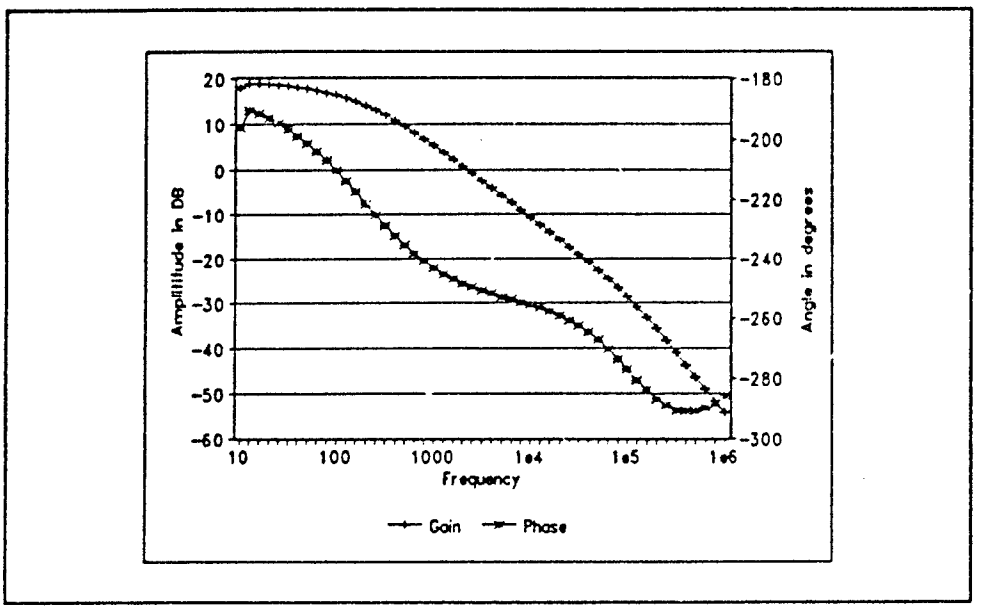

Figure 138. Succinyl Chloride Thin Film Gain Response to DMMP and DFP Challenge Gas at 30° C.

Succinylcholine Chloride Supplemental Graphs

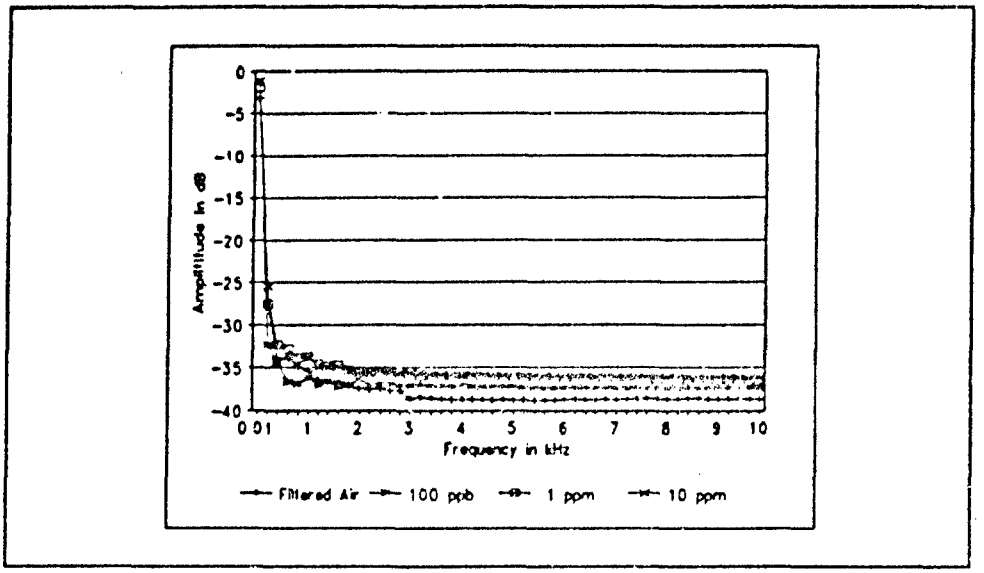

Figure 139. Succinylcholine Chloride Thin Film Low-Frequency Response to DMMP Challenge Gas at 30° C.

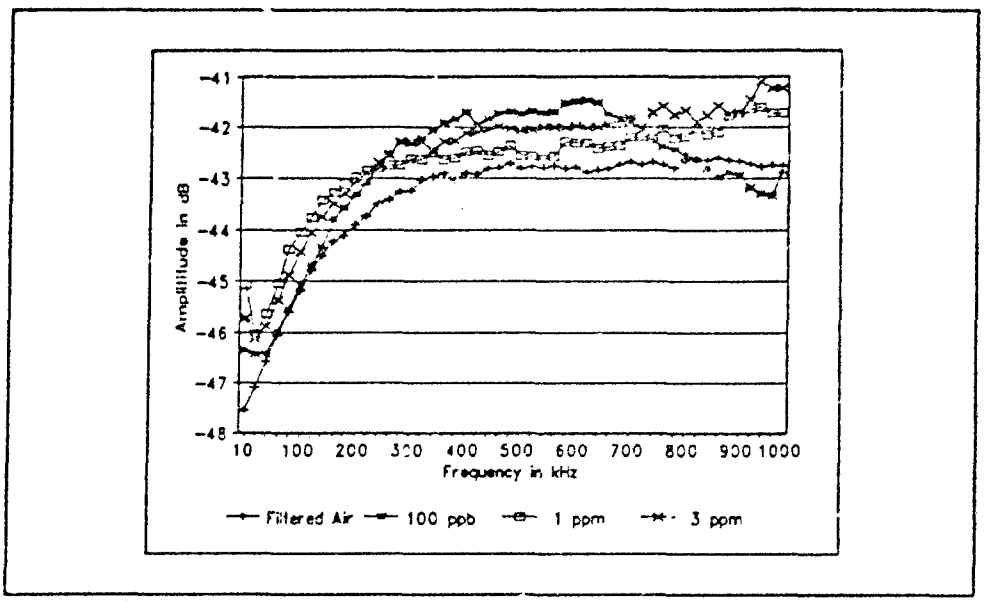

Figure 140. Succinylcholine Chloride Thin Film High-Frequency Response to DFP Challenge Gas at 30° C.

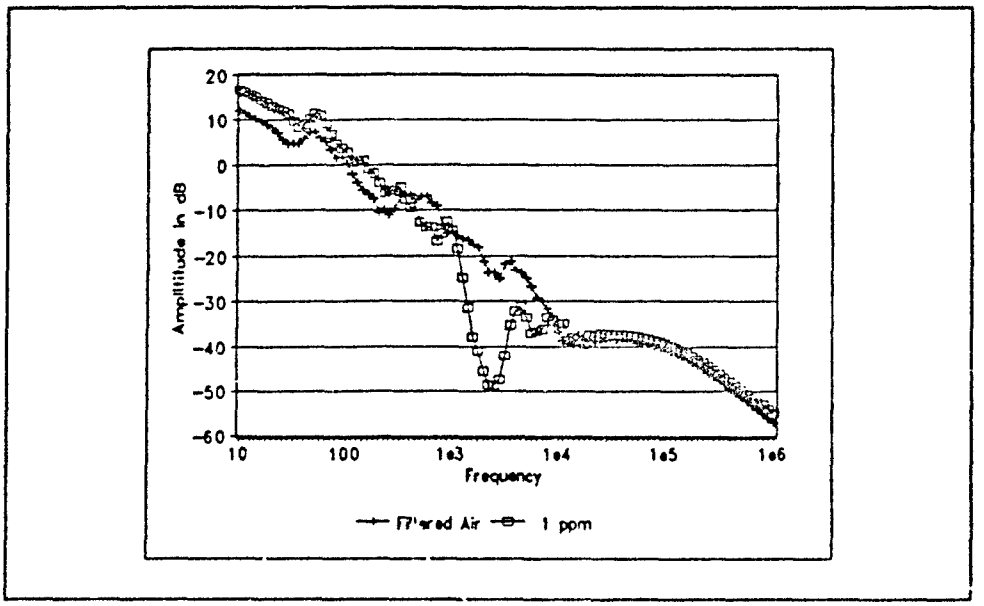

Figure 141. Succinylcholine Chloride Thin Film Gain Response to DFP Challenge Gas at 30° C.

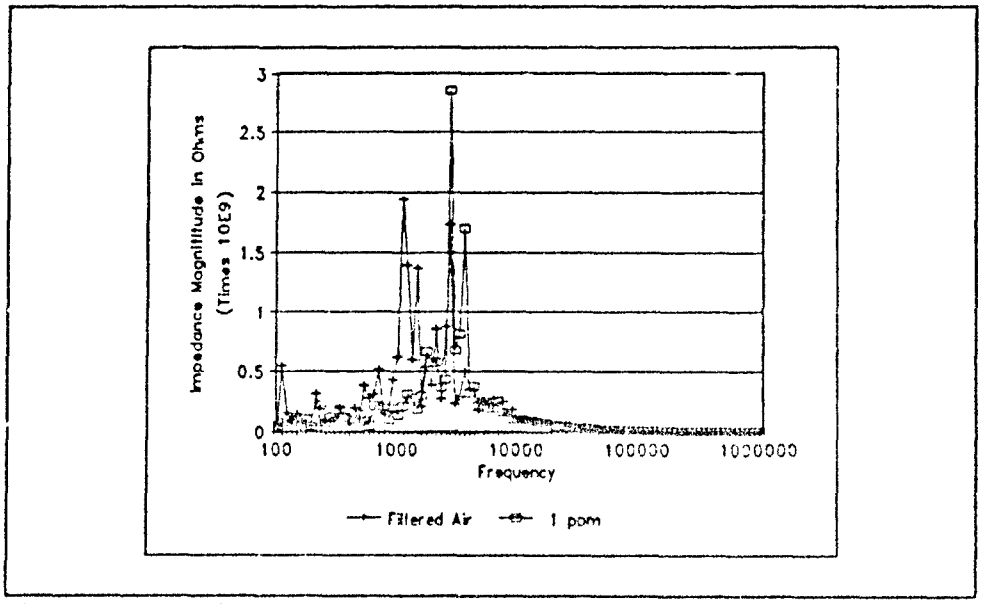

Figure 142. Succinylcholine Chloride Thin Film AC Impedance Response to DFP Challenge Gas at 30° C.

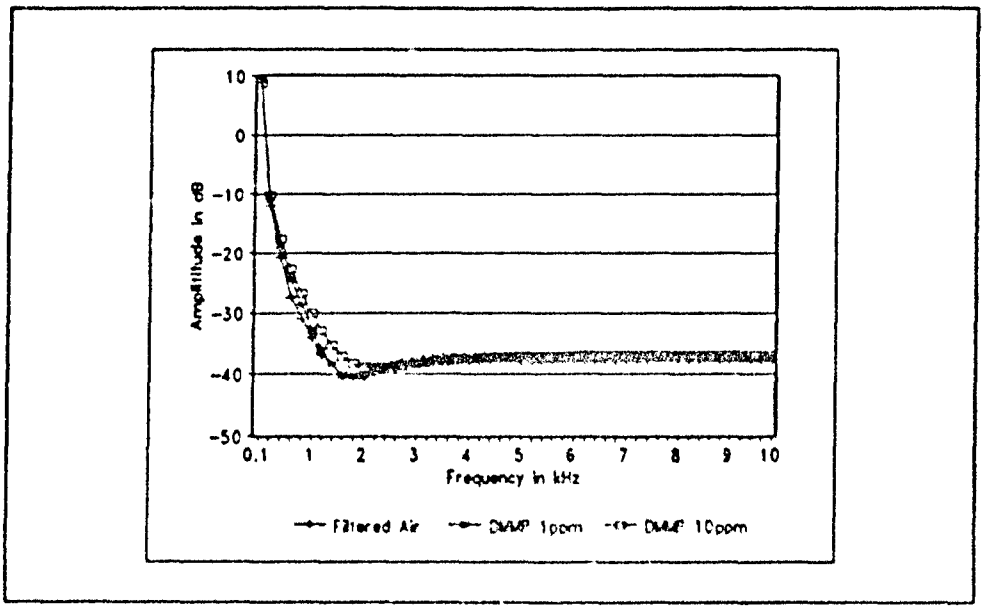

Figure 143. Succinylcholine Chloride Thin Film Low-Frequency Response to DIMP and DMMP Challenge Gas at 30° C.

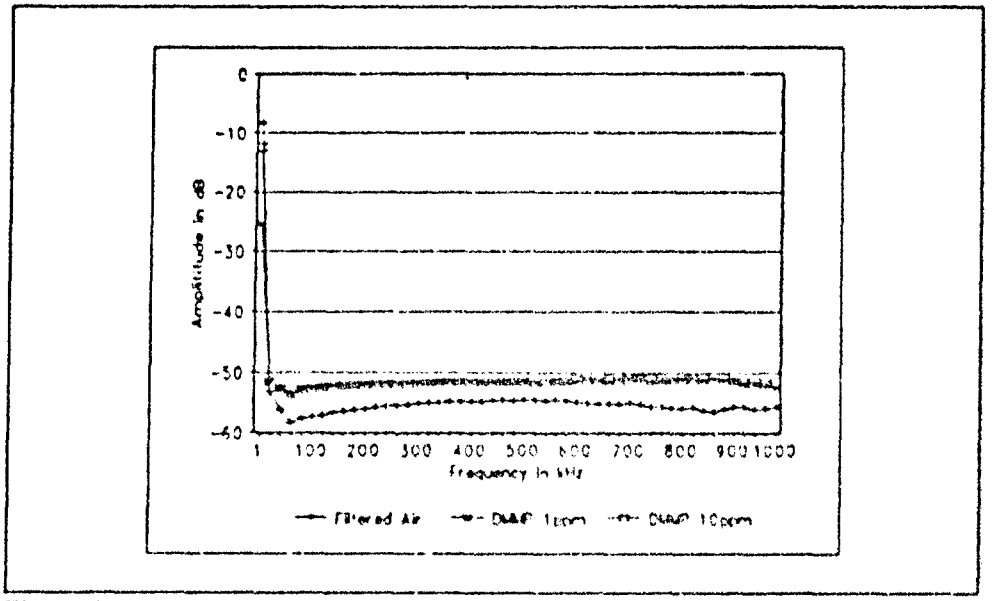

Figure 144. Succinylcholine Chloride Thin Film High-Frequency Response to DIMP and DMMP Challenge Gas at 30° C.

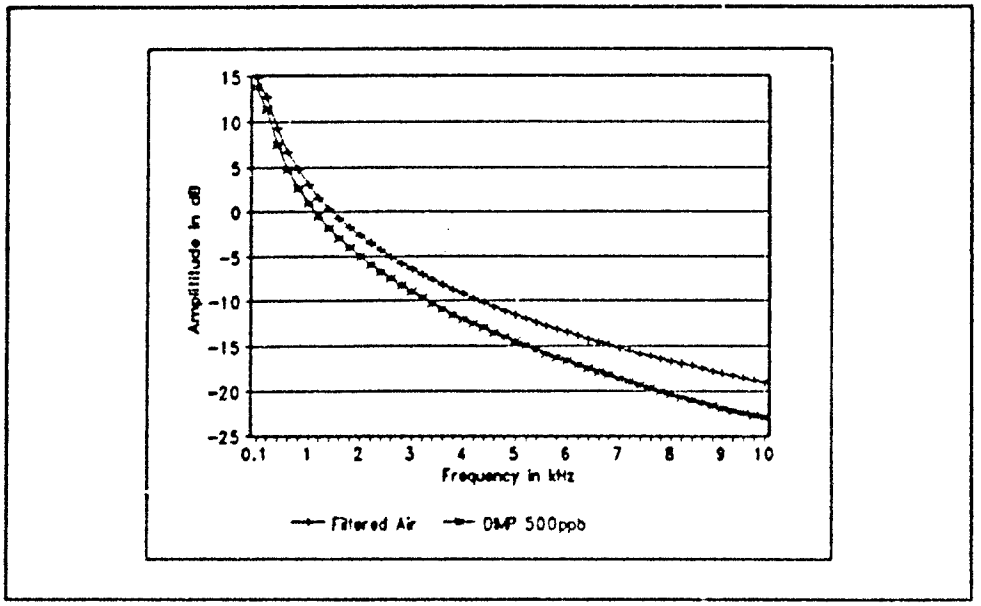

Figure 145. Succinylcholine Chloride Thin Film Low-Frequency Response to DIMP and DFP Challenge Gas at 30° C.

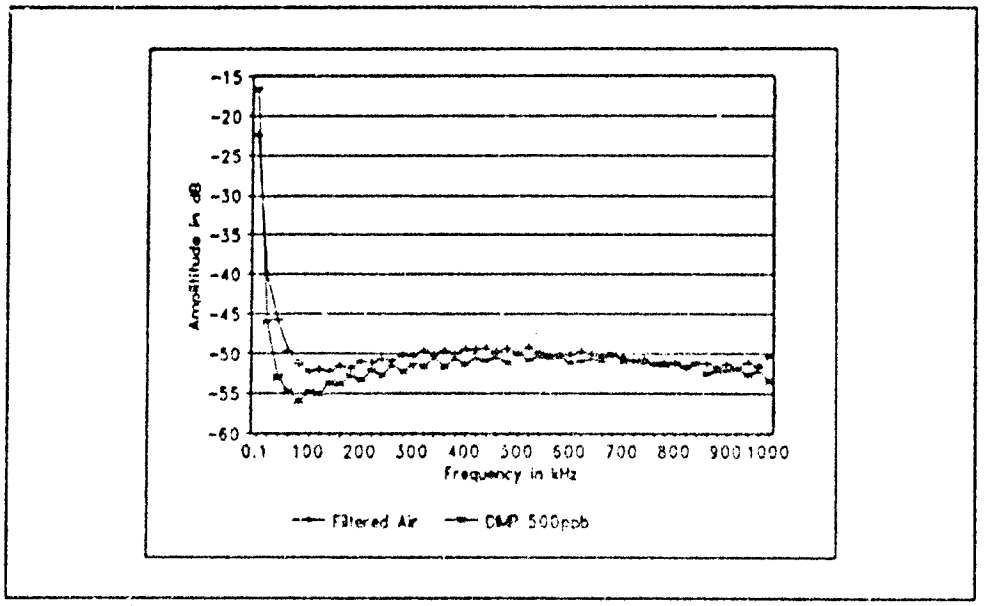

Figure 146. Succinylcholine Chloride Thin Film High-Frequency Response to DIMP and DFP Challenge Gas at 30° C.

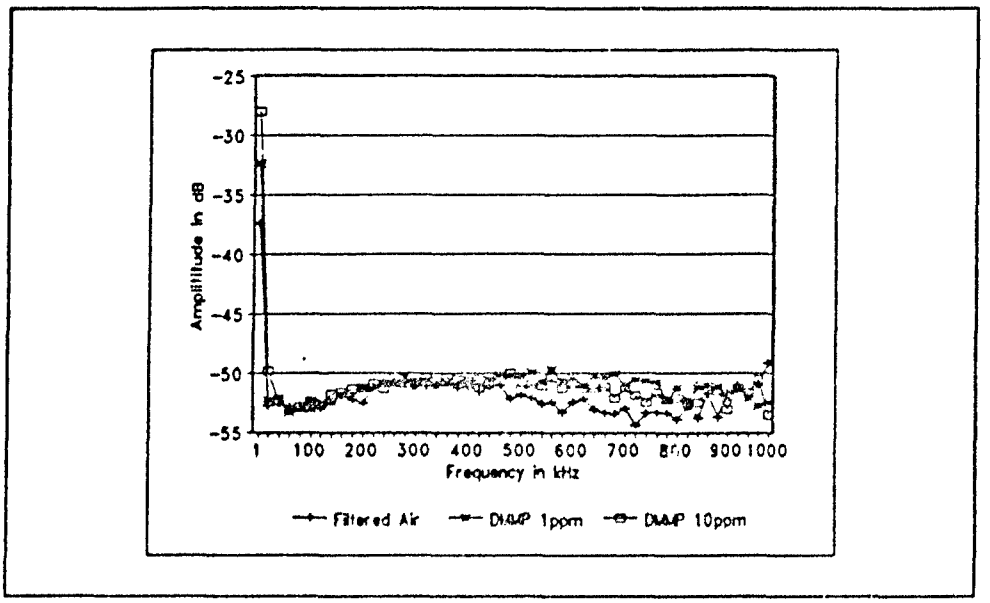

Figure 147. Succinylcholine Chloride Thin Film High-Frequency Response to DMMP and DFP Challenge Gas at 30° C.

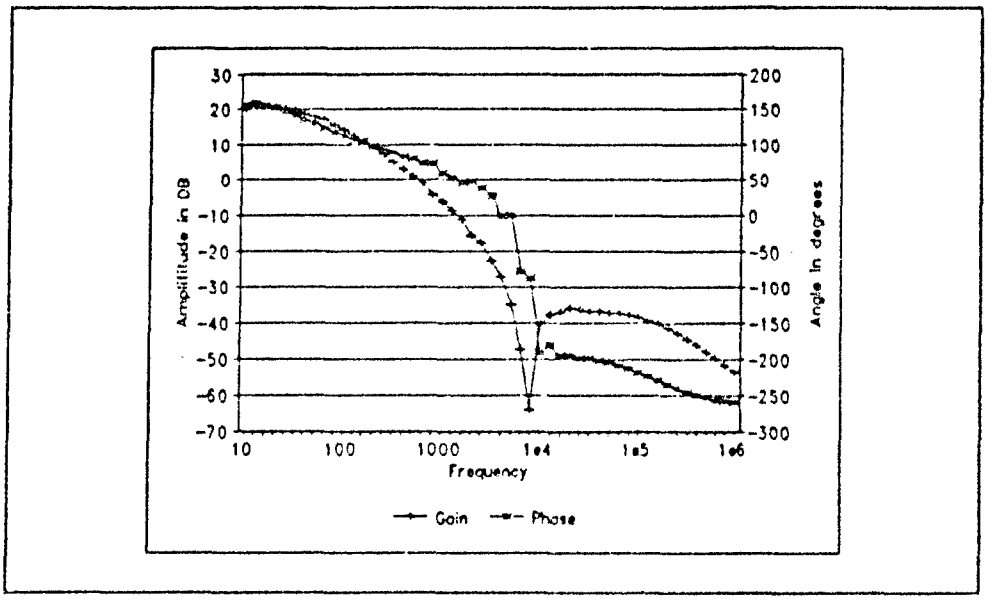

Figure 148. Succinylcholine Chloride Thin Film Gain Response to DMMP and DFP Challenge Gas at 30° C.

2-Naphthol(β) Supplemental Graphs

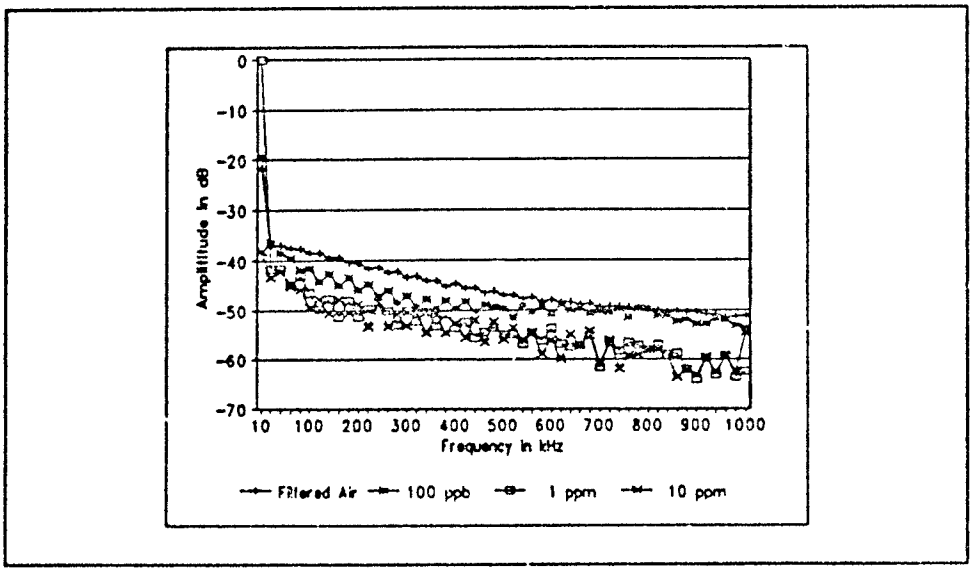

Figure 149. 2-Naphthol(β) Thin Film High-Frequency Response to DIMP Challenge Gas at 30° C.

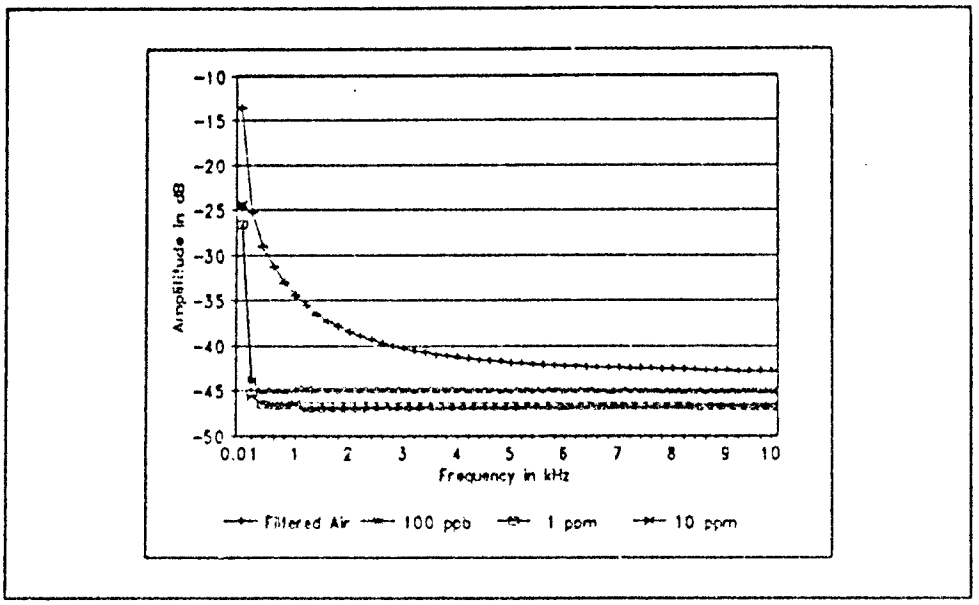

Figure 150. 2-Naphthol(β) Thin Film Low-Frequency Response to DMMP Challenge Gas at 30° C.

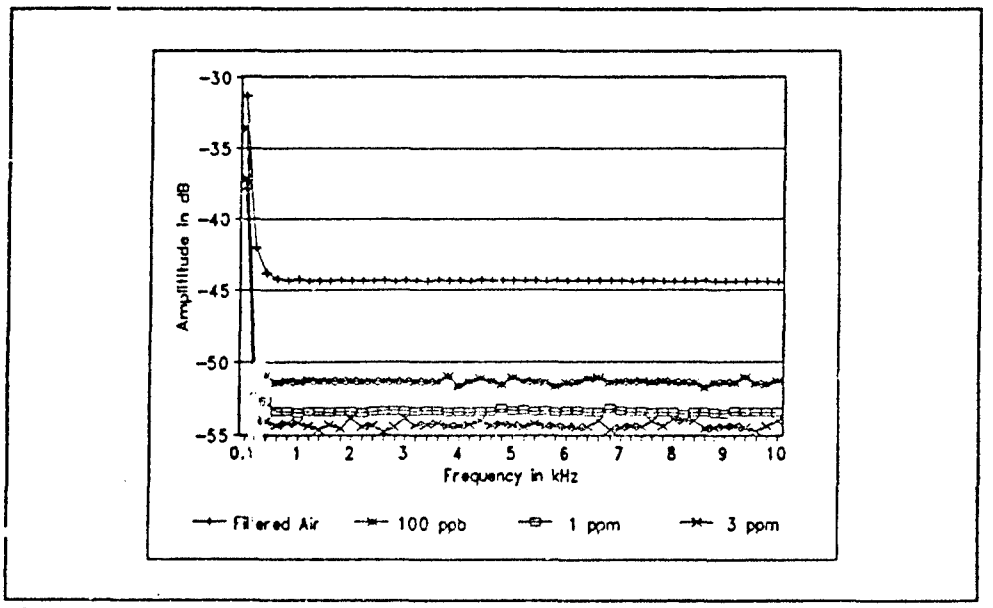

Figure 151. 2-Naphthol(β) Thin Film Low-Frequency Response to DFP Challenge Gas at 30° C.

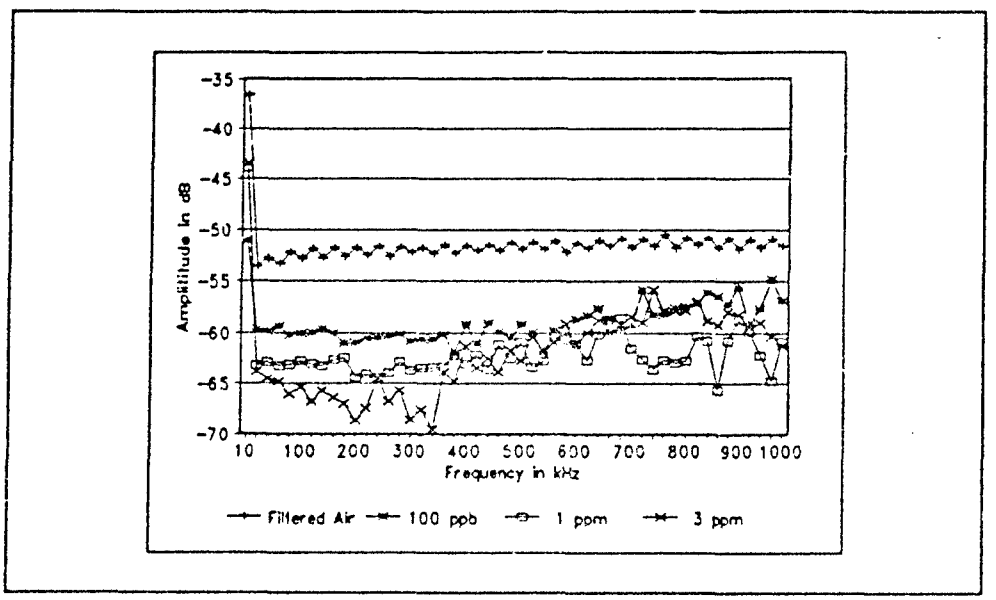

Figure 152. 2-Naphthol(β) Thin Film High-Frequency Response to DFP Challenge Gas at 30° C.

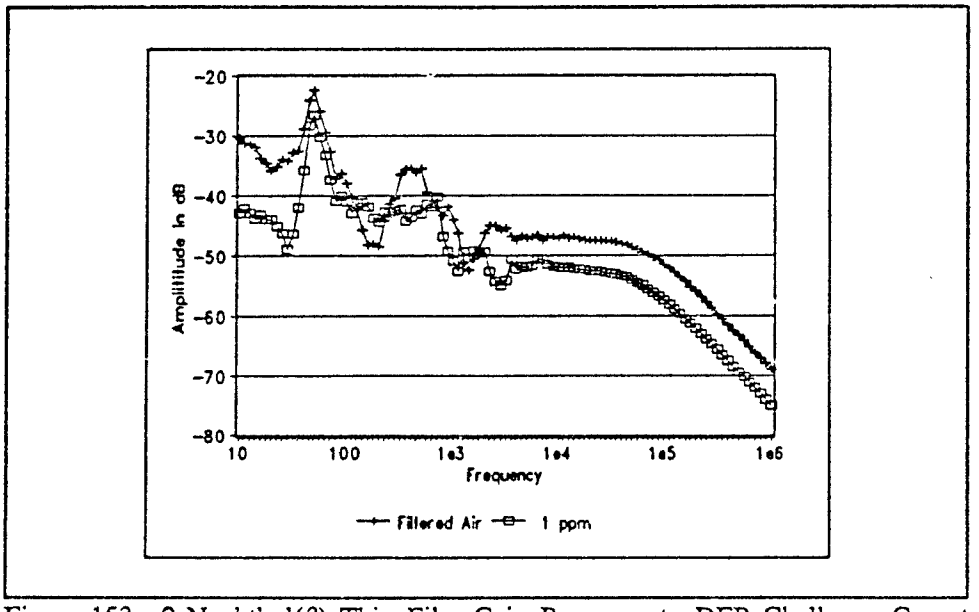

Figure 153. 2-Naphthol(β) Thin Film Gain Response to DFP Challenge Gas at 30° C.

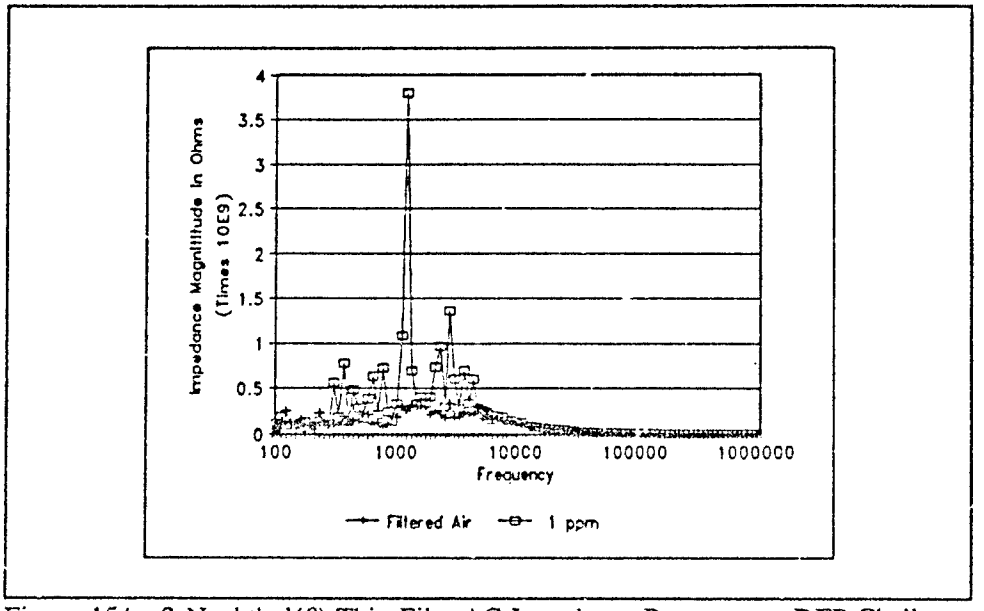

Figure 154. 2-Naphthol(β) Thin Film AC Impedance Response to DFP Challenge Gas at 30° C.

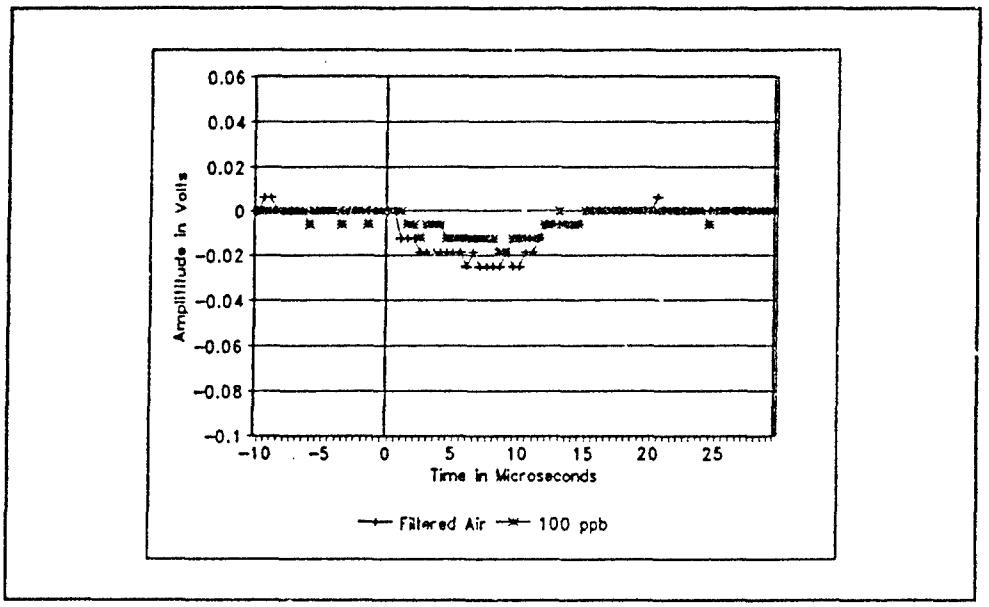

Figure 155. 2-Naphthol(β) Thin Film Time-Domain Response to a 3 Volt 10 Microsecond Excitation Pulse With DFP Challenge Gas at 30° C.

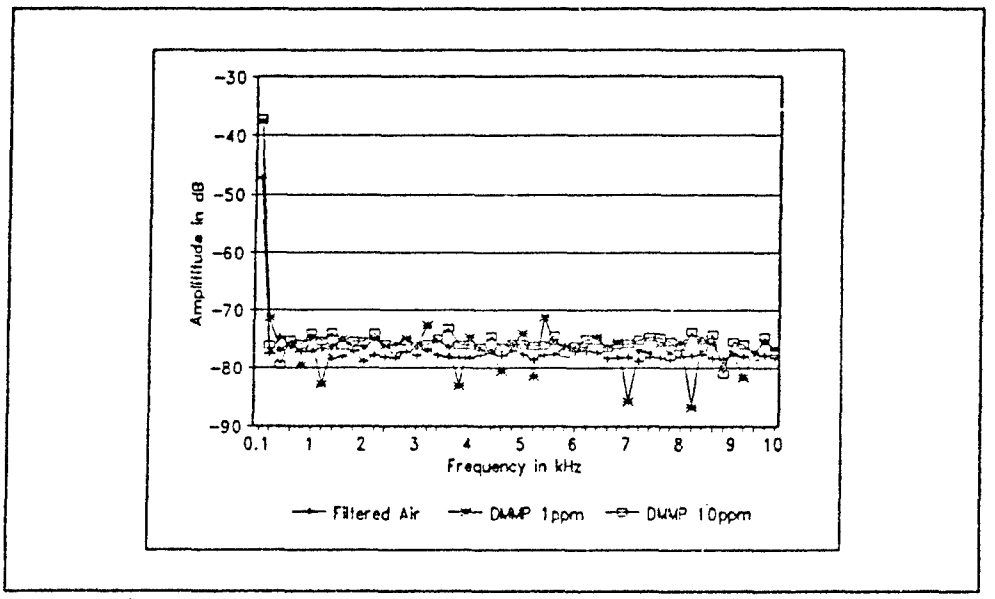

Figure 156. 2-Naphthol(β) Thin Film Low-Frequency Response to DIMP and DMMP Challenge Gas at 30° C.

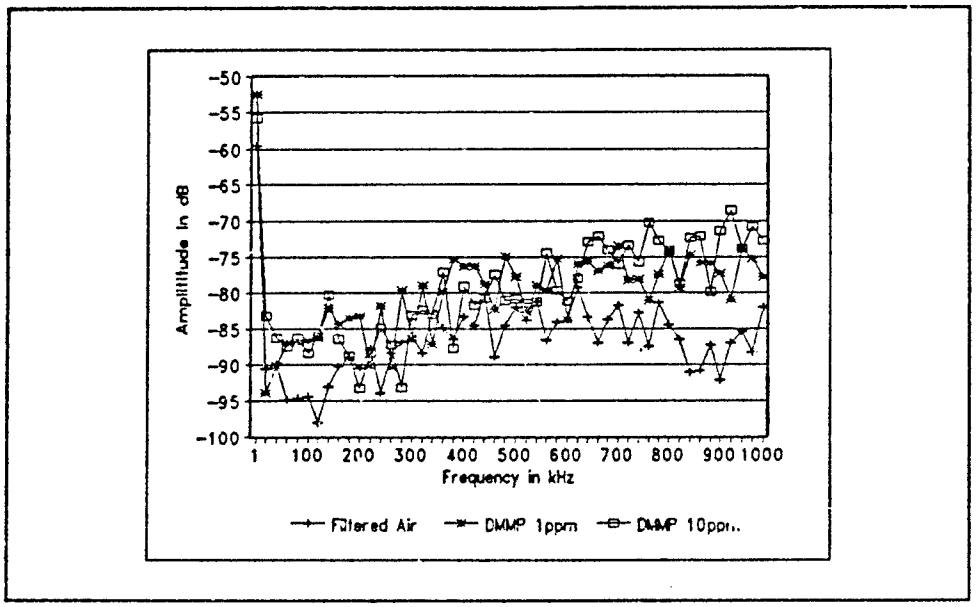

Figure 157. 2-Naphthol(β) Thin Film High-Frequency Response to DIMP and DMMP Challenge Gas at 30° C.

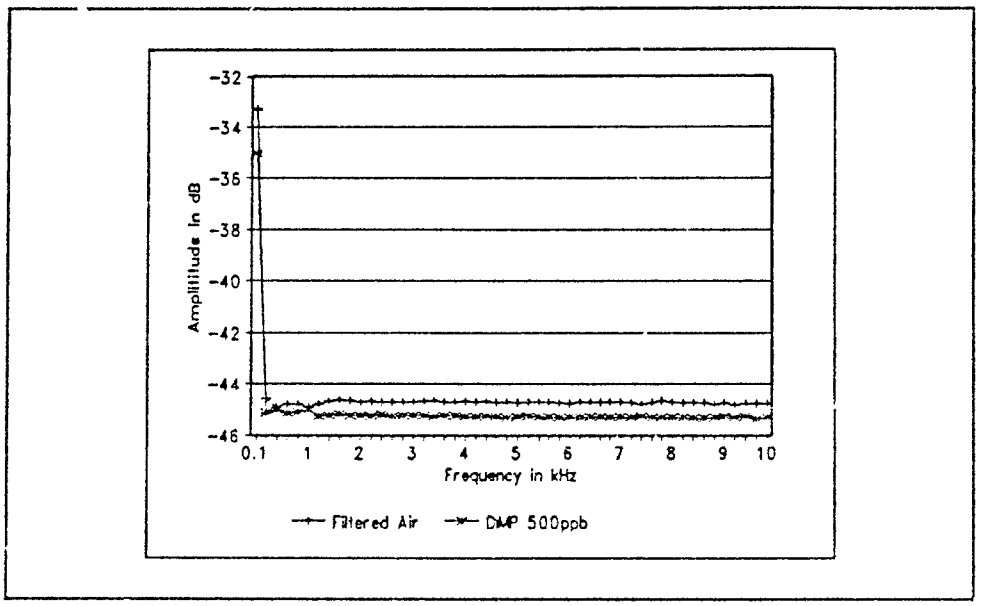

Figure 158. 2-Naphthol(β) Thin Film Low-Frequency Response to DIMP and DFP Challenge Gas at 30° C.

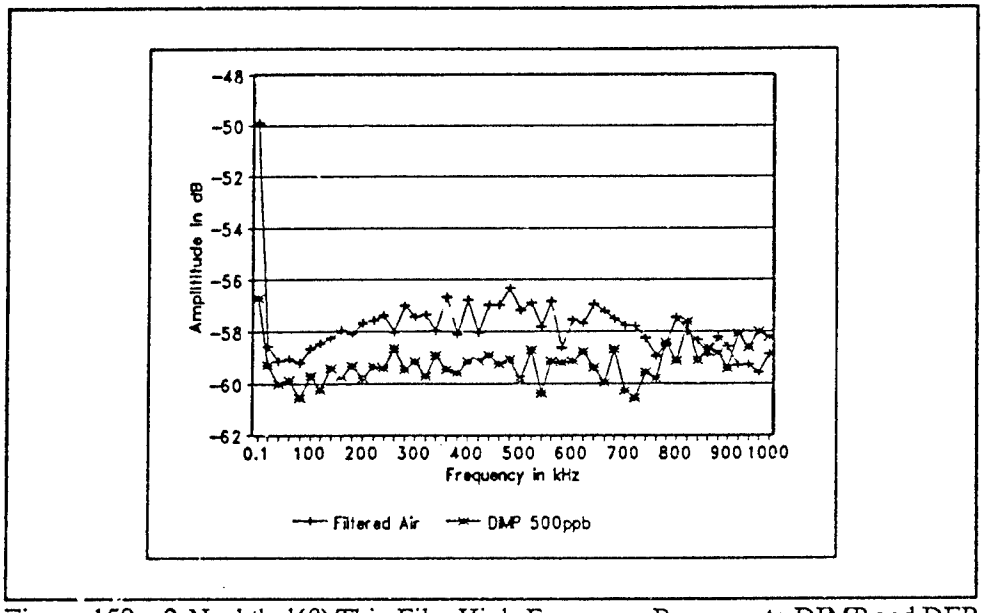

Figure 159. 2-Naphthol(β) Thin Film High-Frequency Response to DIMP and DFP Challenge Gas at 30° C.

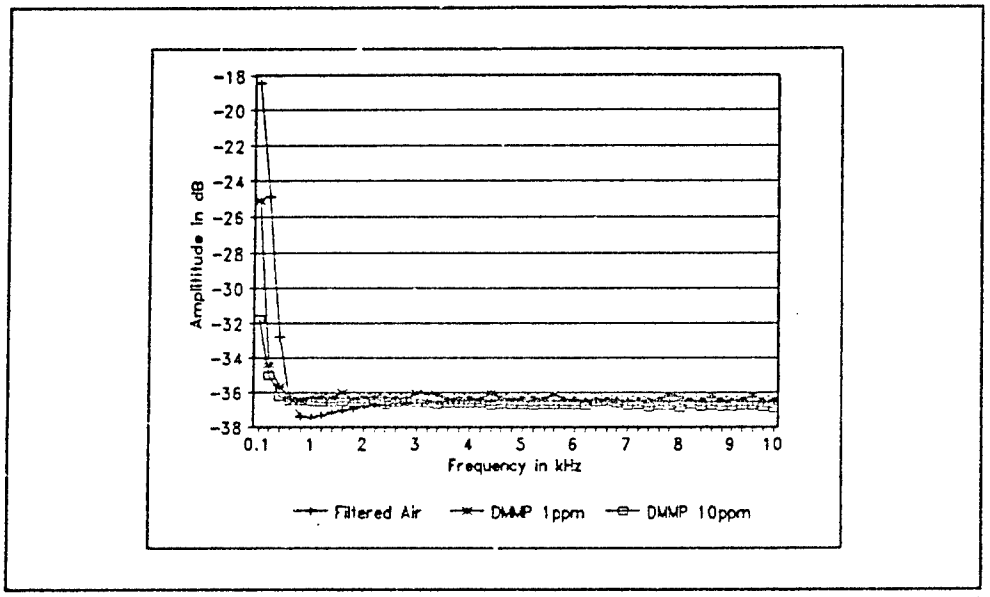

Figure 160. 2-Naphthol(β) Thin Film Low-Frequency Response to DMMP and DFP Challenge Gas at 30° C.

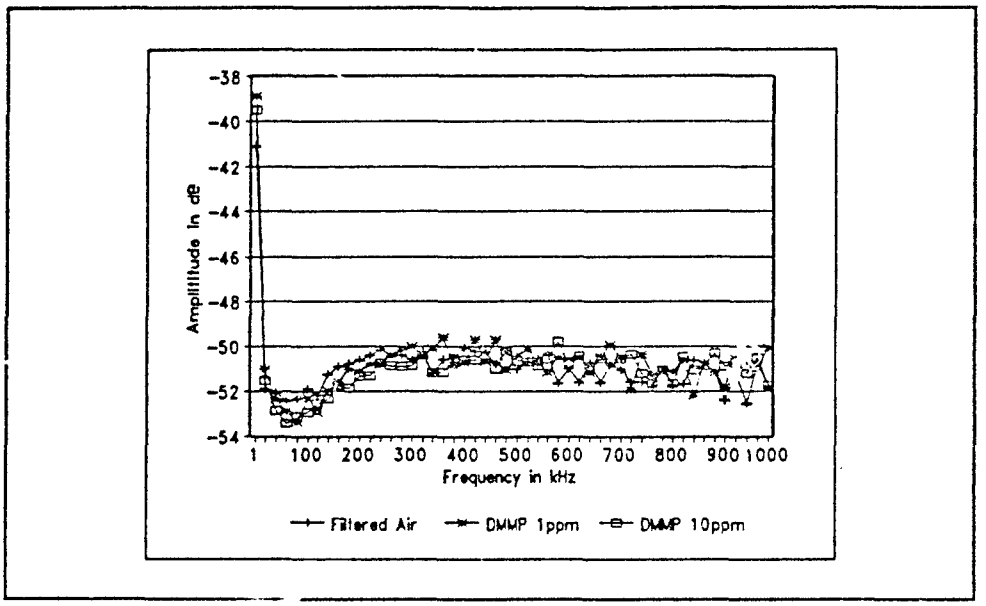

Figure 161. 2-Naphthol(β) Thin Film High-Frequency Response to DMMP and DFP Challenge Gas at 30° C.

L-Histidine Dihydrochloride Supplemental Graphs

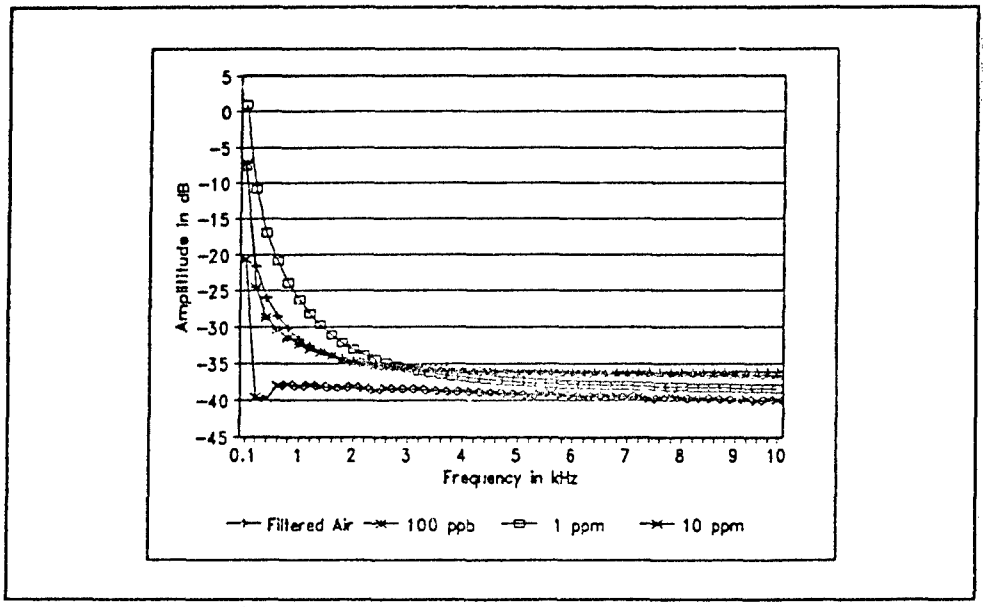

Figure 162. L-Histidine Dihydrochloride Thin Film Low-Frequency Response to DIMP Challenge Gas at 30° C.

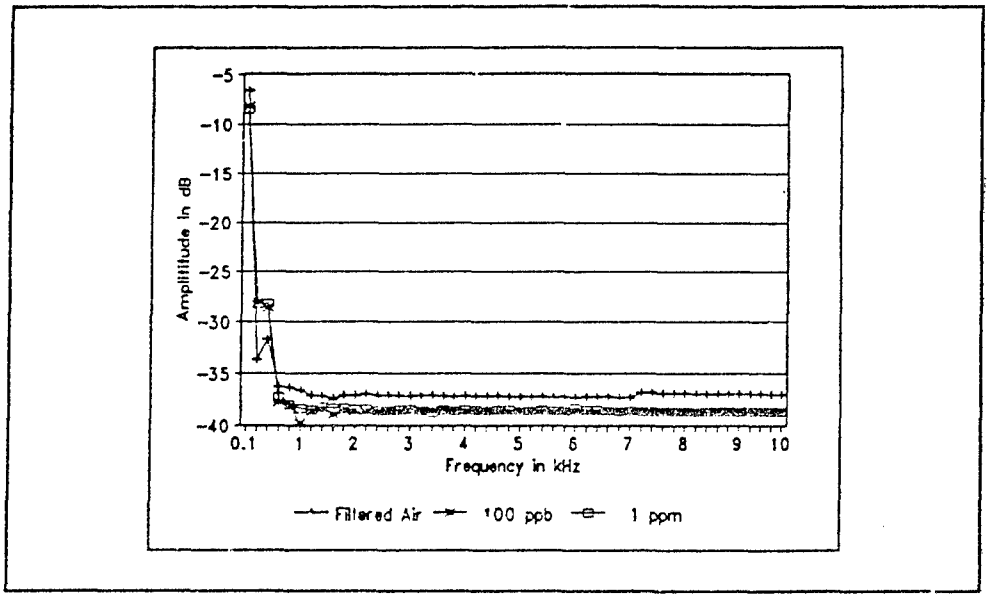

Figure 163. L-Histidine Dihydrochloride Thin Film Low-Frequency Response to DIMP Challenge Gas at 50° C.

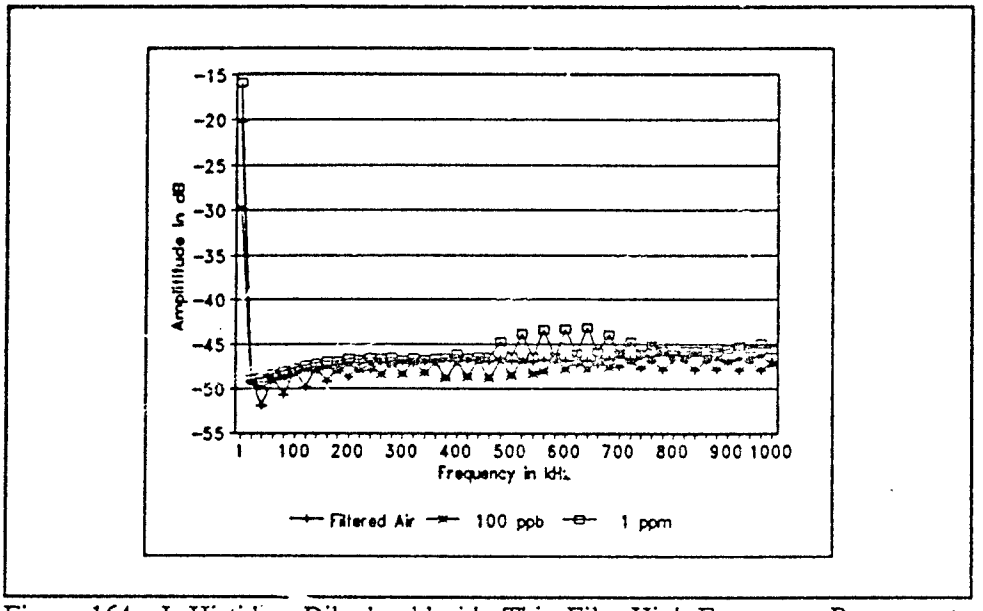

Figure 164. L-Histidine Dihydrochloride Thin Film High-Frequency Response to DIMP Challenge Gas at 50° C.

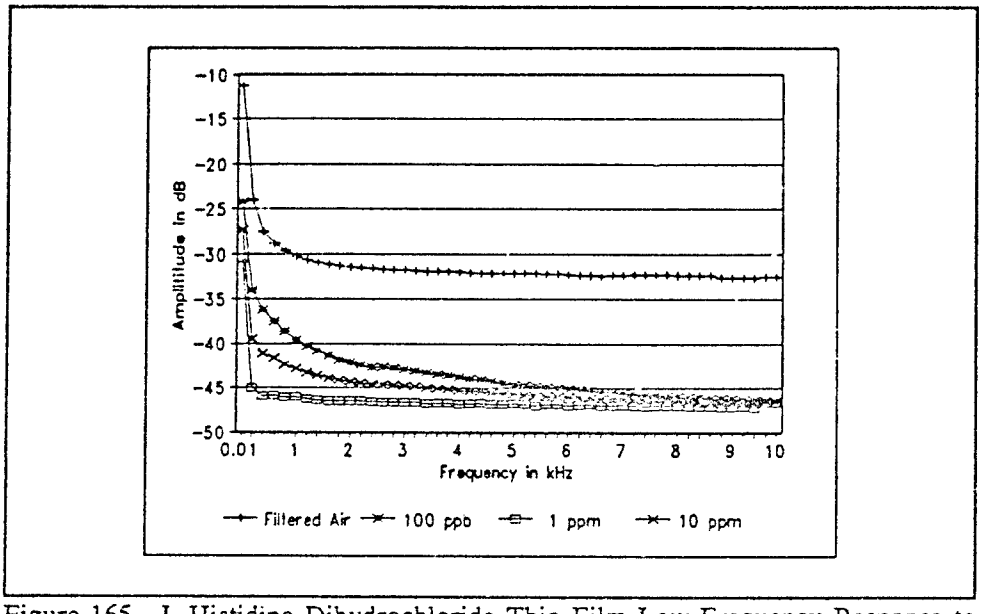

Figure 165. L-Histidine Dihydrochloride Thin Film Low-Frequency Response to DMMP Challenge Gas at 30° C.

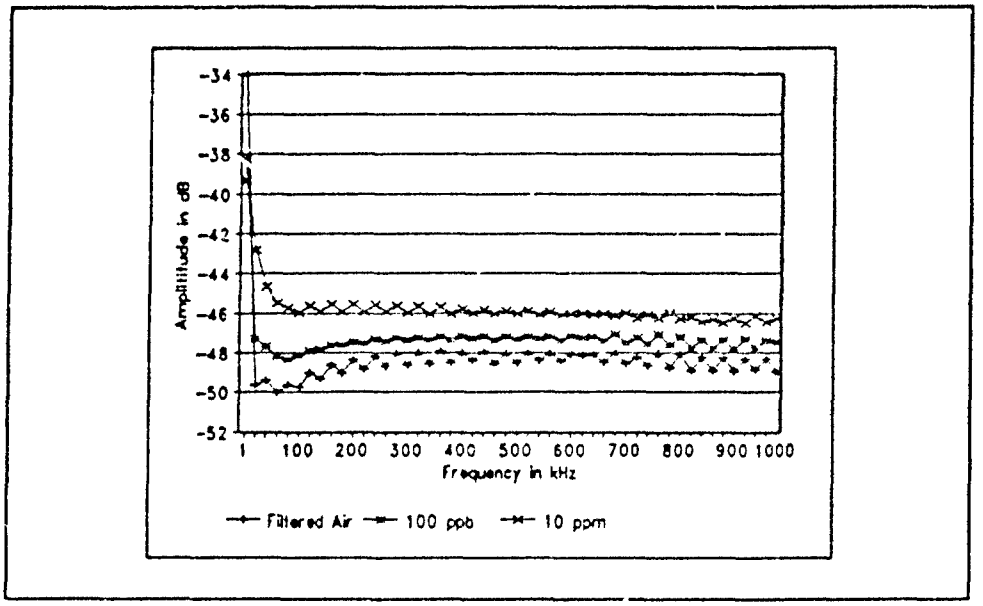

Figure 166. L-Histidine Dihydrochloride Thin Film High-Frequency Response to DMMP Challenge Gas at 30° C.

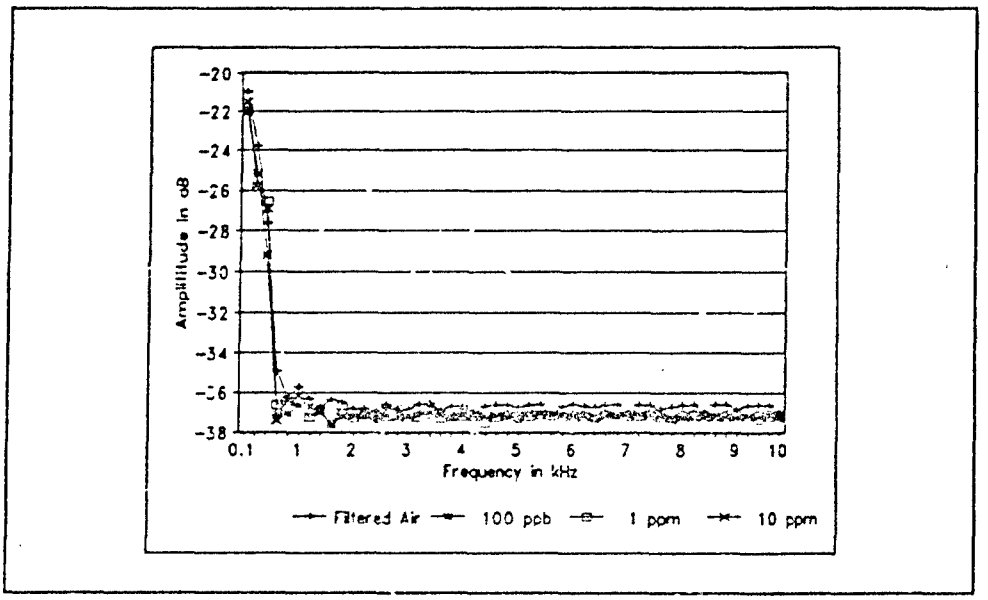

Figure 167. L-Histidine Dihydrochloride Thin Film Low-Frequency Response to DMMP Challenge Gas at 50° C.

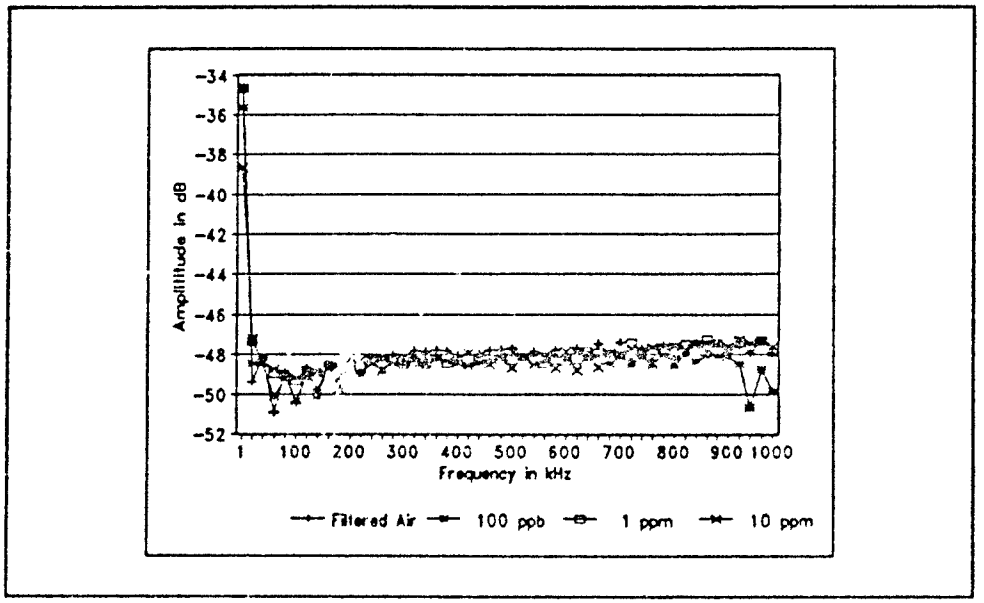

Figure 168. L-Histidine Dihydrochloride Thin Film High-Frequency Response to DMMP Challenge Gas at 50° C.

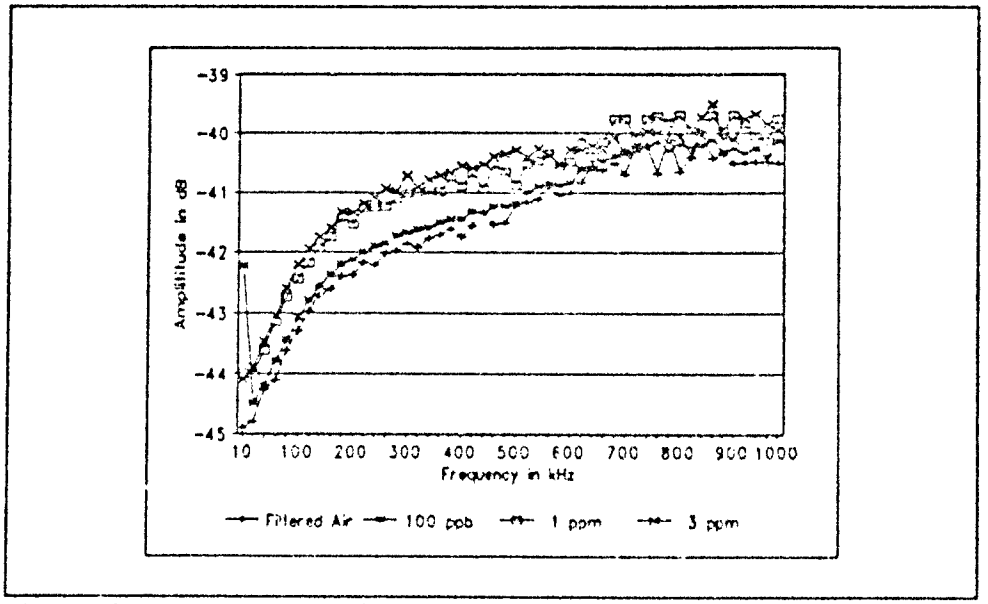

Figure 169. L-Histidine Dihydrochloride Thin Film High-Frequency Response to DFP Challenge Gas at 30° C.

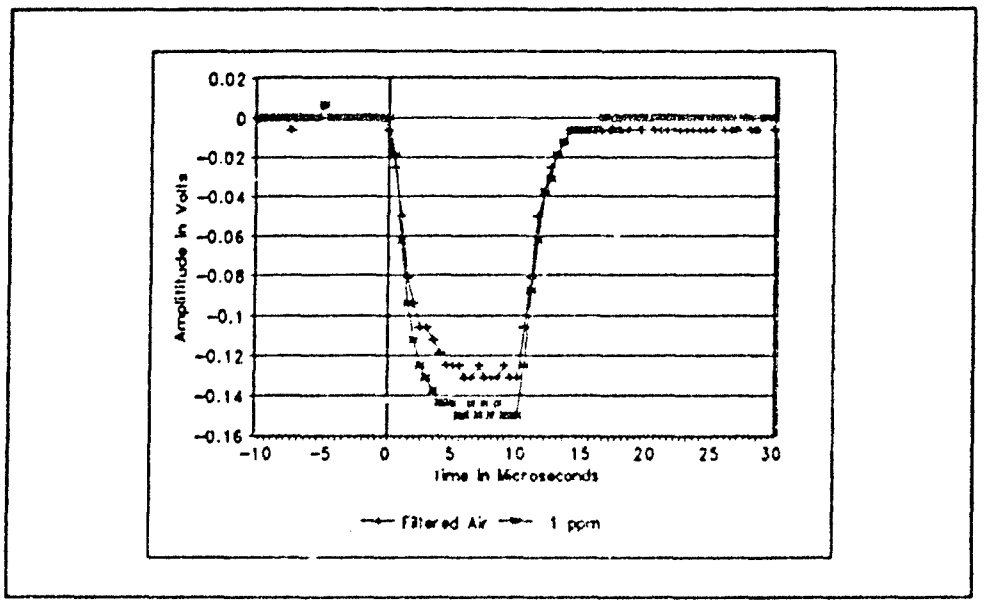

Figure 170. L-Histidine Dihydrochloride Thin Film Time-Domain Response to a 3 Volt 10 Microsecond Excitation Pulse With DFP Challenge Gas at 30° C.

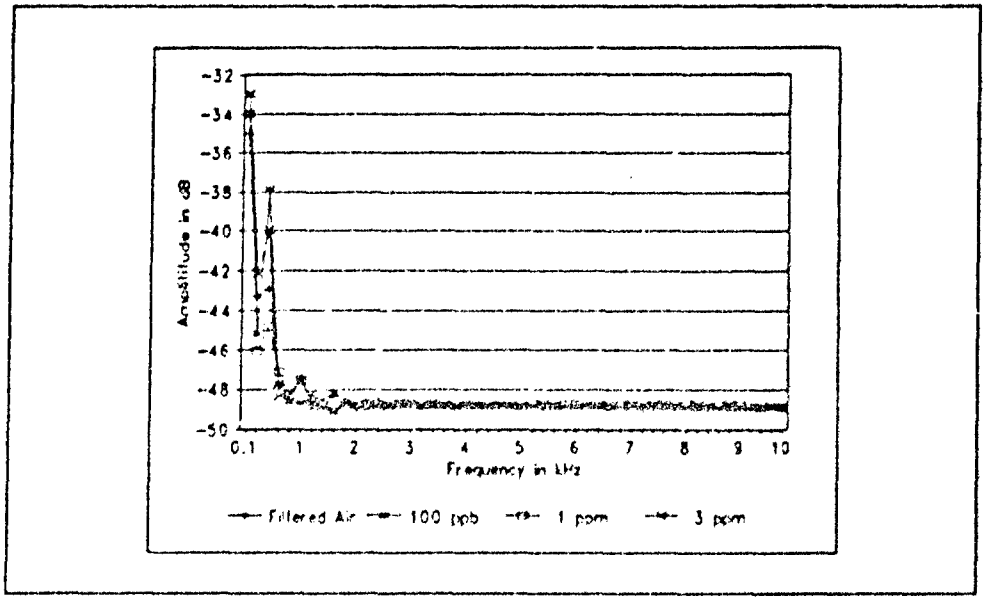

Figure 171. L-Histidine Dihydrochloride Thin Film Low-Frequency Response to DFP Challenge Gas at 50° C.

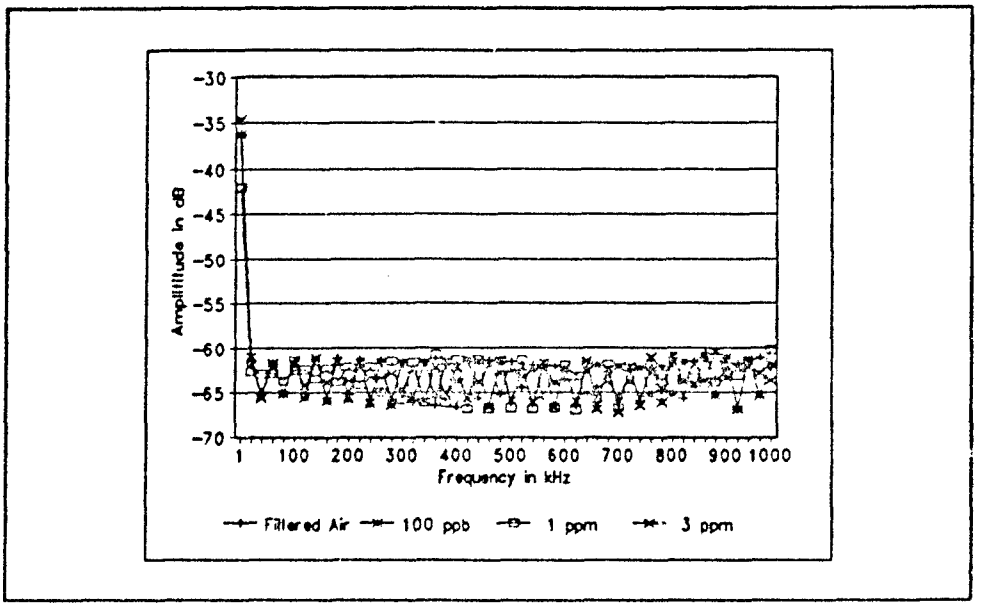

Figure 172. L-Histidine Dihydrochloride Thin Film High-Frequency Response to DFP Challenge Gas at 50° C.

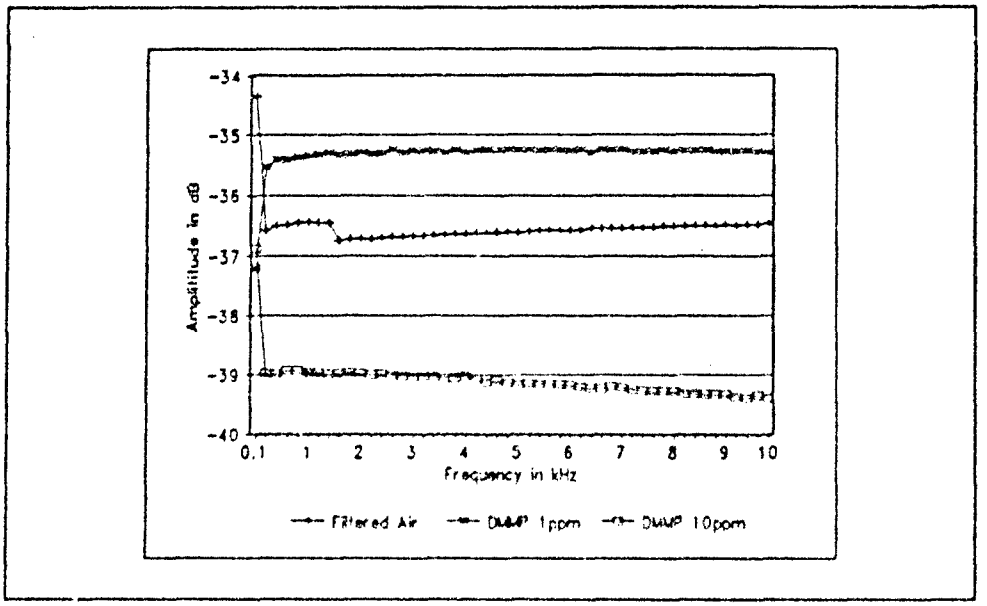

Figure 173. L-Histidine Dihydrochloride Thin Film Low-Frequency Response to DIMP and DMMP Challenge Gas at 30° C.

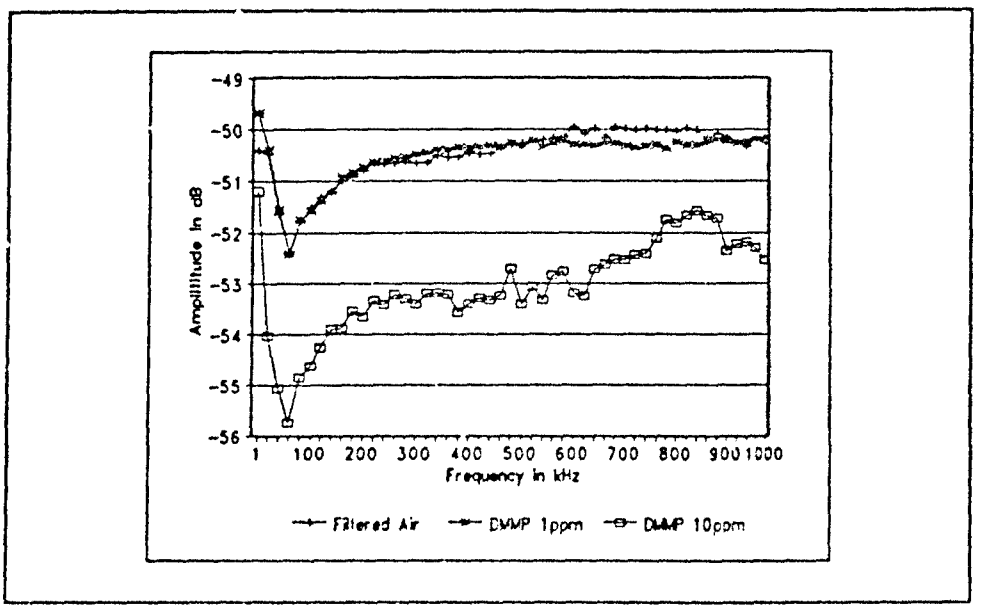

Figure 174. L-Histidine Dihydrochloride Thin Film High-Frequency Response to DIMP and DMMP Challenge Gas at 30° C.

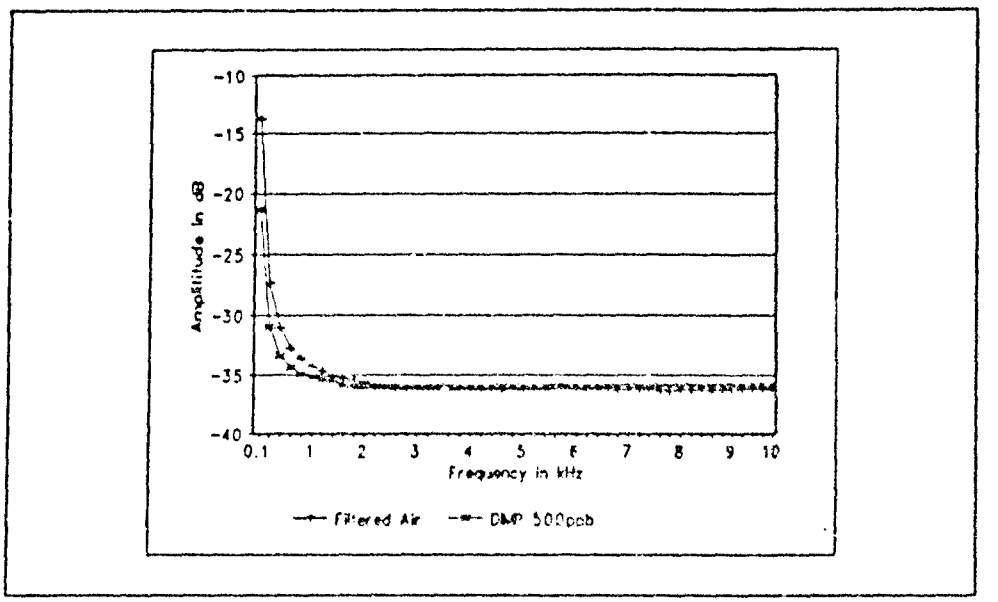

Figure 175. L-Histidine Dihydrochloride Thin Film Low-Frequency Response to DIMP and DFP Challenge Gas at 30° C.

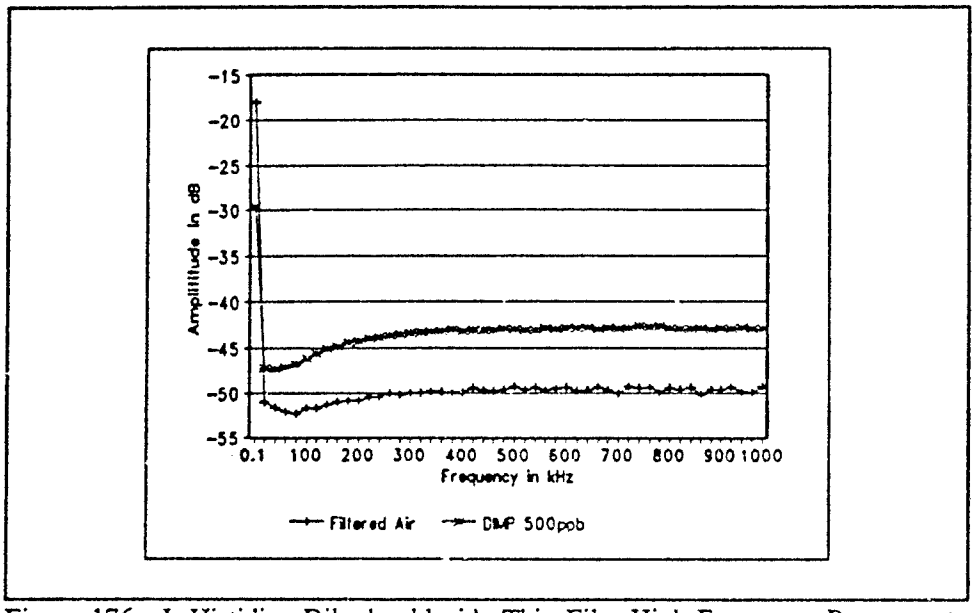

Figure 176. L-Histidine Dihydrochloride Thin Film High-Frequency Response to DIMP and DFP Challenge Gas at 30° C.

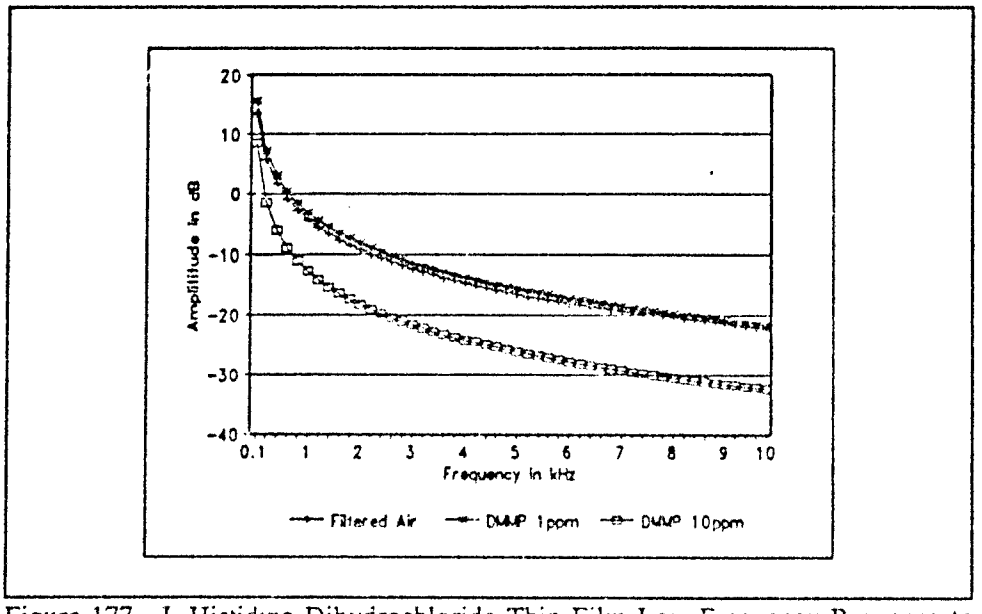

Figure 177. L-Histidine Dihydrochloride Thin Film Low-Frequency Response to DMMP and DFP Challenge Gas at 30° C.

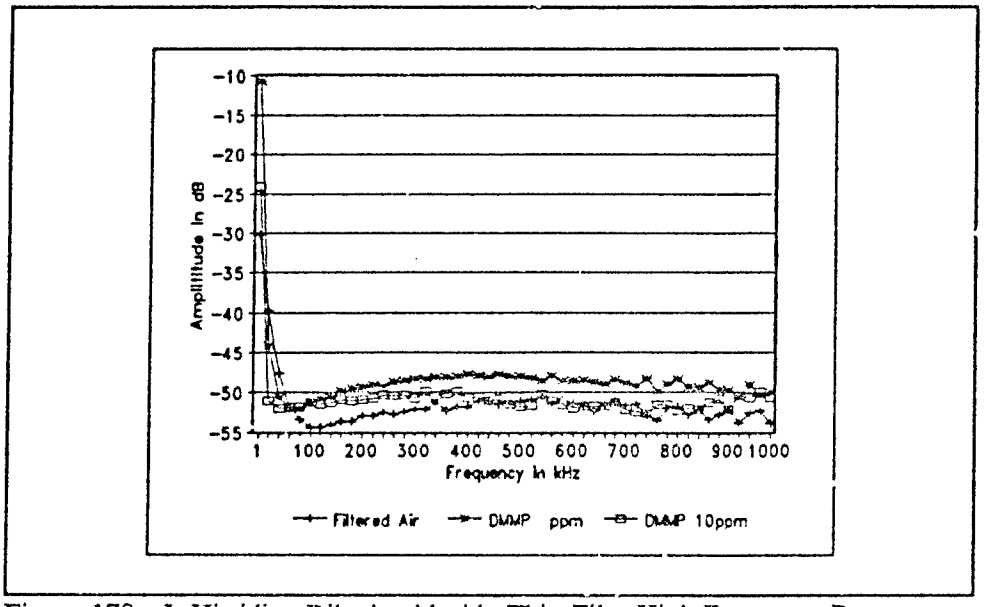

Figure 178. L-Histidine Dihydrochloride Thin Film High-Frequency Response to DMMP and DFP Challenge Gas at 30° C.

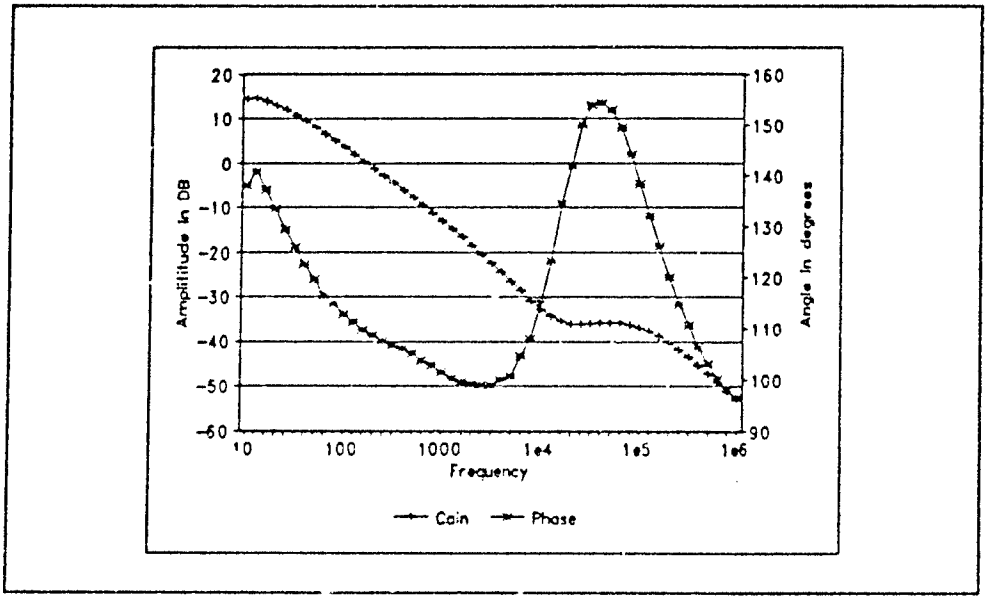

Figure 179. L-Histidine Dihydrochloride Thin Film Gain Response to DMMP and DFP Challenge Gas at 30° C.

Appendix G

Resistance Capacitance Frequency-Domain Model

The band-reject filter response is modeled using data obtained from measurements taken from the IGEFET while installed in the test cell. The capacitance values for the driven and floating gate to ground were provided by Captain John Wiseman (28). The value for the input resistance was taken from the instrumentation providing the input signal (Figure 180). The driven to floating gate resistance and capacitance values were derived from the measurements taken during testing.

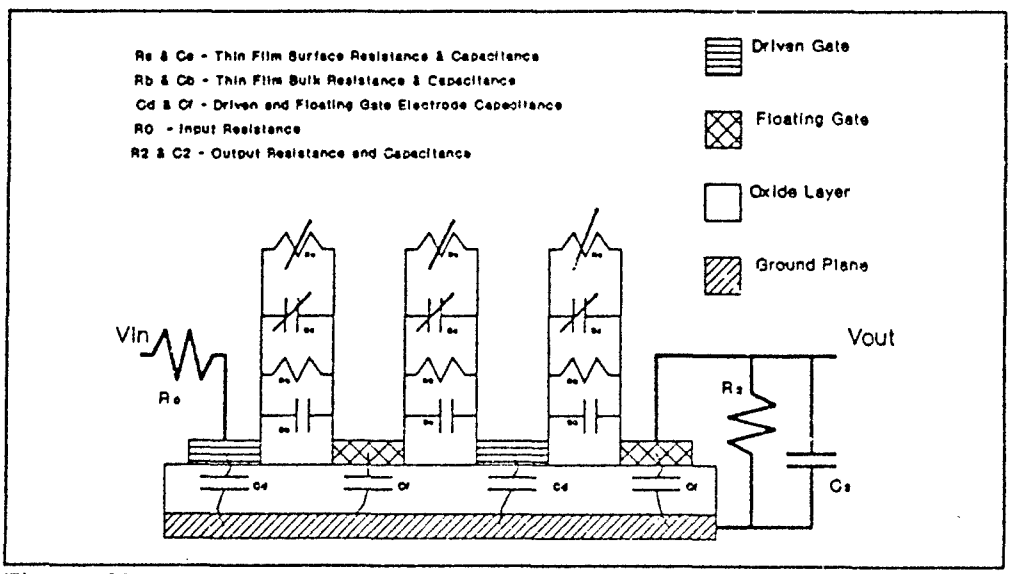

Figure 180. The Resistance and Capacitance Model for the IGE Structure Where the Driven Gate Electrodes Shown are Shorted to Each Other as are the Floating Gate Electrodes.

A simplified π equivalent model is used to demonstrate how the interdigitated gate electrode (IGE) structure may be modeled to produce the band-reject (notch) filter response observed in the succinylcholine chloride response when exposed to the diisopropyl fluorophosphate challenge gas. A schematic representation of the model is shown in Figure 181.

The values used for this model are given for the following relationships, where the first column of terms (R_0, C_d, R_s, C_s, R_b, C_b, C_f, R_2, and C_2) are the lumped values for the IGE structure and the connecting hardware, the second column grouping of terms (R_0, C_0, R_1, C_1, R_2, and C_2) are the ones used in the π model, and the values are the values obtained for calculating the results.

Listed below are the terms and values used in the calculation of the data presented in Figure 182:

R_0 =	R_0 =	50 Ω	
C_d =	C_0 =	15 pF	
$R_s + R_b$ =	R_1 =	3.95 GΩ	=2.95 GΩ (response to air)
$C_s + C_b$ =	C_1 =	810 fF	=800 fF (response to air)
R_2 =	R_2 =	34.4 MΩ	
$C_f + C_2$ =	C_2 =	45 pF	

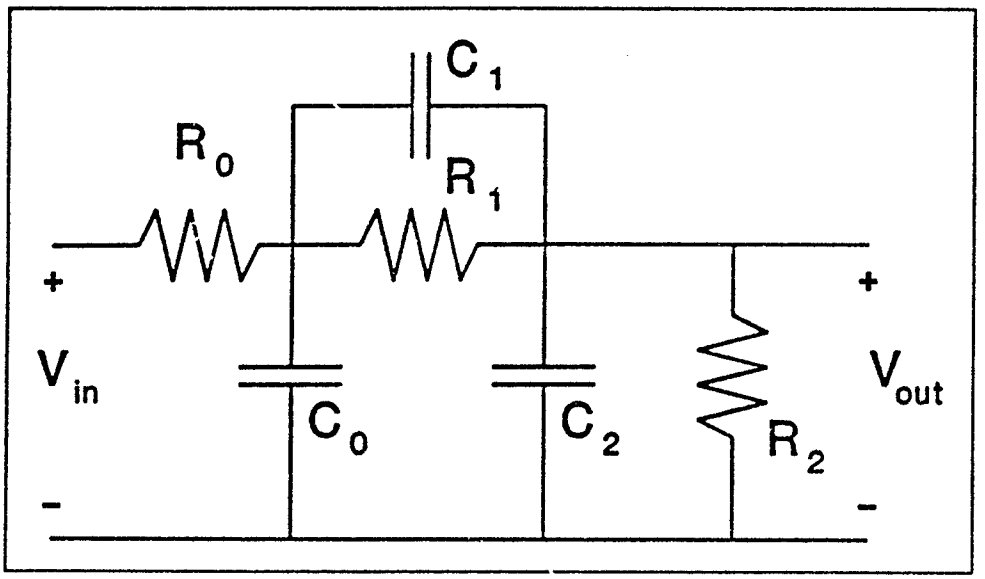

Figure 181. Simplified Schematic Diagram of the π Equivalent Model as Used to Evaluated the IGE Structure Response.

The frequency-domain output power response of the results (assuming a 0 dB input) obtained are shown in Figure 182. The only values changed for the response to filtered laboratory versus the DFP challenge gas are R_1 and C_1 representing the changes observed in R_x and C_x in the IGE structure.

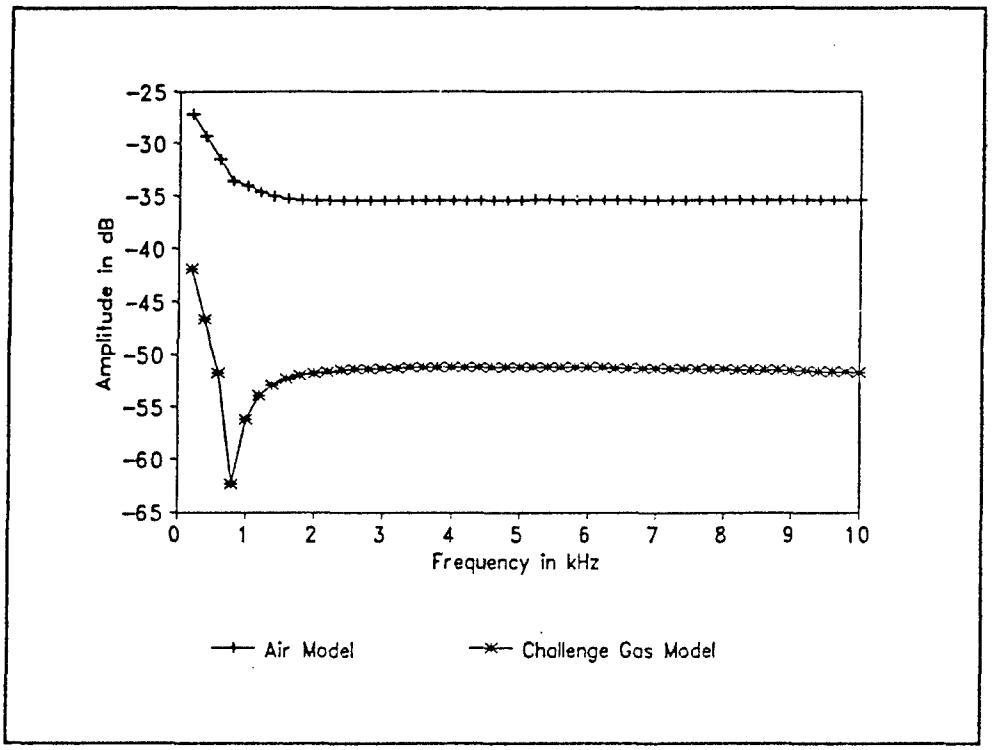

Figure 182. Frequency-Domain Power Response of the π Equivalent Model of the IGE Structure Using Succinylcholine Chloride as the Chemically-Sensitive Thin Film When Exposed to Laboratory Air and the DFP Challenge Gas.

Bibliography

1. Handout distributed in "Medical Management of Chemical Casualties Course," US Army Medical Research Institute of Chemical Defense, Aberdeen Proving Ground, MD, (14 November 1988).

2. Wiseman, Capt J. *Investigation of the Impedance Modulation of Thin Films With a Chemically-Sensitive Field-Effect Transistor*. MS Thesis, AFIT/GE/ENG/88D-6.61. Department of Electrical and Computer Engineering, Air Force Institute of Technology (AU), Wright-Patterson AFB OH, (5 December 1988). (AD-A202-766)

3. Shin, Capt J. *Evaluation of Chemically-Sensitive Field-Effect Transistors for Detection of Organophosphorus Compounds*. MS Thesis, AFIT/GE/ENG/89D-47. Department of Electrical and Computer Engineering, Air Force Institute of Technology (AU), Wright-Patterson AFB OH, (5 December 1989). (AD-A215-536)

4. Jenkins, Capt T. *Evaluation of Doped Phthalocyanine Polymers for use with a Chemically-Sensitive Field-Effect Transistor*. MS Thesis, AFIT/GE/ENG/89D-18. Department of Electrical and Computer Engineering, Air Force Institute of Technology (AU), Wright-Patterson AFB OH, (4 December 1989). (AD-A215-662)

5. Smith, P. *et al.* "Cholinesterase Inhibition in Relation to Fitness to Fly," *Aerospace Medicine, 39*: 754-758, (July 1968).

6. Russell R. W. and Overstreet D. H. "Mechanisms Underlying Sensitivity to Organophosphorus Anticholinesterase," *Progress In Neurobiology, 28*: 97-129, Pergamon Journals Ltd, Great Britain, 1987.

7. Rose-Pehrsson, S. L. and Ballantine, D. B. "Data Analysis of Surface Acoustic Wave Device Coating Responses Using Pattern Recognition Methods," *Proceedings of the 1986 US Army Chemical Research, Development and Engineering Center Scientific Conference on Chemical Defense Research, 1*: US Army Armament, Munitions & Chemical Command, Aberdeen Proving Ground MD, (June 1987).

8. "SAW Chip to Detect Chemical Warfare Agents," *Microwave System News, 12*: 36, (December 1989).

9. Ruihua W. and Jones T. "The Characteristics of Gas-Sensitive Multilayer Devices Based on Lead Phthalocyanine," *Sensors and Actuators B, 12*: 33-42, Elsevier Sequoia, Netherlands, (1990).

10. Shin, Capt J. Graduate Engineering Student. Interview. Air Force Institute of Technology, Air University, Wright-Patterson AFB OH, (11 December 1989).

11. Jenkins, Capt T. Graduate Engineering Student. Interview. Air Force Institute of Technology, Air University, Wright-Patterson AFB OH, (14 December 1989).

12. Hayes, T. *et al.* "Development of Gas Chromatographic Analytical Methods Using Solid Sorbents for Detecting HD, GA, GD, GB, and VX at Monitoring Levels," U. S. Army Medical Research and Development Command. Contract DAMD17-83-C-3129 with Battelle Memorial Institute. Aberdeen Proving Ground, MD, (15 August 1989).

13. Kerenyi, Capt S. Project Scientist. Telephone interview. USAF School of Aerospace Medicine, Human Systems Division (AFSC), Brooks AFB TX, (24 April 1990).

14. Goodman, L. and Gilman, A. *The Pharmacological Basis of Therapeutics* (Third Edition). New York: The MacMillan Company, 441-463, 1965.

15. Janata, J. "Chemical Sensors," *Analytical Chemistry, 62, 12*: 33R-44R, (15 July 90).

16. Ballantine, D. "Correlation of Surface Acoustic Wave Device Coating Responses with Solubility Properties and Chemical Structure Using Pattern Recognition," *Analytical Chemistry, 58, 14*: 3058, (December 1986).

17. Janata J. and Huber R. "Chemically Sensitive Field Effect Transistors," *Ion-Selective Electrodes in Analytical Chemistry, 2*: 107-171, edited by Henry Freiser. Plenum Press, New York, (1980).

18. Wohltjen, H. *et al.* "A Vapor-Sensitive Chemiresistor Fabricated with Planar Microelectrodes and a Langmuir-Blodgett Organic Semiconductor Film," IEEE *Transactions On Electron Devices, ED-32*: 1170-1170 (July 1985).

19. Josowicz, M. and Janata, J. "Suspended Gate Field Effect Transistor," *Chemical Sensor Technology*, Volume 1, edited by Seiyama. Tokyo: Kodansha Ltd. and Elsevier Science Publishers, 1988.

20. Kolesar, E. "Theory and Practice of Dielectric-Supported Thin Film Chemiresistors," *Chemical Sensor Technology*, Volume 3, edited by Yamazoe. Tokyo: Kodansha Ltd. and Elsevier Science Publishers, (In press).

21. Fluka Chemical Co. *Catalog 1988/1989.* Ronkonkoma NY, 1988.

22. Senturia, S. "The Role of the MOS Structure in Integrated Sensors," *Sensors and Actuators, 4*: 507-526, (1983)

23. Rajan, K. *et al.* "Stability of Squid-Type DFPase and its Recovery in CW-Agent Decontamination Application," *Proceedings of the 1988 US Army Chemical Research, Development and Engineering Center Scientific Conference on Chemical Defense Research, 1*: US Army Armament, Munitions & Chemical Command, Aberdeen Proving Ground, MD, (August 1989).

24. Graham, Capt T. Personal communication. Air Force Institute of Technology, Air University, Wright-Patterson AFB OH, (1 June 1990).

25. Jerse, T. "Shielding Basics," *RF Design, 13*: 83-88, (March 1990).

26. Weast, R. ed. *CRC Handbook of Chemistry and Physics* (61st Edition). Boca Raton, FL: CRC Press Inc., 1980.

27. Kraus, J. *Electromagnetics* (Third Edition). New York: McGraw Hill Book Company, 1984.

28. Wiseman, Capt J. Graduate Engineering Student. Interview. Air Force Institute of Technology, Air University, Wright-Patterson AFB OH, (29 November 1990).

Vita

Captain Charles P. Brothers, Jr. was born 10 April 1958 in Portland, Oregon. He graduated from Bend Senior High School in Bend, Oregon in 1976. He served in the United States Air Force as a Precision Measurement Equipment Specialist from 1976 until 1980. He then attended Central Oregon Community College, Bend, Oregon followed by Portland State University, Portland, Oregon where he received a Bachelor of Science in Electrical Engineering with honors in 1985. Reentering the Air Force, he graduated from Officer Training School 4 October 1985. He served as a project engineer Peacekeeper Guidance and Control, Ballistic Missile Organization, Norton AFB, CA from October 1985 through May 1989. While stationed at Norton AFB, he attended the University of Southern California receiving a Masters of Science in Systems Management in 1987. He entered the School of Engineering, Air Force Institute of Technology in May 1989.

Permanent Address: 11525 NE Coos St
Newport, OR 97365

REPORT DOCUMENTATION PAGE

	December 1990	Master's Thesis

EVALUATION OF AN INTERDIGITATED GATE ELECTRODE FIELD-EFFECT TRANSISTOR FOR DETECTING ORGANOPHOSPHORUS COMPOUNDS

Charles P. Brothers, Jr., Captain, USAF

Air Force Institute of Technology, WPAFB OH 45433-6583

AFIT/GE/ENG/90D-07

Approved for public release; distribution unlimited.

This study used integrated circuit microsensors to detect organophosphorus compounds. Chemically-sensitive thin films, copper phthalocyanine, DFPase, succinyl chloride, succinylcholine chloride, 2-naphthol(β), and L-histidine dihydrochloride, were deposited on interdigitated gate electrode (IGE) structures, with an average thickness of 2000Å. Thin film electrical performance characteristics were measured for several parameters, including: DC resistance, AC impedance, time-domain, and spectral responses from 10 Hz to 1 MHz. Each microsensor contained nine IGEs; each IGE possessed an *in situ* field-effect transistor amplifier. After purging each sensor with filtered air, it was exposed to one or two of the following gases: diisopropyl fluorophosphate (DFP), diisopropyl methylphosphonate, and dimethyl methylphosphonate at concentrations spanning 100 ppb to 10 ppm (at 90% relative humidity and 23° C). Testing was conducted with microsensors heated to 30, 50, and 70° C. All six candidate films demonstrated various degrees of sensitivity to the challenge gases at 30° C. DFPase was especially sensitive to the challenge gases at 100 ppb. Only copper phthalocyanine and L-histidine dihydrochloride demonstrated sensitivity above 30° C. In particular 2-naphthol(β) showed complete reversibility and succinyl chloride demonstrated partial reversibility at 30° C. Copper phthalocyanine was reversible only at 70° C. Succinylcholine chloride demonstrated a unique band-reject filter response to the presence of DFP in any challenge gas sample.

Chemically-Sensitive Microsensor, Microsensor, Chemical Sensor, IGEFET, DFPase, Organophosphorus Compounds

245

Unclassified | Unclassified | Unclassified | UL